

Cardiovascular Magnetic Resonance Imaging for the Investigation of Ischaemic Heart Disease

James Robert John Foley

Submitted in accordance with the requirements for the degree of Doctor of Medicine (MD)

The University of Leeds

Faculty of Medicine and Health

Leeds Institute of Cardiovascular and Metabolic Medicine

November 2018

Intellectual Property and Publication Statements

The candidate confirms that the work is his own, except where work which has formed part of jointly authored publications has been included. The contribution of the candidate and the other authors to this work has been explicitly indicated below. The candidate confirms that appropriate credit has been given within the thesis where reference has been made to the work of others:

This copy has been supplied on the understanding that it is copyright material and that no quotation from the thesis may be published without proper acknowledgement.

Chapter 1

Publication:

Foley JR, Plein S, Greenwood JP. Assessment of stable coronary artery disease by cardiovascular magnetic resonance imaging: Current and emerging techniques. *World J Cardiol.* 2017 Feb 26;9(2):92-108. doi: 10.4330/wjc.v9.i2.92.

PMID: 28289524

Authorship:

JF: Conception, design, literature search, drafting and revision of manuscript. **SP:** Revision of the manuscript. **JPG:** Conception and Revision of the manuscript.

Chapter 3

Publication:

Foley JRJ, Kidambi A, Biglands JD, Maredia N, Dickinson CJ, Plein S, Greenwood JP. A comparison of cardiovascular magnetic resonance and single photon emission computed tomography (SPECT) perfusion imaging in left main stem or equivalent coronary artery disease: a CE-MARC substudy *J Cardiovasc Magn Reson.* 2017 Nov 6;19(1):84. doi: 10.1186/s12968-017-0398-7. PMID: 29110669

Authorship:

JF: Conception, design, collection of data, data analysis and interpretation of data. Drafting and revision of manuscript. **AK:** Data analysis and interpretation, revision of manuscript. **JDB:** Data analysis and revision of manuscript. **NM:** Recruitment of patients, data analysis, revision of manuscript. **CJD:** Data analysis and revision of manuscript **SP:** Data analysis and revision of manuscript **JPG:** Data analysis and interpretation,

revision of manuscript.

Chapter 4:

Publication:

Foley JRJ, Swoboda PP, Fent GJ, Garg P, McDiarmid AK, Ripley DP, Erhayiem B, Musa TA, Dobson LE, Plein S, Witte KK, Greenwood JP. Quantitative deformation analysis differentiates ischaemic and non-ischaemic cardiomyopathy: sub-group analysis of the VINDICATE trial. Eur Heart J Cardiovasc Imaging. 2018 Jul 1;19(7):816-823. doi: 10.1093/ehjci/jex235. Erratum in: Eur Heart J Cardiovasc Imaging. 2018 Mar 1;19(3):278.

Authorship:

JF: Conception, design, patient recruitment, collection of data, data analysis and interpretation of data. Drafting and revision of manuscript. **PPS:** Conception, data interpretation, revision of manuscript. **GJF:** data analysis and revision of manuscript. **PG:** data analysis and revision of manuscript. **AKM:** patient recruitment, collection of data, revision of manuscript. **DPR:** collection of data, revision of manuscript. **BE:** collection of data, revision of manuscript. **TAM:** collection of data, revision of manuscript. **LED:** revision of manuscript. **SP:** revision of manuscript. **KKW:** Conception, patient recruitment, revision of manuscript. **JPG:** Conception, data interpretation, revision of manuscript.

Chapter 5

Authorship:

JF: Conception, design, patient recruitment, collection of data, data analysis and interpretation of data. Drafting and revision of manuscript. **CCE:** data analysis and interpretation of data. **JMB:** revision of manuscript **PJB:** patient recruitment, collection of data, revision of manuscript. **DPR:** patient

recruitment, collection of data, revision of manuscript. **SP**: revision of manuscript. **JPG**: Conception, data interpretation, revision of manuscript.

Chapter 6

Publication:

Foley JRJ, Fent GJ, Garg P, Broadbent D, Dobson LE, Chew PG, Brown LA, Swoboda PP, Plein S, Higgins DM, Greenwood JP. Feasibility Study of a Single Breath-hold,3D mDIXON Pulse Sequence for Late Gadolinium Enhancement Imaging of Ischemic Scar. Journal of Magnetic Resonance Imaging 2018 accepted and in press

Authorship:

JF: Conception, design, patient recruitment, collection of data, data analysis and interpretation of data. Drafting and revision of manuscript. **GJF**: data analysis and revision of manuscript. **PG**: patient recruitment, collection of data, revision of manuscript. **DAB**: data interpretation, revision of manuscript. **LED**: revision of manuscript. **PGC**: revision of manuscript. **LAB**: data analysis and revision of manuscript. **PPS**: revision of manuscript. **SP**: revision of manuscript. **DMH**: Conception, design, interpretation of data, revision of manuscript. **JPG**: Conception, revision of manuscript.

Chapter 7

Authorship:

JF: Conception, design, patient recruitment, collection of data, data analysis and interpretation of data. Drafting and revision of manuscript. **DAB**: data interpretation, revision of manuscript. **GJF**: data analysis and revision of manuscript. **PG**: patient recruitment, collection of data, revision of manuscript. **LAB**: data analysis and revision of manuscript. **PGC**: revision of manuscript. **LED**: revision of manuscript. **PPS**: revision of manuscript. **SP**: revision of manuscript. **DMH**: Conception, design, interpretation of data, revision of manuscript. **JPG**: Conception, revision of manuscript.

Contributors initials/names:

AK: Ananth Kidambi

AKM: Adam McDiarmid

BE: Bara Erhayiem

CCE: Colin Everett

CJD: Catherine Dickinson

DAB: David Broadbent

DMH: David Higgins

DPR: David Ripley

GJF: Graham Fent

JDB: John Biglands

JF: James Foley

JMB: Julia Brown

JPG: John Greenwood

KKW: Klaus Witte

LAB: Louise Brown

LED: Laura Dobson

NM: Neil Maredia

PG: Pankaj Garg

PGC: Pei Ge Chew

PJB: Petra Bijsterveld

PPS: Peter Swoboda

SP: Sven Plein

TAM: Tarique Musa

Publications arising from this work

Papers:

1. Foley JR, Plein S, Greenwood JP. Assessment of stable coronary artery disease by cardiovascular magnetic resonance imaging: Current and emerging techniques. *World J Cardiol.* 2017 Feb 26;9(2):92-108. doi: 10.4330/wjc.v9.i2.92. PMID: 28289524
2. Foley JRJ, Kidambi A, Biglands JD, Maredia N, Dickinson CJ, Plein S, Greenwood JP. A comparison of cardiovascular magnetic resonance and single photon emission computed tomography (SPECT) perfusion imaging in left main stem or equivalent coronary artery disease: a CE-MARC substudy. *J Cardiovasc Magn Reson.* 2017 Nov 6;19(1):84. doi: 10.1186/s12968-017-0398-7. PMID: 29110669
3. Foley JRJ, Swoboda PP, Fent GJ, Garg P, McDiarmid AK, Ripley DP, Erhayiem B, Musa TA, Dobson LE, Plein S, Witte KK, Greenwood JP. Quantitative deformation analysis differentiates ischaemic and non-ischaemic cardiomyopathy: sub-group analysis of the VINDICATE trial. *Eur Heart J Cardiovasc Imaging.* 2018 Jul 1;19(7):816-823. doi: 10.1093/ehjci/jex235. Erratum in: *Eur Heart J Cardiovasc Imaging.* 2018 Mar 1;19(3):278. PMID: 29029139
4. Foley JRJ, Fent GJ, Garg P, Broadbent D, Dobson LE, Chew PG, Brown LA, Swoboda PP, Plein S, Higgins DM, Greenwood JP. Feasibility Study of a Single Breath-hold,3D mDIXON Pulse Sequence for Late Gadolinium Enhancement Imaging of Ischemic Scar *Journal of Magnetic Resonance Imaging* 2018 accepted and in press

Under peer review

1. Foley JRJ, Everett CC, Brown JM, Bijsterveld P, Ripley DP, Plein S, Greenwood JP. Development and validation of a contemporary pre-test likelihood model of coronary artery disease referenced to invasive angiography, with comparison to pre-existing risk models. Submitted to International Journal of Cardiology July 2018.
2. Foley JRJ, Broadbent DA, Fent GJ, Garg P, Brown LA, Chew PG, Dobson LE, Swoboda PP, Plein S, Higgins DM, Greenwood JP. Clinical Evaluation of two dark blood methods of late gadolinium quantification of ischaemic scar. Submitted to Journal of Magnetic Resonance Imaging August 2018.

Abstracts:

1. Foley JRJ, Fent GJ, Garg P, Broadbent D, Dobson LE, Chew PG, Brown LAE, Swoboda PP, Plein S, Higgins DM, Greenwood JP. Single breath-hold, 3D MDIXON pulse sequence for late gadolinium enhancement imaging of ischaemic scar: a feasibility study. *Heart*, May 2018, 104 (Suppl 5) A12; DOI: 10.1136/heartjnl-2018-BCVI.32. Poster presentation at BCVI 2018, Edinburgh, UK May 2018.
2. Foley JRJ, Fent GJ, Garg P, Broadbent DA, Dobson LE, Chew PG, Brown LAE, Dall'Armellina E, Swoboda PP, Plein S, Higgins DM, Greenwood JP. Feasibility Study of a Single Breath-hold, 3D mDIXON Pulse Sequence for Late Gadolinium Enhancement Imaging of Ischaemic Scar. Poster presentation at CMR 2018, Barcelona, Spain January 2018.
3. Foley JRJ, Everett CC, Cairns D, Bijsterveld P, Ripley DP, Plein S, Sharples L, Brown J, Greenwood JP. Development and external validation of a multivariable model of pre-test likelihood of coronary artery disease based on a contemporary UK population, with comparison to existing risk models. *Heart* Jun 2017, 103 (Suppl 5) A64-A66. Poster presentation at BCS Manchester June 2017.
4. Foley JRJ, Swoboda PP, Fent GJ, Garg P, Ripley DP, McDiarmid AK, Dobson LE, Musa TA, Plein S, Witte KK, Greenwood JP. Differences in myocardial mechanics between ischaemic and non-ischaemic cardiomyopathy assessed by CMR: a sub-group analysis of the VINDICATE trial. *Heart* Jun 2017, 103 (Suppl 5) A77-A78. Poster presentation at BCS Manchester June 2017.
5. Foley JRJ, Swoboda PP, Fent GJ, McDiarmid AK, Garg P, Ripley DP, Musa TA, Plein S, Witte KK, Greenwood JP. Differences in CMR global strain assessment in ischaemic and non-ischaemic

cardiomyopathy: sub-group analysis of the VINDICATE trial. Poster presentation at SCMR, Washington DC, USA January 2017.

Acknowledgements

This work would not have been possible without the contribution and support of others. I would like to express my gratitude to my supervisors Professor John Greenwood and Professor Sven Plein. Their guidance, leadership and support has been invaluable and is something that will stay with me through the rest of my career.

The working environment in the University of Leeds CMR Department has been fantastic and I would also like to express my thanks to the other staff involved in its day-to-day running. My colleagues Drs Swoboda, Garg, Fent, Kidambi, Dobson, Musa, Ripley, Chew, Brown, McDiarmid, Erhayiem, Biglands and Broadbent have all provided creative input, valuable experience and insight as well as a sense of humour when needed. I am grateful to the research nurses Petra, Michelle, Lisa, Hannah and Fiona for their assistance in recruiting patients and smooth running of studies. Special thanks go to the radiographers Gavin, Margaret, Caroline, Lisa, Georgina, Graham and Stephen for their technical know-how, scanning of patients and flexibility in accommodation of my requests. I am grateful to the assistants Debbie and Anne for their help. Additionally I owe a debt of gratitude to Dr David Higgins for his help and extensive physics knowledge and support. I am grateful to the team at the CTRU particularly Colin for his statistical help.

Additionally I am most grateful to all the patients who participated in this research project. Their time and altruism has hopefully furthered our knowledge of this field and lead to progress in patient care.

Lastly, I would like to acknowledge the support of my family- particularly my long suffering partner Lauren for her endless patience and unrelenting support, my mother for instilling in me a solid work ethic, my father for teaching me the value of quiet endeavour.

List of abbreviations

2D	two dimensional
3D	three-dimensional
4D flow	four-dimensional flow CMR
ACEi	angiotensin-converting enzyme inhibitor
ACS	acute coronary syndrome
AF	atrial fibrillation
AHA	American Heart Association
ANOVA	analysis of variance
ARB	aldosterone receptor blocker
AUC	area under the curve
BHF	British Heart Foundation
BMI	Body mass index
BN	blood nulled PSIR
BNP	natriuretic peptide
BOLD	Blood Oxygen Level Dependent
BSA	body surface area
CABG	coronary artery bypass grafts
CAC	coronary artery calcium score
CAD	coronary artery disease
CCS	Canadian Cardiovascular society
CMRA	coronary magnetic resonance angiography
CMR	cardiovascular magnetic resonance
CNR	contrast-to-noise ratio
COPD	chronic obstructive pulmonary disease
CRT	cardiac resynchronization therapy

CT	computed tomography
CTCA	CT coronary angiography
DSE	stress echocardiography
DSMR	dobutamine Stress CMR
DTI	diffusion tensor MRI
E _{cc}	circumferential strain.
ECG	electrocardiogram
ECV	extracellular myocardial volume fraction
EDV	end diastolic volume
EDVI	end diastolic volume indexed to body surface area
EF	ejection fraction
eGFR	estimated glomerular filtration rate
ESC	European Society of Cardiology
ESV	end systolic volume
ETT	exercise tolerance test
FFR	fractional flow reserve
FIDDLE	Flow-Independent Dark-blood DeLayed Enhancement
FOV	field of view
FPP	first pass perfusion,
FWHM	full width half max
GBCA	gadolinium based contrast agent
Gad-DTPA	gadopentate-dimeglumine
GLS	global longitudinal strain
HF	heart failure
HFrEF	Heart failure with reduced ejection fraction
ICD	internal cardiac defibrillators
ICM	ischaemic cardiomyopathy

iFR	instantaneous flow reserve
IHD	ischaemic heart disease
IQR	interquartile range
IR	Inversion Recovery
IVUS	intravascular ultrasound
KE	kinetic energy
LAD	left anterior descending
LCx	circumflex coronary
LDD	low-dose dobutamine
LGE	late gadolinium enhancement
LMS	left main stem
LV	left ventricle
LVEDV	left ventricular end diastolic volume.
LVEDVi	left ventricular end diastolic volume indexed to body surface area
LVEF	left ventricle ejection fraction.
LVESV	left ventricular end systolic volume
LVM	left ventricular mass.
LVMi	left ventricular mass indexed
MACE	major adverse cardiovascular events
MBF	myocardial blood flow
mDIXON	modified Dixon
METs	metabolic equivalent
MI	myocardial infarction
MN	myocardium nulled PSIR LGE
MPR	myocardial perfusion reserve
MPS -SPECT	myocardial perfusion scan

MRA	magnetic resonance angiography
MRI	magnetic resonance imaging
MVO	microvascular obstruction
NHS	National Health Service
NICE	National Institute for Health and Care Excellence
NICM	non-ischaemic cardiomyopathy
NIHR	National Institute for Health Research
NPV	negative predictive value
NSA	number of signal averages
NSF	nephrogenic systemic fibrosis
NYHA	New York Heart Association functional class
OCT	optical coherence tomography
OMT	optimal medical therapy
PCI	percutaneous coronary intervention
PET	positron emission tomography
PPV	positive predictive value
PSIR	Phase sensitive inversion recovery
PTL	pre-test likelihood
QCA	quantitative coronary angiography
RACPC	rapid access chest pain clinic
RF	radio frequency
ROC	receiver operating characteristic curve analysis
ROI	region of interest
RV	right ventricle
RWMA	regional wall motion abnormality
SE	stress echocardiography
SNR	signal-to-noise ratio

SPAMM	spatial modulation of magnetization
SPECT	single-photon emission computed tomography
SSFP	steady state free precession
SSS	summed stress score
STEMI	ST elevation myocardial infarction
T	tesla
T1 ρ	T1rho
TE	echo time
TID	transient left ventricular dilatation
TI	inversion time
TOE	trans-oesophageal echocardiography
TR	repetition time
TTE	thoracic echocardiography
VLA	vertical long axis

Abstract

Introduction: Coronary artery disease (CAD) remains the number one cause of mortality worldwide; improving diagnosis and treatment is a priority. Multi-parametric cardiovascular magnetic resonance (CMR) offers quantitative assessment of the cardiovascular system with a variety of techniques allowing assessment of anatomy, function, myocardial composition and perfusion during a single scan.

Aims: To assess 1.) diagnostic accuracy of visual and quantitative perfusion CMR to single-photon emission computed tomography (MPS-SPECT) in patients with left main stem CAD. 2.) the hypothesis that patients with ischaemic (ICM) and non-ischaemic cardiomyopathy (NICM) have different torsion and strain parameters 3.) development and validation of a contemporary multivariable risk model of CAD from a large population undergoing X-ray angiography. 4.) a rapid 3D mDIXON pulse sequence for image quality and quantitation of MI. 5.) T1 rho prepared (T1 ρ) dark blood sequence and compare to blood nulled PSIR (BN) and standard myocardium nulled PSIR (MN) for detection and quantification of scar.

Methods: Patients were recruited between 2008 and 2017. Patients in chapters 3,4,6,7 underwent multi-parametric CMR including late gadolinium enhancement (LGE) imaging at 1.5 or 3.0T. Patients in chapter 5 underwent angiography.

Results:

1.) CMR demonstrated significantly higher area under the curve for detection of LMS or equivalent disease over MPS-SPECT(P=0.0001).

2.) Despite no difference in LV dimensions, EF and strain between ICM and NICM, NICM patients had significantly lower LV twist(P=0.023) and torsion(P=0.017) compared to ICM.

3.) The developed model discriminated well and was well-calibrated. Diamond and Forrester and Duke scores substantially over-predicted CAD risk, whilst CAD Consortium risk models slightly under-estimated risk.

4.) Image quality was comparable between 3D and 2D LGE($P=0.162$). Time for 3D image acquisition was only 5% of the time required for a standard 2D acquisition.

5.) $CNR_{\text{scar-blood}}$ was significantly increased for BN and T1 ρ compared to MN LGE. BN LGE demonstrated significantly higher reader confidence scores.

Table of contents

Cardiovascular Magnetic Resonance Imaging for the Investigation of Ischaemic Heart Disease.....	i
Intellectual Property and Publication Statements	ii
Publications arising from this work.....	vii
Acknowledgements.....	xi
List of abbreviations	xii
Abstract.....	xvii
Table of contents.....	xix
List of figures	xxiv
List of Tables	xxvi
List of equations.....	xxvii
1. General Introduction	1
1.1. Background.....	1
1.2. Coronary artery disease	1
1.2.1. Stable versus unstable coronary disease.....	1
1.2.2. Epidemiology of CAD	2
1.2.3. Presentation of stable coronary artery disease	2
1.2.4. Presentation of Acute Coronary syndromes.....	4
1.2.5. Pathophysiology of CAD	4
1.3. Cardiac Imaging	6
1.3.1. Assessment of coronary artery disease	6
1.3.2. Risk stratification in stable CAD	7
1.3.3. Computed tomography coronary angiography	9
1.3.4. MPS-SPECT	12
1.3.5. Stress echocardiography	14
1.3.6. PET	16
1.3.7. Coronary angiography.....	17
1.4. Cardiovascular Magnetic Resonance.....	18
1.4.1. CMR in stable CAD	19
1.4.2. Diagnosis of CAD.....	21
1.4.3. Stress Perfusion CMR.....	24
1.4.4. Dobutamine Stress CMR (DSMR).....	30
1.4.5. Early and late gadolinium enhancement imaging.....	32

1.4.6.	Viability assessment.....	35
1.4.7.	Cost effectiveness.....	38
1.4.8.	Recently published and future studies	39
1.4.9.	Coronary artery evaluation	41
1.4.10.	Future directions	42
1.5.	Conclusion	43
2.	Methods	45
2.1.	Study Populations	45
2.1.1.	Common patient population for Chapters 3 and 5.....	45
2.1.2.	Patient population for Chapter 4.....	47
2.1.3.	Patient population for Chapter 6.....	48
2.1.4.	Patient population for Chapter 7.....	48
2.2.	Ethics and approvals.....	48
2.3.	MRI Scanner Hardware.....	49
2.4.	Common CMR protocols.....	49
2.4.1.	Survey images	49
2.4.2.	Localisers.....	50
2.4.3.	The CE-MARC CMR protocol	50
2.4.4.	Cine imaging	51
2.5.	Common CMR analysis.....	52
2.5.1.	Assessment of LV function.....	52
2.5.2.	Tagging	53
2.5.3.	Late Gadolinium Enhancement quantification.....	54
2.6.	X-ray coronary angiography	55
2.7.	Statistical Analysis	56
3.	A comparison of Cardiovascular Magnetic Resonance and Single Photon Emission Computed Tomography Perfusion Imaging in Left Main Stem or Equivalent Coronary Artery Disease.....	57
3.1.	Background.....	57
3.2.	Methods	58
3.2.1.	Subjects	58
3.2.2.	CMR protocol	58
3.2.3.	MPS-SPECT protocol	59
3.2.4.	X-ray Angiography	59
3.2.5.	CMR Analysis.....	59

3.2.6.	X-ray Angiography Analysis	61
3.2.7.	MPS-SPECT Analysis	62
3.2.8.	Data analysis and Statistics	62
3.3.	Results	63
3.3.1.	Visual analysis	63
3.3.2.	Quantitative CMR perfusion analysis	66
3.4.	Discussion.....	69
3.4.1.	Limitations.....	72
3.4.2.	Conclusion	73
4.	Quantitative deformation analysis differentiates ischaemic and non-ischaemic cardiomyopathy: sub-group analysis of the VINDICATE trial	74
4.1.	Background.....	74
4.1.	Methods	75
4.1.1.	Study participants.....	75
4.1.2.	Cardiac Magnetic Resonance Protocol	76
4.1.3.	Image Analysis.....	77
4.2.	Statistical Analysis	77
4.3.	Results	79
4.4.	Discussion.....	86
4.4.1.	Limitations.....	89
4.5.	Conclusion	90
5.	Development and validation of a contemporary pre-test likelihood model of coronary artery disease referenced to invasive angiography, with comparison to pre-existing risk models.....	91
5.1.	Introduction	91
5.2.	Methods	93
5.2.1.	Patients	93
5.2.2.	Classification of Chest Pain and Risk Factors.....	95
5.2.3.	X-ray Angiography	95
5.2.4.	Model Development	96
5.2.5.	Validation	98
5.3.	Results	99
5.3.1.	Development and internal validation	99
5.3.1.	External Validation	104

5.3.2.	Validation of other coronary artery disease risk models	104
5.4.	Discussion.....	108
5.4.1.	Strengths of our study	109
5.4.2.	Clinical implications.....	109
5.4.3.	Limitations.....	111
5.4.4.	Conclusions.....	111
6.	Feasibility Study of a Single Breath-hold, 3D mDIXON Pulse Sequence for Late Gadolinium Enhancement Imaging of Ischemic Scar	113
6.1.	Introduction	113
6.2.	Material and Methods.....	116
6.2.1.	Study population	116
6.2.2.	CMR data acquisition.....	116
6.2.3.	CMR data analysis.....	117
6.2.4.	Qualitative LGE assessment.....	118
6.2.5.	Quantitative LGE assessment.....	118
6.2.6.	CNR measurements.....	119
6.2.7.	Statistical analysis.....	119
6.3.	Results	120
6.3.1.	Demographics.....	120
6.3.2.	Image quality.....	120
6.3.3.	CNR	122
6.3.4.	Quantitative LGE Analysis	122
6.3.5.	Segmental and transmural assessment	125
6.3.6.	Image acquisition time	125
6.4.	Discussion.....	126
6.4.1.	Limitations.....	130
6.4.2.	Conclusion	131
7.	Clinical Evaluation of two dark blood methods for late gadolinium enhancement imaging and quantification of ischaemic scar	132
7.1.	Introduction	132
7.2.	Methods	134
7.2.1.	Study population	134
7.3.	CMR data acquisition	134
7.3.1.	CMR data analysis.....	136

7.3.2.	Image analysis	136
7.3.3.	Statistical analysis.....	138
7.4.	Results.....	138
7.4.1.	Study population	138
7.4.2.	MR imaging.....	138
7.4.3.	Qualitative image analysis	138
7.4.4.	Quantitative image analysis	142
7.5.	Discussion.....	143
7.5.1.	Limitations.....	145
7.5.2.	Conclusion	146
8.	Discussion.....	147
8.1.	Discussion, study limitations and future direction relating to Chapter 3	148
8.2.	Discussion, study limitations and future direction relating to Chapter 4	150
8.3.	Discussion, study limitations and future direction relating to Chapter 5	151
8.4.	Discussion, study limitations and future direction relating to Chapter 6	153
8.5.	Discussion, study limitations and future direction relating to Chapter 7	155
8.6.	Overall future directions	156
8.6.1.	Studies showing outcomes in ischaemic heart disease.....	157
8.7.	Conclusions.....	158
9.	References.....	159
10.	Appendix.....	206
10.1.	Ethical approval, Patient information sheets and consent form for Chapters 3 and 5	206
10.2.	Ethical approval, Patient information and consent forms for Chapter 4	230
10.3.	Ethical approval, Patient information and consent forms for Chapters 6 and 7.....	240

List of figures

Figure 1-1 Image panel showing CT FFR	11
Figure 1-2 Image panel showing MPS-SPECT and corresponding angiogram.....	14
Figure 1-3 Image panel showing contrast enhanced stress echocardiography and corresponding coronary angiogram	16
Figure 1-4 CMR Imaging techniques	19
Figure 1-5 CMR multi-parametric scanning protocols for the investigation of suspected coronary artery disease.....	20
Figure 1-6 Image panel showing CMR perfusion techniques.....	25
Figure 1-7 Image panel showing early and late gadolinium enhancement.....	34
Figure 2-1 Image panel showing CE-MARC scanning protocol	51
Figure 2-2 Image panel showing an example image of an LV slice using the semi-automated full width half maximum LGE quantification method on Circle CVI	55
Figure 3-1 Image panel showing angiography and CMR perfusion of patient with LMS disease.	60
Figure 3-2 ROC curves for visual summed stress scores for CMR and MPS-SPECT.....	66
Figure 3-3 ROC curves for CMR quantitative perfusion results.....	67
Figure 3-4 ROC curves for quantitative summed stress score for MBF, visual CMR and MPS-SPECT.....	69
Figure 4-1 Tagged images in inTag© analysis.....	78
Figure 4-2 Plots showing apical and basal rotation and twist of individual patients with ischaemic and non-ischaemic cardiomyopathy respectively.....	85
Figure 4-3 Schematic image of LV torsion in normal, ischaemic and non-ischaemic cardiomyopathy:.....	87
Figure 5-1 Image panel showing angiography and CMR perfusion.....	93
Figure 5-2 Image panel showing angiography and CMR perfusion.....	94
Figure 5-3 predictors used in developing the risk model	97
Figure 5-4 Calibration plots showing relation between predicted PTL and observed rates of CAD in the validation population	102

Figure 5-5 Calibration plots showing the relation between predicted pre-test-likelihood of CAD and observed rates of CAD by decile in the development population for the Diamond and Forrester model, the Duke Risk Score, CAD Consortium Basic risk score and CAD Consortium Clinical risk score.....	107
Figure 6-1 Short axis LGE images from basal, mid-ventricular and apical slices from 2D PSIR acquisitions, and basal, mid-ventricular and apical slices from 3D mDIXON acquisitions of the same patient showing antero-lateral scar following a left anterior descending artery territory infarction	121
Figure 6-2 Bland-Altman analysis of 3D and 2D LGE acquisitions for assessment of (A) absolute scar tissue mass and (B) scar tissue as a percentage of LV myocardial mass.....	123
Figure 6-3 Laminated thrombus in a chronic myocardial infarction in an apical slice of a 2D PSIR acquisition and 3D mDIXON acquisition of the same patient.....	124
Figure 7-1 shows the T1 rho preparation for the FIDDLE (T1ρ) pulse sequence	136
Figure 7-2 Patient 1 shows a small sub-endocardial anterior infarct imaged with each of the pulse sequences.....	140
Figure 7-3 2 patients with acute infarctions with each of the pulse sequences.....	141
Figure 7-4 2 patients with chronic infarction imaged with each of the pulse sequences	142
Figure 7-5 CNR for the respective LGE sequences.....	143

List of Tables

Table 1-1	Canadian Cardiovascular Society grading of angina pectoris	3
Table 1-2	Classification of Myocardial Infarction	5
Table 1-3	Typicality of chest pain for angina	8
Table 1-4	Pre-test likelihood of coronary artery disease based on typicality of symptoms, age, gender, and risk factors	9
Table 1-1	ESC and ACCF/AHA Recommendations for CMR in stable CAD	22
Table 3-1	Baseline Demographics	63
Table 3-2	Imaging findings	64
Table 3-3	Quantitative CMR perfusion analysis	67
Table 3-4	Sensitivity, specificity and predictive values for detection of IHD in LMS patients by visual CMR analysis, MPS-SPECT and quantitative CMR.....	68
Table 4-1	Demographic details for HF and healthy control group	80
Table 4-2	CMR data for HF group and controls	81
Table 4-3	Baseline demographic data for ischaemic and non-ischaemic cardiomyopathy patients	82
Table 4-4	CMR characteristics for ischaemic and non-ischaemic cardiomyopathy patients	84
Table 5-1	Characteristics of risk models used.....	92
Table 5-2	Demographic and clinical characteristics of participants in the development and validation populations	100
Table 5-3	Developed CE-MARC model.....	103
Table 5-4	Model performance statistics	105
Table 6-1	Reasons for impaired subjective image quality ratings (for any rating other than excellent)	122

List of equations

Equation 1	LV ejection fraction.....	53
Equation 2	Calculation of Torsion	54

1. General Introduction

1.1. Background

Coronary artery disease (CAD) is a leading cause of death and disability worldwide (1), and remains the leading cause of death in Europe and the UK (2). Despite major advances in the treatment of CAD resulting in significantly decreased mortality rates, CAD remains the single most common cause of death in the European Union, leading to 19% of deaths in men and 20% of deaths in women (2); in the United States, CAD causes 1 in every 7 deaths, accounting for 370,213 deaths in 2013 (3). The mortality rate for CAD remains higher in the UK and particularly Scotland compared to Europe and it is currently estimated that in the UK there are 2.3million people living with ischaemic heart disease (IHD) (2, 4). The economic health burden of CAD is substantial with an estimated cost of CAD management at €60 billion in the European Union (5), and \$182 billion in the US (3). Admissions with chest pain account for a significant proportion of admissions to the acute medical take and whilst it is important to remain vigilant for acute coronary syndromes a reasonable proportion of these admissions will represent stable coronary disease/angina (6, 7).

1.2. Coronary artery disease

1.2.1. Stable versus unstable coronary disease

Coronary artery disease presents in several manners – typically these are divided into stable or unstable CAD. The main symptomatic presentations of stable CAD are classical angina caused by an epicardial coronary stenosis, ischaemic cardiomyopathy and less frequently vaso-spastic angina or angina caused by microvascular obstruction/dysfunction (8). Unstable CAD encompasses the acute coronary syndromes (ACS) typically caused by

rupture of an atherosclerotic plaque with consequent thrombosis and consequent myocardial necrosis.

1.2.2. Epidemiology of CAD

Angina prevalence increases as age increases in both men and women with an incidence of about 4% in men and women aged 75-84 years. Myocardial infarction is one of the leading causes of mortality worldwide (1). Myocardial infarction (MI) is defined as 'myocardial cell death due to prolonged ischaemia' (9). In the UK, over 915,000 people are estimated to have previously had an MI and coronary artery disease was responsible for 73,500 deaths in 2012, representing 16% of all male and 12% of all female deaths (4). National health service (NHS) spending on treating coronary artery disease is estimated at £6.8 billion pounds each year, representing a significant proportion of the total spending budget (4).

1.2.3. Presentation of stable coronary artery disease

Stable CAD encompasses a variety of different presentations i.) stable angina pectoris due to stenotic CAD, ii.) patients with CAD who are asymptomatic, iii.) patients with left ventricular (LV) dysfunction from prior myocardial infarction, iv.) ischaemic cardiomyopathy (8).

Stable angina pectoris was first described by William Heberden in 1768 to the Royal College of Physicians:

"They who are afflicted with it, are seized while they are walking, (more especially if it be up hill, and soon after eating) with a painful and most disagreeable sensation in the breast, which seems as if it would extinguish life, if it were to increase or to continue; but the moment they stand still, all this uneasiness vanishes."

Stable angina is typically exercise related and caused by a mismatch between supply and demand of coronary bloodflow to myocardium (ischaemia) due to an epicardial coronary stenosis. Typical symptoms of angina are retrosternal chest pain, radiating to the neck, jaw and arm brought

on by exertion and relieved by rest or nitroglycerine. The degree of symptoms however does not necessarily reflect the underlying extent of CAD and patients may be asymptomatic despite a large burden of ischaemia. Severity of symptoms have been quantified by the Canadian Cardiovascular society (CCS).

Table 1-1 Canadian Cardiovascular Society grading of angina pectoris

Grade	Description
Grade I	Ordinary physical activity does not cause angina, such as walking and climbing stairs. Angina with strenuous or rapid or prolonged exertion at work or recreation
Grade II	Slight limitation of ordinary activity. Walking or climbing stairs rapidly, walking uphill, walking or stair climbing after meals, or in cold, or in wind, or under emotional stress, or only during the few hours after awakening. Walking more than two blocks on the level and climbing more than one flight of ordinary stairs at a normal pace and in normal conditions
Grade III	Marked limitation of ordinary physical activity. Walking one or two blocks on the level and climbing one flight of stairs in normal conditions and at normal pace
Grade IV	Inability to carry on any physical activity without discomfort, anginal syndrome may be present at rest

Ischaemic cardiomyopathy is the end-stage manifestation of stable coronary artery disease. Heart failure attributed to IHD is independently associated with an increased mortality over non-ischaemic cardiomyopathy. A variety of pathophysiological processes can result in ischaemic cardiomyopathy, myocardial hibernation, scarring and mechanical and neuro-humoral factors

(10). Hibernating myocardium is the concept of downregulation of myocardium following chronic ischaemia and is a retrospective diagnosis following functional recovery once revascularisation has occurred (11). Revascularisation of hibernating myocardium is the basis of viability assessment. The role of revascularisation in ischaemic cardiomyopathy remains a subject of debate currently with the results of the STICH study showing no benefit contrary to the results of a number of large observational studies showing benefit (12, 13).

1.2.4. Presentation of Acute Coronary syndromes

The typical features of an ACS are severe retrosternal chest pain radiating to the arm and jaw, with associated diaphoresis, nausea and dyspnoea. ACS does not always present in this manner with some patients (e.g. diabetics) either asymptomatic or may have vague symptoms; frequently in these instances MI is unrecognised at the time of its occurrence (14).

1.2.5. Pathophysiology of CAD

CAD is a chronic progressive disease that develops in adult life through a process of lipoprotein dysregulation and immune cell/inflammatory mediated events that occur within the coronary vasculature (15). Atherosclerosis begins with a long quiescent phase that initially develops from fatty streaks that are typically present from the teenage years onwards. Progressively these fatty streaks develop into mature atherosclerotic plaques that comprise a fibrous cap overlying a central core of lipid (16). A wide variety of different pathologically and structurally distinct subtypes of lesions can occur that give rise to varying degrees of vulnerability to manifest in a clinical event (16, 17).

In stable CAD as the plaque grows the coronary artery will remodel outward in order to retain lumen patency and can remain undetected on angiography or stress testing. Ultimately however the plaque will encroach on the vessel lumen leading to obstruction of blood flow leading to ischaemia. In unstable CAD, coronary events occur as consequence of plaque rupture with a

resultant thrombotic event. Acute coronary syndromes are typically caused triggered by acute fibrous cap rupture, which exposes the thrombogenic, tissue factor-rich lipid core to circulating blood (18), although in about 30% of cases of infarction, plaque erosion of the endothelium overlying the fibrous cap can lead to the formation of a platelet-rich thrombus (19). “Vulnerable” plaques tend to have common characteristics that make them distinct from plaques that cause stable angina such as a thin fibrous cap, positive remodeling, a large necrotic core, inflammation, microcalcification, angiogenesis, and plaque hemorrhage (16, 18).

Following the onset of ischaemia myocardial necrosis can occur within 20 minutes, with complete cell death occurring after between 2 and 4 hours (9). A ‘wavefront phenomenon’ of cell death is seen with the distal sub-endocardial myocytes affected first followed by the more proximal epicardial myocytes that are adjacent to the coronary arteries (20). Reduction to the blood supply of the myocardium resulting in myocardial infarction can be caused by various mechanisms that are summarised in the table 1-2:

Table 1-2 Classification of Myocardial Infarction

(adapted from Thygesen et al. The Fourth Universal Definition of Myocardial Infarction. EHJ 2018. 33 (20); 2551-67)(21)

MI Classification	Description
Type 1	Spontaneous plaque rupture or dissection within an epicardial coronary artery.
Type 2	MI secondary to ‘ischaemic imbalance’ – myocardial oxygen supply is temporarily outstripped by demand as a result of brady- or tachycardia, hypotension, respiratory failure etc.
Type 3	Myocardial infarction resulting in death
Types 4a/4b/5	Myocardial infarction resulting from PCI (4a) or thrombosis of existing coronary stent (4b) or restenosis associated with PCI (4c) or coronary artery bypass grafting (5)

Myocardial infarction, causes a complex pattern of ventricular remodelling. Infarcted myocardium is replaced by fibrotic scar, whilst the remote healthy myocardium compensates for the reduced contribution of the infarcted regions to maintain cardiac output (22). This process typically takes around 6 weeks according to autopsy studies (23). Cardiovascular magnetic resonance (CMR) imaging identifies that the infarcted LV mass is reduced by around 40% at 4 months compared with at the time of infarction, with minimal further change at 12 months, suggesting remodelling is largely complete by 4 months (24). Following MI, LV dilatation can occur; this typically occurs with larger infarcts involving the left anterior descending (LAD) artery as opposed to right (RCA) or circumflex (LCx) coronary artery territories (25). LV chamber dilatation occurs due to thinning and expansion along the circumferential length of the scarred myocardium, combined with a concurrent compensatory circumferential hypertrophy of remote myocardium (26).

1.3. Cardiac Imaging

Cardiac imaging has a wide array of potential methods of investigation that are available to the cardiologist for the investigation of CAD. These range from invasive tests such as angiography to non-invasive imaging tests that give anatomical and/or functional information; however currently there is no one perfect test and all have potential benefits and limitations. The focus of this thesis is stable CAD and the role of these imaging modalities are discussed in this context.

1.3.1. Assessment of coronary artery disease

Invasive coronary X-ray angiography has long been recognised as the reference standard for the investigation of coronary artery disease (8, 27). Invasive coronary X-ray angiography gives anatomical information and identifies coronary stenoses in patients presenting with chest pain, as well as allowing invasive pressure measurements. Angiography however does not give information on the burden of ischaemia (% of the myocardium that is

ischaemic) although invasive pressure wire assessment can be used to give lesion specific ischaemia if used (28). X-ray angiography is an invasive investigation, and confers both morbidity in terms of radiation burden and potential vascular complications and a very low but potential 1/1000 risk of mortality. Furthermore there is a low yield of obstructive CAD, around 60% of those referred for elective invasive angiography have no significant disease (29). Non-invasive imaging modalities such as myocardial perfusion scintigraphy by single-photon emission computed tomography (MPS-SPECT), stress echocardiography (SE), CMR, CT coronary angiography (CTCA) or positron emission tomography (PET) aim to diagnose CAD, as well as quantify ventricular function, ischaemic burden, assess viability and confer prognostic information and are therefore identified for these roles in current clinical practice guidelines (8, 30).

1.3.2. Risk stratification in stable CAD

In the UK, rapid access chest pain clinics (RACPC) in accordance with the National Service Framework for CAD previously utilised clinical history and examination followed by an exercise tolerance test (ETT) to risk stratify patients presenting with chest pain, followed by MPS-SPECT or invasive coronary angiography if warranted. ETT however has a limited diagnostic ability estimated at sensitivity of 45-50% (31, 32) and consequently has been removed from current guidelines (8, 30). Given the wide variety of non-invasive imaging modalities available, National institute of health and clinical excellence NICE 2010 CG95 guidelines proposed the use of pre-test likelihood” (PTL) of underlying CAD to choose between different investigations (table 1-4). The PTL estimation is based on typicality of symptoms and co-existent risk factors to give a percentage risk. ‘Typical’ symptoms of angina pectoris include retrosternal chest pain, radiating to the neck or arm that occurs during exercise and is relieved with rest or GTN (table 1-3)(30, 33). Those with a low to intermediate risk should undergo a “rule out test” i.e. CTCA; the intermediate risk patients should have a functional test (CMR, MPS-SPECT, DSE); with invasive angiography reserved for those with a high PTL. Notably for those patients in the very high risk PTL of CAD, NICE

guidelines suggested performing no investigation and to treat as angina; however this may potentially be denying this group assessment of their “ischaemia burden”, a discriminator that is known to confer prognostic information (34). The recently published CE-MARC 2 trial identified that the 2010 NICE guidelines led to higher rates of unnecessary angiography compared to functional imaging guided care; a strategy that potentially increases patient morbidity and healthcare costs (35). The mechanism is likely a result of overestimation of risk of CAD by the PTL model used in the 2010 CG95 guideline; notably the more recent European Society of Cardiology (ESC) guidelines have used an updated PTL model to risk stratify patients (8, 30). Subsequently, the NICE CG95 guideline has been updated in 2016 and PTL estimation is no longer recommended (36). This is in contrast to US and European practice guidelines that still recommend PTL estimation prior to investigation. The 2016 update to CG95 now recommends referral for CTCA in all patients with typical or atypical chest pain (table 1-3) and in those with non-anginal pain but with ECG changes, with functional imaging reserved for those who have previously documented coronary disease or revascularisation (36). Direct referral to angiography is no longer recommended in current guidelines thus a thorough understanding of the contemporary non-invasive imaging modalities is paramount.

Table 1-3 Typicality of chest pain for angina (30)

<i>Typical</i> angina (definite)	Meets all three of the following: <ul style="list-style-type: none">• Substernal chest discomfort of characteristic quality and duration• Provoked by exertion or emotional stress• Relieved by rest and/or nitrates within minutes
<i>Atypical</i> angina (probable)	Meets two of the above characteristics
<i>Non-cardiac</i> chest pain	Meets one or none of the above characteristics

Table 1-4 Pre-test likelihood of coronary artery disease based on typicality of symptoms, age, gender, and risk factors (30)

Age (years)	Non-anginal chest pain				Atypical angina				Typical angina			
	Men		Women		Men		Women		Men		Women	
	Low	High	Low	High	Low	High	Low	High	Low	High	Low	High
35	3	35	1	19	8	59	2	39	30	88	10	78
45	9	47	2	22	21	70	5	43	51	92	20	79
55	23	59	4	25	45	79	10	47	80	95	38	82
65	49	69	9	29	71	86	20	51	93	97	56	84

Values represent percentage likelihood at mid-decade age of significant CAD.

Men over 70 with atypical or typical symptoms estimate PTL at >90%.

Women over 70, assume a risk of 61 to 90%, except women with high risk with typical symptoms risk of >90% is estimated.

High = high risk factors that are diabetes, smoking and hyperlipidaemia (total cholesterol > 6.47 mmol/l), resting ECG ST-T changes or Q waves.

Low = low risk when none of the above risk factors are present.

Non-anginal chest pain should not be investigated for stable angina routinely.

1.3.3. Computed tomography coronary angiography

Computed tomography (CT) can be used in the assessment of coronary artery calcium score (CAC) which uses an estimate of calcium burden within the heart to predict the presence or absence of CAD and CTCA which allows visualisation of the coronary arteries. CAC score is a quick and simple test acquired in a single breath hold, without the need for any contrast agent. It is used to estimate the degree of calcification within the coronary arteries with an excellent correlation to total coronary calcium burden in histological samples (37). A score of 0 is associated with low CV risk, whereas scores above 1 are associated with an incremental increase in CV risk (38). Coronary calcium scoring predicts future risk of coronary events (MI, death from coronary heart disease or resuscitated cardiac arrest) in asymptomatic patients, more accurately than clinical risk scoring alone (39). Coronary

calcium scores in symptomatic patients have been shown to correlate positively with the degree of luminal coronary artery obstruction (40). However, more recently, a large international, multi-centre trial demonstrated that a CAC score of 0 is insufficient to rule-out significant coronary artery disease (41). For this reason, CAC score is now nearly always combined with CTCA in the assessment of patients with chest pain at low to intermediate risk of chest pain.

CTCA allows visualisation of the lumen and wall of coronary arteries and image acquisition only takes minutes, with few contraindications. An intravenous cannula is required and allows the administration of the iodinated contrast agent required to produce images. Contraindications include allergy to iodinated contrast agent or poor renal clearance as contrast is nephrotoxic and significant cardiac arrhythmia. CTCA's key strength lies in its high negative predictive value, meaning it correctly classifies a high proportion of patients not to have significant CAD. Its ability to visualise the coronary arteries, which typically measure 3-4mm in diameter in adults, stems from its high spatial resolution (42) (the ability to discriminate between two adjacent high contrast objects). The level of spatial resolution (around 0.625mm with 64 slice scanners) of modern scanners allows detection of atherosclerotic plaque within coronary arteries and thereby a diagnosis of CAD to be made (43).

Meta-analyses comparing the diagnostic accuracy of 64 slice or more CTCA in detecting significant coronary artery stenosis have estimated the sensitivity to be between 98% and 99%, and the specificity to be between 64% and 89% (44–46). Specificity is limited mainly due to a phenomenon called 'blooming artefact' where, in the presence of a high calcium burden (typically a CAC score > 400), an exaggerated bright signal is seen which frequently leads to overestimate of the degree of luminal stenosis (47).

Limitations of CT include the potential nephrotoxic effects of the intravenous contrast used, exposure of the patient to ionising radiation and its very limited ability to assess heart structure and function beyond the coronary arteries. Recently however a novel method of CT fractional flow reserve (FFR) to measure flow dynamics has been described (48, 49). CT FFR uses computational flow dynamics in order to calculate "3 Vessel" FFR from

normally acquired CTCA images (49). Recent trials have suggested that as these models have progressively evolved, diagnostic accuracy has improved for CT FFR compared to invasive FFR (50, 51) and suggest that care guided by CT FFR is comparable to that guided by routine invasive FFR (52, 53). A recent meta-analysis however is more circumspect identifying that the accuracy of CT FFR varies markedly across the spectrum of disease, with diagnostic accuracy as low as 46.1%(95% CI:42.9%-49.3%) for vessels with an invasive FFR of 0.8-0.9 (54). With current methodology, the radiation exposure from CTCA is in the region of 3-4 millisievert or below (55). The typical radiation dose associated with CAC scoring is less than 1 millisievert (56).

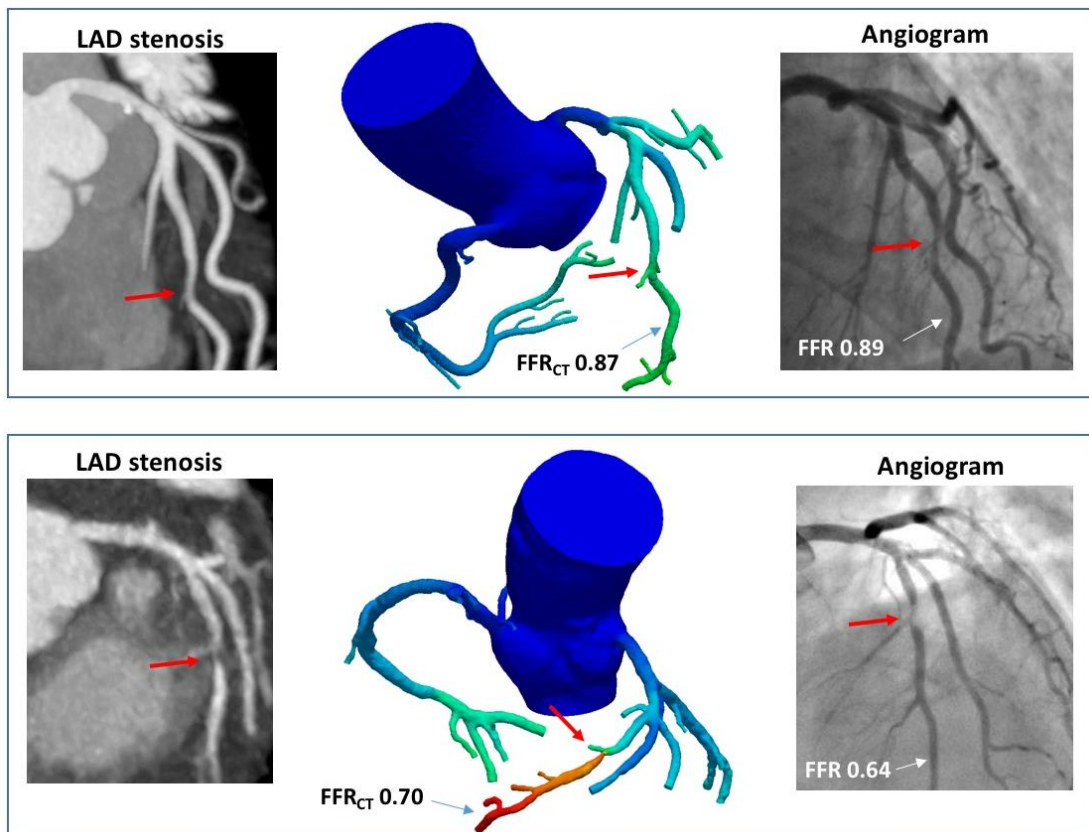


Figure 1-1 Image panel showing CT FFR

Figure with two case examples with left anterior descending coronary artery lesions, showing CTCA images on the left, corresponding CT FFR images and corresponding invasive coronary angiograms.

(Image courtesy of HeartFlow)

1.3.4. MPS-SPECT

MPS-SPECT is noninvasive nuclear imaging test that uses radioactive tracers in order to evaluate myocardial perfusion and systolic function in patients with suspected CAD. MPS-SPECT requires the administration of a radioactive perfusion tracer, which is usually administered intravenously, and a gamma camera system, utilizing single-photon emission computed tomography, for the detection of the gamma photons. MPS-SPECT is based upon the flow-dependent and metabolism-dependent selective uptake of the radioactive tracer by functional myocardial tissue. MPS-SPECT images are commonly taken at rest and following stress. Largely, two-day rest-first MPS-SPECT protocols are used. Some centres with expertise in nuclear imaging have moved on to the one-day stress-only imaging. Stress testing is performed using either exercise (treadmill or bicycle), pharmacologic agents (mainly vasodilators, but if contraindicated, dobutamine), or a combination of both vasodilator stress and low-level exercise. The vasodilator stressors most commonly used are adenosine and dipyridamole. More recently, many centres are progressively using regadenoson. Adenosine produces vasodilation of the coronary vasculature through activation of the adenosine A_{2A} receptor subtypes. Due to its nonselectivity, adenosine also has the ability to activate the remaining adenosine receptors (A₁, A_{2B}, and A₃), which limits its use in patients with pronounced bronchospastic airway disease, hypotension, or sick sinus syndrome (57). Regadenoson is a selective adenosine A_{2A} receptor agonist that was developed to reduce the adverse effects experienced with adenosine (58). The benefit of the rest-stress myocardial perfusion scan (MPS) protocol is that it also provides information on the presence or absence of myocardial infarction and viability. For example, if there is a fixed perfusion defect at rest and stress, it implies the presence of scar with no perfusion. Conversely, if there is perfusion defect at stress versus no defect at rest, it implies myocardial ischaemia in the given territory. Radiation dose from MPS-SPECT varies around 8-14mSv, depending on the sequence and hardware used (59, 60).

MPS-SPECT is a well-validated diagnostic tool for the detection of myocardial ischaemia. American and European guidelines recommend the use of MPS-SPECT for investigating patients with stable chest pain where the PTL is intermediate to high (8, 61). Additionally, it is a well-validated non-invasive technique with documented sensitivity as high as 90% for the detection of angiographically defined coronary disease (62), although more recent studies have suggested more modest values (63, 64). Large data derived from several large population studies demonstrate the prognostic power of MPS-SPECT. In a pooled analysis of 20,963 patients from 16 published studies with a follow up of slightly more than two years, the event rate of cardiac death and non-fatal MI was only 0.7% per year (65).

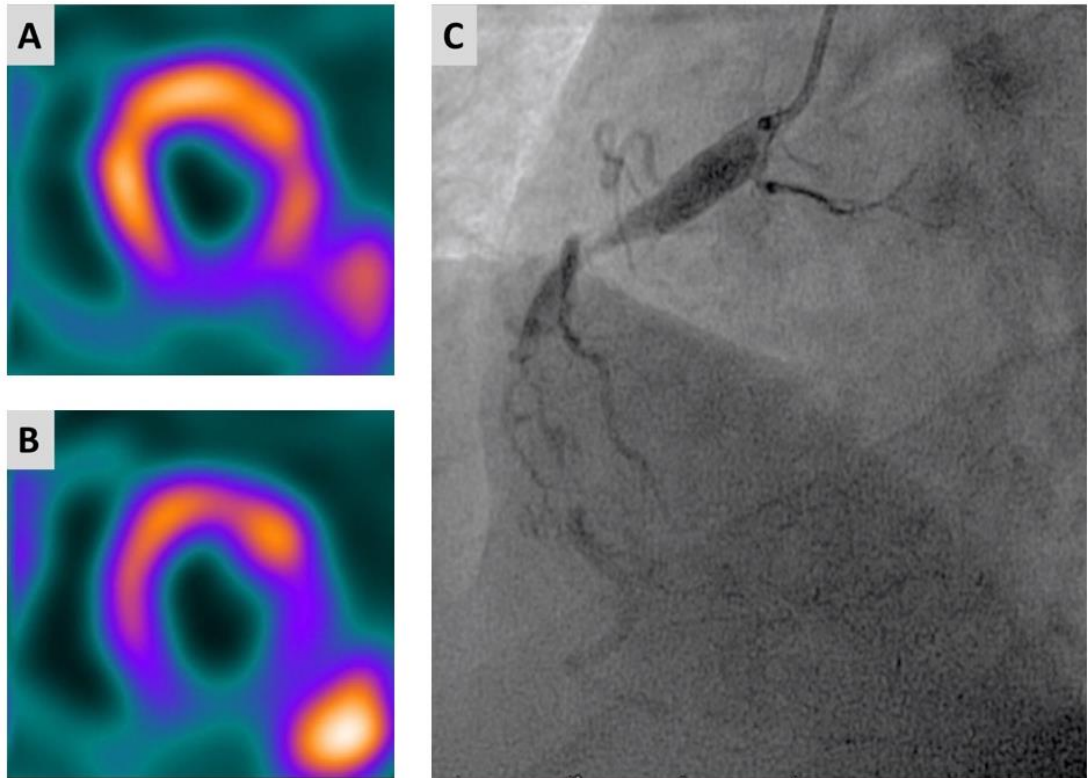


Figure 1-2 Image panel showing MPS-SPECT and corresponding angiogram

Image panel showing Single photon emission computed tomography myocardial perfusion scintigraphy in a 66-year old male patient who presented with typical cardiac chest pain. Image A is a resting short axis MPS-SPECT images demonstrating reducing perfusion to the mid inferior wall. This is suggestive of sub-endocardial scar with viability. Image B is a stress MPS-SPECT images demonstrating reduced perfusion in the infarct and peri-infarct zone. Image C is the corresponding chronic total occlusion of the proximal right coronary artery seen at elective diagnostic invasive coronary angiography.

1.3.5. Stress echocardiography

Stress echocardiography enables the detection of significant coronary artery disease through the use of transthoracic echocardiography to detect the characteristic changes in the contraction of the LV myocardium that occur with increasing myocardial oxygen demand. The test is simple, cost effective and

does not involve the use of ionising radiation. A full study takes around 30 minutes and requires continuous ECG monitoring and an intravenous cannula (66). In addition to ischaemia testing, it provides useful information regarding valvular and left ventricular function. Contraindications include severe aortic stenosis and severe uncontrolled hypertension. The diagnostic accuracy of stress echocardiography is dependent on the patient having good acoustic windows to allow visualisation of the LV endocardial borders. Where acoustic windows are poor, microbubble contrast agent may be used to improve endocardial definition and test accuracy (67). Incremental increases in myocardial oxygen demand are brought about through either increasing levels of physical exercise (e.g. exercise bike or treadmill) or pharmacologically (usually with increasing doses of intravenous dobutamine). These stimuli in turn bring about changes in the contraction of the LV myocardium with increasing levels of exercise or increasing concentrations of intravenous medication. Myocardial ischaemia is suggested when a region of LV myocardium contracts less well with exercise or pharmacological stress compared with rest. Prior myocardial infarction is indicated when a region of LV myocardium fails to contract at both rest and with either exercise or pharmacological stress.

Stress echocardiography has a good safety record, with a recorded incidence of life threatening complications of 1 in 6574 with exercise and 1 in 557 with dobutamine in a large international registry (68). For this reason and also due its similar diagnostic accuracy, exercise echocardiography is preferred to pharmacological stress whenever possible (66). Overall accuracy of stress echocardiography has been demonstrated by meta-analysis to be in the region of 81% in terms of sensitivity, and a specificity of 82% (69). A negative stress echocardiogram in a patient with chest pain and suspected coronary artery disease is associated with a low risk of cardiac death with one study demonstrating a risk of 0.6% per annum over a mean 7 year follow up period (70).

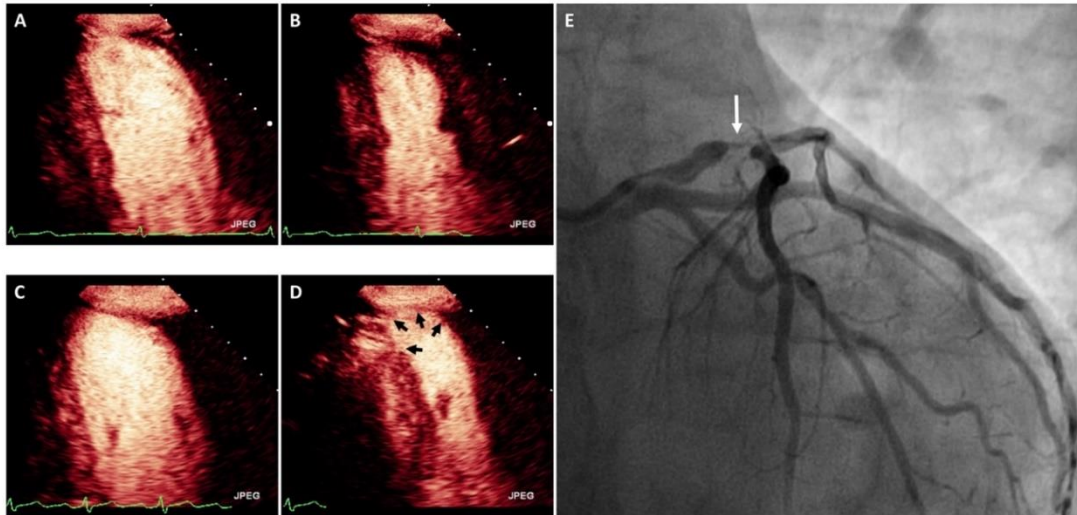


Figure 1-3 Image panel showing contrast enhanced stress echocardiography and corresponding coronary angiogram

Contrast enhanced stress echocardiography in a male patient who presented to chest pain clinic with stable angina symptoms. Panel A-B demonstrate resting end-diastolic (Panel A) and end-systolic (Panel B) frames of the two chamber view on contrast enhanced stress-echocardiography. Panel C-D demonstrate end-diastolic (Panel C) and end-systolic (Panel D) frames of the two chamber view at peak stress. In the peak stress end-systolic frame (Panel D), apical dyskinesia (black arrows) is seen with hyper-contraction of all other segments. Panel E identifies a severe stenosis of the left anterior descending artery (white arrow) at corresponding diagnostic invasive coronary angiography.

Image courtesy of Dr Ripley – published in Interventional Cardiology (third edition)

1.3.6. PET

Positron emission tomography (PET) is a highly sensitive imaging modality that measures metabolic activity of disease processes as they occur in the patient. PET imaging depends on a radioactive tracer targeted toward the pathological process being investigated. In cardiac metabolism ^{11}C -labelled fatty acids are used and ^{18}F -fluorodeoxyglucose that can be used in the context of assessing myocardial viability and inflammation (71, 72). The majority of

studies assessing the diagnostic accuracy of PET perfusion imaging for the detection of CAD, have been conducted with static uptake images of ^{82}Rb and $^{13}\text{NH}_3$ (73). ^{18}F -fluoride–PET/CT has recently been identified as a novel tracer that can identify high risk coronary artery plaques in coronary arteries (74, 75). PET imaging is somewhat limited by the anatomical information it provides and progressively is being combined as hybrid imaging with either MR or CT scanners in order to localise tracer activity to specific anatomical sites. Currently cardiac PET is predominantly a research tool, but hybrid PET/CT imaging is being progressively used in oncology and as scanner hardware becomes more widely available clinical adoption in cardiovascular medicine may become more widespread.

1.3.7. Coronary angiography

Coronary angiography is recognised as the invasive reference standard for the assessment of CAD. Cardiac catheterisation was first performed in 1929 by Werner Forsmann who inserted a catheter into his cubital vein and published an x-ray of his chest to prove it was in the right ventricle. Subsequently Mason Sones developed the technique of selective coronary angiography. Angiography enables visualisation of the coronary arteries, accurate pressure measurements and functional assessment of the heart chambers and major vessels. Angiography requires percutaneous access via a flexible sheath that is inserted in a peripheral vessel (previously predominantly the femoral artery though progressively more commonly the radial artery) that allows catheters to be passed to the heart. Catheters enable accurate pressure monitoring or under fluoroscopic guidance allow injection of radio-opaque contrast agent to opacify vessels, as well as providing access for interventional procedures.

The most common diagnostic use of angiography is for the direct visualisation of the anatomy of the coronary arteries. However, the 2D representation of the coronary anatomy is open to wide interobserver variability (76–78). Even the use of quantitative coronary angiography (QCA) is beset by diagnostic variability and thus “lumenology” as a purely anatomical investigation has

been somewhat superseded by invasive measurements by wire based pressure assessments (28, 79, 80). Both fractional flow reserve (FFR) or instantaneous wave-free ratio (iFR) require a pressure sensor mounted on a coronary wire to measure pressure before and distal to a coronary stenosis. FFR is defined as the ratio of the pressure distal to a stenosis relative to the pressure proximal to the stenosis measured during maximal hyperaemia induced by a vasodilating agent (typically adenosine). FFR has been shown in a number of trials in single and multivessel disease to reduce rates of major adverse cardiovascular events (MACE) for FFR guided care compared to visual angiography and optimal medical therapy in patients with stable CAD (28, 81, 82). In contrast iFR measures the ratio of the pressure of the distal coronary (beyond a stenosis) during the “wave free period” of diastole (removing the confounders of myocardial contraction) to the aortic pressure. Most notably iFR does not require the induction of hyperaemia. Recently 2 major trials have shown non-inferiority of iFR to FFR for the invasive assessment of stenoses of ambiguous haemodynamic significance in patients with stable CAD (79, 80). Furthermore, 2 trials have demonstrated superiority of FFR guided care of non-infarct related arteries in patients with ACS (83, 84). In addition to invasive coronary pressure assessments, two intracoronary imaging techniques are available to complement coronary catheterisation in the management of CAD; intravascular ultrasound (IVUS) and optical coherence tomography (OCT). IVUS and OCT enable visualisation of atherosclerotic plaque burden and composition, intracoronary structures and assist in stent implantation but have little role in ischaemia testing.

1.4. Cardiovascular Magnetic Resonance

CMR is a unique multi-parametric imaging modality producing high spatial resolution images that can be acquired in any plane for the assessment of global and regional cardiac function, myocardial perfusion and viability, tissue characterisation and proximal coronary artery anatomy, all within a single study and without exposure to ionising radiation (figure 1-4). Historically, long scanning times, limited scanner availability and narrow bore sizes restricted

the use of CMR, but these issues have been largely resolved, such that CMR has become a first line investigation for suspected stable angina in many centres in the UK and Europe. Consequently CMR is part of international clinical practice guidelines for the assessment of known and unknown stable CAD and for the identification of those who may benefit from revascularisation (8, 27, 85, 86).

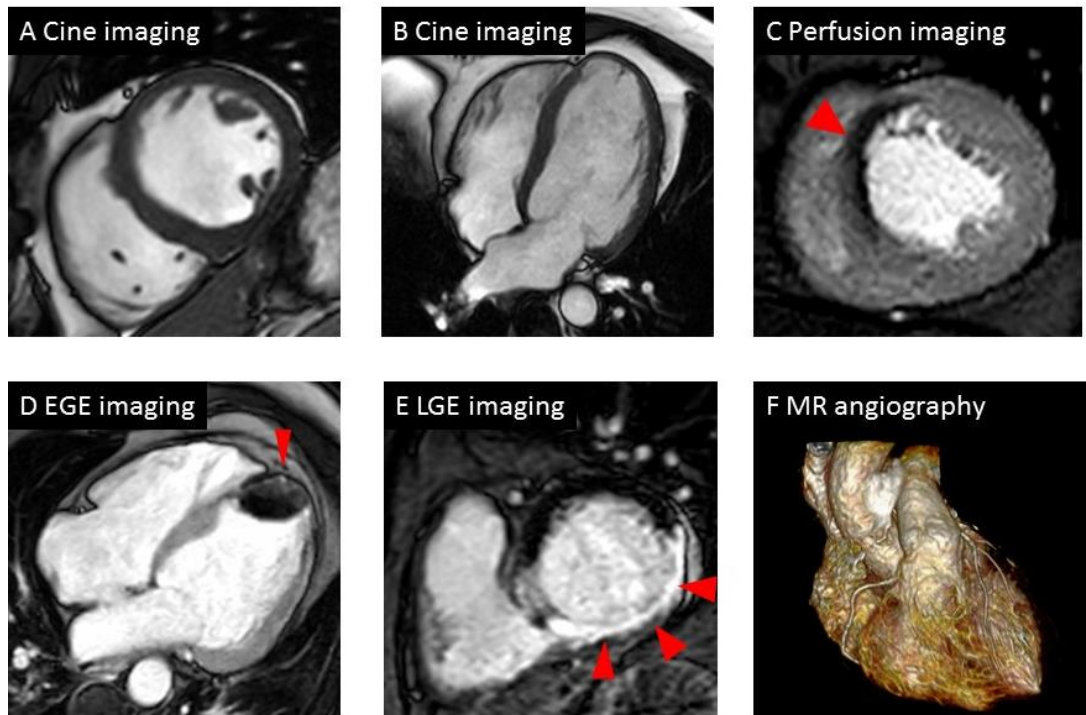


Figure 1-4 CMR Imaging techniques

Images A and B show short axis and 4 chamber cine images respectively for anatomical and functional assessment. Image C shows stress perfusion with a septal perfusion defect (arrow). Image D shows EGE imaging with a large apical thrombus (arrow). Image E is LGE imaging with a transmural inferior infarction (arrows). Image F is 3D whole heart MR angiography. (87)

1.4.1. CMR in stable CAD

A CMR protocol for the investigation of stable CAD will typically take between 30-60 minutes and involves the acquisition of cine images in multiple planes

for the assessment of left ventricular function and volumes, stress and rest myocardial perfusion imaging and late gadolinium enhancement (LGE) imaging for the assessment of myocardial viability and scar quantification (figure 1-5).

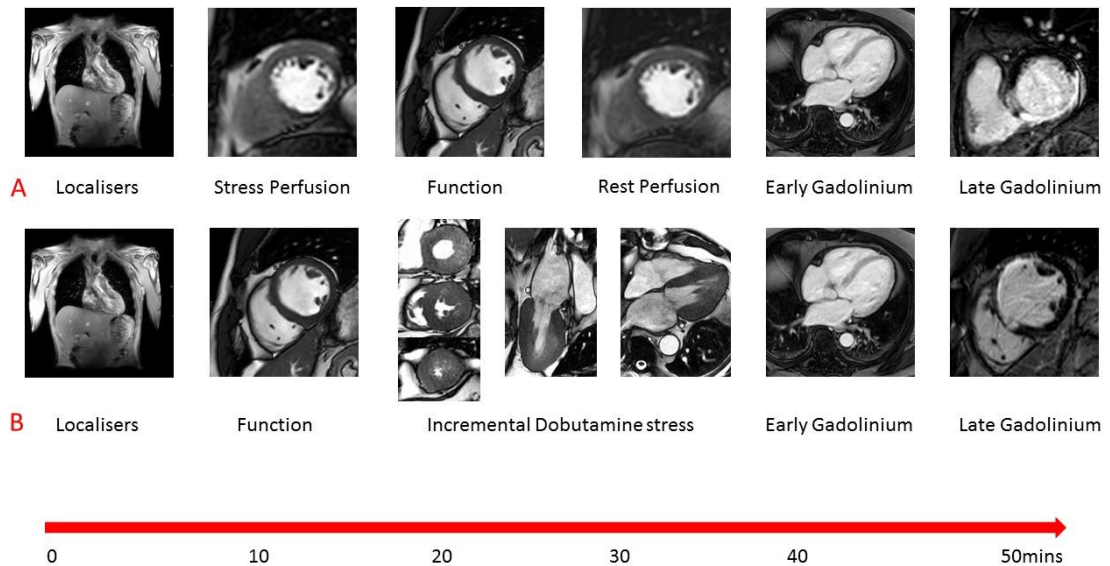


Figure 1-5 CMR multi-parametric scanning protocols for the investigation of suspected coronary artery disease

Panel A shows a typical multi-parametric CMR protocol for the investigation of stable coronary artery disease with adenosine stress perfusion, and B with incremental dose dobutamine stress. (87)

CMR is the reference standard non-invasive technique for the measurement of left ventricular (LV) and right ventricular (RV) volumes, and ejection fraction (EF), with high intra- and inter-observer reproducibility (88, 89). Steady State Free Precession (SSFP) cine imaging is typically performed for the assessment of LV function to enable visual assessment of global and regional myocardial function in a similar manner to echocardiography; however, there are no limitations due to poor acoustic windows or large body habitus degrading image quality. CMR volumetric analysis is performed by acquiring a stack of contiguous breath held cine images from the base of the heart to the apex; the endocardial and epicardial borders are subsequently contoured giving mass, volumes and function. Thus CMR provides a true 3D analysis of LV and RV function unlike 2D echocardiography that relies on geometric assumptions for volumetric calculations. Furthermore specific myocardial tagging pulse sequences can be performed that enable more detailed assessment of intra-myocardial mechanics beyond ejection fraction, including torsion, twist, strain and strain rates (90). Additionally, feature tracking is a novel post-processing method of quantitatively assessing strain and strain rate using standard cine images without having to acquire further imaging sequences as is the case with standard CMR tissue tagging (90, 91).

1.4.2. Diagnosis of CAD

Ischaemia detection by CMR is performed using either vasodilator or inotropic stress. Ischaemia detection by CMR is recommended as a first line strategy for investigating suspected angina in patients with an intermediate pre-test likelihood of CAD in both the current ESC and NICE guidelines (table 1.)(8, 30), whilst the US guidelines are more conservative and give a grade IIa recommendation for stress perfusion CMR in patients with uninterpretable ECGs or unable to exercise (27).

Table 1-5 ESC and ACCF/AHA Recommendations for CMR in stable CAD

ESC guidelines

Suspected/stable coronary artery disease(8)

In patients with suspected stable coronary artery disease and pretest probability of 15 % - 85 % stress imaging is preferred as the initial test option if local expertise and availability permit.	Class I
An imaging stress test is recommended in patients with resting ECG abnormalities, which prevent accurate interpretation of ECG changes during stress.	Class I
CMR should be considered in symptomatic patients with prior revascularisation (PCI or CABG).	Class IIa
Risk stratification is recommended based on clinical assessment and the results of the stress test initially employed for making a diagnosis of stable coronary artery disease.	Class I
CMR is recommended in the presence of recurrent or new symptoms once instability has been ruled out.	Class I
In symptomatic patients with revascularised stable coronary artery disease, CMR is indicated rather than stress ECG.	Class I
CMR is recommended for risk stratification in patients with known stable coronary artery disease and a deterioration in symptoms if the site and extent of ischemia would influence clinical decision making.	Class I
<i>Recommendations for imaging to determine ischemia to plan revascularisation(8, 92)</i>	
An imaging stress test should be considered to assess the functional severity of intermediate lesions on coronary arteriography.	Class IIa

To achieve a prognostic benefit by revascularisation in patients with coronary artery disease, ischemia has to be documented by non-invasive imaging.	Class I
Following MI with multivessel disease, or in whom revascularisation of other vessels is considered, CMR for ischaemia and viability is indicated before or after discharge.	Class I
<i>Heart Failure(85)</i>	
CMR should be considered in patients with HF thought to have CAD, and who are considered suitable for coronary revascularization, to determine whether there is reversible myocardial ischaemia and viable myocardium.	Class IIa
AHA guidelines	
<i>Diagnosis and management of stable coronary artery disease(27)</i>	
CMR can be used for patients with an intermediate (10-90%) to high (>90%) pretest probability of obstructive IHD who have an <i>uninterpretable</i> ECG and at least moderate physical functioning or no disabling comorbidity.	Class IIa
CMR is reasonable for patients with an intermediate to high pretest probability of IHD who are incapable of at least moderate physical functioning or have disabling comorbidity.	Class IIa
Pharmacological stress CMR is reasonable for risk assessment in patients with SIHD who are unable to exercise to an adequate workload regardless of interpretability of ECG.	Class IIa
CMR is reasonable in patients with known SIHD who have new or worsening symptoms (not unstable) and who are incapable of at least moderate physical functioning or have disabling comorbidity.	Class IIa

1.4.3. Stress Perfusion CMR

Stress perfusion CMR requires the induction of hyperaemia by a vasodilating agent, and then observation of the first-pass of a gadolinium based contrast agent (GBCA) through the myocardium to identify perfusion defects. Typically, the vasodilating agent used is adenosine though regadenason and less commonly dipyridamole and nicorandil are also used. Adenosine produces vasodilatation in most vascular beds, including the coronary circulation, via A_{2A} and A_{2B} receptors (57). Adenosine is given as an intravenous infusion typically at a rate of 140mcg/kg/min, though this can be increased if there is no haemodynamic response; the main side effects of adenosine are transient heart block, and bronchospasm can be caused in those with reversible airways disease(57). Regadenason is a new selective A_{2A} adenosine receptor agonist that is given via an intravenous bolus, has less respiratory side effects than adenosine, and has recently been approved by both the FDA and in Europe for this indication (93, 94). The coronary micro-vasculature can dilate up to 4 or 5 times from the resting state to ensure adequate tissue perfusion for example during exercise. However, the microvasculature distal to a stenosed coronary artery is already near-maximally vasodilated at rest and consequently when hyperaemia is provoked a coronary steal effect is caused. GBCAs increase the signal intensity in T1 weighted images and the first-pass of GBCAs through the myocardium causes healthy myocardium to become brighter while regions of hypoperfusion ('ischaemia') remain dark (figure 1-6).

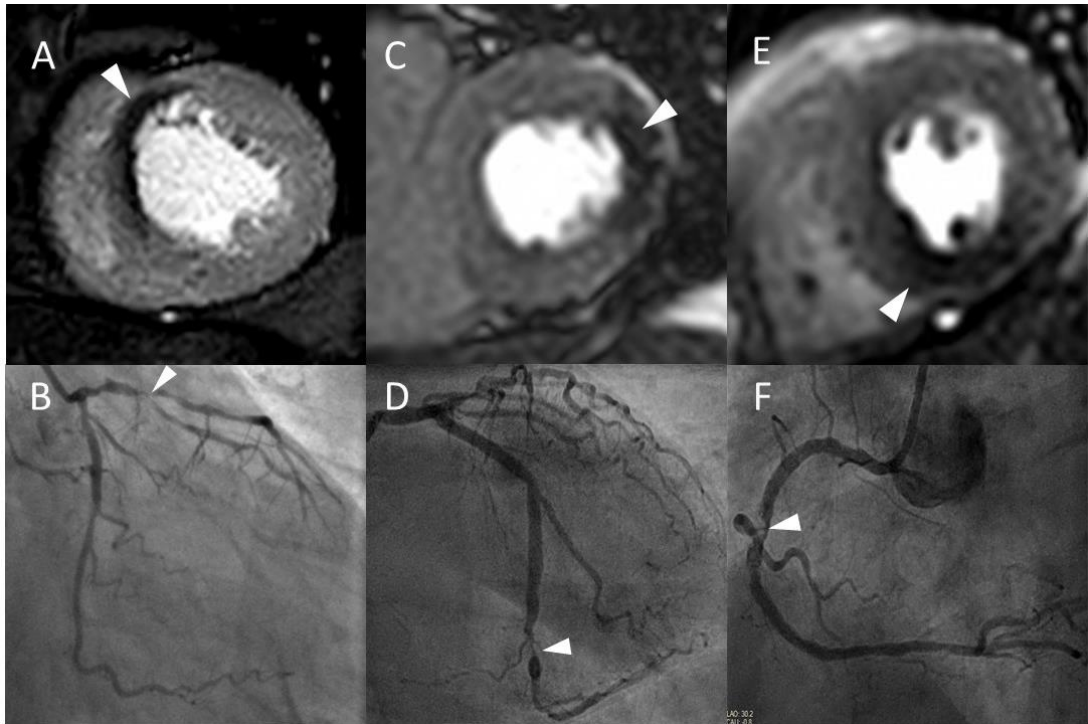


Figure 1-6 Image panel showing CMR perfusion techniques

Image A is a high spatial resolution *k-t* BLAST stress perfusion CMR study at 3.0T showing an antero-septal perfusion defect with corresponding left anterior descending lesion at angiography in image B. Image C shows a transmural lateral perfusion defect at standard resolution at 1.5T with corresponding circumflex lesion in image D. Image E shows a transmural inferior perfusion defect at standard resolution at 1.5T with corresponding right coronary artery lesion in image F. (87)

The diagnostic accuracy of stress perfusion CMR for the detection of CAD is well validated. A meta-analysis of 37 studies demonstrated a combined sensitivity of 89% (95%CI: 88%-91%) and specificity of 76% (95%CI: 73%-78%) for perfusion CMR for the diagnosis of CAD (95). The CE-MARC study (n=752), the largest prospective randomised single-centre trial of CMR in this context showed superiority of perfusion CMR over MPS-SPECT, with a higher sensitivity (87% vs. 67%, $p < 0.0001$) and negative predictive value (91% vs. 79%, $p < 0.0001$) but similar specificity (83% vs. 83% $p = 0.916$) and positive predictive values (77% vs. 71%, $p = 0.061$) (63, 96). Furthermore in a pre-specified gender sub analysis of CE-MARC, CMR showed similar sensitivity for CAD detection in both males and females, whilst MPS-SPECT had significantly lower sensitivity in females compared to males (97).

The multi-centre, multi-vendor MR-IMPACT II trial (n=515) also confirmed CMR's superior sensitivity compared to MPS-SPECT (67% vs. 59%, $p = 0.024$) but with a lower specificity (61% vs. 72%, $p = 0.038$) (98); however unlike CE-MARC only the stress/rest perfusion component of the CMR protocol was analysed. CE-MARC included analysis of LGE for scar detection, cine imaging for regional ventricular function and magnetic resonance angiography (MRA) for coronary artery anatomy, and a subsequent sub-analysis of CE-MARC demonstrated the additive diagnostic accuracy of the summation of these components of the multi-parametric protocol (99).

Stress perfusion CMR has also been validated against FFR in a recent meta-analysis with a pooled sensitivity and specificity of 0.90 (95% confidence interval [CI]: 0.86 to 0.93) and 0.87 (95% CI: 0.82 to 0.90) at the patient level and 0.89 (95% CI: 0.83 to 0.92) and 0.86 (95% CI: 0.77 to 0.92) at the coronary artery and territory levels (100). Furthermore CMR stress perfusion had comparable sensitivity and specificity to cardiac CT and PET in a recent meta-analysis of non-invasive imaging modalities, and was superior to both MPS-SPECT and DSE when using FFR as the reference standard (73). Most trials thus far have excluded patients with arrhythmia amid concerns regarding ECG

gating, however the diagnostic accuracy of stress perfusion CMR remains high in suspected CAD patients with AF or frequent ectopy (sensitivity 80%, specificity 74%) (101).

1.4.3.1. 1.5T versus 3T field strength

Although 1.5T is remains the standard field strength used in clinical CMR, imaging at a higher field strength of 3.0T offers increased signal to noise (SNR) and contrast to noise ratios (CNR) thereby giving improved spatial and temporal resolution (102). Consequently, the diagnostic accuracy of perfusion imaging at 3.0T may be improved, and in a small direct comparison of CMR perfusion at 1.5T, 3.0T (n=61) showed greater diagnostic accuracy in both single vessel (AUC: 0.89 vs. 0.70; $p < 0.05$) and multi-vessel disease (AUC: 0.95 vs. 0.82 $p < 0.05$) (103). Furthermore, 3.0T has been compared to 1.5T using FFR as reference standard, corroborating it's superior diagnostic accuracy (104, 105). The higher 3.0T field strength does however pose challenges with greater field inhomogeneity, susceptibility artefacts and higher local energy deposition. Also, many implants deemed "MR compatible" at 1.5T cannot be scanned at 3.0T (106). These issues are however being overcome with improved technology and the use of multi-transmit radiofrequency CMR techniques improving field homogeneity (107).

1.4.3.2. Improving perfusion imaging

Currently typical CMR perfusion imaging acquires 3 short axis slices of the left ventricle with an in-plane spatial resolution of 2-3mm. Developments in CMR technology however now allow faster scan speeds; these novel acquisition techniques allow accelerated data acquisition based on spatio-temporal undersampling (*k-t* SENSE or *k-t* BLAST and highly constrained back projection HYPR, compressed sensing and others)(108). These faster data acquisition techniques have been applied to achieve in-plane spatial resolution < 2 mm or full-coverage of the LV using 3D whole-heart perfusion imaging. High spatial-resolution imaging offers benefits by significantly reducing dark rim artefacts, as these are directly proportional to voxel size (109). Moreover there

is improved ability to detect sub-endocardial ischaemia which is critical in multi-vessel disease where there is a lack of reference healthy myocardium for comparison (110, 111). High spatial-resolution perfusion CMR has been validated at both 1.5 T and 3.0T against QCA with improved diagnostic accuracy at both field strengths compared to standard resolution perfusion imaging (102, 111, 112). Furthermore, validation against FFR gave sensitivity and specificity to detect stenoses at a threshold of FFR <0.75 of 0.82 and 0.94 ($p < 0.0001$) respectively, and an area under the curve of 0.92 ($p < 0.0001$) (113).

Conventional stress perfusion CMR is typically acquired in 3 short -axis slices, and thus unlike MPS-SPECT does not truly calculate global ischaemia burden. Accelerated acquisition techniques can also be employed to achieve full LV coverage using a 3D whole-heart single shot acquisition. Such 3D acquisitions can overcome the assumptions made about 'missing' myocardium between the slices from conventional 2D multi-slice perfusion imaging. Two studies have validated the feasibility and diagnostic accuracy of 3D stress perfusion CMR against FFR; at 1.5T 3D perfusion demonstrated a sensitivity, specificity and diagnostic accuracy of 90%, 82% and 87% respectively and 91%, 90% and 91% respectively at 3.0T (114, 115). Furthermore, in a recent multicentre trial of 3D stress perfusion at 3.0T, sensitivity and specificity were 84.7% and 90.8% relative to the FFR reference (116). The main motivation for 3D perfusion is to give a more accurate quantification of total myocardial ischaemia burden; evidence from MPS-SPECT suggests a prognostic benefit for revascularisation in those with an ischaemia burden >10%, with an ischaemia burden of 10% conferring a risk of ~5% for death or MI per year (117, 118). Ischaemia burden as measured by 3D stress perfusion CMR has been compared to MPS-SPECT and showed good correlation ($r = 0.70$, $p < 0.001$) (119). Intriguingly a recent pilot study compared ischaemia burden by high-resolution perfusion (using 3 short axis slices) and 3D perfusion imaging (providing whole heart coverage) suggesting that there was also a good correlation between the techniques ($r = 0.72$; $p = 0.001$), and that therefore the two methods are potentially interchangeable (120).

1.4.3.3. Quantitative perfusion

CMR stress perfusion studies are normally reported in a qualitative manner; however this can prove challenging in diffuse or multi-vessel disease where there is no healthy reference myocardium to use as a visual comparator. These situations can introduce subjectivity into the analysis and consequently quantitative measurement techniques have been developed to provide an objective assessment of myocardial blood flow. A number of different methods of quantitative analysis have been assessed with the Fermi deconvolution method showing most accuracy when compared to microspheres in an explanted porcine model at 1.5T and mice at 3.0T (121, 122), and when compared to MPS-SPECT and with QCA (123). When compared to angiography with FFR, an MPR threshold of 1.58 detected a stenosis with an FFR <0.75 with a sensitivity of 0.80, specificity of 0.89 ($p < 0.0001$), and area under the curve of 0.89 ($p < 0.0001$) (113). Myocardial perfusion reserve derived from quantitative CMR perfusion has also shown good correlation to PET imaging, the imaging modality that is widely regarded as the reference standard non-invasive measure of myocardial blood flow (124, 125). Currently, time consuming post-processing has limited quantitative perfusion methods to a research tool, but automated methods are being developed that may potentially overcome this (126). To date however quantitative perfusion has not been shown to improve diagnostic accuracy over visual CMR analysis (127, 128).

Recently a dual sequence fully automated quantitative perfusion method was proposed (129). This fully automated CMR perfusion mapping method for quantification of myocardial perfusion was validated using $^{13}\text{N-NH}_3$ cardiac positron emission tomography as the reference method (130). Twenty-one patients underwent adenosine stress and rest perfusion imaging with $^{13}\text{N-NH}_3$ PET and a dual sequence, single contrast bolus CMR on the same day. Global and regional myocardial perfusion were quantified both at stress and rest using PET and CMR. The study demonstrated good correlation between global and segmental myocardial perfusion and myocardial perfusion reserve (130).

1.4.4. Dobutamine Stress CMR (DSMR)

GBCAs have an excellent safety profile (131), but in patients with poor renal clearance (e.g. on dialysis) there is a risk of nephrogenic systemic fibrosis (NSF)(132). In those patients unable to have GBCAs inotropic stress CMR is an alternative. Inotropic stress CMR is typically performed with dobutamine in a similar manner to DSE with inducible regional wall motion abnormalities (RWMA) identified in territories supplied by a stenosed coronary artery at peak stress. Unlike DSE however, DSMR's accuracy is not limited by body habitus or in those with poor acoustic windows and in a single centre study DSMR was shown to have significantly greater diagnostic performance to DSE in this context (133). However echocardiography in this study was performed without harmonic imaging and contrast agents, so that the performance of DSE is likely to be underreported compared with contemporaneous methods. DSMR has a comparable safety profile to DSE with an event rate of 0.1% for sustained VT and 0.4% for non-sustained VT, and 1.6% for atrial fibrillation; patients thus require close monitoring during scanning and resuscitation equipment needs to be available (134). DSMR has been shown to have high diagnostic accuracy for the detection of CAD with one meta-analysis of 14 trials showing a pooled sensitivity of 0.83 (95%CI: 0.79-0.88) and specificity of 0.86 (95%CI: 0.81-0.91)(135); furthermore a single centre trial of DSMR versus perfusion CMR showed similar diagnostic accuracy (136). First-pass perfusion can be performed additionally at peak dobutamine stress to provide incremental diagnostic accuracy (137), and can be a useful adjunct in challenging patient groups such as those with pre-existing wall motion abnormalities or dyssynchrony from left bundle branch block (138).

Exercise is commonly used rather than pharmacological agents as the stressor in echocardiography, and gives useful prognostic information such as workload in metabolic equivalent (METs) in addition to ischaemia testing (139, 140). CMR is limited in this respect due to the need for supine scanning and consistent positioning within the scanner. Recent studies however have

assessed the feasibility of exercise stress CMR and showed comparable accuracy to echocardiography, though it has yet to reach mainstream clinical use (141, 142). Promising developments are 'steppers' and cycle ergometers that can attach directly to the MRI scanner, and thereby eliminate the need to transfer the patient from the exercise equipment into the scanner (143, 144).

1.4.4.1. Prognosis from stress CMR

Both perfusion CMR and DSMR provide excellent prognostic information, and this has recently been shown in two large meta-analyses. One meta-analysis of 14 studies including 12,178 patients showed that a negative stress CMR was associated with a 1.03% annualised event rate, comparable to the normal population (145). A further meta-analysis of 19 studies including 11,636 patients showed a similar annualised event rate of 0.8% for a negative stress CMR over a mean follow up of 32 months (146). In a large prospective study of 1,229 patients undergoing adenosine stress with a mean follow-up period of 4.2 ± 2.1 years, patients with reversible perfusion deficits had a 3-fold increased risk of major adverse cardiovascular events, with significantly more cardiac deaths ($p < 0.0001$) and nonfatal myocardial infarctions ($p < 0.001$) (147). Similarly the data from DSMR mirrors the results of first-pass perfusion CMR with a negative study conferring an equally low annual event rate of 1.3% (145, 148). Recently the five-year outcome data from CE-MARC were published with prognostic data for both CMR and MPS-SPECT in the same patient population. The analysis showed that although an abnormal result from both tests was a strong indicator of future MACE, CMR was superior at predicting time to MACE in this population (149). Furthermore CMR remained the only independent predictor of outcome after adjustment for major cardiovascular risk factors, stratification for initial patient treatment and coronary angiographic findings (149). These findings likely reflect CMR's overall greater diagnostic accuracy, combined with CMR's higher spatial resolution enabling greater identification of subendocardial scar compared to MPS-SPECT (150); a feature known to confer prognostic significance beyond ejection fraction, and clinical or angiographic features (151).

1.4.5. Early and late gadolinium enhancement imaging

GBCAs have a large molecular weight and cannot penetrate an intact cell membrane; consequently GBCAs are constrained to the extracellular space. In healthy myocardium the extracellular space is limited and contrast enters and clears rapidly. The extracellular space in infarcted myocardium however is substantially increased compared to normal myocardium and is less vascular. Thus in chronic myocardial infarction scar tissue composed of a matrix of collagen fibres has significantly increased extracellular space, leading to GBCA accumulation (slow washout), whilst in acute infarction GBCAs passively diffuse across disrupted myocardial cell membranes and into the intracellular space (greater volume of distribution)(152). Thus both acute and chronic myocardial infarctions retain more GBCAs. Imaged with T1 sensitive acquisition methods, this results in a higher signal in infarcted tissue compared to normal reference myocardium.

Early gadolinium enhancement imaging is performed immediately following contrast administration; this allows mainly the visualisation of ventricular thrombi that appear 'dark/black' due to a lack of contrast uptake as they are non-vascular (figure 1-7). CMR has been shown to be superior to both trans-thoracic echocardiography (TTE) and trans-oesophageal echocardiography (TOE) for the identification of ventricular thrombi(153–155). LGE imaging is performed between 10-20mins after contrast administration, an appropriate inversion time (TI) is set to null the normal myocardium and the areas where gadolinium is retained enhances (figure 1-7). Typically a stack of short axis slices, a 4-chamber view and vertical long axis (VLA) are acquired. Alternatively, 3D LGE CMR imaging enables whole heart quantification of scar burden to be acquired in a shorter time period (although with a reduction in image quality), which may provide an alternative for patients that struggle to breath-hold (156, 157).

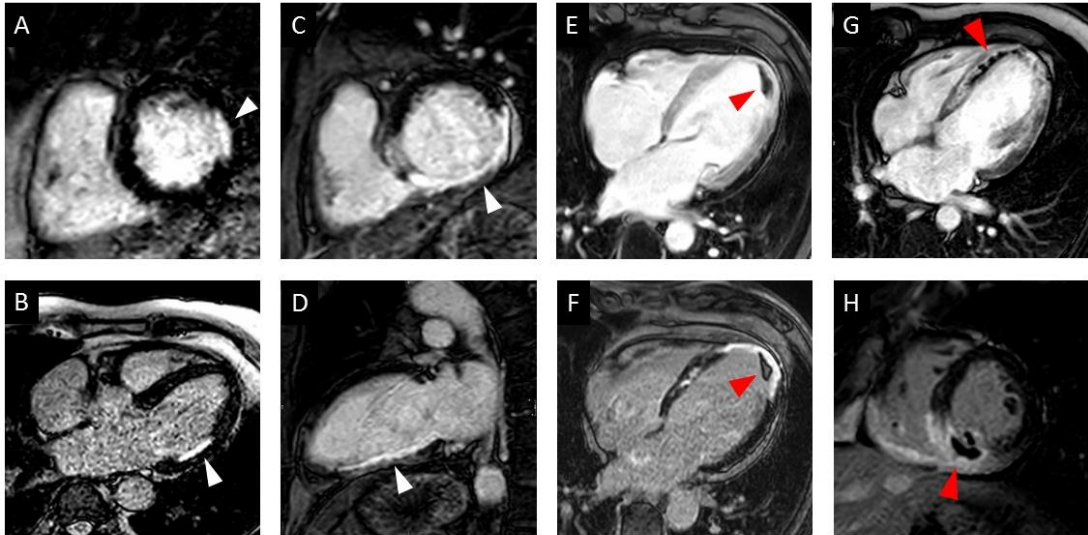


Figure 1-7 Image panel showing early and late gadolinium enhancement

Images A and B show a lateral sub-endocardial infarction on short axis and 4 chamber LGE respectively. Images C and D show a full thickness inferior infarction on LGE imaging on short axis and VLA respectively. Images E and F show EGE and LGE imaging respectively of a full thickness apical infarction with an apical thrombus appearing black (highlighted by red arrow). Images G shows an extensive acute antero-apical infarction with a core of microvascular obstruction visible within the hyperenhancement on EGE (red arrow). Image H shows an acute inferior wall infarction with MVO and extension into the right ventricle on LGE (red arrow) imaging. (87)

1.4.6. Viability assessment

CMR viability assessment using LGE enables the accurate detection, and extent and trans-murality of previous myocardial infarction to be determined, and identifies regions with potential to recover function following revascularisation. Hibernating myocardium is dysfunctional myocardium that has been down-regulated through a process of chronic/repetitive ischaemia and which has the potential for functional recovery when blood flow is restored. LGE imaging detects replacement of normal viable myocytes by focal necrosis or fibrosis with high spatial resolution, and has excellent correlation to histopathology (152). Furthermore the degree of transmural extent of hyper-enhancement on LGE imaging has a direct association to the potential for functional recovery following revascularisation; Kim et al demonstrated that segments with less than 25% hyper-enhancement were most likely to attain functional recovery whilst segments with over 75% hyper-enhancement were unlikely to improve, notably this was irrespective of whether the region was initially hypokinetic, dyskinetic or akinetic (158). A meta-analysis of 331 patients using 50% trans-murality of hyper-enhancement reported a sensitivity of 95% (95%CI: 93-97%) and specificity of 51% (40-62%) for predicting functional recovery (159).

CMR viability assessment is not however limited to just LGE imaging; whilst LGE identifies the transmural extent of scarring, the use of low-dose dobutamine (LDD) identifies the contractile reserve. Myocardium is considered viable if there is a 2mm or more increase in systolic wall thickening within a segment following administration of LDD (5-10mcg/kg/min)(160). While scar burden on LGE has been shown to be most sensitive method for assessment for functional recovery compared to LDD and diastolic wall thickness (161), LDD CMR offers higher specificity and PPV for prediction of functional recovery (91% and 93%, respectively)(159). Consequently a stepwise approach utilising LGE first followed by LDD if the trans-mural extent of LGE in the territory of the diseased coronary is between 1-50% has been proposed

(162). Recently both tissue tagging and feature tracking have been used to give quantitative viability assessment with LDD and have been suggested as possible methods to reduce reliance on operator experience in what is currently a qualitative method of assessment (163–165).

LGE imaging has a grade A recommendation to determine myocardial viability prior to revascularisation in the ACCF/AHA/SCMR appropriate use guidelines (166), though viability assessment by LGE is currently not recommended for this indication in ESC or US practice guidelines for management of stable CAD or coronary revascularisation (8, 27, 86, 167). The utility of viability assessment has been questioned recently following the results of the STICH trial and the subsequently published viability sub-study that showed no mortality benefit from revascularisation following viability assessment (12, 168). This is contrary to prior observational data in large meta-analyses including over 3000 patients with viability; revascularisation was associated with 79.6% reduction in annual mortality ($p < 0.0001$) compared with medical treatment (13, 169) and presence of dysfunctional viable myocardium by LGE-CMR without revascularisation is an independent predictor of mortality in patients with ischaemic LV dysfunction (170). Questions have been asked however whether the STICH sub-study results would have been different if CMR had been used rather than MPS-SPECT, and consequently in Europe the third highest indication for CMR remains the assessment of viability (171).

1.4.6.1. Dark Blood

LGE imaging has become the reference standard for myocardial viability assessment giving excellent depiction of myocardial infarction and identification of myocardial viability. Many myocardial infarctions due to the wavefront of ischaemia are sub-endocardial (20). Identification of contrast enhanced sub-endocardial scar that is adjacent to the contrast enhanced blood pool can consequently prove challenging. Thus interest has turned to methods that suppress the contrast enhanced blood pool yet to retain the conspicuity of the gadolinium enhanced scar. Multiple different dark blood

methods have been proposed to null the signal from blood pool and more clearly delineate sub-endocardial infarction by the addition of extra magnetization pulses (172–178). More recently a novel method that does not require a separate preparation pulse but by adjusting the TI to null the blood pool utilises the phase sensitive inversion recovery (PSIR) reconstruction to provide a dark blood method (179). These have not had widespread clinical adoption yet but are surely on the horizon.

1.4.6.2. Scar beyond viability assessment

In addition to identifying viable myocardium, the presence and extent of LGE provides valuable prognostic information, and the extent of scar burden by LGE is readily quantified and reproducible on CMR (180). Impairment of left ventricular ejection fraction is well recognised as an independent risk factor in those with coronary artery disease (85, 181); LGE can provide additive prognostication in these patients and a recent study of 1560 patients established that the presence of scar by LGE irrespective of LVEF identified those at risk of increased mortality (182). Furthermore, a meta-analysis showed that the presence of LGE increases the risk of death by 4.77% and MACE by 3.9% and that each gram of scar measured by LGE increased the hazards of death and MACE by 4% and 5%, respectively (183). Additionally the identification of previously unrecognised MI by LGE confers a significantly increased risk of both mortality and MACE (151, 184).

The extent of scar burden by LGE in patients with IHD has also been identified in a number of studies to be an independent predictor of ventricular arrhythmias in patients with internal cardiac defibrillators (ICD)(185–187), and a recent meta-analysis of 1105 patients with ICDs determined that the extent of LGE was predictive of ventricular arrhythmia whilst LVEF was not (188). Additionally in a high risk cohort of patients with a mean LVEF of 35% being considered for ICD implantation, LGE demonstrated that significant scarring (>5% LV) in patients with LVEF>30%, conferred a risk similar to those with LVEF≤30% (189). Equally, in patients with LVEF≤30%, minimal or no scar

burden established a lower risk cohort similar to those with LVEF>30% (189). Other studies have identified the presence of a “grey zone” on LGE imaging, a heterogeneous region of viable and non-viable myocardium at the infarct periphery, as predictive of VT (190, 191).

LGE and quantification of scar burden has also been used to predict responsiveness to cardiac resynchronization therapy (CRT)(192), and identification of scarring in the pacing region of the LV lead has been associated with non-response to device therapy (193, 194). In a similar method to imaging the coronary artery anatomy, coronary venous anatomy can be reliably demonstrated using GBCAs, which can potentially aid planning of device implantation (195). The combination of coronary venous imaging (not typically an MR based assessment), assessment of ventricular function and LGE may be a useful adjunct in the management of patients with ischaemic cardiomyopathy being considered for CRT, as well as risk stratifying those being considered for defibrillator therapy.

1.4.7. Cost effectiveness

The economic burden of CAD is enormous with £6.8billion spent in 2012 in the UK; in the US over 15 million people have CAD costing the US economy \$108.9 billion/yr (4, 196). Cost effectiveness analyses help to inform optimal management pathways in order to maximise health care benefit within the constraints of limited resources. In the US a low yield has been reported at diagnostic angiography with just over 40% of patients referred having obstructive CAD (29). CMR can act as a potential gatekeeper to invasive coronary angiography in order to reduce downstream costs as well as reduce risk from unnecessary invasive assessments.

Health economic analyses based on the CE-MARC dataset identified that despite the higher initial cost of CMR to MPS-SPECT, the superior diagnostic accuracy of CMR led to an overall greater cost effectiveness in models of the

UK, German and Swiss healthcare systems (197–199). A study of 1,158 German patients being investigated for suspected CAD were randomised to either DSMR prior to angiography or direct to angiography; DSMR prior to invasive angiography led to a saving of 12,466€ of hospital costs per life year, furthermore this cost saving was maintained through a median period of 7.9 years follow up (200).

In a cost analysis comparing CMR and X-ray angiography versus angiography and FFR to determine the need for revascularisation, CMR and angiography was more cost-effective below a CAD prevalence of 62%, 65%, 83%, and 82% for the Swiss, German, UK, and the US health care systems, respectively (201). These studies confirm that as well as the established high diagnostic accuracy, CMR is also a financially advantageous investigative strategy in patients with CAD.

1.4.8. Recently published and future studies

Studies thus far have predominantly focused on the diagnostic accuracy of CMR; forthcoming multi-centre clinical effectiveness trials are however focused on evaluating clinical pathways to improve patient outcomes. The recently published CE-MARC 2 trial was a prospective, multi-centre, 3-arm parallel group, randomised controlled trial comparing multi-parametric CMR versus UK NICE CG95 guidance (30) versus AHA/ACCF MPS-SPECT appropriate-use criteria (202) to investigate patients with suspected CAD (pre-test likelihood 10%-90%) requiring further investigation (35, 203). The primary outcome measure was FFR defined unnecessary angiography (FFR >0.8) with the important safety secondary outcome measure of MACE at 1 and 3 years. CE-MARC 2 showed overall that CMR guided care resulted in significantly reduced rates of unnecessary angiography at 12 months compared to routine guideline directed care (35).

Contemporary registry data from the US suggests roughly 12-26% of elective PCI are deemed inappropriate with considerable variation in practice between sites (204, 205). Both FAME and DEFER showed improved outcomes using FFR guided revascularisation based on ischaemia detection, compared to reliance on visual assessment at angiography (28, 81). These trials would suggest that a better way of selecting patients prior to invasive revascularisation procedures is required. CMR offers a non-invasive ischaemia assessment and the MR-INFORM trial aims to establish if perfusion CMR could act as a non-invasive surrogate to FFR to determine the need for revascularisation in patients with stable CAD (206). MR-INFORM is a multi-national, multi-centre, non-inferiority study comparing adenosine stress perfusion CMR versus angiography with FFR measurement to guide revascularisation decisions in patients with stable angina and moderate to high probability of CAD; the primary endpoint was the occurrence of MACE at one year. The trial has completed recruitment and the preliminary findings were reported at ACC in 2017. The primary outcomes demonstrated that using CMR stress perfusion to guide initial management of patients with stable angina and an intermediate to high risk for coronary artery disease is non-inferior to a strategy with invasive angiography supported by FFR during a follow-up of one year. Both strategies CMR and FFR guidance resulted in a low overall clinical event rate. The number of revascularization procedures was significantly lower when guided by CMR stress perfusion imaging in comparison to invasive angiography supported by FFR.

The prognostic benefit of revascularisation in stable coronary artery disease is a topic of debate; both the COURAGE trial and BARI-2D failed to show any prognostic benefit of revascularisation over optimal medical therapy (OMT) in patients with stable CAD (207, 208). Determination of extent of ischaemia in both these 2 trials was however limited; in COURAGE only 33% of patients had moderate/severe ischaemia and moreover around 40% had <5% ischaemia(209). In both trials however those with a higher residual ischaemia burden had a worse prognosis (209–211). The ISCHEMIA trial aims to test the hypothesis that a routine invasive strategy with early cardiac catheterisation

and revascularisation plus OMT is superior to a conservative management strategy of OMT for patients with moderate or severe ischaemia (117). The trial aims to recruit over 8000 patients worldwide with ischaemia determined by non-invasive imaging (CMR, stress echocardiography, MPS-SPECT) with a primary endpoint of time to cardiovascular death or non-fatal myocardial infarction.

1.4.9. Coronary artery evaluation

Coronary Magnetic Resonance Angiography (CMRA) allows the non-invasive anatomical assessment of coronary arteries; currently clinical indications are limited to the detection of aberrant origin of coronary arteries, coronary ectasia and/or aneurysms (class I indication) and evaluation of bypass grafts (class II indication)(212, 213). CMRA for diagnosis of CAD is not presently part of routine clinical practice. The initial multi-centre experience using CMRA in this context showed interpretable image quality in 84% of proximal and middle coronary artery segments, though with a specificity of 42%; CMRA did however exclude triple-vessel disease and left main coronary artery stenosis with a negative predictive value (NPV) of 100% (214). Progress in CMRA techniques have improved significantly however, and a recent multi-centre study showed that CMRA at 1.5T detects significant CAD with a sensitivity of 88% and specificity of 72% and a negative predictive value of 88% (215). Furthermore one study showed in a direct comparison between CMRA and CTCA there was no significant difference between coronary imaging at 3.0T and 64-slice CTCA for the detection of CAD with a sensitivity of 87% versus 90% ($p=0.16$) and specificity of 77% versus 83% ($p=0.06$) respectively (216).

Currently CMRA techniques are time consuming and there are questions over the incremental diagnostic merit they provide in addition to established perfusion protocols; the CE-MARC study found no additional diagnostic benefit by including CMRA into a full multi-parametric protocol versus the perfusion/LV function/LGE combination (overall accuracy 84.6% vs. 84.2% ($p=0.5316$))(99). Moreover there was no significant improvement in diagnostic

accuracy when CMRA was added to perfusion imaging at 1.5T and compared to FFR as the reference standard (217).

1.4.10. Future directions

T1 mapping

T1 mapping and extra cellular volume fraction quantification are novel methods for CMR tissue characterisation. These techniques are currently research tools that have shown promise for diagnosis and prognostication in rare disease processes (e.g. Amyloid and Fabry's Disease); presently however they do not have an established role in the diagnosis or management of stable IHD (218, 219). Post myocardial infarction however a role for these imaging "biomarkers" is being established in predicting both prognosis and adverse LV remodelling (220, 221).

Blood Oxygen Level Dependent (BOLD) CMR uses the paramagnetic properties of deoxyhaemoglobin as an endogenous contrast agent; increasing deoxyhaemoglobin content leads to a reduction of signal intensity on T2 or T2* weighted images (222). The magnitude of the BOLD effect depends on the static magnetic field strength, with an exponential increase at 3.0T from 1.5T; consequently, most studies have used 3.0T. Thus far BOLD has shown good correlation with QCA and conventional CMR perfusion imaging, but studies are generally small and single centre, limiting its clinical validation (223, 224).

Diffusion tensor MRI (DTI) is another method that has recently been gaining interest in CMR. DTI is a technique that relies on measuring restricted diffusion of water to reveal in vivo anatomical structures such as the myocardial microstructure by assessing myofiber orientation (225). Although, currently a research tool it is giving insight in how histology relates to physiology (226, 227).

Four-dimensional flow cardiovascular magnetic resonance imaging (4D flow CMR) enables mapping and quantification of intra ventricular flow and can measure its kinetic energy (KE) (228). This method is uniquely placed to provide new insight into the manner of intra-ventricular flow in both health and disease. 4D flow techniques allow quantification of intra-cardiac flow in a three-dimensional plane, and as it is automated has the potential to reduce intra-/inter-observer variability and measure flow indices with high accuracy.

Finally, hyperpolarised CMR is making the transition from animal studies to human applications. Hyperpolarisation methods artificially increase the number of molecules in one orientation resulting in a significant increase in MR signal; combined with ¹³C enriched metabolic tracers enable real time imaging of *in vivo* substrate metabolism, coronary angiography and quantitative perfusion imaging (229). The results of human hyperpolarisation studies are eagerly awaited.

1.5. Conclusion

Over the last decade, the evidence base for the diagnostic accuracy of CMR for the investigation of stable coronary artery disease has been confirmed through the publication of large-scale clinical trials and meta-analyses, and CMR is now firmly established in clinical practice guidelines. CMR enables assessment of cardiac dimensions, function, ischaemia, scar burden and tissue viability in a single study without exposure to ionising radiation. CMR also offers prognostic information with a normal stress CMR associated with a <1% risk of death or MI at 2 years, whilst the presence of LGE confers added prognostication above and beyond simple LV ejection fraction. New technical developments continue apace and ongoing large clinical trials will further clarify the role of CMR in routine clinical practice and guide the future development of international guidelines.

The aim of this thesis is to study and refine the utility of both existing and emerging CMR imaging techniques in the context of IHD, with a particular emphasis on prior myocardial infarction and LGE techniques, risk prediction and diagnostic accuracy of ischaemia testing in severe CAD.

2. Methods

Methods common to all the following results chapters are detailed in this section. Further relevant methodology specific to individual results chapters is included within the methods section of relevant chapters.

2.1. Study Populations

The details of each specific patient population by chapter are listed in the following individual sections. The exclusion criteria common to all patient groups undergoing CMR in Chapters 3,4,5,6,7 included the following:

- Contraindication to CMR (e.g. intra-orbital metal, intracranial clips, claustrophobia, non-CMR conditional permanent pacemaker or defibrillator, etc.)
- Pregnant or breastfeeding patients
- Weight $\geq 120\text{kg}$ or obesity where girth exceeds scanner diameter
- Inability to lie flat for the duration of the CMR scan
- Inability to give written, informed consent
- Known adverse reaction to gadolinium based contrast agents
- glomerular filtration rate $< 30\text{mL}/\text{min}/1.73\text{m}^2$

2.1.1. Common patient population for Chapters 3 and 5

Both these chapters derived part or all their study populations from the CE-MARC study. The CE-MARC study protocol has been published previously (96). 752 patients were recruited between March 2006 and August 2009 from 2 hospitals (Leeds General Infirmary and Pinderfields General Hospital). Inclusion criteria for CE-MARC were stable chest pain symptoms thought to be angina pectoris, at least one cardiovascular risk factor (smoking, family history of premature cardio-vascular disease, arterial hypertension, hyperlipidaemia, diabetes mellitus), body weight less than 110 kg, suitability for coronary revascularisation if required and currently in sinus rhythm.

Recruited prior to commencement of my MD, I reviewed Leeds angiographic database for the enrichment population.

2.1.1.1. Patient population for Chapter 3

The patient population in this chapter was derived from the CE-MARC study (63). Twenty-seven patients (4% of CE-MARC) with left main stem (LMS) coronary disease $\geq 50\%$ ($n=22$), and left main equivalent ($\geq 70\%$ stenosis of proximal LAD and circumflex arteries) ($n=5$) by QCA were selected from the CE-MARC population, together with 27 control patients without significant stenosis on X-ray angiography. The control patients were independently matched to the LMS group for age, sex and cardiovascular risk factors. All patients had undergone CMR, MPS-SPECT and angiography. Recruited prior to commencement of my MD, I reviewed all CRFs for appropriate patients and controls.

2.1.1.2. Patient population for Chapter 5

The patient population in this chapter was derived from patients in the CE-MARC study that had undergone angiography (63, 96), the CE-MARC 2 trial (35, 203) and a further enrichment population from the Leeds General Infirmary. 675 patients of the 752 CE-MARC patients were included (inclusion criteria outlined above). 264 patients from the multi-centre CE-MARC 2 trial that had undergone angiography within 12 months of randomisation (which enrolled 1,202 patients) from November 2012 to March 2015 (35, 203). Inclusion criteria for CE-MARC 2 were an estimated PTL of CAD of 10-90% who were aged ≥ 30 yrs with suspected stable angina requiring further investigation, and no prior MI/ACS, and no prior revascularization. Anonymised data for 105 patients consecutively undergoing elective coronary angiography for the investigation of suspected CAD at Leeds General Infirmary with an estimated PTL $< 10\%$ or $> 90\%$ further enriched the population to make it generalisable.

2.1.2. Patient population for Chapter 4

The study population for Chapter 4 was derived from the VINDICATE (Vitamin D treating patients with Chronic heart failure) trial (230). 223 patients were enrolled in the VINDICATE trial and a subgroup of 69 patients underwent a baseline CMR scan. Of these 53/69 had myocardial tagging sequences performed as part of their multi-parametric CMR protocol and were included in the analysis.

Inclusion criteria were, patients had stable (>3 months) New York Heart Association (NYHA) functional class II or III symptoms, a left ventricular ejection fraction $\leq 45\%$ on maximally tolerated medical therapy (>3 months) and a 25(OH) vitamin D level of < 50 nmol/l (< 20 ng/ml). All patients were invited to enter the CMR substudy at their initial enrolment visit. Exclusion criteria included history of taking calcium or other vitamin supplements in the preceding 3 months; aetiology of chronic heart failure (HF) due to untreated valvular heart disease, anaemia or thyrotoxicosis; existing indications for vitamin D supplementation; history of primary hyperparathyroidism, sarcoidosis, tuberculosis or lymphoma; cholecalciferol concentration > 50 nmol/l (20 ng/ml); or if there was significant renal dysfunction (estimated glomerular filtration rate < 30 ml/min/1.73m²)(230). Aetiology of heart failure was determined by the enrolling clinician. Ischaemic cardiomyopathy (ICM) was defined as left ventricular dysfunction associated with previous significant coronary disease ($> 70\%$ in at least one major epicardial coronary artery) on angiography, positive ischaemia testing with MPS-SPECT or stress echocardiography and/or history of previous myocardial infarction or revascularisation (230); non-ischaemic cardiomyopathy (NICM) was defined as left ventricular dysfunction in the absence of the previous conditions. A further healthy 25 age-matched controls with no co-morbidity and taking no regular medication underwent an identical CMR scan protocol. Recruited prior to commencement of my MD, I supervised/performed CMR scanning.

2.1.3. Patient population for Chapter 6

For Chapter 6, 92 patients with prior myocardial infarction were prospectively recruited between June 2016 and June 2017. Of these, 53 patients had chronic and 39 patients had acute MI. MI was diagnosed by cardiac biomarkers, electrocardiography and coronary angiography. Patients were classified as Acute MI if scanned within 7 days of their index admission with the acute coronary syndrome. Chronic MI was defined as being scanned at least 3 months following the initial presentation of the acute coronary syndrome. Inclusion criteria were ≥ 18 years of age, no contra-indication to contrast-enhanced CMR, glomerular filtration rate $\geq 60\text{mL/min/1.73m}^2$. Exclusion criteria were patients with atrial fibrillation, non-MR compatible implants, renal failure or claustrophobia. I recruited and scanned patients.

2.1.4. Patient population for Chapter 7

The study population for Chapter 7 encompassed 30 patients with prior MI who were prospectively recruited between April 2017 and June 2017. MI was diagnosed by cardiac biomarkers, electrocardiography and coronary angiography. Inclusion criteria were ≥ 18 years of age, no contra-indication to contrast-enhanced CMR, glomerular filtration rate $\geq 60\text{mL/min/1.73m}^2$. Exclusion criteria were patients in atrial fibrillation, non-MR compatible implants, renal failure or claustrophobia. I recruited and scanned patients.

2.2. Ethics and approvals

All Chapters were performed in accordance with the Declaration of Helsinki, approved by the National Research Ethics Service, with all patients providing informed written consent. Ethics for the respective chapters had been attained prior to my commencing my MD but in the course of my research time I gained experience in applying for ethical approval. For the VINDICATE study (Chapter 4), the protocol and other relevant documentation had been approved by the National Research Ethics Service [12/YH/0206]. CE-MARC and CE-MARC 2

(Chapters 3 and 5) were conducted in accordance with the Declaration of Helsinki (2000); CE-MARC was approved by the UK National Research Ethics Service (05/Q1205/126); CE-MARC 2 was approved by the UK National Research Ethics Service (12/YH/0404) (35, 63). For Chapters 6 and 7, the study protocol was performed in accordance with approval from the National Research Ethics Service (12/YH/0169). CE-MARC and CE-MARC 2 were funded by the British Heart Foundation (BHF); grant references RG/05/004 and SP/12/1/29062. Additional support was received from the Leeds Teaching Hospital Charitable Foundation and the National Institute for Health Research (NIHR) Leeds Clinical Research Facility. VINDICATE was funded by the Medical Research Council, UK.

2.3. MRI Scanner Hardware

In Chapter 3, patients underwent stress perfusion-CMR on a Philips Intera 1.5T scanner (Philips Medical Systems, Best, The Netherlands) equipped with “Master” gradients (30 mT/m peak gradient, 150 mT/m/ms slew rate) and a five-element cardiac phased-array receiver coil.

For patients scanned in Chapter 4, CMR was performed on a 3.0 Tesla Philips Achieva system (Philips Healthcare, Best, The Netherlands) equipped with a 32 channel coil and MultiTransmit® technology.

In Chapters 6 and 7, CMR was performed on a 1.5 Tesla Philips Ingenia system (Philips Healthcare, Best, The Netherlands) equipped with a 24 channel digital receiver coil and patient-adaptive RF shimming.

2.4. Common CMR protocols

2.4.1. Survey images

At the start of any CMR protocol, free breathing low-resolution survey scans of the chest were performed to mark anatomical landmarks. For each pulse

sequence, images with artefact were repeated until any artefact was removed or minimised. The highest quality images were used for analysis.

2.4.2. Localisers

Cardiac localiser scans which define short axis, vertical long axis and horizontal long axis acquired with a balanced SSFP, single slice, breath-hold pulse sequence. Pulse sequence parameters: echo time (TE) 1.6 ms, repetition time (TR) 3.2 ms, slice thickness 8 mm, matrix 192 × 192, field of view 320–400 mm according to patient size, SENSE factor 1.7 to 2.0, 30–50 phases per cardiac cycle.

2.4.3. The CE-MARC CMR protocol

The protocol commenced with a low-resolution survey scan and localisers. Intravenous adenosine was then administered for approximately 4 minutes at 140 mcg/kg/min, following which first pass stress perfusion imaging was undertaken after the injection of 0.05 mmol/kg dimeglumine gadopentetate. Stress and Rest perfusion was carried out using a “3 of 5” technique, planned from long axis cine images. Three-dimensional whole heart MR coronary angiography was performed but not used in the analysis here. Rest perfusion imaging was undertaken a minimum of 15 minutes following stress perfusion, with a further injection of 0.05 mmol/kg dimeglumine gadopentetate. A final injection of 0.1 mmol/kg dimeglumine gadopentetate was given following this sequence, bringing the overall gadolinium dose to 0.2 mmol/kg. Resting left ventricular function was then assessed, initially for three slices planned identically to the perfusion slices, and then for the entire left ventricle using contiguous slices. A modified Look-Locker inversion time scout was performed prior to LGE imaging in short axis, vertical long axis and horizontal long axis orientations.

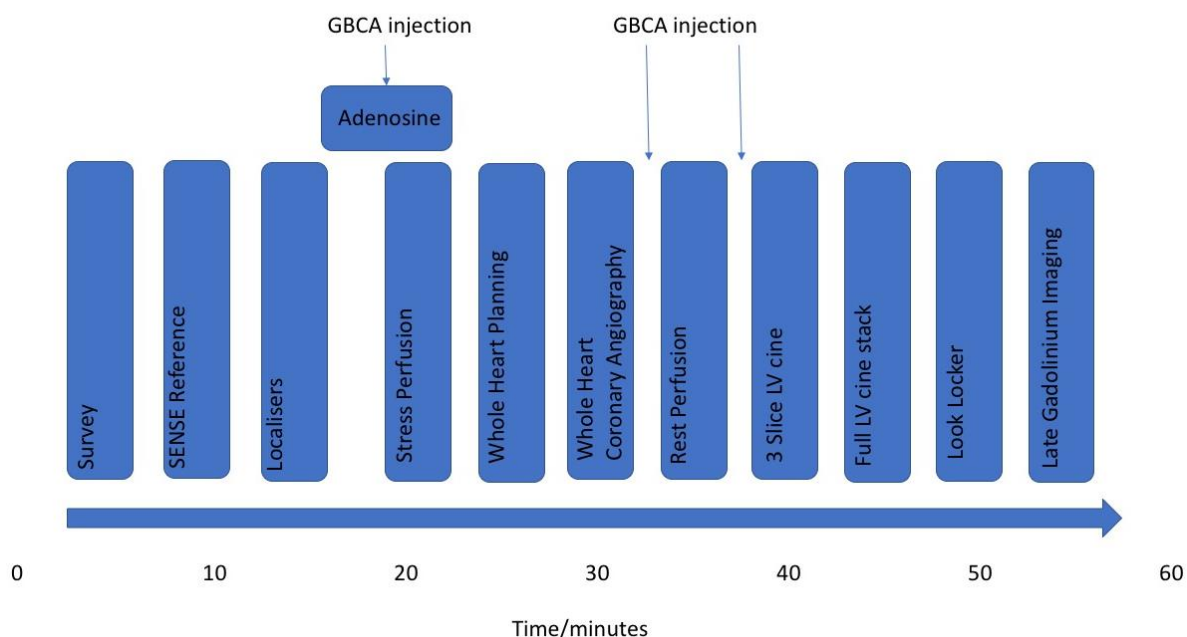


Figure 2-1 Image panel showing CE-MARC scanning protocol

2.4.4. Cine imaging

2.4.4.1. Chapter 3

A contiguous cine stack covering the entire left ventricle in 10–12 slices (depending on left ventricular long axis length). Three additional slices, with identical slice positioning to the perfusion sequence were also be acquired. Pulse sequence parameters: balanced SSFP, TE 1.7 ms, TR 3.5 ms, flip angle 60°, SENSE factor 2, matrix 192 × 192, field of view 320–460 mm, slice thickness 10 mm, at least 20 phases per cardiac cycle, 1–2 slices per breath-hold.

2.4.4.2. Chapter 4

A contiguous cine stack were acquired covering the entire heart in the LV short axis plane (balanced steady state free precession), spatial resolution 1.2x1.2x10mm³, 30 cardiac phases TR/TE 2.6/1.3ms, flip angle 40°, field of

view 300-420mm, typical temporal resolution 39ms) and in orthogonal long-axis planes.

2.4.4.3. Chapters 6 and 7

Assessment of myocardial function using standard SSFP cine imaging in a contiguous cine stack were acquired covering the entire heart in the LV short axis (spatial resolution 1.09x1.09x8mm³, 30 cardiac phases TR/TE 3.0/1.48ms, flip angle 40°, field of view 360-360mm, SENSE acceleration).

2.5. Common CMR analysis

CMR analysis in Chapter 3 was carried out by JF, JPG and SP with additional post processing by JB. Specifically JF performed the quantitative perfusion analysis. CMR analysis in Chapter 4 was conducted by 2 observers (JF overall analysis and PS for interobserver variability). CMR analysis in Chapter 6 was conducted by 3 observers (JF overall analysis, GF and LAB for interobserver variability). CMR analysis in Chapter 7 was conducted by 2 observers (JF overall analysis, GF for interobserver variability). All post-processing CMR analysis was carried out using the same software (CVI⁴², Circle Cardiovascular Imaging, Calgary, Canada) with the exception of tissue tagging analysis which used separate software (inTag version 1.0, Creatis, Lyon, France) and the post processing analysis of perfusion imaging in LMS which is described below. Specific methods of CMR analysis are detailed in the respective chapters.

2.5.1. Assessment of LV function

The short axis LV cine stack was used to generate LV end systolic and end diastolic volumes according to the summation of discs methodology (231). The left ventricular endocardial and epicardial borders were manually traced from the short axis LV cine stack at both end systole and end diastole in order to generate systolic and diastolic volumes. The LV ejection fraction was derived from the equation:

Equation 1 LV ejection fraction

$$LVEF(\%) = ((LVEDV - LVESV) / LVEDV) * 100$$

Where EDV= end diastolic volume(ml), ESV= end systolic volume

Both trabeculations and the papillary muscles were excluded. The LV mass values were calculated from the end diastolic myocardial volume according to established methods (232). The Mosteller equation was used to index volumetric data to body surface area.

2.5.2. Tagging

For tagging analysis, endocardial and epicardial contours were drawn on the short axis spatial modulation of magnetization images using a semi-automated process. Peak circumferential LV strain was measured for the three slices at apex, mid-ventricle, and base. Strain was measured in the mid-myocardial layer which has previously been reported to be the most reproducible (233). LV twist was calculated by subtracting the basal from apical rotation. Basal and apical radius was calculated from cine images in diastole at the same slice location as the tagged images. The equation used to determine torsion was (234):

Equation 2 Calculation of Torsion

$$Torsion = \frac{Peak\ Twist \times (Apical\ Radius + Basal\ Radius)}{2 \times Apex\ to\ Base\ length}$$

2.5.3. Late Gadolinium Enhancement quantification

In Chapters 4,6 and 7, quantitative assessment of myocardial scar burden was performed using a threshold of 50% of the maximum intensity within the scar (full width half max method). This method has been proposed as the most reproducible quantitative measure of late enhancement of myocardial scar (180). On the LGE short-axis images endocardial and epicardial contours were manually outlined (excluding trabeculations and papillary muscles); manual delineation of two separate user-defined regions of interest (ROIs) were then made on the LGE short axis slice where infarcted myocardium was present. One ROI was drawn in remote myocardium (where no scar was present); a second ROI was drawn around hyperenhanced myocardium where infarcted myocardium was present. Automated calculation for the scar tissue mass (grams) was then calculated on each LV short axis slice based on these ROIs.

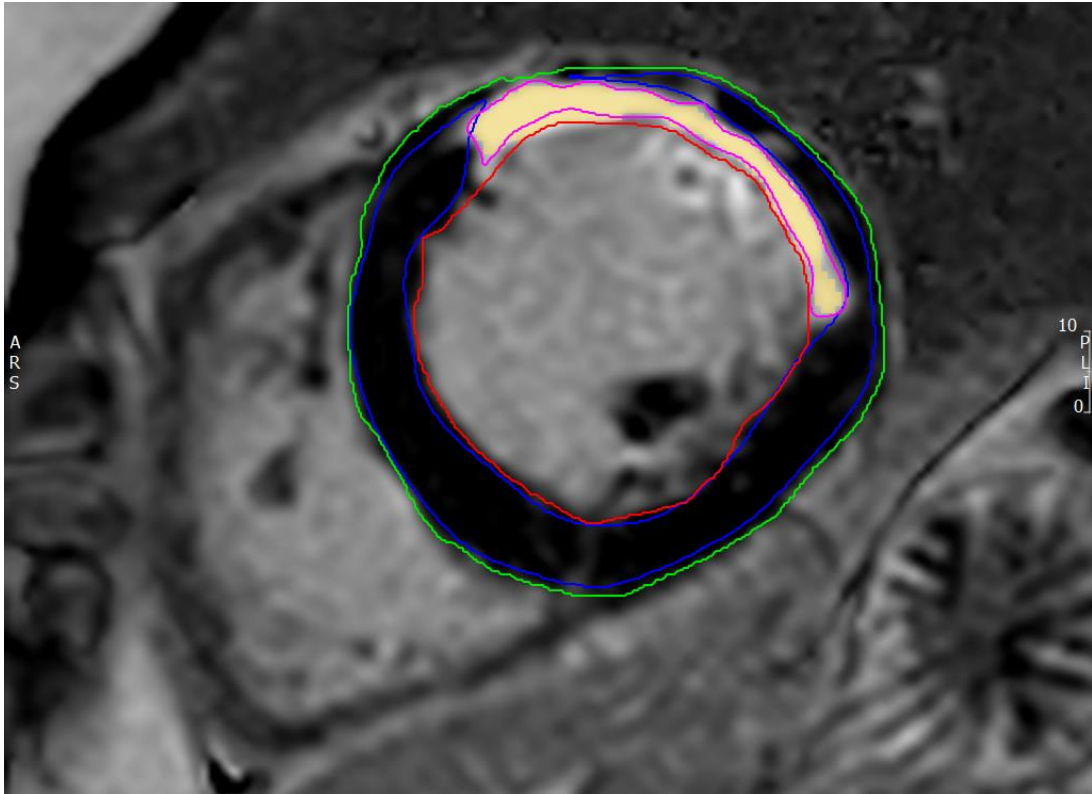


Figure 2-2 Image panel showing an example image of an LV slice using the semi-automated full width half maximum LGE quantification method on Circle CVI

2.6. X-ray coronary angiography

All patients in the CE-MARC study were scheduled to undergo invasive X-ray coronary angiography by a cardiologist blinded to the MPS-SPECT and CMR results. Angiography was performed by standard methods from the femoral or radial approach. X-ray angiography images were analysed by two cardiologists (JY and NM) with experience in invasive coronary angiography for CE-MARC. Quantitative coronary angiography analysis was performed off-line using QCAPlus software (version 8.11.19, Sanders Data Systems, Palo Alto, California, USA). Clinically significant coronary disease was defined as $\geq 70\%$ stenosis of a first order coronary artery measuring 2 mm or greater in diameter, or left main stem stenosis 50% or more as measured by QCA. The same QCA parameters were applied to the CE-MARC 2 population

undergoing angiography where FFR was not possible and in the enrichment population derived from the Leeds General Infirmary (performed by JF).

In the population derived from CE-MARC 2 fractional flow reserve (PressureWire; St Jude Medical, Minneapolis, MN) was performed in all vessels ≥ 2.5 mm with a stenosis considered $\geq 40\%$ and $\leq 90\%$, following intracoronary nitrates. Adenosine at a rate of 140 to 210 $\mu\text{g}/\text{kg}/\text{min}$ was given intravenously to achieve maximal hyperaemia and haemodynamic steady state. Totally occluded coronary arteries were assigned a default FFR value of 0.50; for lesions with a visual stenosis of $>90\%$, FFR was also considered positive (0.50), and for lesions $<40\%$, FFR was considered normal (0.90). If FFR was not able to be performed in patients in the CE-MARC 2 trial, then QCA measurements were made during offline analysis by a single independent blinded observer at the Glasgow Angiographic core laboratory.

2.7. Statistical Analysis

All statistical analysis was performed using the PASW software package (V21, SPSS, IBM, Chicago, Illinois, USA). Data are presented as mean \pm SD, median (interquartile range, IQR) or frequency (percentage). Data were tested for normality using the Shapiro-Wilks test. For normally distributed data, two-tailed unpaired Student's t tests were used for comparisons between groups, and paired Student's t tests were used for intragroup comparisons. For non-normally distributed data, the Related-Samples Wilcoxon Signed Rank Test and independent samples Mann-Whitney U test were used. To compare between groups an analysis of variance (ANOVA) and Tukey post-hoc tests were used. The Chi-squared test was used for comparing categorical variables. Pearson's correlation coefficients were used to assess the correlation of dependent and independent variables. P values <0.05 were considered statistically significant.

3. A comparison of Cardiovascular Magnetic Resonance and Single Photon Emission Computed Tomography Perfusion Imaging in Left Main Stem or Equivalent Coronary Artery Disease

3.1. Background

Left main stem coronary artery disease is found in approximately 5% of patients with stable angina and in approximately 7% of patients presenting with an acute myocardial infarction (235). Significant LMS disease is typically defined as a stenosis of $\geq 50\%$ and LMS equivalent as $\geq 70\%$ stenosis of both the proximal left anterior descending artery and proximal circumflex artery. Significant LMS disease is associated with poor clinical outcomes, with an untreated 3-year survival of 50% in those with $>50\%$ stenosis dropping to 41% in those with stenosis $>70\%$ (236, 237). Several studies have demonstrated survival benefit for revascularisation of significant LMS stenosis (238, 239). Thus, accurate detection and functional assessment of the degree of LMS stenosis has both important prognostic and therapeutic implications.

Patients evaluated for suspected CAD frequently undergo functional imaging, which may include MPS-SPECT or CMR imaging. A normal myocardial perfusion study by either of these techniques is associated with an excellent long-term prognosis (146, 149, 240). Published data on the utility of MPS-SPECT for the diagnosis of LMS disease are limited, with variable diagnostic accuracy reported (241–244). Equally, the diagnostic accuracy of stress perfusion CMR is poorly established in LMS disease.

The Clinical Evaluation of MAgnetic Resonance imaging in Coronary heart disease study (63, 96) was a large prospective study of patients with suspected CAD; 752 patients were enrolled and all were scheduled to undergo CMR, MPS-SPECT and the reference standard invasive coronary angiography. Using the CE-MARC dataset, we hypothesised that CMR would

have a greater diagnostic accuracy than MPS-SPECT for the detection of LMS or LMS equivalent CAD, and that quantitative CMR perfusion analysis would improve diagnostic discrimination compared to visual analysis.

3.2. Methods

3.2.1. Subjects

All patients with LMS disease $\geq 50\%$, and left main equivalent ($\geq 70\%$ stenosis of proximal LAD and LCx arteries) by QCA were selected from the CE-MARC population, together with an equal number of control patients without significant stenosis on X-ray angiography. The control patients were independently matched to the LMS group for age, sex and cardiovascular risk factors. The inclusion criteria and full imaging protocol for CE-MARC have been previously reported (96). In brief, inclusion criteria were: stable chest pain thought to be angina pectoris, at least one cardiovascular risk factor, suitability for coronary revascularisation if required and in sinus rhythm. Exclusion criteria were: previous coronary artery bypass surgery, evidence of crescendo angina or acute coronary syndrome, contraindication to CMR imaging or adenosine infusion, and chronic renal failure. The study was performed in accordance with the Declaration of Helsinki (October 2000), with all patients providing informed written consent. The study protocol and other relevant documentation had been approved by the National Research Ethics Committee.

3.2.2. CMR protocol

Patients underwent perfusion-CMR on a Philips 1.5T scanner (Philips Medical Systems, Best, The Netherlands) equipped with "Master" gradients (30 mT/m peak gradient, 150 mT/m/ms slew rate) and a five-element cardiac phased-array receiver coil. Stress perfusion imaging was performed using intravenous adenosine (140mcg/kg/min) infused for 4 minutes. Perfusion imaging was performed every heartbeat during the first-pass in 3 short-axis imaging planes,

representing the basal, midventricular, and apical myocardial segments. Images were acquired by using a T1-weighted saturation recovery turbo field-echo imaging sequence, using a shared (non–slice-selective) saturation pulse. A bolus of 0.05mmol/kg gadopentetate dimeglumine [Gd-DTPA], (Magnevist, Bayer Schering Health Care Limited, UK) followed by a 15ml saline flush was administered at 5ml/s into an antecubital vein by a power injector (Medrad Spectris Solaris, Medrad, USA). Resting myocardial perfusion was then assessed and the data obtained with identical parameters as for the resting perfusion acquisition. The CMR protocol also included cine imaging for assessment of LV function and LGE imaging (96).

3.2.3. MPS-SPECT protocol

MPS-SPECT radionuclide imaging was carried out on a dedicated cardiac gamma camera (MEDISO Cardio-C, Budapest, Hungary), using a two-day scanning protocol, the radioisotope tracer ^{99m}Tc tetrofosmin (Myoview), with a standard dose of 400 MBq, weight-adjusted to a maximum of 600 MBq, per examination. Stress and rest ECG-gated MPS-SPECT images were acquired. The stress imaging protocol was performed using intravenous adenosine (140mcg/kg/min) for 4 minutes followed by isotope injection to minimise variation between MPS-SPECT and CMR (96).

3.2.4. X-ray Angiography

All patients underwent invasive X-ray coronary angiography by a cardiologist (blinded to MPS-SPECT and CMR results).

3.2.5. CMR Analysis

The methods for the visual analysis of CMR in CEMARC have been described previously (96). As per the original analysis, CMR was deemed positive if one or more abnormality of perfusion, wall motion abnormality or scar was present (63, 96).

For quantitative perfusion analysis, perfusion CMR data were exported in DICOM format and post-processed off-line using the software cvi42, (version 5.1.0, Circle Cardiovascular Imaging, Calgary, Alberta, Canada.) Contours depicting the myocardium and a region within the left ventricular blood pool were drawn manually (Figure 3-1). These contours were copied to all time frames and manually adjusted for breathing motion by using rigid translation. The myocardium was subdivided into six circumferentially equidistant regions in the basal and middle sections and four in the apical section according to the standard American Heart Association (AHA) model (245).

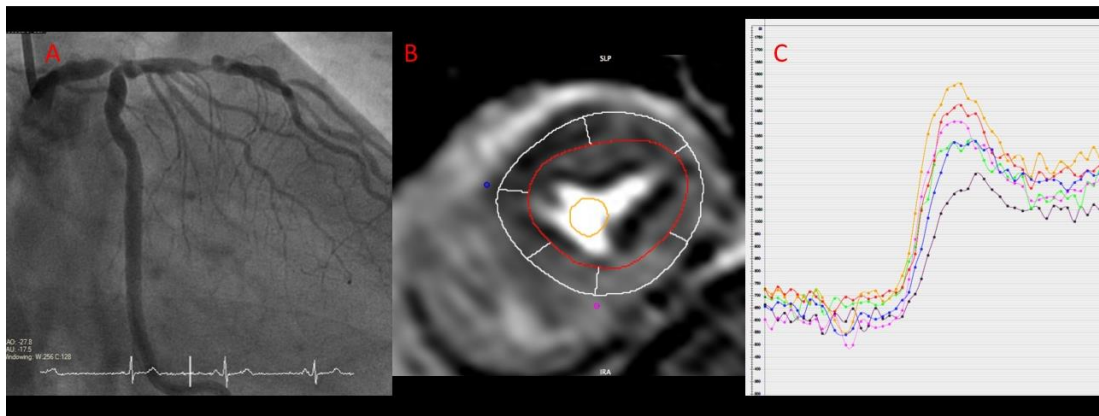


Figure 3-1 Image panel showing angiography and CMR perfusion of patient with LMS disease.

Panel A shows angiography with a critical distal LMS lesion. The corresponding mid-slice CMR stress perfusion (B) demonstrates a perfusion defect in septum, anterior and lateral wall. Myocardial curves (C) of the same mid ventricular slice demonstrates hypoperfusion in the segments subtended by the LMS. Orange and red lines represent the inferior and infero-lateral segments respectively and show higher signal intensity corresponding with no hypoperfusion in these segments. Notably a significant LAD stenosis is seen which may contribute to the perfusion defect. (128)

Quantitative perfusion parameters were calculated using in-house software written in Matlab (Mathworks, Natick, MA) (123). Myocardial blood flow (MBF) was estimated using Fermi-constrained deconvolution (246). Blood pool and myocardial curves were converted to contrast agent concentrations assuming a linear relationship between signal intensity and concentration as previously described (123). An assumed native blood T_1 value of 1435ms and a contrast agent relaxivity of $4.3 \text{ sec}^{-1} \cdot \text{mM}^{-1}$ was used. The arterial input function was taken from the basal slice (which had the shortest preparation delay). Concentration curves were baseline subtracted, corrected for temporal shifts between the arterial input function and the myocardial curves and limited to the first pass of contrast through the left ventricle using previously described automated methods (123, 247). Myocardial perfusion reserve (MPR) was calculated as the ratio of stress MBF to rest MBF. Segmental MBF and MPR were averaged to produce per-patient indices for statistical analysis. This was performed with 16 segments to give a global myocardial value, and separately for segments in the LMS territory. The LMS territory comprised segments 1, 2, 5-8, 11-14 and 16 (245). A quantitative summed stress score (SSS) was produced by applying the optimal MBF value derived by Youden's index (as detailed in the statistical methods) to the MBF generated in each of the 16 segments for each patient.

3.2.6. X-ray Angiography Analysis

X-ray angiography images were analysed by two cardiologists experienced in invasive coronary angiography. QCA analysis was performed off-line using QCAPlus software (Sanders Data Systems, Palo Alto, California, USA). For all LMS patients, visual and quantitative analysis of the invasive angiogram were concordant.

3.2.7. MPS-SPECT Analysis

MPS-SPECT data sets were analysed in a blinded manner, simultaneously by a cardiologist with >10 years' experience in nuclear cardiology and an experienced medical physicist. Evidence of ischaemia by visual comparison of rest/stress perfusion scans, based on the standard 17-segment AHA model, was performed. Additionally, evidence of ischaemia by semi-quantitative scoring (using the QPS 20 segment) (QPS, Cedars-Sinai Medical Center, USA) was also performed. Non-perfusion markers of significant coronary artery disease, such as transient left ventricular dilatation (TID) and increased right ventricular uptake were also taken in to consideration as felt appropriate by the reporting team.

3.2.8. Data analysis and Statistics

Statistical analysis was performed using commercially available software (SPSS, version 22.0, SPSS Inc., Chicago, USA). Two-sided p values ≤ 0.05 were considered to be statistically significant. Data were compared using Student's t-test for continuous variables and Fisher's Exact test for proportions, independent samples t tests and Pearson's correlation coefficients as necessary. Normality for MBF values in the normal comparison group was evaluated using a Q-Q plot and Shapiro-Wilk test. Receiver operating characteristic (ROC) curve analysis for diagnostic tests were compared using the method described by DeLong et al (248). For quantitative perfusion analysis, the optimal sensitivity and specificity of quantitative parameters were derived by calculating Youden's index (249). The sensitivity and specificity and ROC analysis were based on the 54 patients.

3.3. Results

3.3.1. Visual analysis

Twenty-seven (4%) patients of the 729 patients that received invasive angiography from CE-MARC were identified to have LMS or LMS equivalent disease by invasive angiography. Twenty-two patients had true LMS disease and 5 patients had LMS equivalent disease. Patient characteristics are shown in Table 1.

Table 3-1 Baseline Demographics

Patient characteristic	LMS	Controls	P
N	27	27	
Age (years)	65 ± 7	64 ± 6	0.45
Male	23 (85%)	23 (85%)	1.0
Body mass index (kg/m ²)	27.5 ± 3.89	27.0 ± 2.87	0.60
Current smoker	5 (19%)	4 (15%)	1.0
Blood pressure	134/74 ± 20/10	140/76 ± 19/7	0.27 / 0.43
Hypertension	12 (44%)	17 (62%)	0.27
Total cholesterol (mmol/L)	5.3 ± 1.4	4.8 ± 1.2	0.25
Diabetes mellitus	5 (19%)	5 (19%)	1.0
Family history of CAD*	14 (52%)	13 (48%)	1.0
Significant CAD*			
- LMS	22 (81%)	0 (0%)	<0.001
- LAD	17 (63%)	0 (0%)	<0.001
- LCx	11 (41%)	0 (0%)	<0.001
- RCA	11 (41%)	0 (0%)	<0.001

Data as mean ± SD or n (%). *CAD coronary artery disease.

Table 3-2 Imaging findings

Imaging finding	LMS	Control	P
CMR			
- RWMA* positive	17 (63%)	0 (0%)	<0.001
- FPP positive	22 (81%)	1 (4%)	<0.001
- LGE positive	15 (56%)	0 (0%)	<0.001
- Overall positive	22 (81%)	1 (4%)	<0.001
MPS-SPECT			
- RWMA positive	10 (37%)	6 (22%)	0.37
- Fixed defect	6 (22%)	5 (19%)	1.0
- Inducible defect	17 (63%)	4 (15%)	<0.001
- TID	1 (4%)	1 (4%)	1.0
- RV uptake	17 (63%)	14 (52%)	0.58
- Overall positive	16 (59%)	3 (11%)	<0.001

Data as n (%). *RWMA regional wall motion abnormality, FPP first pass perfusion, LGE late gadolinium enhancement, TID left ventricular transient ischaemic dilatation, RV right ventricular isotope uptake.

All patients had completed CMR, MPS-SPECT and angiography studies. Detection rates for CAD by both CMR and MPS-SPECT are shown in Table 3.2. Multi-parametric CMR detected evidence of CAD in a non-significantly higher proportion of patients with LMS disease than MPS-SPECT (81% vs. 59%, $p=0.14$). All patients with abnormal multi-parametric CMR also had abnormal perfusion CMR by visual analysis. One patient was deemed a false negative by MPS-SPECT that had 1 segment of inferior ischaemia. For CMR, the average SSS for LMS patients was 13.0 ± 9.5 , and for controls 0.67 ± 1.0 ($p<0.001$). For MPS-SPECT, the average SSS for LMS patients was 5.15 ± 6.5 , and for controls 1.93 ± 2.3 ($p=0.02$). ROC analysis demonstrated a significantly higher area under the curve (AUC) for detection of LMS disease by visual CMR analysis compared to MPS-SPECT (0.95 vs. 0.63; $p=0.0001$, Figure 3-2).

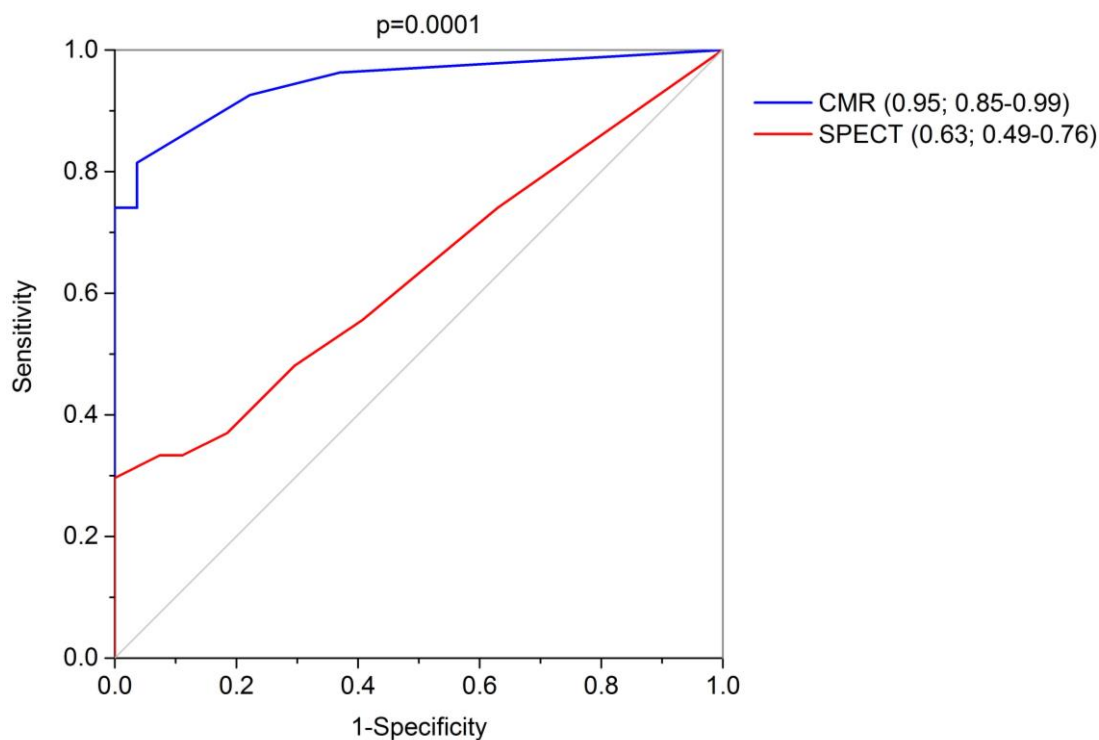


Figure 3-2 ROC curves for visual summed stress scores for CMR and MPS-SPECT. Numbers in parentheses indicates AUC with 95% confidence intervals.

3.3.2. Quantitative CMR perfusion analysis

Table 3.3 shows the results of the quantitative CMR perfusion analysis. Mean stress MBF and mean MPR were both significantly lower in LMS patients compared to controls ($p < 0.001$); resting MBF was similar between the LMS and control groups ($p = 0.14$).

ROC analysis (Figure 3-3) demonstrated the highest AUC (0.88) for global MBF as an association with LMS disease. Global MBF of < 2.08 ml/g/min was associated with a sensitivity of 78% and specificity of 85% for diagnosis of significant LMS disease. A quantitative SSS was produced using this value;

this score had an AUC not significantly different to CMR visual analysis ($p=0.18$), and more accurate than MPS-SPECT ($p=0.003$, Figure 3-4).

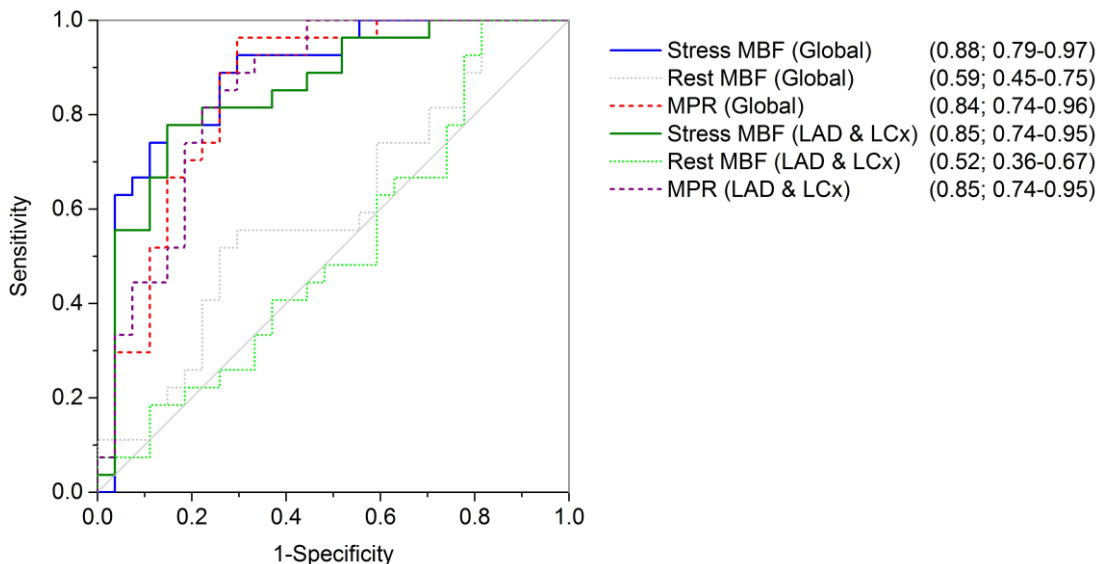


Figure 3-3 ROC curves for CMR quantitative perfusion results. Numbers in parentheses indicates AUC with 95% confidence intervals.

Table 3.4 shows sensitivity, specificity and predictive values for overall visual analysis by multi-parametric CMR and MPS-SPECT, and quantitative analysis by CMR global MBF.

Table 3-3 Quantitative CMR perfusion analysis

	LMS	Control	P-value
Global stress MBF	1.77 ± 0.72	3.28 ± 1.20	<0.001
Global rest MBF	1.28 ± 0.42	1.48 ± 0.55	0.14
Global MPR	1.42 ± 0.44	2.31 ± 0.76	<0.001
LMS territory stress MBF	2.03 ± 0.77	3.38 ± 1.15	<0.001
LMS territory rest MBF	1.42 ± 0.36	1.54 ± 0.56	0.36
LMS territory MPR	1.53 ± 0.44	2.34 ± 0.64	<0.001

MBF values are in ml/g/min.

Table 3-4 Sensitivity, specificity and predictive values for detection of IHD in LMS patients by visual CMR analysis, MPS-SPECT and quantitative CMR.

	Sensitivity	Specificity	PPV	NPV
CMR Visual	81	96	48	99
CMR MBF	78	85	18	98
MPS-SPECT	63	89	19	98

Predictive values are corrected based on the prevalence of LMS disease in the CE-MARC population. *PPV positive predictive value, NPV negative predictive value

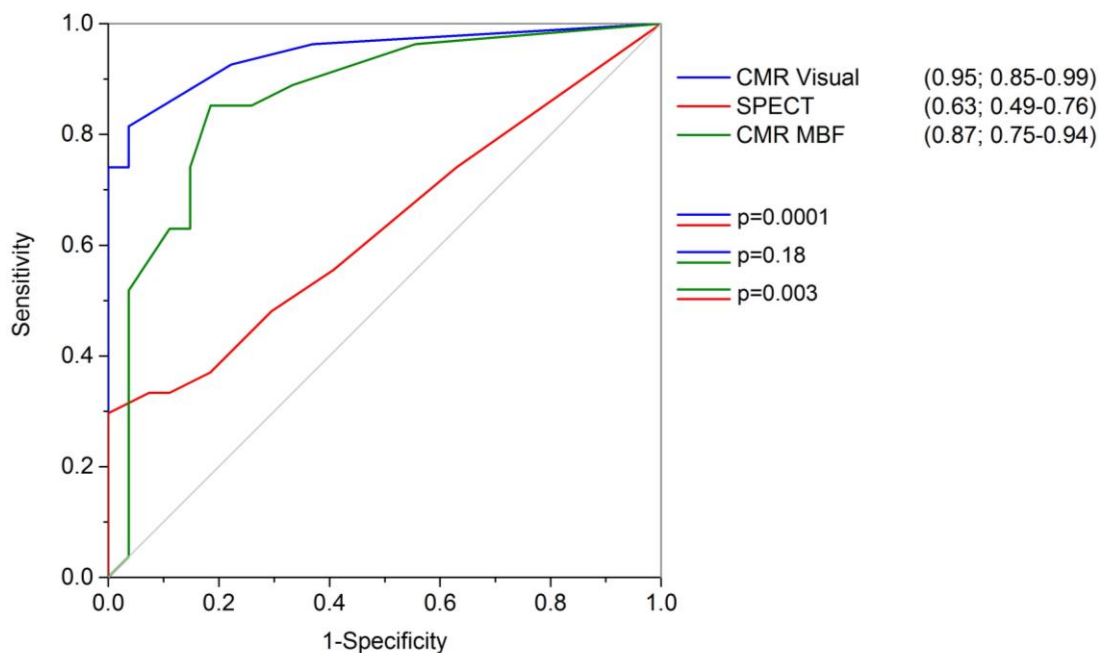


Figure 3-4 ROC curves for quantitative summed stress score for MBF, visual CMR and MPS-SPECT. Numbers in parentheses indicates AUC with 95% confidence intervals.

3.4. Discussion

This post hoc exploratory analysis of the CE-MARC study has demonstrated the diagnostic accuracy of CMR and MPS-SPECT in the setting of LMS (or equivalent) CAD. The main finding is that in patients with stable suspected CAD, CMR first-pass perfusion imaging as part of a multi-parametric protocol more accurately detected evidence of LMS or equivalent disease than MPS-SPECT. Additionally, quantitative CMR perfusion showed high diagnostic accuracy for the detection of LMS disease with global MBF as the most diagnostic, however quantitative perfusion did not outperform visual CMR perfusion analysis.

CMR is established as a cost effective investigation with high diagnostic accuracy compared to MPS-SPECT for the diagnosis of suspected CAD (63,

97, 197, 250). Previous data on the diagnostic accuracy of MPS-SPECT and CMR in LMS disease are sparse. Thus far there are no studies specifically investigating the diagnostic accuracy of CMR for LMS disease. The MR-IMPACT study (251), a multicentre comparison of CMR and MPS-SPECT in 234 patients, included eight patients with LMS disease, while MR-IMPACT II analysed 465 patients of which 14 had LMS disease (250); in neither of these studies were patients with LMS disease separately analysed. The majority of studies validating CMR perfusion techniques have less than five LMS patients, effectively precluding meaningful analysis of this subset. In contrast, the CE-MARC study had a LMS population of sufficient size to allow reasonable conclusions to be drawn (63). MPS-SPECT studies of LMS disease have largely been un-blinded, retrospective and derived from angiographic databases (241–243); in this context referral bias potentially leads to an over-estimation of the sensitivity of MPS-SPECT for the detection of LMS disease (242), as the false negative MPS-SPECT scans go unevaluated.

Non-invasive detection of CAD is clinically useful to both determine the presence of clinically significant disease and to estimate the severity and extent of disease. The classical finding of an inducible perfusion abnormality involving both the LAD and LCx coronary artery territories was not robustly seen in LMS patients by either CMR or MPS-SPECT. This perfusion defect pattern has been described with varying frequency from 12-59% of MPS-SPECT patients with documented significant LMS stenosis in retrospective analyses (241, 243, 244). This perfusion defect pattern was seen in just 8 LMS patients (30%) by CMR and 2 patients (7%) by MPS-SPECT in our study. The low diagnostic yield specific for LMS disease may be due, in part, to distal and bifurcation LMS lesions, which may have a differential effect on myocardial perfusion to the LAD and LCx territories, resulting in underestimation of LMS disease. Furthermore, although a visual or QCA reported stenosis of 50% of the LMS is deemed significant by convention, not all 50% coronary stenoses are haemodynamically significant when assessed by invasive FFR (252). In addition, a myocardial perfusion abnormality consistent with LMS disease may be less apparent in the presence of coronary collateralisation, or flow-limiting

stenosis in the right coronary artery (i.e. 3-vessel disease). However, these haemodynamic factors do not account for the differential detection rates of CMR and MPS-SPECT (overall 81% vs. 59% for detection of CAD). The phenomenon of “balanced ischaemia” in multivessel disease potentially leads to an underestimation of disease, in MPS-SPECT this effect is reported with variable frequency (253, 254). In this context, CMR has been shown to have an advantage over MPS-SPECT to detect perfusion defects (in multivessel disease) due to a higher spatial resolution (255, 256). Furthermore, multivessel disease has been shown to not be significantly associated with false negatives in CMR (257).

Wide interobserver variability for visual severity of stenoses of the LMS have been reported (77, 78). In our study QCA was used to determine the severity of angiographic stenoses, as per the CE-MARC study protocol (63, 96). In this context, there is a potential limitation of the invasive reference standard; however FFR and intra-vascular ultrasound are only recommended as adjuncts in LMS disease assessment in current guidelines and revascularisation decisions are, for the mainstay, based on severity of angiographic stenosis (27, 86).

Additional diagnostic aids have been proposed to improve the sensitivity of MPS-SPECT for the diagnosis of LMS disease. TID of the left ventricular cavity in response to stress has been identified to be a strong predictor of cardiac events (258), reflecting global subendocardial ischaemia or stress-induced left ventricular dysfunction from left main or three vessel disease (259). Increased right ventricular radiotracer uptake has also been independently associated with LMS disease, with a 60% increase from 0.33 ± 0.07 at rest to 0.51 ± 0.07 with stress in LMS patients ($p < 0.001$ compared to controls) (260, 261). When non-perfusion markers of widespread ischaemia are used alongside perfusion data, the proportion of patients with LMS stenosis identified by MPS-SPECT increased from 56% to 83% in one study (241). In our population, however TID was seen less frequently, with no significant difference in right ventricular uptake between LMS patients and controls suggesting limited discriminatory value. These markers were used for MPS-SPECT analysis in this study, but

to date have not been used as standard in CMR, and were not prospectively evaluated here.

This study also examined the utility of quantitative CMR perfusion as a potential approach to account for balanced myocardial hypoperfusion that theoretically limits visual analysis in LMS or 3-vessel disease. Other studies have shown that quantitative estimation of myocardial perfusion reserve by CMR over visual analysis improved sensitivity from 74% to 88% and specificity from 58% to 90% for patients suspected to have coronary artery disease, but not confined to LMS (262). The Fermi deconvolution method used in our study has been shown to perform as well as any other model for the detection of CAD (123). Patel et al identified increased ischaemia burden by quantitative perfusion methods using Fermi deconvolution over qualitative assessment as severity of coronary disease increased in patients undergoing perfusion CMR with multi-vessel disease (263). The value of quantitative CMR analysis for LMS lesions has not been previously detailed. In our study, global MBF was the best quantitative marker and showed high sensitivity and specificity (78% and 85% respectively) for the diagnosis of LMS disease. Quantitative perfusion analysis however was not significantly better than visual CMR perfusion analysis, suggesting that visual perfusion analysis is sufficient to detect heterogeneities in myocardial contrast distribution in LMS disease, a finding supported by dedicated analysis of false-negative CMR (257). Furthermore, our results suggest there is little additive value to be gained from the quantification of rest perfusion when quantitation of stress perfusion is performed.

3.4.1. Limitations

Given the low prevalence of LMS disease, the numbers in this prospective study are limited. In our study MPS-SPECT analysis did not use attenuation correction; however this was not routine practice when the study was performed (264). We did not use FFR as our invasive reference standard, however we did use QCA in line with the main CE-MARC paper. The pulse

sequence used for perfusion imaging in CE-MARC was not fully optimised for quantitative analysis as it used a single preparation pulse for all three slices and a relatively high contrast agent dose. This may have led to a lower performance of quantitative analysis in this study compared to recent approaches. The lack of a completely linear arterial input function measurement for MBF analysis, with the assumption that concentration is linearly related to signal intensity will result in an overestimate of absolute myocardial blood flow. However, *post-hoc* correction based on baseline signal intensity values would introduce noise into the measurements that could reduce diagnostic accuracy (265). Furthermore, studies comparing dual-bolus and uncorrected single bolus myocardial blood flow estimates have not shown significant differences in diagnostic accuracy (266). Our diagnostic accuracy values agree well with other studies in the literature, suggesting that these limitations have not significantly impacted on our findings. Bystander disease in the way of significant LAD or CX or concomitant RCA disease was not excluded but may contribute to perfusion defects seen; this would have decreased numbers further and LMS disease is rarely seen in isolation.

3.4.2. Conclusion

This study shows that visual stress perfusion CMR had higher diagnostic accuracy than MPS-SPECT to detect significant LMS or LMS equivalent disease. Quantitative perfusion CMR by Fermi-constrained deconvolution had similar performance to visual CMR perfusion analysis.

4. Quantitative deformation analysis differentiates ischaemic and non-ischaemic cardiomyopathy: sub-group analysis of the VINDICATE trial

4.1. Background

Heart failure with reduced ejection fraction (HFrEF) is caused by a diverse range of pathologies that contribute to the overall syndrome (267–269). Identification of the aetiology of cardiomyopathy provides both insights into the pathophysiology, as well as directing specific therapeutic interventions, whilst conferring prognostic information (268, 269). Ischaemic and non-ischaemic cardiomyopathy can manifest extremely similar phenotypes, though management may be divergent and consequently current guidelines suggest clarification of the aetiology for this reason (268, 269). Multi-parametric CMR can help to distinguish these aetiologies (269).

Strain, twist and torsion are measures of myocardial performance beyond ejection fraction. Strain is an index of deformation from the initial to maximal length of a myocardial segment (%) (270). Twist ($^{\circ}$) describes the relative rotation between the apex and base of the ventricle (peak difference between systolic rotation of LV apex and base viewed from the apex/). Torsion ($^{\circ}$) describes the complex “wringing” motion of the left ventricle that is influenced by of both the twisting motion of the heart and size of the ventricular cavity (271). The torsional shear angle ($^{\circ}$) is calculated by measuring the radius of the apical and basal slices multiplied by the twist and divided by the distance between them (234). In the normal heart the base of the ventricle rotates clockwise during systole whilst the apex rotates counter clockwise (234). Left ventricular torsion is a primary component of normal systolic function and has been identified as a sensitive marker for transplant rejection, myocardial ischaemia and infarction, successful ventricular reconstruction surgery as well as a predictor of responsiveness to cardiac resynchronisation therapy (272–277). These parameters can be quantified by CMR tissue tagging techniques, which are highly reproducible and recognised as the reference standard non-invasive measures of myocardial strain and torsion (233, 273, 278–280).

The VINDICATE (Vitamin D treating patients with Chronic heart failure) trial was a randomised placebo-controlled double-blind trial designed to describe the safety and efficacy of long-term, high-dose vitamin D₃ supplementation on submaximal exercise capacity and cardiac function in vitamin D-deficient patients with chronic heart failure due to left ventricular systolic dysfunction already established on optimal medical therapy (230). A subgroup of the study underwent additional investigation using multi-parametric CMR. In this sub-study we investigated the relationship between strain-derived parameters and aetiology of HFrEF and hypothesised that in a prospectively recruited random sample of HFrEF patients ICM and NICM would have distinctive myocardial torsion patterns.

4.1. Methods

4.1.1. Study participants

The inclusion criteria for VINDICATE have been previously reported (230). In summary, all patients had stable (>3 months) NYHA functional class II or III symptoms, a LVEF \leq 45% on maximally tolerated medical therapy (>3 months) and a 25(OH) vitamin D level of <50 nmol/l (<20 ng/ml). Patients were invited to enter the CMR substudy at their initial enrolment visit. Exclusion criteria included history of taking calcium or other vitamin supplements in the preceding 3 months; aetiology of chronic HF due to untreated valvular heart disease, anaemia or thyrotoxicosis; existing indications for vitamin D supplementation; history of primary hyperparathyroidism, sarcoidosis, tuberculosis or lymphoma; cholecalciferol concentration >50 nmol/l (20 ng/ml); or if there was significant renal dysfunction (estimated glomerular filtration rate <30 ml/min/1.73m²)(230). Aetiology of heart failure was determined by the enrolling clinician. ICM was defined as left ventricular dysfunction associated with previous significant coronary disease (>70% in at least one major epicardial coronary artery) on angiography, positive ischaemia testing with MPS-SPECT or stress echocardiography and/or history of previous myocardial infarction or revascularisation (230); NICM was defined as left

ventricular dysfunction in the absence of the previous conditions. A control group of age-matched volunteers with no significant co-morbidities were enrolled and underwent an identical CMR protocol.

The study was performed in accordance with the Declaration of Helsinki, with all patients providing informed written consent. The study protocol and other relevant documentation had been approved by the National Research Ethics Service [12/YH/0206]; VINDICATE was funded by the Medical Research Council, UK.

4.1.2. Cardiac Magnetic Resonance Protocol

CMR was performed on a 3 Tesla Philips Achieva system (Philips Healthcare, Best, The Netherlands) equipped with a 32 channel coil and MultiTransmit® technology. Data was acquired at end expiration during breath-holding. Cine images were acquired covering the entire heart in the LV short axis plane (balanced steady state free precession), spatial resolution $1.2 \times 1.2 \times 10 \text{mm}^3$, 30 cardiac phases TR/TE 2.6/1.3ms, flip angle 40° , field of view 300-420mm, typical temporal resolution 39ms) and in orthogonal long-axis planes. Tissue tagging by spatial modulation of magnetization (spatial resolution $1.51 \times 1.57 \times 10 \text{mm}^3$, tag separation 7 mm, ≥ 18 phases, typical TR/TE 5.8/3.5ms, flip angle 10° , typical temporal resolution 55ms) was acquired in three short axis slices at the apex, mid-ventricle, and base. Consistent slice positioning was performed according to the widely accepted “3 of 5 technique” (281). LGE imaging was undertaken 15 minutes following administration of 0.15mmol/kg gadolinium DTPA (Gadovist, Bayer Schering) using an inversion recovery-prepared T1-weighted gradient echo pulse sequence. Selection of the appropriate TI to null normal myocardial signal was ascertained by the Look-Locker approach. Between 10 and 12 short axis slices and, 2 chamber and 4 chamber images were acquired for each participant. Imaging on 3.0T would yield analogous results if imaged at 1.5T.

4.1.3. Image Analysis

CMR data were analysed quantitatively using commercially available software (CVI42, Circle Cardiovascular Imaging Inc. Calgary, Canada and inTag v1.0, CREATIS lab, Lyon, France). Endocardial borders were traced on the LV cine stack at end-diastole and end-systole to calculate end diastolic volume, end systolic volume, stroke volume and ejection fraction. Contours were traced to exclude papillary muscles and trabeculations. Volumetric data were indexed to body surface area calculated by the Mosteller equation. LGE was assessed quantitatively using the semi-automated full width half maximum method.

For tagging analysis, endocardial and epicardial contours were drawn on the short axis spatial modulation of magnetization images using a semi-automated process (Figure 4-1). Peak circumferential LV strain was measured for the three slices at apex, mid-ventricle, and base. Strain was measured in the mid-myocardial layer which has previously been reported to be the most reproducible (233). LV twist was calculated by subtracting the basal from apical rotation. Basal and apical radius was calculated from cine images in diastole at the same slice location as the tagged images. The equation used to determine torsion was (234):

$$Torsion = \frac{Peak\ Twist \times (Apical\ Radius + Basal\ Radius)}{2 \times Apex\ to\ Base\ length}$$

Feature tracking rather than spatial modulation of magnetization was used for the analysis of global longitudinal strain. For this, endocardial and epicardial contours were drawn on 4 chamber cine images using a semi-automated process and peak longitudinal strain and systolic strain rate were measured for the LV.

4.2. Statistical Analysis

Statistical analysis was performed using IBM SPSS® Statistics 20.0 (IBM Corp., Armonk, NY). Continuous variables were expressed as means \pm SD. Categorical variables were expressed as N (%). Normality of data was tested using a Shapiro-Wilk test. Unpaired Student t-test and Mann-Whitney were

used as appropriate to compare continuous variables. Chi-square test was used for categorical data. $P < 0.05$ was considered statistically significant.

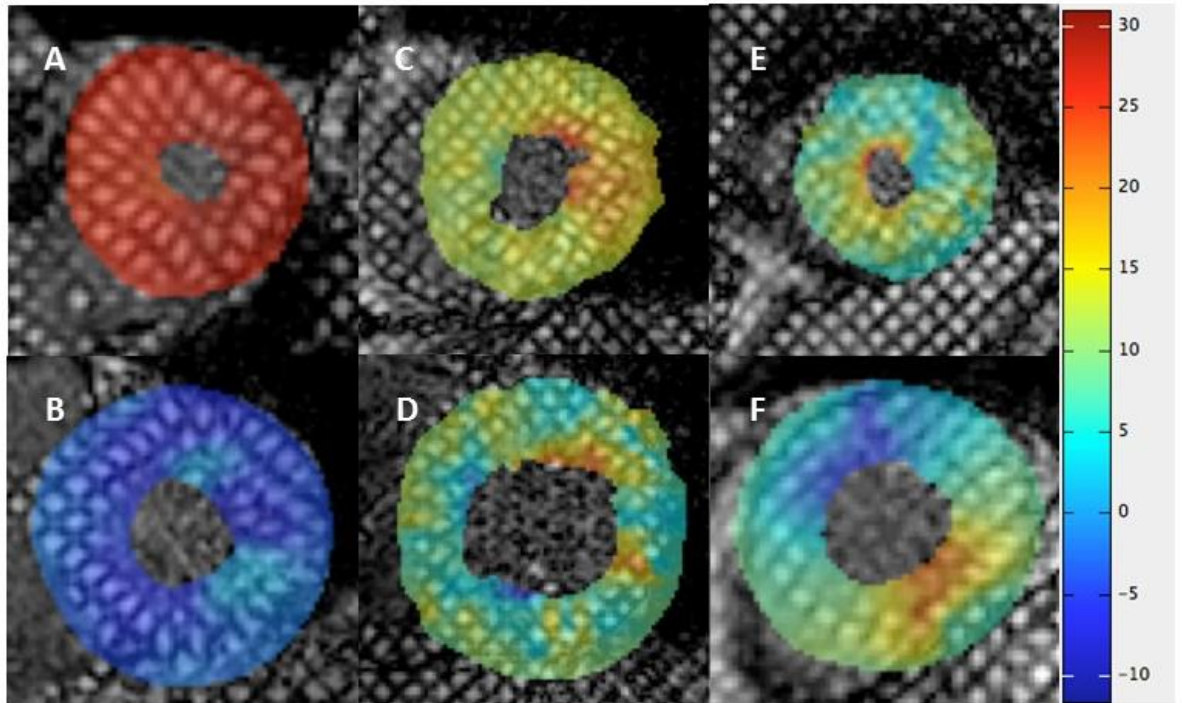


Figure 4-1 Tagged images in inTag© analysis.

Images A shows apical systolic anticlockwise rotation (red) and **B** clockwise basal rotation (blue) in a healthy control. **Images C** shows reduced apical (yellow/red) and **D** basal (yellow/green) rotation in a patient with ischaemic cardiomyopathy. **Images E** shows markedly reduced apical (yellow/green) and **F** basal rotation (yellow/green blue) in a patient with non-ischaemic cardiomyopathy. (282)

4.3. Results

223 patients were enrolled in VINDICATE, but as CMR was not mandated in the clinical trial protocol, only a subgroup of 69 patients underwent a baseline CMR scan. Of these 53 had myocardial tagging sequences performed and were included in this analysis. 25 age-matched controls with no co-morbidity and taking no regular medication underwent an identical CMR scan. Table 4.1 shows the demographic data for the combined HF group and controls. There were no significant differences between age, height, weight and body mass index (BMI). Table 4.2 shows the CMR imaging characteristics and strain parameters of both the HF and control groups. Compared with controls, patients with HF had significantly larger ventricles when indexed to body surface area and significantly lower values of LVEF, LV torsion and twist, circumferential and longitudinal strain.

Table 4.3 shows the baseline demographics between the ICM and NICM patients. There were no significant differences between groups in terms of age, blood pressure, heart rhythm or baseline NYHA status. ICM patients had undergone significantly more prior revascularisation (PCI, CABG) than NICM patients. Table 4.4 shows CMR volumetric data and functional parameters between the ICM and NICM patients. There was no significant difference in LV dimensions, LV mass and EF between the two groups. ICM patients had significantly more infarct pattern LGE than NICM (77% vs. 0% $p < 0.001$). Mean percentage of infarction was $19.0 \pm 7.6\%$ in the ICM group. Three patients in the NICM group had mid wall pattern late enhancement, no other late enhancement patterns were seen in this group. Strain parameters showed no differences in circumferential strain at any short axis level or in terms of global longitudinal strain (GLS) between the two groups. NICM patients had significantly lower LV twist ($6.0 \pm 3.7^\circ$ vs. $8.8 \pm 4.3^\circ$, $p = 0.023$) (figure 4-2) and torsion ($5.9 \pm 3.5^\circ$ vs. $8.8 \pm 4.7^\circ$, $p = 0.017$) compared to the ICM group. There was no significant correlation of twist ($r = -0.113$ $P = 0.424$) or torsion ($r = -0.096$ $P = 0.4938$) with patient functional assessment measures from a standard six minute walk test.

Table 4-1 Demographic details for HF and healthy control group

	HF group (53)	Controls (25)	P-value
Age, years	62.6±16.4	58.0±12.2	0.164
Sex (female)	17 (32.1)	7 (28)	0.716
Height, cm	170.1±7.8	172.9±12.6	0.389
Weight, kg	78.9±15.1	80.2±18.6	0.762
Body Mass Index, kg/m ²	27.2±4.7	26.6±3.3	0.527
Systolic Blood Pressure, mmHg	117.3±19.8	127.7±14.6	0.026
Diastolic Blood Pressure, mmHg	70.8±10.9	70.2±12.1	0.828
Diabetes Mellitus, %	7 (13)	0	0.122
CABG, %	10 (18.9)	0	0.020
PCI, %	17 (32.1)	0	0.001
AF, %	34 (64.2)	0	<0.001
COPD, %	2 (3.8)	0	0.325

Data as mean ± SD or n (%). AF, atrial fibrillation. CABG, coronary artery bypass grafting. COPD, chronic obstructive pulmonary disease. PCI, percutaneous coronary intervention.

Table 4-2 CMR data for HF group and controls

	HF (53)	Controls (25)	P-value
LVEDV, ml	210.5±85.4	160.0±44.7	0.007
LVEDVi, ml/m ²	109.2±38.9	82.2±19.9	<0.001
LVESV, ml	141.6±81.8	68.6±25.3	<0.001
LVEF, %	35.5±10.9	57.6±7.0	<0.001
LGE, (%)	26 (49.0)	0	<0.001
LV twist, °	7.6±4.3	14.6±4.2	<0.001
LV torsion, °	7.6±4.5	13.4±3.1	<0.001
E _{cc} Apex, %	10.4±6.8	22.2±5.3	<0.001
E _{cc} Mid, %	10.4±6.6	21.7± 2.3	<0.001
E _{cc} Base, %	9.6±6.2	20.5±2.6	<0.001
LV longitudinal strain, %	11.0 ±7.3	18.4±2.2	<0.001
LV longitudinal strain rate, %/s	56.5±39.9	93.7±15.9	<0.001

Data as mean ± SD or n (%). E_{cc}, Circumferential strain. LVEDV, left ventricular end diastolic volume. LVEDVi, left ventricular end diastolic volume indexed to body surface area. LVEF, left ventricle ejection fraction. LVESV, left ventricular end systolic volume.

Table 4-3 Baseline demographic data for ischaemic and non-ischaemic cardiomyopathy patients

	ICM (31)	NICM (22)	P-value
Age, years	65.2±15.9	59.0±16.9	0.182
Sex (female)	9, 29%	8, 36%	0.573
Height, cm	170.1±8.1	170.0±7.4	0.970
Weight, kg	78.5±14.2	79.7±16.6	0.773
Body Mass Index, kg/m ²	26.9±3.9	27.6±5.6	0.654
Systolic Blood Pressure, mmHg	119±21	115±18	0.399
Diastolic Blood Pressure, mmHg	70±11	72±11	0.601
Heart rate, bpm	69.2±10.8	69.6±9.5	0.903
Diabetes Mellitus, %	6 (19)	1 (4.5)	0.117
COPD, %	1 (3.2)	1 (4.54)	0.804
CABG, %	10 (32)	0 (0)	0.03
PCI, %	17 (55)	0 (0)	<0.001
AF, %	20 (65)	14 (64)	0.948
BNP, pg/mL	1084±1196	1118±1172	0.421
VO ₂ max, mlO ₂ /min/kg	16.8±5.0	19.7±7.7	0.162
NYHA class II, %	30 (96.8)	22 (100)	0.395
NYHA class III, %	1 (4)	0 (0)	0.395
Beta blockers, %	29 (93.5)	19 (86.4)	0.378
ACEi/ARB, %	28 (90.3)	22 (100)	0.133
Aldosterone antagonist, %	17 (54.8)	11 (50)	0.728
Creatinine, µmol/l	87.5±20.9	80.4±20.6	0.227

Data as mean \pm SD or n (%). AF, atrial fibrillation. ACEi, angiotensin-converting enzyme inhibitor. ARB, aldosterone receptor blocker. BNP, natriuretic peptide. CABG, coronary artery bypass grafts. COPD, chronic obstructive pulmonary disease. NYHA, New York Heart Association functional class. PCI, percutaneous coronary intervention.

Table 4-4 CMR characteristics for ischaemic and non-ischaemic cardiomyopathy patients

	ICM	NICM	P-value
LVEDV, ml	199.4±56.7	226±113.9	0.317
LVEDVi, ml/m ²	104.9±30.5	115.3±48.5	0.343
LVESV, ml	132.8±56.0	153.9±108.8	0.359
LVEF, %	35.1±10.6	36.0±11.7	0.767
LVM, g	134.9±42.6	141.8±70.1	0.655
LVMi, g/m ²	70.4±20.9	72.2±28.9	0.795
LVM/EDV g/ml	0.7±0.3	0.7±0.2	0.378
LGE infarct pattern, %	24. 77.4%	0. 0%	<0.001
LGE mid wall pattern, %	0. 0%	2. 9.0%	0.162
LGE, % of myocardial mass	19.0±7.6%	1.4±4.5	<0.001
LV twist, °	8.8±4.3	6.0±3.7	0.023
LV torsion, °	8.8±4.7	5.9±3.5	0.017
E _{cc} Apex, %	10.1±6.5	10.9±7.4	0.689
E _{cc} Mid, %	10.3±6.8	10.7±6.6	0.828
E _{cc} Base, %	8.2±6.8	11.4±4.8	0.064
LV longitudinal strain, %	10.8±7.3	11.3±7.5	0.837
LV longitudinal strain rate, %/s	54.2±37.1	59.7±44.2	0.629

Data as mean ± SD or n (%). E_{cc}, Circumferential strain. LGE, Late gadolinium enhancement. LVEDV, left ventricular end diastolic volume. LVEDVi, left ventricular end diastolic volume indexed to body surface area. LVEF, left ventricle ejection fraction. LVESV, left ventricular end systolic volume. LVM, left ventricular mass. LVMi left ventricular mass indexed.

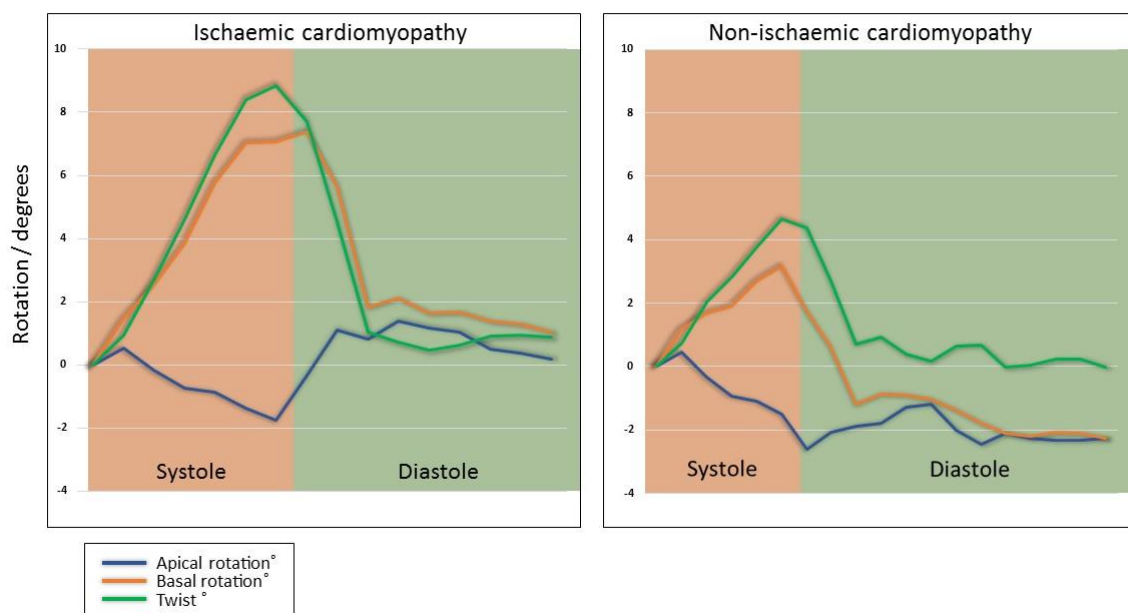


Figure 4-2 Plots showing apical (blue) and basal (orange) rotation and twist (green) of individual patients with ischaemic and non-ischaemic cardiomyopathy respectively.

In patients with ICM and no LGE (n=7), again there were no significant differences compared to NICM patients in CMR volumetric data (LVEDVi $95.5 \pm 15.4 \text{ ml/m}^2$ vs. $115.3 \pm 48.5 \text{ ml/m}^2$ $p=0.272$) or LVEF ($40.9 \pm 12.2\%$ vs. $36.0 \pm 11.7\%$ $p=0.332$). Furthermore, there were no significant differences between these groups in any strain parameters (E_{ccApex} $10.7 \pm 7.6\%$ vs. $10.9 \pm 7.4\%$ $p=0.947$, E_{ccMid} $11.8 \pm 9.3\%$ vs. $10.7 \pm 6.6\%$ $p=0.721$, E_{ccBase} $8.0 \pm 7.3\%$ vs. $11.4 \pm 4.8\%$ $p=0.168$, GLS $12.6 \pm 3.5\%$ vs. $11.3 \pm 7.5\%$ $p=0.627$). Notably, there was no significant difference in twist or torsion between the ICM patients without LGE and the NICM patients (twist $9.6 \pm 4.9^\circ$ vs. $6.0 \pm 3.7^\circ$ $p=0.051$, torsion $7.9 \pm 5.6^\circ$ vs. $5.9 \pm 3.5^\circ$ $p=0.248$).

4.4. Discussion

We have shown that all myocardial mechanical parameters including strain, twist and torsion were reduced in HF patients compared to age-matched controls. More importantly, despite having similar left ventricular dimensions, EF and strain parameters, patients with NICM have significantly less LV twist and torsion than patients with ICM.

Thus far there have been no comparisons of LV mechanics performed between different aetiologies of HFrEF. Our study identified a significant difference between LV torsion and twist in patients with different aetiologies of heart failure. Torsion and strain are currently not routinely measured during CMR imaging for cardiomyopathy, although CMR is the reference standard for these measurements and it is increasingly recommended to guide management (269). Our study shows that measurements of LV strain and torsion parameters measured by CMR can give potential mechanistic insights into the aetiology and pathophysiology of LV dysfunction. Prognostic benefit is seen with therapeutic interventions according to aetiology (283) and thus accurate delineation of aetiology becomes paramount (269).

Left ventricular torsion has been proposed as a mechanism to reduce myocardial fibre strain in order to improve energy efficiency and decrease oxygen demand (284, 285), whilst untwisting contributes to the diastolic function of the ventricle during isovolumetric relaxation (234). Torsion can be influenced by different loading conditions such as hypertension, athletic training and alters with increasing age (234, 286). LV torsion results as a consequence of the fibrous architecture of the heart (figure 4-3). Subepicardial fibres of the ventricle are arranged helically in a right handed oblique orientation of around 60°, whilst subendocardial fibres run in an opposing left handed helix of around 80° (234, 271, 287). This opposing arrangement of fibres results in shear deformation, with the predominant direction of force occurring in a clockwise direction as a result of the greater rotational radius of the subepicardial layer (284, 288).

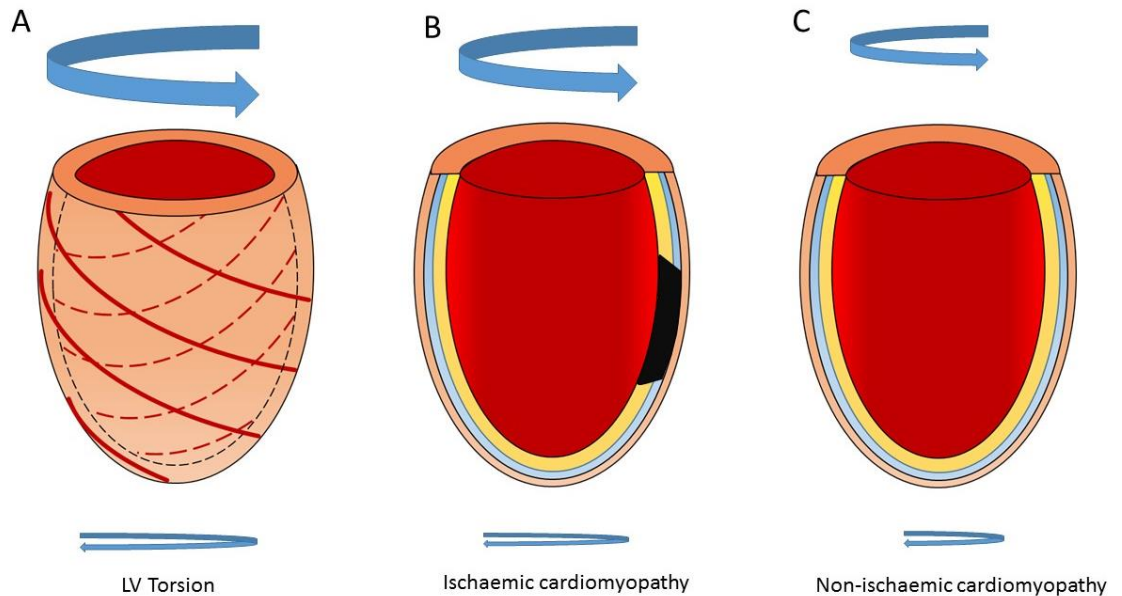


Figure 4-3 Schematic image of LV torsion in normal, ischaemic and non-ischaemic cardiomyopathy:

Image A shows the subepicardial fibres in red lines that are predominantly responsible for LV torsion. Dotted red lines represent subendocardial fibres arrayed in an opposing helix. The blue arrows show the predominant direction of twist with the base of the ventricle rotating clockwise during systole whilst the apex rotating counter clockwise. Image B shows ischaemic cardiomyopathy, with infarction/ischaemia in black typically affecting subendocardial fibres (yellow) and radial fibres (blue) with preferential sparing of the subepicardial fibres. Torsion is reduced (blue arrows) compared to normal due to some subepicardial fibres being affected. Image C shows non-ischaemic cardiomyopathy with global myocardial fibre dysfunction leading to significant reduction in torsion due to the effect on subepicardial fibres. (282)

In patients with IHD, the wave-front of myocardial ischaemia first affects subendocardial fibres prior to the subepicardial layer, with a similar effect on myocardial contraction patterns (20). In dog models of infarction, endocardial fibres show loss of tissue and function, while epicardial fibres demonstrate functional recovery, likely as a result of early reperfusion (289, 290). Correspondingly in man, Wu et al demonstrated by diffusion tensor MRI (291),

subendocardial right handed fibres reduced following infarction whilst the percentage of left handed fibres in the subepicardium increased, potentially as a result of a compensatory remodelling process (291). These structural changes are reflected in imaging studies of LV mechanics that show, according to the degree of transmural infarction, that subendocardial function is similarly reduced in both small and large STEMI, whilst subepicardial fibre function is reduced only in large STEMI (full thickness infarction) and is severely reduced in those with chronic ischaemic HF (the latter finding corresponding with the lack of significant difference seen in twist and torsion between the chronically ICM without scar and NICM) (274, 292, 293).

ICM tends to show regional dysfunction compared to NICM that shows more global myocardial fibre dysfunction (267). Torsion and twist have both been shown to be reduced in a variety of NICM (294–296). NICM can result in a variety of altered contraction patterns including a global reduction in torsion (297); paradoxical reversal of LV rotation with the base rotating counter clockwise and the apex rotating clockwise (298); and in some cases both apical and basal segments rotate in the same direction leading to “rigid body rotation” where the wringing motion of the ventricle is lost altogether (296). Furthermore a reduction in LV torsion is noted in tandem with the degree of spherical LV remodelling (294). These findings are consistent with our study that shows that patients with cardiomyopathy have a reduction of torsion compared to healthy controls, but also that patients with NICM have reduced torsion relative to ICM. The relative preservation of LV torsion in ICM compared to NICM ($8.8 \pm 4.7^\circ$ vs. $5.9 \pm 3.5^\circ$ $p=0.017$) seen in our study is explained by the differential effect on subepicardial fibres by necrosis and ischaemia in ICM with some regions spared, contrary to the global myocyte dysfunction seen in NICM. Furthermore it has been hypothesised that remaining subepicardial fibres in ICM undergo hypertrophy and recruitment as an active remodelling process following ischaemic insults thus contributing to the higher torsion values seen in ICM compared to NICM (290, 291).

Strain is a measure of myocardial deformation and has been proposed as being more sensitive to changes in LV mechanics than ejection fraction and is influenced by compensatory changes such as ventricular dilatation or geometrical change (270). Furthermore global longitudinal strain has been identified as a marker of prognosis over and above ejection fraction in a variety of conditions (299, 300). In our study, neither EF nor strain parameters were significantly different between cardiomyopathy of either aetiology. GLS is predominantly a result of subendocardial longitudinal fibres, whilst circumferential strain is attributed to the radial fibres that are distributed in the mid-wall of the ventricle and the subepicardial fibres (271, 287, 300–302). These fibres in, or adjacent to, the subepicardium are affected by ischaemia prior to the subepicardial fibres and thus intuitively circumferential and longitudinal strain are reduced greater than LV torsion in ICM, whilst leading to the similar strain values seen in patients with NICM.

4.4.1. Limitations

Our observational study has a number of limitations. The sample size is relatively small and differences in baseline demographics, comorbidities and treatment may be a potential source of bias. However both cardiomyopathy groups and controls were prospectively enrolled, and were age-matched, which is an important consideration as age has been shown to affect strain, torsion and twist (303). Through plane motion is a limitation of using 2D tagging methods. This may have an effect due to the global deformation changes seen in NICM versus local changes in contractile properties in ICM. The 2D method used in our paper has consistently been shown to be reliable and reproducible in a variety of patient groups(233, 286, 304, 305), and 2D and 3D tagging methods for LV torsion have been shown to strongly related (306). Currently 3D methods of CMR tagging are time consuming requiring multiple breath holds of long duration (307, 308), thus from a pragmatic point of view we used a reproducible 2D method that required a single breath hold per slice that in general HF patients would be able to tolerate. Estimation of diffuse fibrosis by T1 mapping and extracellular myocardial volume fraction

extracellular myocardial volume fraction (ECV) calculation were not performed in this study, which may have provided further insight.

4.5. Conclusion

Twist, torsion and strain are reduced in patients with cardiomyopathy compared to controls. Torsion and twist are significantly lower in patients with NICM compared to ICM, despite similar volumetric dimensions, circumferential and longitudinal strain parameters and LVEF.

5. Development and validation of a contemporary pre-test likelihood model of coronary artery disease referenced to invasive angiography, with comparison to pre-existing risk models

5.1. Introduction

Coronary artery disease remains a leading cause of death worldwide and invasive X-ray coronary angiography is frequently performed in the investigation pathway (8). Increasingly non-invasive imaging acts as a gatekeeper to invasive angiography and is recommended by Societal guidelines,(8, 27) in which pre-test likelihood scores quantify coronary artery disease risk and guide further investigation. US guidelines historically recommended the Diamond and Forrester risk model,(27, 33) based on Bayesian principles according to age, gender and typicality of chest pain symptoms. The 2010 UK National Institute for Health and Care Excellence CG95 guidelines and current US practice guidelines, the Duke Score, a modified Diamond and Forrester model incorporating additional clinical risk factors was advocated (27, 30, 309) (Table 5.1). These risk models however, are over three decades old and derived from highly selected patient populations; consequently they have been shown to overestimate coronary artery disease risk (310–313). Subsequently the CAD Consortium Basic and Clinical risk models were developed, based on contemporary patient populations and are recommended in the ESC guidelines (8, 311, 312). The CAD Consortium study population however, was derived from a number of diagnostic accuracy studies with considerable heterogeneity of disease prevalence between different sites, and variation between endpoints (computed tomography coronary angiography or invasive catheter angiography with different methods of analysis); furthermore until recently there has been no external validation of the scores (312–314).

The 2016 update to the UK NICE CG95 guideline no longer recommend pre-test likelihood calculation to determine investigation strategy (315). Whilst controversial, this may be in part due to perceived limitations of the previously recommended Duke Score and lack of applicability to a contemporary UK population. The aim of this study was to both develop and validate a contemporary multivariable risk model based entirely on invasive angiographic data (using data from two recent UK studies of stable coronary artery disease (CE-MARC and CE-MARC 2: Clinical evaluation of magnetic resonance imaging in coronary heart disease study)), and compare this to pre-existing risk models used in clinical guidelines (35, 63, 96, 203).

Table 5-1 Characteristics of risk models used

	Risk Scores			
	DF	Duke	CAD Basic	CAD Clinical
Year	1979	1993	2012	2012
Population	4952	168	5677 (3283 male)	5677 (3283 male)
Risk factors	Age, sex, angina typicality	Age, sex, angina typicality, previous MI, smoking, DM, hyperlipidaemia, ECG Q waves or ST-T changes	Age, sex, angina typicality	Age, sex, angina typicality, DM, smoking, HTN, hyperlipidaemia
Setting	US	US single centre	Europe and US (18 hospitals)	Europe and US (18 hospitals)
Investigation	Angiography/ Autopsy	Angiography	CTCA (5190) Angiography (2062)	CTCA (5190) Angiography (2062)
Outcome – coronary stenosis	≥50%	≥75%	≥50%	≥50%

DF – Diamond and Forrester

5.2. Methods

5.2.1. Patients

The development population was derived from the CE-MARC study,(63, 96) which recruited from May 2006 to August 2009 in a single centre (Leeds General Infirmary, Leeds, UK); inclusion criteria and study protocol have been described previously (96). In brief, inclusion criteria were stable chest pain symptoms thought to be angina pectoris, aged 35-79 years, in sinus rhythm, and suitable for revascularisation if required. Exclusion criteria included prior coronary artery bypass grafting, unstable chest pain symptoms, and pregnancy. By protocol, all participants were expected to undergo invasive angiography. Of 752 CE-MARC participants, 77 were excluded from this analysis due to prior percutaneous coronary intervention or myocardial infarction/acute coronary syndrome, in whom pre-test likelihood was already 100%. Figure 5-1 shows the derivation of participants in the development population.

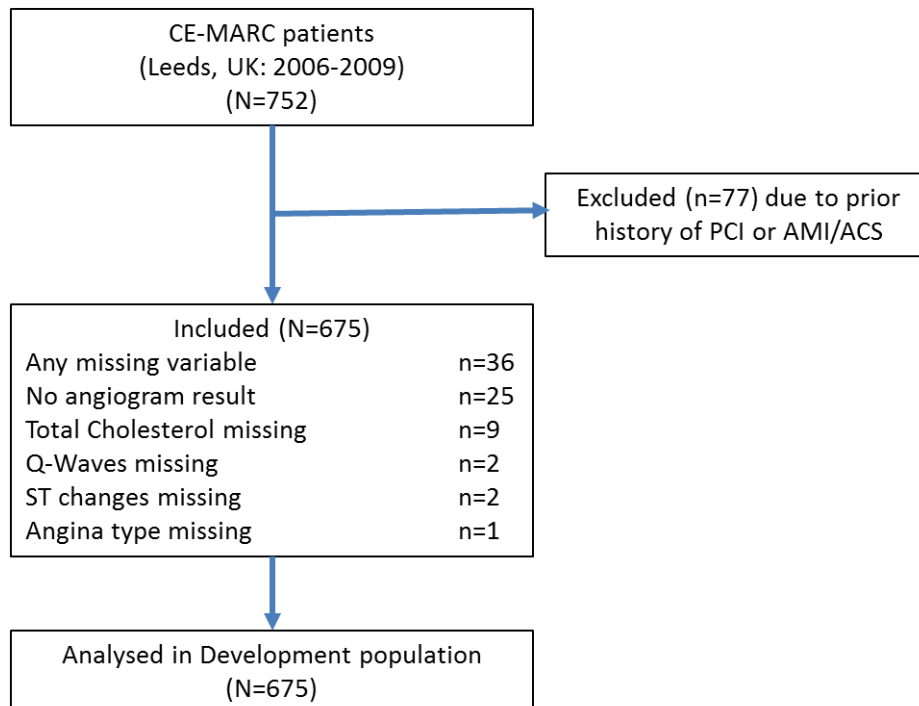


Figure 5-1 Image panel showing angiography and CMR perfusion

The validation population was drawn from two sources: 1) The multi-centre CE-MARC 2 trial which enrolled 1,202 patients from November 2012 to March 2015,(35, 203) with estimated pre-test likelihood of coronary artery disease of 10-90% aged ≥ 30 yrs with suspected stable angina requiring further investigation, no prior myocardial infarction/acute coronary syndrome or revascularisation. From this trial, 264 patients were included in the validation population based on them having invasive angiography within 12 months of randomisation. 2) The validation population was added to by an “enrichment population” by obtaining anonymised data of patients consecutively undergoing elective coronary angiography for investigation of suspected coronary artery disease at Leeds General Infirmary with estimated pre-test likelihood $< 10\%$ or $> 90\%$ during the period October 2014 to 2016.

CE-MARC and CE-MARC 2 were conducted in accordance with the Declaration of Helsinki (2000); CE-MARC was approved by the UK National Research Ethics Service (05/Q1205/126); CE-MARC 2 was approved by the UK National Research Ethics Service (12/YH/0404) (35, 63). Figure 5-2 shows derivation of the validation population.

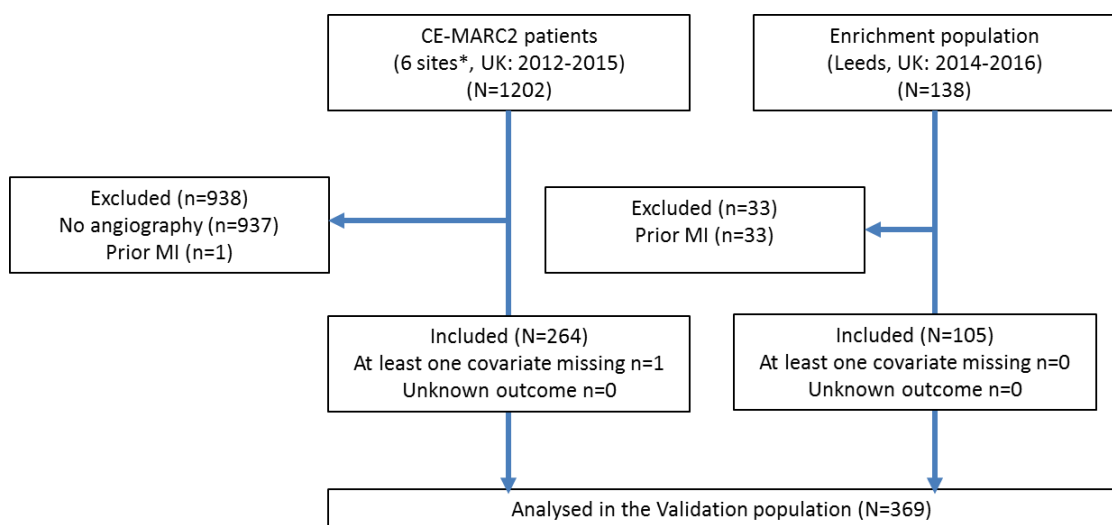


Figure 5-2 Image panel showing angiography and CMR perfusion

5.2.2. Classification of Chest Pain and Risk Factors

Chest pain symptoms were classified as typical, atypical, or non-anginal (8, 27, 316). Typical chest pain was defined as all following criteria: (1) substernal chest pain or discomfort (2) provoked by exertion or emotional stress and (3) relieved by rest or nitroglycerine (or both). Atypical chest pain was defined as any two of these criteria. If one or none of the criteria was present, symptoms were classified as non-anginal (8, 27, 316). Systemic arterial hypertension was defined as systolic blood pressure >140 mmHg, diastolic blood pressure >90 mmHg (at >1 occasion) or current diagnosis of hypertension or treatment with blood pressure lowering drugs. Hyperlipidaemia was defined as either serum cholesterol >6.47 mmol/L or patient on medication for hyperlipidaemia. Diabetes mellitus was defined as a prior physician based diagnosis (HbA1c ≥ 6.5) or use of glucose lowering drugs. Smoking was defined as current, former or never. Family history of premature coronary artery disease was defined as any first degree relative with history of myocardial infarction, or revascularisation <55 years in men and <65 years in women. All patients had an ECG performed at their initial clinic visit.

5.2.3. X-ray Angiography

All patients enrolled in CE-MARC were scheduled by protocol for X-ray coronary angiography, (63, 96) and analysed by two experienced cardiologists. Clinically significant coronary artery disease was defined as $\geq 70\%$ stenosis of a first order coronary artery measuring ≥ 2.5 mm in diameter, or LMS stenosis $\geq 50\%$ as measured by quantitative coronary angiography with use of QCAPlus software (version 8.11.19 Sanders Data Systems, Palo Alto, California, USA); a post-stenosis diameter was used as the reference vessel diameter in cases of ostial disease.

In those patients that underwent X-ray angiography in CE-MARC 2, (203) fractional flow reserve measurement (St Jude Medical) was recorded in all arteries ≥ 2.5 mm with visually recorded diameter stenosis $\geq 40\%$ and $\leq 90\%$. Where fractional flow reserve could not be performed due to clinical/safety

reasons, quantitative coronary angiography was performed. Fractional flow reserve and quantitative coronary angiography measurements were made by a single independent blinded observer at the Glasgow Angiographic Core Laboratory. For the enrichment population, quantitative coronary angiography analysis was performed as per the CE-MARC study (63, 96).

5.2.4. Model Development

From the demographic and clinical variables collected in CE-MARC, we specifically examined patient age, sex, angina type, diabetes mellitus, current smoking, hypercholesterolaemia, diagnosis of hypertension, ECG Q-wave abnormalities and ST segment changes. These covariates were chosen as they were used in existing Duke risk score and CAD Consortium Clinical models (309, 312). Family history of premature heart disease was not thought to be as strongly related and was not fully available in the enrichment population, so was not considered further for model development. We treated age as a linear term in our model, and did not consider any interaction terms. Figure 5-3 illustrates selection of predictors for use in developing the risk model.

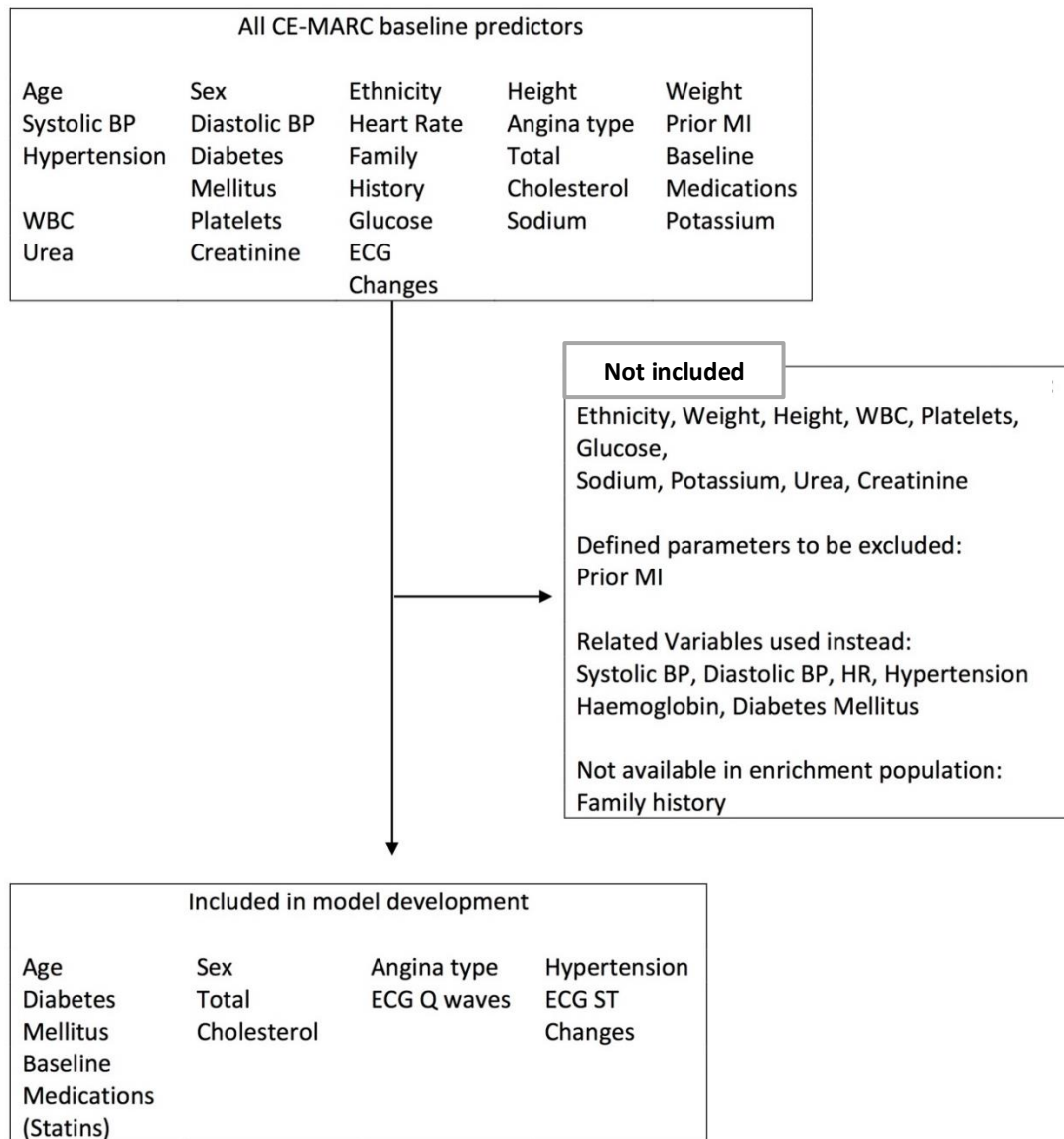


Figure 5-3 predictors used in developing the risk model

Binary logistic regression was used to model log-odds of significant angiographic stenosis as a function of all candidate predictors. We did not employ stepwise selection methods: all covariates were included in the development model, regardless of statistical significance or size of effect. Since 84 patients (12.4%) of the development population had incomplete data for either one or more predictor and/or the outcome (Figure 5-1) we used multiple imputation (fully conditional specification or multiple imputation by chained equations)(317, 318) to create 20 fully-complete datasets. We then

fitted our regression model to each dataset, and combined the resulting parameter estimates across all analyses using the methods of Rubin,(319) to give the overall apparent risk model. Internal validation was performed by the regular bootstrap validation method using 200 bootstrap samples to assess any need to penalise model performance or adjust estimated coefficients due to overfitting (320). We estimated discrimination (area under the receiver operating characteristic curve) and calibration in the development population. Calibration was assessed in a two-step process: calibration-in-the-large (representing difference in overall coronary artery disease prevalence) was assessed by fitting a new intercept term holding the existing risk score constant; logistic miscalibration was estimated by fitting the risk score to a model that included the risk model itself, and the calibration-in-the-large term as offset variables (set equal to one), and the risk model again as a covariate. Logistic miscalibration would be concluded if the regression parameter was significantly different from zero (311, 312). Model 'optimism' was calculated, which is a measure of how different the discrimination/calibration metric is for the model we developed, compared to what it was on average during the internal validation process. Small values of 'optimism' are preferred, since they suggest that model performance reported will be similar to what others may see in clinical practice.

5.2.5. Validation

The developed model was validated in the independent external validation population. We derived the risk score for all participants, and from that the predicted pre-test likelihood of coronary artery disease using our new model. We then estimated the discrimination and calibration in the same manner as for development. Any missing covariates were imputed using multiple imputation. However, positive angiography (or not) was known for all participants in the validation population, since angiography defined inclusion for CE-MARC 2 patients, and was not missing for any patient in the enrichment population.

To put our results into current clinical context, we used the validation populations to independently validate the performance of four existing coronary artery disease risk models: Diamond and Forrester (extended version), Duke clinical risk score and CAD Consortium Basic and Clinical risk models (33, 309, 311, 312). We estimated their discrimination and calibration in the same manner. For completeness, we also repeated this for the development population.

5.3. Results

5.3.1. Development and internal validation

Of 752 CE-MARC patients, 675 were included in the development population. Twenty-five of these (3.7%) had unknown angiogram results and 36 (5.3%) had at least one covariate and/or angiogram outcome unknown. Table 5.2 shows patient demographic characteristics according to presence or absence of significant angiographic stenosis. After multiple imputation of missing baseline and outcome data, and fitting all covariates, the CE-MARC risk model (Table 5.3) was derived. Internal validation of the model by regular bootstrap did not reveal any concerns of overfitting: the apparent discrimination measured by area under the receiver operating characteristic curve was 0.779 (95% CI:0.742, 0.814; bootstrap estimated optimism -0.001) and parameters of apparent calibration under a 2-parameter approach were $\alpha=-0.02$ (95%CI:-0.22, 0.18; optimism=0.005) and $\beta=0.998$ (95%CI:0.81, 1.19; optimism=0.002). Since estimated model 'optimism' resulting from overfitting was small, the model was not changed between development and external validation. Our 'optimism' in performance estimates was close to zero for all, i.e. final model performance was very close to that seen in internal validation.

Table 5-2 Demographic and clinical characteristics of participants in the development and validation populations

	CE-MARC (2006-2009) Development population				CE-MARC II (2012-2015) + Enrichment (2014-16) Validation population		
	Not CAD (n=415)	CAD (n=235)	No angiogram result (n=25)	Total (n=675)	Not CAD (n=211)	CAD (n=158)	Total (n=369)
Patient Age (Derived)							
Mean (SD)	57.9 (9.83)	62.1 (8.34)	57.5 (12.74)	59.4 (9.66)	58.2 (10.08)	61.5 (9.85)	59.6 (10.10)
Median (IQR)	59.0 (50.0, 66.0)	63.0 (57.0, 69.0)	59.0 (48.0, 66.0)	60.0 (52.0, 67.0)	58.0 (51.0, 65.0)	60.0 (54.0, 69.0)	59.0 (52.0 , 66.0)
Range	(35.0, 79.0)	(40.0, 79.0)	(37.0, 77.0)	(35.0, 79.0)	(25.0 , 85.0)	(39.0 , 86.0)	(25.0 , 86.0)
Male sex	213 (51.3%)	189 (80.4%)	15 (60.0%)	417 (61.8%)	94 (44.5%)	66 (41.8%)	160 (43.4%)
Chest Pain (Derived)							
Non-anginal chest pain	24 (5.8%)	5 (2.1%)	3 (12.0%)	32 (4.7%)	33 (15.6%)	-	33 (8.9%)
Atypical Angina	344 (82.9%)	139 (59.1%)	14 (56.0%)	497 (73.6%)	98 (46.4%)	56 (35.4%)	154 (41.7%)
Typical Angina	47 (11.3%)	90 (38.3%)	8 (32.0%)	145 (21.5%)	80 (37.9%)	102 (64.6%)	182 (49.3%)
Hypertension	211 (50.8%)	128 (54.5%)	15 (60.0%)	354 (52.4%)	74 (35.1%)	91 (57.6%)	165 (44.7%)
Current Smoker	79 (19.0%)	38 (16.2%)	9 (36.0%)	126 (18.7%)	44 (20.9%)	33 (20.9%)	77 (20.9%)
Dyslipidaemia	197 (47.5%)	149 (63.4%)	12 (48.0%)	358 (53.0%)	75 (35.5%)	95 (60.1%)	170 (46.1%)
Diabetic Type II	43 (10.4%)	27 (11.5%)	6 (24.0%)	76 (11.3%)	33 (15.6%)	28 (17.7%)	61 (16.5%)
ECG Q-Wave abnormality	22 (5.3%)	14 (6.0%)	-	36 (5.3%)	2 (0.9%)	13 (8.2%)	15 (4.1%)

	CE-MARC (2006-2009) Development population				CE-MARC II (2012-2015) + Enrichment (2014-16) Validation population		
	Not CAD (n=415)	CAD (n=235)	No angiogram result (n=25)	Total (n=675)	Not CAD (n=211)	CAD (n=158)	Total (n=369)
ECG ST segment abnormality	43 (10.4%)	29 (12.3%)	2 (8.0%)	74 (11.0%)	9 (4.3%)	11 (7.0%)	20 (5.4%)
CEMARC Clinical PTL							
Median (IQR)	24.5% (13.8% , 40.1%)	47.4% (34.0% , 69.0%)	37.9% (15.6% , 51.4%)	32.8% (17.6% , 51.3%)	32.7% (13.2% , 49.2%)	56.2% (39.3% , 69.2%)	42.2% (21.7% , 60.7%)
Diamond/Forrester (1979/2011) PTL*							
Median (IQR)	46.3% (31.4% , 69.8%)	77.6% (57.4% , 91.1%)	58.2% (23.0% , 82.0%)	57.4% (35.4% , 79.9%)	63.9% (31.4% , 83.3%)	85.1% (73.5% , 92.8%)	75.2% (48.5% , 89.1%)
Duke Risk Score (1993) PTL							
Median (IQR)	39.9% (21.2% , 68.6%)	75.8% (55.7% , 90.1%)	64.1% (17.5% , 85.1%)	56.2% (27.1% , 80.2%)	56.0% (18.9% , 75.9%)	79.7% (61.1% , 89.5%)	67.4% (35.6% , 83.3%)
CAD Consortium (2012) Basic PTL							
Median (IQR)	12.9% (7.3% , 24.6%)	30.9% (18.3% , 48.6%)	21.6% (8.0% , 42.5%)	18.3% (9.5% , 34.1%)	12.6% (6.5% , 39.3%)	22.7% (10.9% , 54.0%)	16.8% (7.7% , 47.0%)
CAD Consortium (2012) Clinical PTL							
Median (IQR)	11.8% (5.8% , 22.3%)	28.2% (16.6% , 48.8%)	26.9% (5.3% , 43.5%)	17.6% (8.2% , 32.7%)	11.4% (5.1% , 31.0%)	21.8% (9.9% , 57.2%)	14.8% (6.6% , 45.5%)

* The Diamond/Forrester risk score was implemented using the 2011 Genders et al model-based risk function, rather than the original 1979 lookup table. In validating this model, patients aged 70 and over had no score calculated. Numbers of participants with incomplete or unknown variable values are noted where they occur. For all other variables, data was 100% complete.

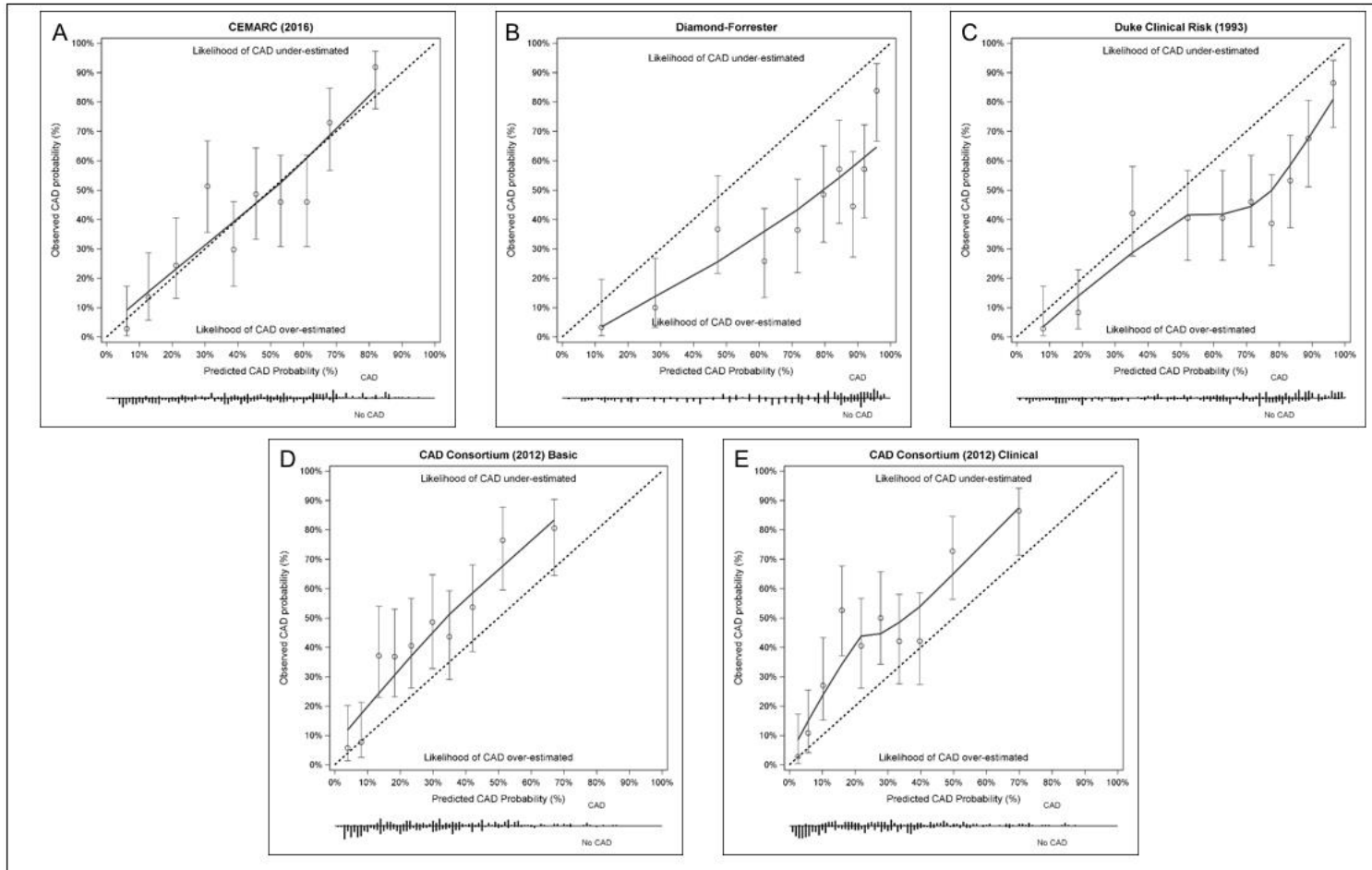


Figure 5-4 Calibration plots showing relation between predicted PTL and observed rates of CAD in the validation population

Figure 5-4 cont. Calibration plots showing the relation between predicted pre-test-likelihood of CAD and observed rates of CAD by decile in the validation population for (A) the CE-MARC risk model, (B) the Diamond and Forrester model, (C) the Duke Risk Score (1993), (D) CAD Consortium Basic risk score and (E) CAD Consortium Clinical risk score. The lower margin of each graph presents a histogram of the numbers of patients with each predicted risk score. * The Diamond/Forrester risk score was implemented using the 2011 Genders et al model-based risk function, rather than the original 1979 lookup table.

Table 5-3 Developed CE-MARC model

Model parameter	Estimated effect	Standard Error	P-Value
Intercept (Baseline: Male, non-anginal chest pain, no other risk factors)	-4.093	0.812	<.001
Per year of patient age	0.046	0.011	<.001
Sex: if female	-1.532	0.212	<.001
Symptoms: if atypical angina	0.609	0.524	0.245
Symptoms: if typical angina	1.997	0.554	<.001
Smoking: if current smoker	0.129	0.258	0.616
Diabetes: if Type II Diabetic	-0.247	0.307	0.420
Cholesterol: if total cholesterol > 6.47mmol/L OR current lipid-lowering therapy	0.481	0.192	0.012
ECG: If Q-Waves present	0.648	0.397	0.103
ECG: if S-T segment changes present	0.012	0.293	0.966
Hypertension: if diagnosed hypertensive	0.140	0.189	0.460

Footnote: to obtain the risk score, add up the intercept and the values related to each characteristic present in the patient (regardless of statistical significance). The pre-test likelihood is then given by the function $\text{Prob}(\text{CAD}) = 1 / (1 + \exp(-\text{Risk Score}))$. For example: For a 70 year old female patient with atypical angina, hypertension and no other risk factors, the Risk Score is $-4.093 + 70 \times 0.046 - 1.532 + 0.609 + 0.140$

= -1.656 and the pre-test probability is $\text{Prob}(\text{CAD}) = 1 / (1 + \exp(-(-1.656))) = 16.0\%$. Alternatively, a 65-year old male patient with non-anginal chest pain, Type II diabetes and currently smoking with no other risk factors has a risk score of $-4.093 + 65 \times 0.046 - 0.247 + 0.129 = -1.221$ and a pre-test likelihood of 22.8%

5.3.1. External Validation

Table 5-2 shows clinical and demographic characteristics of patients in the validation population. After imputing missing covariate values for the validation population, the CE-MARC model was found to discriminate well between patients with and without significant angiographic stenosis (c-statistic=0.777; 95%CI:0.731, 0.824). Figure 5-4 shows calibration of the CE-MARC model by plotting observed coronary artery disease proportions by calculated coronary artery disease rates for deciles of the population. An additional intercept term added to the model was not statistically significant (0.045; 95%CI:0.190, 0.280; P=0.71), neither was a coefficient representing logistic miscalibration (0.0275; 95%CI-0.214, 0.269; P=0.82).

5.3.2. Validation of other coronary artery disease risk models

Table 5-4 summarises discrimination and calibration of the models in the two populations. The performance of these models in development and validation populations were similar.

The Diamond and Forrester model and Duke Score were both very poorly calibrated. The “calibration-in-the-large” estimates were -1.548 (95%CI:-1.816, -1.279; P<0.001) and -1.016 (95%CI:-1.265, -0.766; P<0.001) respectively in the validation population indicating substantial overestimation of pre-test likelihood compared to the average in the two populations. After adjusting for the average over-estimation of coronary artery disease prevalence, the Duke model remained miscalibrated in the

validation population (logistic calibration -0.207: 95%CI:-0.363, -0.050; P=0.010) indicating that predicted probabilities of coronary artery disease at the extremes were in fact too extreme. After adjustment of the Diamond and Forrester model the overall miscalibration effect was not significant (-0.109: 95%CI:-0.256, 0.039; P=0.148). Figure 5-4B and 5-4C illustrate performance of the Diamond and Forrester model and Duke Clinical Risk score in the Validation population respectively.

Table 5-4 Model performance statistics (95% CI)

Model	Discrimination (c-statistic)	Calibration in the large (alpha)	Logistic miscalibration (beta)
Development			
CE-MARC	0.779 (0.742, 0.814)	-[a]	-[a]
Diamond- Forrester (1979)	0.7703 (0.7287, 0.8119)	-1.334 (-1.547,-1.121) P<0.001	-0.170 (-0.317, -0.023) P=0.024
Duke Risk Score (1993)	0.763 (0.725, 0.800)	-1.108 (-1.305, 0.911); P<0.001	-0.298 (-0.416, -0.180); P<0.001
CAD Consortium (2012) Basic	0.770 (0.733, 0.806)	0.713 (0.532, 0.893); P<0.001	-0.015 (-0.131, 0.101); P=0.803
CAD Consortium (2012) Clinical	0.762 (0.725, 0.7995)	0.822 (0.639, 1.005); P<0.001	-0.051 (-0.159, 0.057); P=0.354
Validation			
CE-MARC	0.777 (0.731, 0.824)	0.045 (-0.190, 0.280); P=0.709	0.028 (-0.214, 0.269); P=0.823
Diamond- Forrester (1979)	0.7547 (0.701, 0.808)	-1.548 (-1.816, -1.279) P<0.001	-0.109 (-0.256, 0.039) P=0.148
Duke Risk Score (1993)	0.752 (0.704, 0.801)	-1.016 (-1.265, -0.766); P<0.001	-0.207 (-0.363, -0.050); P=0.010
CAD Consortium (2012) Basic	0.755 (0.706, 0.803)	0.738 (0.507, 0.969); P<0.001	-0.007 (-0.182, 0.169); P=0.940
CAD Consortium (2012) Clinical	0.752 (0.703, 0.800)	0.866 (0.629, 1.103); P<0.001	-0.054 (-0.121, 0.105); P=0.507

Discrimination (c-statistic) is equivalent to the Area Under the ROC Curve, with 0.5 meaning no ability to discriminate. Calibration in the large (alpha) is found by fitting a logistic model in which only an intercept term can be fit, and the risk model's linear predictor is an offset term, set equal

to 1. Positive and negative values indicate that a model under or over estimates risk compared to the average for the population. Logistic miscalibration (beta) is estimated by taking the linear predictor for the model (adjusted for calibration-in-the-large) and fitting a logistic model with no-intercept, said linear predictor as an offset variable (set equal to 1) and the same linear predictor as a variable in the model. Positive and negative values indicate that the range of predicted values is too variable or too similar in relation to the spread of risk among the population. [a] A model that is validated in the same population as it was derived has perfect calibration, so no results are presented for this model.

The CAD Consortium Basic risk score underestimated risk of coronary artery disease in the validation population (0.738: 95%CI:0.507, 0.969; $P < 0.001$). Once this under-estimation was adjusted for, however, the recalibrated CAD Consortium Basic model performed well, with predicted probabilities more in line with observed rates of coronary artery disease (logistic miscalibration was -0.007: 95%CI:-0.182, 0.169; $P = 0.940$). Finally, the CAD Consortium Clinical risk model performed similarly to the Basic risk model. Calibration in the large showed that this model also underestimated risk of coronary artery disease in the validation population (0.866: 95%CI:0.629, 1.103; $P < 0.001$). Again, once adjusted, there was no evidence of logistic miscalibration in the validation population (-0.054: 95%CI:-0.121, 0.105; $P = 0.507$). Figures 5-4D and 5-4E illustrate the calibration performance of CAD Consortium Basic and Clinical risk models in the validation population. Figure 5-5 illustrates calibration of these four models when validated in the development population.

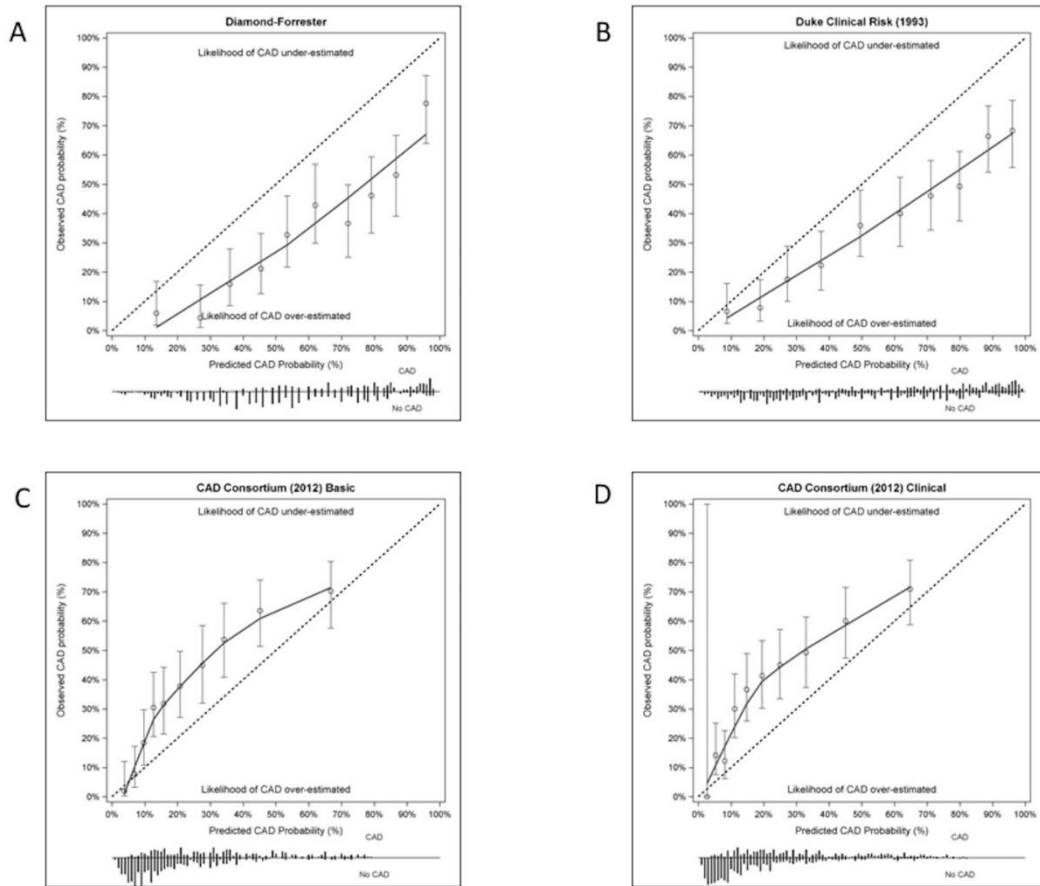


Figure 5-5 Calibration plots showing the relation between predicted pre-test-likelihood of CAD and observed rates of CAD by decile in the development population for (A) the Diamond and Forrester model (B) the Duke Risk Score (1993), (C) CAD Consortium Basic risk score and (D) CAD Consortium Clinical risk score. The lower margin of each graph presents a histogram of the numbers of patients with each predicted risk score.

5.4. Discussion

The newly-developed CE-MARC risk model, derived from a large contemporary UK population undergoing invasive angiography, performed very well for estimation of pre-test likelihood in the independent validation sample, without needing any adjustment for different risk prevalence or for miscalibration. In contrast, the earlier Diamond and Forrester and Duke risk models substantially over-predicted risk of coronary artery disease (and remained poorly-calibrated once this was corrected). The more recent CAD Consortium models (recommended in the ESC guidelines) slightly underestimated risk of coronary artery disease, but performed well once this was accounted for.

Both Diamond and Forrester and Duke Scores (recommended in US and prior UK NICE guidelines) have been recognised to overestimate presence of coronary artery disease in contemporary populations (33, 309–313). These models were developed over 30 years ago from high risk populations in the US (prevalence >60%). Since the inception of the Diamond and Forrester and Duke risk scores, prevalence of coronary artery disease has declined, with a reduction in rates of smoking, and significantly altered pharmacological management of cardiovascular risk factors (3, 321). Furthermore, with increased life expectancy many patients with stable chest pain present over the age of 70 whilst the Diamond and Forrester score only estimates risk for patients up to the age of 69 (33). As the performance of a prediction model is related to the population from which it is derived, unless these models are applied to a population with a high prevalence of coronary artery disease, risk will be overestimated. In contrast, the CAD Consortium models have been developed from lower risk populations derived from a constellation of diagnostic imaging studies (312). The CAD Consortium models have thus far been externally validated by Bittencourt, in a low risk US population referred for computed tomography coronary angiography, and recently the anatomical arm of the PROMISE trial (312–314, 322). The good fit of the CAD Consortium model observed in the study by Bittencourt however reflects the low-risk nature of

a population referred for non-invasive assessment (only 9% had typical chest pain and 47% had non-anginal chest pain symptoms) (312, 313). Application of the CAD Consortium models to the PROMISE dataset is significantly limited by the lack of 87% of the population having the primary endpoint (invasive angiography); furthermore addition of Coronary Artery Calcium scoring is of limited clinical benefit, as this information is unlikely to be available to physicians at time of initial patient consultation (314, 322).

5.4.1. Strengths of our study

The CE-MARC development population was derived prospectively from across the full spectrum of pre-test likelihood risk groups, as opposed to previous studies that have been derived from the amalgamation of diagnostic studies of non-invasive imaging modalities (leading to lower risk cohorts) or retrospective registries of invasive catheterization (leading to high risk cohorts) (63, 310–313, 323). Moreover, the CE-MARC protocol mandated all patients underwent invasive angiography regardless of non-invasive imaging findings or pre-test likelihood of coronary artery disease, thereby minimising verification bias (63, 96). Furthermore, we used consistent, clinically relevant endpoints from invasive angiography, contrary to recent studies estimating pre-test likelihood, principally derived from diagnostic accuracy studies of computed tomography coronary angiography, where correlation with invasive angiography was not mandated (310, 312, 313). Furthermore, in our study a stenosis of $\geq 70\%$ or fractional flow reserve < 0.8 was considered significant for coronary artery disease and applied to the pre-test likelihood score, as opposed to a threshold stenosis severity of $\geq 50\%$ or indeed a binary yes/no for the presence of coronary artery disease that has been used previously (33, 310–313).

5.4.2. Clinical implications

Despite a recognition of disease risk overestimation, Diamond and Forrester and Duke Scores are recommended in US guidelines, whilst the

updated 2016 NICE guidelines have dispensed with pre-test likelihood estimation altogether in favour of an anatomically guided approach with computed tomography coronary angiography (27, 33, 309, 315). Our results support findings by Bittencourt, which suggest that Diamond and Forrester and Duke Score overestimate pre-test likelihood of coronary artery disease and that adoption of a contemporary risk score potentially re-classifies patients from higher to lower risk groups, thus potentially leading to a reduction in the requirement for additional investigations (313). The use of a reliable contemporary model that does not over-estimate risk could be both reassuring and safer for patients and financially beneficial for healthcare systems, as some potentially unnecessary investigations could be avoided. The wholesale adoption of computed tomography coronary angiography as the initial method of risk stratification, rather than pre-test likelihood estimation, potentially leads to increased diagnostic testing and exposure to ionizing radiation in what is an increasingly a lower risk population (149, 324). Furthermore, the anatomically-guided arm of the PROMISE trial, computed tomography coronary angiography led to increased rates of invasive catheterisation and revascularisation, with no apparent improvement on clinical outcomes (322). Given the derivation and validation of the CE-MARC model from contemporary populations referenced entirely to invasive angiography, this method of pre-test likelihood risk stratification may be appropriate for adoption in future guidelines.

Finally, whilst our findings of the effective estimation of pre-test likelihood of coronary artery disease by the CE-MARC model are pertinent to patients in the hospital setting, future research should evaluate whether this estimate is suitable for a primary care setting. Future validation of our model in a larger dataset would also be useful to corroborate our findings and further scrutinise effect of predictors that we found to be non-significant.

5.4.3. Limitations

Despite the total sample size of 1044 patients our prospective development and validation datasets are small by standards set by the CAD Consortium. Consequently, some established clinical predictors were not found to be statistically significant (smoking, hypertension, type II diabetes; indeed the latter had a small reduction in likelihood of coronary artery disease in our population). We included these established major clinical predictors in our model, regardless of significance, to take a clinical approach to risk model development, rather than a statistical one. In addition, while our development dataset was sufficiently-sized (in terms of events per variable), and was derived from a study with low risk of work-up bias, it was a single-centre study. In addition, although the validation set was largely drawn from a 6-centre randomised controlled trial, adding the enrichment set to the population meant nearly two thirds of the data came from the same hospital as the development set. Excluding the enrichment set from the validation of the CE-MARC model did not change the overall calibration in the large, but a statistically significant miscalibration effect was observed (-0.305; 95%CI -0.611, 0.000; P=0.050) indicating “extreme” predictions to be too extreme. However, as the study population in CE-MARC 2 was patients with a Duke pre-test likelihood between 10-90%, excluding the enrichment set would also mean that the validation population would not have the same distribution of pre-test likelihood as the development population.

5.4.4. Conclusions

The developed CE-MARC risk model performed very well in the independent validation sample, without needing any adjustment for different disease prevalence or for miscalibration. In contrast, earlier Diamond and Forrester model and Duke Scores substantially over-predicted coronary artery disease risk, and the Duke score remained poorly-calibrated even when this over estimation was corrected for. The

CAD Consortium risk models slightly under-estimated average coronary artery disease risk, but performed well once this under estimation was accounted for.

6. Feasibility Study of a Single Breath-hold, 3D mDIXON Pulse Sequence for Late Gadolinium Enhancement Imaging of Ischaemic Scar

6.1. Introduction

Late gadolinium enhancement imaging is the reference standard for myocardial scar assessment by CMR (152). LGE imaging is both diagnostic for myocardial infarction, and confers prognostic information in patients with IHD (99, 151, 158). The transmural extent of myocardial infarction delineated by LGE imaging has been shown to accurately identify the likelihood of myocardial functional recovery following revascularisation therapy and is the cornerstone of viability assessment by CMR (158).

LGE imaging relies on the altered washout kinetics of gadolinium contrast agents caused by expansion of the interstitial space of damaged myocardium, with a consequent higher signal intensity compared to healthy myocardium demarcating scarred territories. Typically, LGE imaging is performed 10-20 minutes following gadolinium contrast administration by a two-dimensional (2D) inversion recovery or phase sensitive inversion recovery spoiled gradient echo sequence (325). 2D IR and PSIR imaging involves a series of repetitive breath holds for the acquisition of each short axis plane to cover the left ventricle (325). Three-dimensional (3D) acquisition methods have been developed in recent years that cover the entire left ventricle in a single breath hold (156, 326–329) or via navigator based free breathing sequences (330–334). Studies evaluating 3D techniques have suggested the potential use of 3D LGE imaging in a variety of different patient groups (156, 332, 335–337). Thus far, single breath hold 3D LGE techniques have typically reported a compromise in image quality, mainly due to movement artefacts resulting from the very long breath hold durations required (156, 326–329). Additionally, typical 3D breath hold durations (>20s) are not possible for some patient populations. Navigator gated methods, where the scan is triggered to synchronise with the patient's breathing pattern, require scan

times in the order of minutes and yield no observed improvement in image quality (330–334).

CMR scans are typically of long duration and require multiple breath holds, this is both challenging for patients and impacts clinical workflow. Faster scans with less breath holds are sought as they are more tolerable for patients, and enable more patients to be scanned per list; the challenge though is to retain the excellent image quality that is the strength of CMR.

A shorter breath-hold 3D LGE acquisition can be enabled by additional acceleration (undersampling) of data acquisition, such as the use of increased parallel imaging factors. However, this naturally yields a loss of signal-to-noise ratio (SNR) which can negatively affect image quality. Therefore, a data acquisition method is needed which provides more SNR so that additional acceleration may be applied whilst maintaining sufficient image quality. In this work, we propose use of the modified Dixon (mDIXON) method for the specific purpose of enabling a 3D acquisition via the additional SNR mDIXON provides (338).

The Dixon method is a historical MRI imaging technique that acquires a minimum of two echoes per repetition time in which fat and water signals are in-phase and opposed-phase. From the two corresponding images, water-only and fat-only images may be calculated (339). The original Dixon method is limited by B₀ field heterogeneity and long scan times. Subsequent three (or more) echo methods were developed that are more robust to field inhomogeneity, and are used in many applications, such as musculoskeletal imaging and in tissue characterisation (340). However, such Dixon techniques are not routinely used in cardiac imaging (173) because they do not accommodate reasonable breath hold durations (338, 341). In this work, we utilised mDIXON in which only two echoes per TR are employed,(338) which allows shorter scan times and so may be suitable for CMR acquisitions with reasonable breath hold durations. Large

field-of-view (FOV) acquisitions with accurate water and fat separation with only two echoes is made possible by a full FOV B0 correction, water-fat shift correction, and a 7-spectral-peak fat model. Compared to traditional Dixon methods, the mDIXON method is uniquely suited to CMR because the echo time is not fixed to in-phase and out-of-phase echo times, and therefore may be shortened, helping to reduce breath hold durations still further.

Moving from 2D to a 3D scan automatically produces an increase in SNR because all k-space measurements now contribute to all pixels in all slices. However, the use of two echoes per TR in mDIXON allows an additional SNR boost compared to a single-echo 3D non-Dixon scan, which can be traded for higher sensitivity encoding (SENSE) acceleration factors, which in turn help to reduce breath hold duration for the 3D acquisition. The further additional signal produced by using 2-echo mDIXON versus a single echo 3D non-Dixon scan can be stated as an equivalent number of signal averages (NSA) as described by Reeder et al. (342).

Whilst mDIXON is used in this work to enable faster 3D data acquisition, it should be noted that from mDIXON data many image contrast types may be calculated (water image, fat image, in-phase image, out-of-phase image). In this work only the water image is used, and additional clinical utility derived from the presence of the other contrast types is not assessed.

The aim of this study was to prospectively evaluate a novel mDIXON 3D-LGE imaging sequence (in terms of image quality and acquisition duration) and compare it to a standard 2D sequence for the detection and quantification of myocardial scar in the setting of ischaemic heart disease.

6.2. Material and Methods

6.2.1. Study population

Patients with prior myocardial infarction were prospectively recruited between June 2016 and June 2017. Myocardial infarction was diagnosed by cardiac biomarkers, electrocardiography and acute coronary angiography at the time of primary PCI. Inclusion criteria were ≥ 18 years of age, no contra-indication to contrast-enhanced CMR, glomerular filtration rate ≥ 60 mL/min/1.73m². Patients with atrial fibrillation, non-MR compatible implants, renal failure or claustrophobia were excluded. Patients were classified as Acute MI if scanned within 7 days of their index admission with the acute coronary syndrome. Chronic MI was at least 3 months following the initial presentation of the acute coronary syndrome. The study had appropriate ethical approval and was performed in accordance with the Declaration of Helsinki, and all patients provided informed written consent.

6.2.2. CMR data acquisition

CMR was performed on a 1.5 Tesla Philips Ingenia system (Philips Healthcare, Best, The Netherlands) equipped with a 24 channel digital receiver coil and patient-adaptive RF shimming. Imaging acquisition included survey images, assessment of myocardial function using standard SSFP cine imaging (spatial resolution 1.09x1.09x8mm³, 30 cardiac phases TR/TE 3.0/1.48ms, flip angle 40°, field of view 360-360mm, SENSE acceleration) and 2D-LGE and 3D-LGE imaging. For LGE imaging, an intravenous bolus of 0.15mmol/kg gadobutrol (Gadovist®, Bayer Inc.) was administered. The optimal TI to null the myocardium was determined by a Look-Locker sequence. 2D and 3D LGE imaging were performed 10 minutes following contrast administration. 2D and 3D sequences were performed separately in random order to avoid bias and systematic error caused by contrast washout. Times taken for the 2D and 3D acquisition sequences were recorded. Imaging parameters were:

(i) 2D breath-hold PSIR sequences with 12 short-axis slices covering the full LV, thickness 10mm, no gap, repetition time 6.1ms, echo time 3.0ms, flip angle 25° , field of view 300 x 300mm, matrix 127/256, acquired in-plane resolution $1.59 \times 2.20 \text{mm}^2$ reconstructed to $0.91 \times 0.91 \text{mm}^2$, effective SENSE factor 2.2. The turbo factor was 20 (7 shots) with an acquisition duration of 123.3ms. The receiver bandwidth was 250.2 Hz/px;

(ii) 3D mDIXON sequences with 24 short-axis slices, slice thickness 5mm, repetition time 4.0 ms/echo times 1.21ms and 2.5ms, flip angle 15° , field of view 300 x 300 x 120mm, matrix 169/384, acquired in-plane resolution $1.83 \times 2.00 \text{mm}^2$ reconstructed to $1.17 \times 1.17 \times 5 \text{mm}^2$, SENSE factors in phase and slice directions were 3 and 2 respectively with effective overall factor 6.86 after oversampling taken into account. The equivalent NSA provided by mDIXON compared to an identical single-echo protocol was 1.52 (342). The turbo factor was 30 (16 shots) with a shot acquisition duration of 148 ms, one shot per heartbeat over 18 beats. The receiver bandwidth was 866 Hz/px. Saturation bands were not used.

Additional 4 Chamber and 2 Chamber 2D LGE images were acquired but not used for analysis/interpretation.

6.2.3. CMR data analysis

CMR data were analysed quantitatively using commercially available software (CVI42, Circle Cardiovascular Imaging Inc. Calgary, Canada). MR data analysis of 2D and 3D LGE images was performed blinded in random order by a cardiologist (JF with 6 years in cardiac imaging). For 15 patients, quantitative analysis was performed again 4 weeks later to assess intra-observer variability, and to assess interobserver variability by a second (GF with 6 years in cardiac imaging) and third cardiologist (LB with 8 years in cardiac imaging). For volumetric analysis, endocardial borders were traced on the LV cine stack at end-diastole and end-systole to calculate end diastolic volume, end systolic volume, stroke volume and ejection fraction. Contours were traced to exclude papillary muscles and trabeculations.

6.2.4. Qualitative LGE assessment

Image quality was defined on a scale of 1-4 (4=non-diagnostic, 3=acceptable diagnostic quality, 2=good quality, 1=excellent quality). For scores other than 1, the reason for impaired quality was categorized as a) motion or blurring artefacts, b) low contrast or high noise, c) inadequate myocardial nulling, or d) wrap around/folding artefacts. Additionally, both 2D and 3D LGE images were evaluated for the presence of ventricular cavity thrombi.

6.2.5. Quantitative LGE assessment

Quantitative assessment of the myocardial scar burden was performed using the semi-automated full-width half-maximum method (threshold of 50% of the maximum intensity within the scar) which has been proposed as the most reproducible method (180, 343). On both the 2D and 3D LGE short-axis images endocardial and epicardial contours were manually outlined (excluding papillary muscles); manual delineation of two separate user-defined ROIs were then made on an LGE short axis slice where infarcted myocardium was present. One ROI was drawn in remote myocardium (where no scar was present); a second ROI was drawn around hyperenhanced myocardium where infarcted myocardium was present. Automated calculations for the remaining LV short axis LGE stack based on these two ROIs were then performed. Scar tissue mass was calculated (grams). Scar tissue percentage and transmural extent were calculated automatically for each segment of 16 segments of the 17 segment model proposed by the American Heart Association (excluding the apex) (245). Infarct transmural extent was automatically calculated by the analysis software and then graded using a 5-point scale from the derived quantitative result (0=no scar, 1=1-25% transmural extent, 2=26-50% transmural extent, 3=51-75% transmural extent and 4=76-100% transmural extent). Time taken for image acquisition of the entire LV for 2D

and 3D was recorded (this included time taken for pauses between breath holds for each LV slice).

6.2.6. CNR measurements

In 25 consecutive patients CNR measurement was performed, a single slice containing both hyperenhanced and healthy myocardium was selected and for this corresponding slice a dedicated noise scan (identical pulse sequence without excitation pulses) was performed immediately afterwards in order to assess the noise levels (179). ROIs were drawn on the normal 3D and 2D LGE images in areas of hyper-enhancement, a remote area of normal appearing myocardium, and in blood pool. ROIs contained at least 30 pixels, aside from the areas of hyper-enhancement where size of the ROI was governed by the size of the scar. A further ROI covering the entire LV myocardium was drawn on the corresponding noise image, the standard deviation of this measurement was then used to calculate CNR measurements. CNR was calculated as the ratio of the difference in mean signal intensity between ROIs on the LGE images to the standard deviation of signal intensity in the whole LV ROI from the separate noise image. The MR system noise level is measured and not organ/image level.

6.2.7. Statistical analysis

Continuous variables are expressed as mean \pm SD. Categorical variables are expressed as N (%) or proportions. Normality of data was tested using a Shapiro-Wilk test. Paired two-tailed student t-test and the Wilcoxon signed rank test were used as appropriate to compare continuous variables. $P < 0.05$ was considered statistically significant. Pearson correlation, linear regression and Bland-Altman analysis were used to show agreement between the 2D and 3D acquisition sequences for scar tissue mass and scar tissue percentage of LV mass. Coefficient of variation was used to assess interobserver and intraobserver variability for scar tissue mass. Cohen κ statistic was used for interobserver agreement for

the image quality score. Cohen K statistic was also used to measure agreement between the 5 point grading of transmuralty and the agreement for the binary detection of viable/non-viable segments. Statistical analysis was performed using IBM SPSS® Statistics 22.0 (IBM Corp., Armonk, NY).

6.3. Results

6.3.1. Demographics

A total of 92 patients (80/92 male, mean age 60.9 ± 11.0 years; BMI $26.7 \pm 4.2 \text{ kg/m}^2$; LVEDV $175.3 \pm 60.8 \text{ ml}$; LVEDVi $90.5 \pm 31.2 \text{ ml/m}^2$; LVESV $97.1 \pm 55.2 \text{ ml}$; ejection fraction $47.2 \pm 12.3\%$) were prospectively examined. Of these, 53 patients had chronic (46/53 male, mean age 59.9 ± 10.9 years; BMI $26.7 \pm 4.2 \text{ kg/m}^2$; ejection fraction $47.9 \pm 13.9\%$) and 39 patients had acute (male 34/39, mean age 62.3 ± 11.2 years; BMI $26.8 \pm 4.25 \text{ kg/m}^2$; ejection fraction $46.3 \pm 9.9\%$;) myocardial infarction. All 92 patients were scanned with both 2D PSIR and 3D mDIXON LGE acquisitions (in random order) without complications, resulting in a total of 1,472 segments per technique.

6.3.2. Image quality

Image quality was graded as excellent for 65/92 (70.6%) of the PSIR images, and 63/92 (68.5%) of the 3D images. No dataset was deemed non-diagnostic in either 3D mDIXON or 2D PSIR images (score of 4). There was no statistically significant difference in image quality between 3D and 2D LGE (1.4 ± 0.6 vs. 1.3 ± 0.5 , $P=0.162$) (Figure 6-1). Table 6-1 shows the reasons why image quality was scored other than excellent for LGE sequence. Image quality impairment was predominantly attributed to blurring/motion (15/27) in the 3D datasets. Interobserver agreement for image quality was good for both observers (between 1 and 2 $\kappa = 0.615$ and between 1 and 3: 0.706).

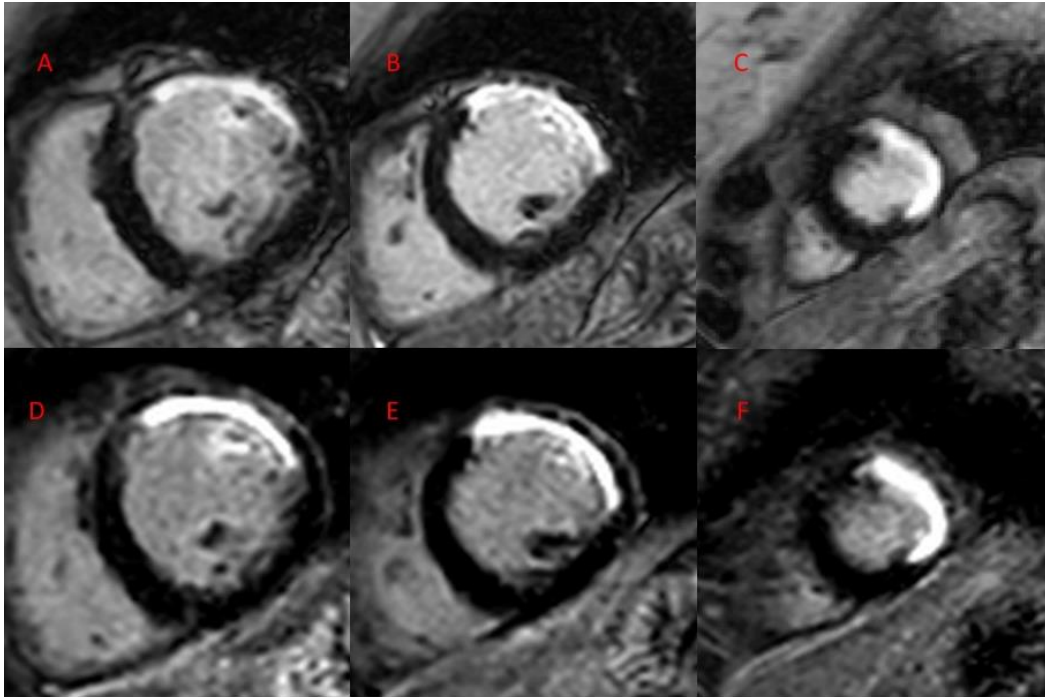


Figure 6-1 Short axis LGE images from (A) basal, (B) mid-ventricular and (C) apical slices from 2D PSIR acquisitions, and (D) basal, (E) mid-ventricular and (F) apical slices from 3D mDIXON acquisitions of the same patient showing antero-lateral scar following a left anterior descending artery territory infarction. (Image from Foley et al. JMRI in press)

Table 6-1 Reasons for impaired subjective image quality ratings (for any rating other than excellent)

	2D PSIR	3D mDIXON
Motion /blurring	7	15
Low contrast/noise	7	4
Nulling	6	5
Folding artefact	4	3
Total	24	27

6.3.3. CNR

The CNR of scar to blood was not significantly different between 3D and 2D LGE techniques respectively (16.1 ± 10.5 vs. 18.8 ± 12.4 , $P=0.337$). The CNR of scar to remote myocardium (36.4 ± 19.8 vs. 56.6 ± 20.8 , $P=0.001$) and CNR of remote myocardium to blood (21.3 ± 12.9 vs. 41.0 ± 17.0 , $P<0.001$) were significantly lower by 3D mDIXON compared to 2D PSIR.

6.3.4. Quantitative LGE Analysis

3D mDIXON compared to 2D PSIR identified statistically significantly more absolute scar tissue mass (18.9 ± 17.5 g vs. 17.8 ± 16.2 g, $P=0.03$) but no significant difference in scar tissue when expressed as a percentage of LV mass ($13.4 \pm 9.9\%$ vs. $12.7 \pm 9.5\%$, $P=0.07$). Bland-Altman analysis of absolute 3D scar tissue mass compared to 2D scar mass showed a small positive bias of 1.1g (95%CI: -5.8 to 8.0); likewise for percentage scar tissue the bias was 0.7% (95%CI: -4.0 to 5.5) (Figure 6-2a and 6-2b).

3D mDIXON identified significantly greater scar tissue mass compared to 2D PSIR in acute myocardial infarction (23.3 ± 19.5 g vs. 21.5 ± 17.3 g, $P=0.012$) and similar scar tissue mass in chronic myocardial infarction (15.6 ± 15.3 g vs. 15.0 ± 14.9 g, $P=0.125$).

There was strong and significant correlation in scar tissue mass ($r=0.981$ $P<0.001$) and scar tissue percentage between 3D and 2D acquisitions ($r=0.970$ $P<0.001$).

A total of 5 patients were identified to have intraventricular thrombi in both 2D and 3D acquisitions, no thrombi were visible in only 2D or 3D images (Figure. 6-3).

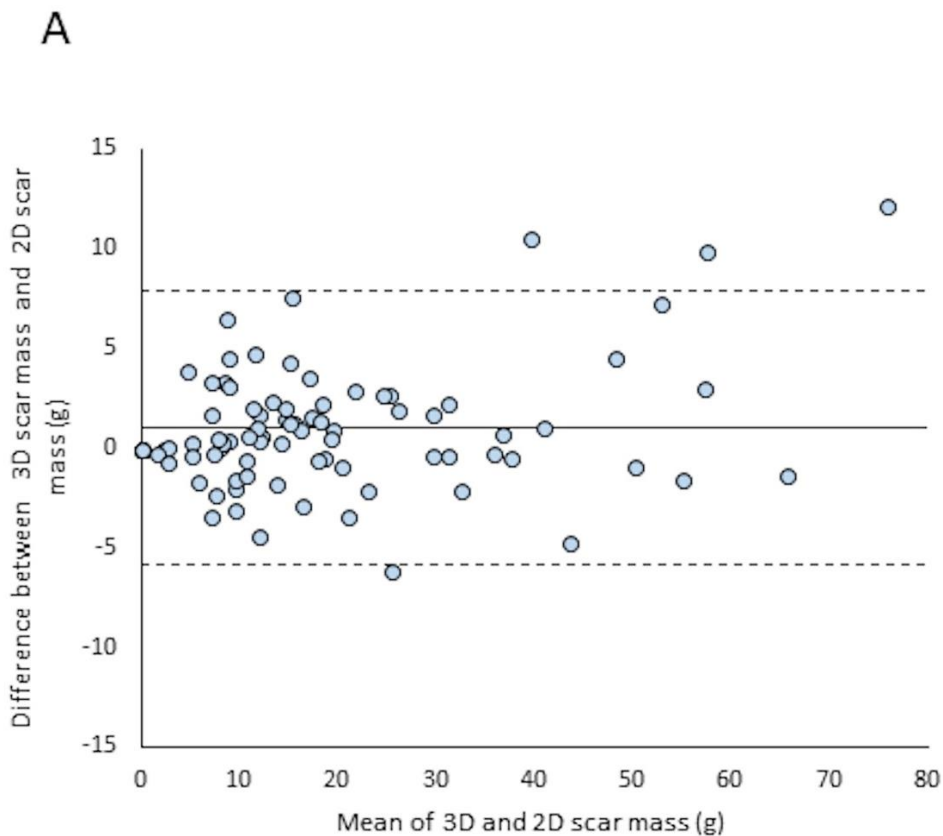


Figure 6-2 Bland-Altman analysis of 3D and 2D LGE acquisitions (± 1.96 Standard deviations – dashed lines) for assessment of (A) absolute scar tissue mass and (B) scar tissue as a percentage of LV myocardial mass.

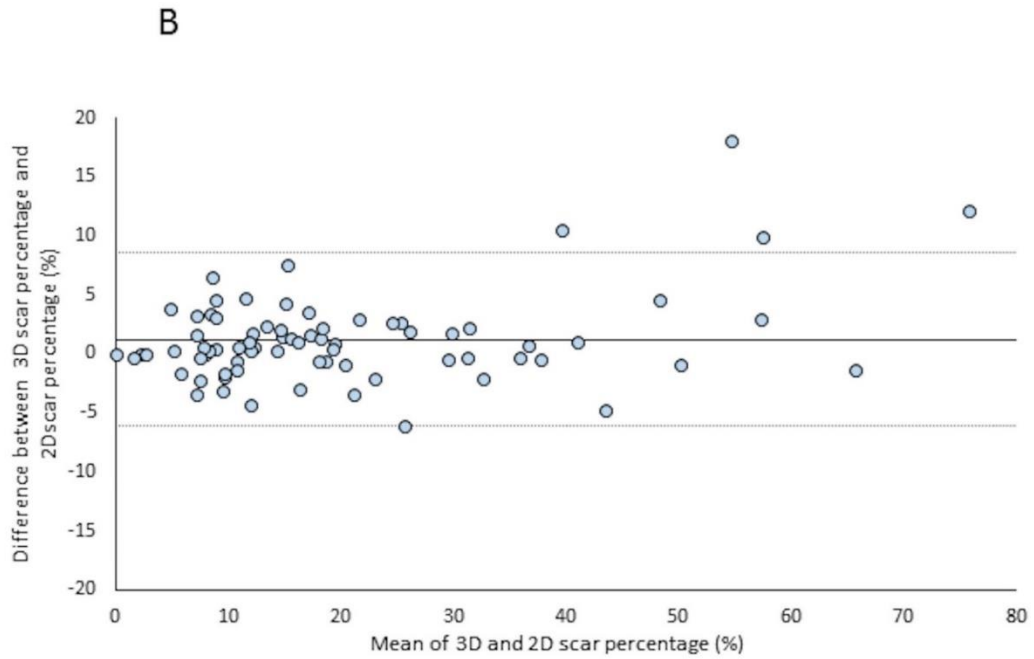
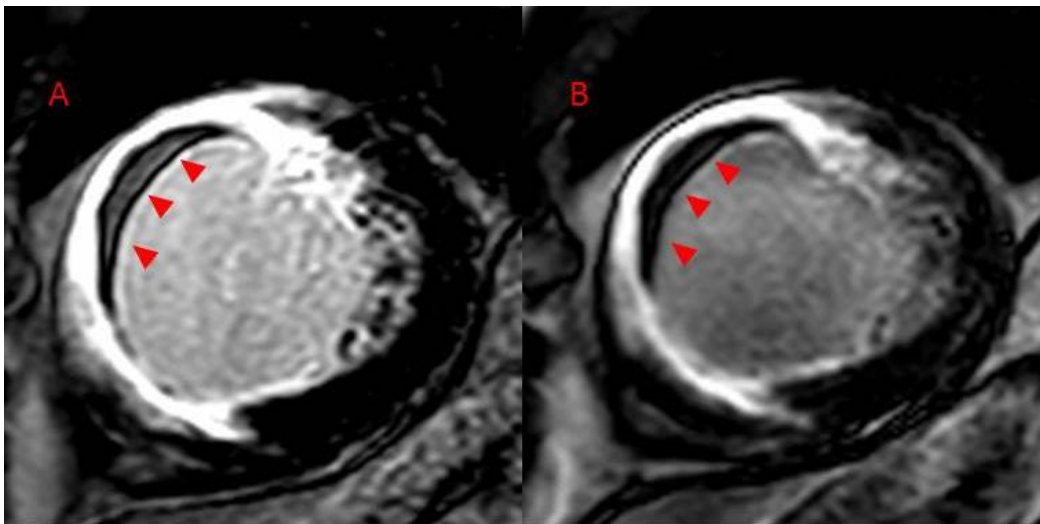


Figure 6-3 Laminated thrombus in a chronic myocardial infarction in an apical slice of a (A) 2D PSIR acquisition and (B) 3D mDIXON acquisition of the same patient (red arrows demarcate the thrombus). (Image from Foley et al. JMRI in press)



Interobserver coefficient of variability was excellent for both 3D and 2D LGE techniques in terms of scar mass (between JF and GF 3D 7.0%; 2D 4.9%; and between JF and LB 3D: 5.8% 2D: 7.3%) and scar tissue percentage (between JF and GF 3D 7.1%; 2D 5.2% and between JF and LB 3D: 6.0% and 2D: 7.8%). Intra-observer coefficient of variability was also excellent for both 3D and 2D LGE for scar mass (3D 5.3%; 2D 4.8%) and scar tissue percentage (3D 5.4%; 2D 5.3%).

6.3.5. Segmental and transmural assessment

There was excellent agreement ($\kappa=0.870$; Pearson's $r=0.956$, $P<0.0001$) between the 3D and 2D LGE techniques based upon a segmental scar transmural threshold of 50% (the threshold typically used for clinical viability status determination); there was also good agreement between the two techniques for the overall 5-point transmural score $\kappa = 0.736$ (Pearson's $r = 0.922$ $P<0.0001$). Results of the segmental 5 point transmural assessment was 1 ± 1.1 for 2D and 1 ± 1.1 and for the binary 50% viable threshold was 0.1 ± 0.3 for 2D and 0.1 ± 0.3 for 3D.

6.3.6. Image acquisition time

Time from contrast injection to image acquisition were as follows: 2D 10.54 ± 0.59 minutes, 3D 13.06 ± 3.12 minutes $P<0.0001$. Time taken to acquire LGE images was much shorter for 3D mDIXON compared to 2D PSIR (15.6 ± 1.4 vs. 311.6 ± 43.2 seconds, $P<0.0001$). For PSIR, 1 slice was acquired per breath hold; average breath hold duration for each PSIR slice acquisition was 10.7 ± 1.2 seconds.

6.4. Discussion

The main findings of this study are i.) 3D mDIXON LGE offers comparable image quality for the evaluation of ischaemic scar compared to 2D LGE imaging; ii.) quantitative assessment of 3D mDIXON LGE of scar mass and transmural thickness has high agreement with 2D LGE imaging; iii.) 3D mDIXON LGE provides a vastly shorter overall scan duration in an acceptable single breath-hold time compared to 2D LGE.

We have used only the water-image calculated from the mDIXON-acquired data. The purpose of the study was to use mDIXON to enable 3D LGE in a reasonable breath hold duration, not to compare the utility of the various contrasts a Dixon-based scan can produce. Others have demonstrated clinical utility of Dixon fat-image, for example in detection of lipomatous metaplasia in scar (344–346). Similar additional clinical value may be available with the 3D mDIXON method used here. Lapinskas et al. describe acquisition of a long axis 3D mDIXON LGE in a single breath hold, this however is not easily comparable to routine 2D PSIR short axis LGE imaging (344). Short axis mDIXON LGE imaging is also described but it is limited in that it requires 2 breath holds, thus leading to increased scan duration and likely corruption of data from different breath hold positions and increasing the potential of breathing artifacts (344).

It is possible to increase the SNR of a single-echo 3D non-Dixon scan by lowering the receiver bandwidth, which might also be considered as an enabler for a 3D LGE protocol within a sufficiently short breath hold duration. However, lowering the receiver bandwidth will also increase the TE, and thus the TR, which increases the acquisition (shot) duration, which would increase blurring due to cardiac motion. In order to shorten the shot again a higher number of readouts is needed necessitates a longer breath hold. mDIXON affords additional SNR without this consequence, which was confirmed by Bloch simulation built into the MR system.

Current 2D LGE imaging techniques are highly discriminatory for the diagnosis of myocardial infarction and form the basis of myocardial viability imaging by CMR (151, 152). Thus, high image quality is of paramount

importance when introducing a new LGE technique, as current 2D methods are so effective. The in-plane resolution of the 2D scan was higher than the 3D, in our study the 2D scan was clinically optimised and established and we wanted to directly compare with it; the 3D scan was separately optimised, balancing resolution and acceleration. Typically, 3D LGE techniques have been shown to have compromised image quality compared to 2D techniques, though differences in qualitative ratings often do not reach significance (156, 328, 336, 347, 348). Our findings were that categorical image scoring of the 3D mDIXON sequence was in fact very comparable to the 2D LGE sequence. This is despite the lower CNR for myocardium to scar and myocardium to blood seen in the 3D images compared to the 2D images. This is likely due to the similar CNR for scar to blood seen between 3D and 2D images; this parameter is arguably more important as poor contrast between scar and blood pool can make it difficult to identify the endocardial border so consequently compromising accurate assessment of scar size and identification of sub-endocardial infarction. Furthermore, despite the CNR differences recorded this does not make an impact on the automated quantitative LGE assessment. PSIR reconstruction used in the 2D protocol mitigates sensitivity of the sequence to the precise TI set by the user to null normal myocardium, which varies from patient to patient. Since the TI required to null normal myocardium changes during contrast washout over the scanning time of the 2D stack of slices, the flexibility PSIR allows is helpful. PSIR reconstruction was not used in the 3D mDIXON protocol, but since the whole stack of slices is acquired in just one breath hold, the effect of contrast washout between slice acquisitions is not an issue. There is no theoretical obstacle to combining the 3D scan we used with PSIR in further work. However, note that since PSIR requires 2 beats, a “3D mDIXON PSIR” scan duration might get significantly longer again (the second beat is used to watch the magnetisation recover and so determine whether the acquisition in the first beat was above or below the null point).

Scar burden by LGE imaging has been shown to be proportional to likelihood of major adverse cardiovascular events and offers prognostic information in patients with ischaemic heart disease (151). Of note, the 3D mDIXON technique identified significantly more scar compared to the 2D sequence. This is likely a result of the contiguous slices which a single breath hold 3D scan affords, compared to the series of breath holds for a 2D stack of slices which can be affected by inconsistent breath hold position even in expiration as used in this work. The 5mm reconstructed slice thickness used in the 3D mDIXON technique compared to the 10mm used in the routine PSIR sequence may also aid perception of scar; a similar result was described by Yin et al who also used a thinner slice thickness in the 3D acquisition compared to the 2D (334). The thinner slice thickness may help identify smaller infarcts and delineate the true border of the scar being imaged.

The transmural extent of infarction has been shown to directly relate to the likelihood of functional recovery following revascularisation. LGE imaging consequently has a grade A rating to determine myocardial viability prior to revascularisation in the ACCF/AHA/SCMR appropriate use criteria and is the third highest indication for CMR in Europe (166, 171) Therefore, accurate discrimination of transmural scar extent is important when considering a new LGE sequence. Previous studies have showed variable results, though more recent studies have shown reasonable agreement (156, 327, 336, 349, 350). The 3D mDIXON technique showed strong agreement with the 2D sequences. Statistical significance was seen in scar mass seen by 3D compared to 2D in the acute but not in the chronic infarctions, overall however there was no difference in viability assessment or the overall % LV mass. This is potentially a reflection of the smaller sample size of acute patients, compared to the overall study group. Furthermore, although the difference in scar tissue mass reached statistical significance, there is in fact little clinical significance in the difference between the two sequences when expressed as a percentage of LV mass (0.7% difference).

Thus far, a significant limitation in the utility of 3D LGE imaging has been that despite a significant reduction in overall scanning time to acquire an entire short axis stack, individual breath holds remain overly long leading to image degradation or scan failure (156, 336). In the patient groups proposed to benefit from shorter scanning times (those with cardio-respiratory disease and those unable to perform long breath holds) this increased breath hold duration negates the perceived advantages. Goetti et al., noted a doubling of blurring artifacts due to breath hold durations of 26.7 ± 4.4 seconds compared to a routine 2D inversion recovery sequence (156). Bratis et al., observed no increase in blurring artifacts, despite 3D acquisitions requiring a breath hold duration of 22-27 seconds, however 60% of patients demonstrated no pathology and comment is made that respiratory motion was the main cause of 3D imaging failure (10/57 cases) (336). Various methods have attempted to overcome the long 3D breath hold duration; Bauner et al., used a 3D acquisition sequence that used 3 consecutive slabs to cover the entire ventricle, however this only resulted in a halving of the acquisition time and generated new artefacts due to misalignment of the 3D volume stacks as a result of variations in breath hold position (350). Alternatively, navigator gated 3D sequences can be acquired in a free-breathing manner; however, navigator gated sequences can lead to prolonged scan times due to navigator inefficiency, with potential scan failure due to drift of respiratory pattern leading to impaired image quality as the TI required to null myocardium alters (330–334). Bizino presented a free breathing motion corrected 3D sequence but this was not compared to 2D LGE for image quality, and still took over 3 minutes for acquisition (351). Recently compressed sensing techniques have been proposed as a method to reduce scanning times, (352) however recent publications of 3D LGE using compressed sensing still require scanning times between 3- 7 minutes and have not been compared to currently used 2D sequences (353, 354). Moreover, the 3D mDIXON method described here can be combined with the product “Compressed SENSE” on the MR system used for this work for further acceleration and reduction in breath

hold duration. Preliminary tests suggest a breath hold duration of just 11 seconds may still preserve sufficient image quality. More extreme methods have also been proposed to overcome the prolonged breath hold durations by increasing the patient's ability to breath hold by supplemental oxygen and hyperventilation techniques, however this approach appears incongruous if this requires training time and resources (355). Our data showed no failed 3D scans in any of the 92 patients, some with significant left ventricular dysfunction, resulting in diagnostic quality studies (none deemed non-diagnostic) that was obtainable in a single breath hold. Our study has shown that a breath hold duration (15.57 ± 1.361 seconds) using the 3D mDIXON technique is sufficiently short to enable most patients to complete, as demonstrated in both acute and chronic MI patient groups.

6.4.1. Limitations

A limitation of our study is the difference in slice thickness between the 2D and 3D acquisitions. We chose to use the slice thickness currently used in our 2D clinical scanning sequence and ongoing clinical trials at our establishment, and used the default 5mm slice thickness on the 3D mDIXON sequence as it was apparent from pilot data that this achieved acceptable SNR within a sufficiently acceptable breath hold duration. Additionally, the 3D LGE scan does not employ a PSIR reconstruction, and so the image contrast is more sensitive to correct inversion time selection. A further limitation is that there is no pathology based reference standard to compare the true size and presence of myocardial infarction from the quantitative analysis of either 2D or 3D LGE approaches. A further limitation is the difference in time from gadolinium injection to image acquisition between the 2 sequences which is inherently impossible to overcome, a pragmatic approach of randomizing test order is what comparable studies on this topic have done previously (156, 328, 335, 336) and although not perfect is an attempt to reduce the effect on image quality of contrast washout from the blood pool.

6.4.2. Conclusion

In conclusion, single breath-hold 3D mDIXON LGE imaging allows quantitative assessment of scar tissue burden and transmural, with comparable image quality, in a significantly shorter acquisition time compared to standard 2D LGE imaging.

7. Clinical Evaluation of two dark blood methods for late gadolinium enhancement imaging and quantification of ischaemic scar

7.1. Introduction

Late gadolinium enhancement imaging is both diagnostic for myocardial infarction as well as prognostic in patients with IHD (99, 151, 158). Presence of late enhancement has been shown to confer increased risk of MACE and cardiovascular mortality above and beyond clinical and angiographic findings (151, 356). Furthermore, transmural extent of MI demarcated on LGE imaging accurately identifies the likelihood of myocardial functional recovery following revascularisation (152, 158). Progress in cardiovascular medicine has resulted in a reduction in the number of fatal STEMI, however this has led to increased numbers of patients living with ischaemic scar. Thus accurate methods of scar quantitation/transmurality assessment are required to guide revascularisation decisions and for prognostication (3).

LGE imaging is typically performed 10-20 minutes following administration of a gadolinium-based contrast agent, by a two-dimensional IR spoiled gradient echo sequence (325). Conventionally this is preceded by a Look-Locker sequence enabling the MR operator to set an appropriate TI to null normal myocardium, and thus give high contrast between 'bright' scarred myocardium (where gadolinium contrast agent is retained), and the darker healthy myocardium. Phase sensitive inversion recovery sequences have been developed to overcome the need to precisely choose the correct TI to null the normal myocardium (357). A large proportion of infarctions are sub-endocardial because ischaemia causes a wavefront-phenomena of necrosis that affects the sub-endocardial fibres of the myocardium first (20). Despite good contrast between scar and normal myocardium, contrast between blood

pool and myocardial scar can be limited leading to uncertainty for the reporting clinician as to the precise location of the scar-blood pool interface, which then can impact on the assessment of the transmural extent of the scar.

Several dark blood sequences have been described that attempt to overcome the issue of poor contrast between contrast enhanced blood pool and sub-endocardial infarction by addition of extra magnetisation pulses (172–178, 358). FIDDLE (Flow-Independent Dark-blood DeLayed Enhancement) incorporates an additional magnetisation preparation prior to the inversion pulse in a PSIR LGE sequence (178, 358). Numerous radiofrequency (RF) preparation types may be employed, such as T1rho (T1 ρ), T2 preparation, additional inversion pulses etc. T1 ρ is the decay rate of magnetisation during application of a RF field applied parallel to the net magnetisation of spins, in the rotating frame. More complex composite RF preparations for T1 ρ weighting can be used to compensate for variations in the B1 field, and B0 inhomogeneity. The preparation pulse incorporates a *spin locking* time (SL) during which T1 ρ decay occurs (359). Then standard LGE imaging follows. The magnetisation preparation effects a different starting value for the magnetisation of tissues before LGE imaging. Then when LGE image acquisition immediately follows, adjusted contrast remains between these tissues. In each case, the intention is that blood pool remains the most incompletely recovered longitudinal magnetisation compared to the other tissues of interest, thus yielding the lowest signal – dark blood – in the PSIR LGE image. A PSIR reconstruction reduces sensitivity to inversion time precision and removes the risk of tissues with different T1 relaxation times appearing isointense. Recently a method using a standard PSIR sequence with the inversion time set to null the blood pool rather than the myocardium was described in a group of 9 patients (179). This method, albeit in a small number of patients, led to improved scar to blood CNR and improved reader confidence (179).

The aim of this study was to prospectively evaluate a novel T1 ρ dark blood sequence and compare this to the recently described blood nulled PSIR (BN)

and the standard 'clinical' myocardium nulled PSIR (MN) technique for the detection and quantification of scar in the setting of ischaemic heart disease.

7.2. Methods

7.2.1. Study population

Patients with prior myocardial infarction were prospectively recruited between April 2017 and June 2017. Myocardial infarction was confirmed by cardiac biomarkers, electrocardiography and coronary angiography. Inclusion criteria were age ≥ 18 years, no contra-indication to contrast-enhanced CMR, glomerular filtration rate ≥ 60 mL/min/1.73m². Patients with atrial fibrillation, non-MR compatible implants, renal failure or claustrophobia were excluded. The study was performed in accordance with the Declaration of Helsinki, approved by the National Research Ethics Service, with all patients providing informed written consent.

7.3. CMR data acquisition

CMR was performed on a 1.5 Tesla Philips Ingenia system (Philips Healthcare, Best, The Netherlands) equipped with a 24 channel digital receiver coil and patient-adaptive RF shimming. Image acquisition included survey images, assessment of myocardial function using standard SSFP cine imaging (spatial resolution 1.09x1.09x8mm³, 30 cardiac phases TR/TE 3.0/1.48ms, flip angle 40°, field of view 360-360mm, SENSE acceleration) and 2D LGE imaging. For LGE imaging, an intravenous bolus of 0.15mmol/kg gadobutrol (Gadovist®, Bayer Inc.) was administered. At 10 minutes post-contrast, the optimal TI to null the myocardium was determined by a Look-Locker sequence. A routine 2D breathhold phase sensitive inversion recovery sequence with 12 slices covering the full LV (thickness 10mm, no gap, repetition time 6.1 ms/echo time 3.0 ms, flip angle 25°) was then performed. A single short axis slice that included scar, remote healthy myocardium and

blood pool was then selected, and a repeat Look-Locker sequence was performed for this slice to re-confirm appropriate inversion times for tissues of interest. The selected short axis slice was then re-acquired using the PSIR LGE sequence with the TI set to null myocardium (MN), the TI set to null the blood pool (BN) and a T1 ρ FIDDLE sequence. A dedicated noise scan (identical pulse sequence without excitation pulses) was performed after each slice acquisition, in order to enable accurate measurement of the signal-noise level (179). The T1 ρ -prepared and the two standard PSIR sequences were all performed in random order to avoid systematic bias caused by differences in contrast washout.

Imaging parameters were as follows:

2D breath-hold phase sensitive inversion recovery sequences with 12 slices covering the full LV, thickness 10mm, no gap, repetition time 6.1ms, echo time 3.0ms, flip angle 25°, field of view 300x300mm, matrix 127/256, acquired in-plane resolution 1.59x2.20mm² reconstructed to 0.91x0.91mm², effective SENSE factor 2.2. The turbo factor was 20 (7 shots) with an acquisition duration of 123.3ms. The receiver bandwidth was 250.2 Hz/px. The same sequence was used for both the single slices of the MN and the BN with the TI set to null myocardium and blood pool respectively.

The T1 ρ preparation employed a ΔB_0 and B1 insensitive spin lock (360) consisting of 90_x, SL_y, 180_y, SL_{-y}, 90_{-x} pulses as seen in Figure 7-1, with the two spin lock (SL) pulses using an locking frequency of 500Hz. The spin lock time was 40ms. The SL pulses with opposed phase compensate for B1 variation, and the central 180 pulse compensates for B0 inhomogeneity. A modified Look-Locker inversion-recovery (MOLLI) T1-mapping scan (3–5 scheme) was performed to determine T1 values of the viable myocardium, LV blood, and scar tissue.

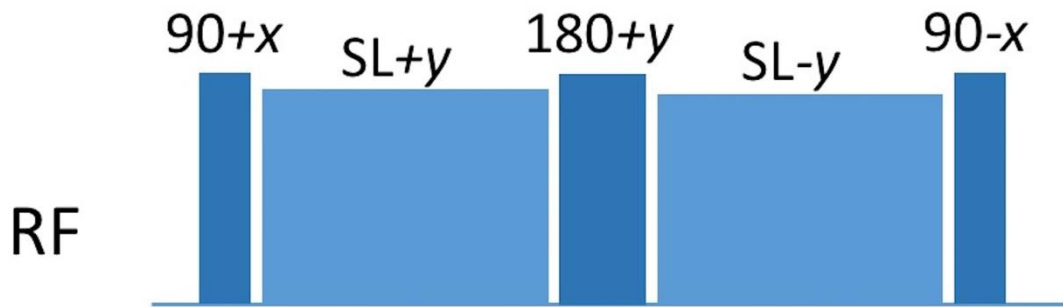


Figure 7-1 shows the T1 rho preparation for the FIDDLE (T1ρ) pulse sequence

7.3.1. CMR data analysis

CMR data were analysed quantitatively using commercially available software (CVI42, Circle Cardiovascular Imaging Inc. Calgary, Canada). MR data analysis of the three types of LGE images was performed blinded in random order by a cardiologist (Observer 1 with 6 years in cardiac imaging). For all patients, quantitative analysis was performed again 4 weeks later to assess intra-observer variability and for all patients by a second cardiologist (Observer 2 with 6 years in cardiac imaging) to assess inter-observer variability. For volumetric analysis, endocardial borders were traced on the LV cine stack at end-diastole and end-systole to calculate end diastolic volume, end systolic volume, stroke volume and ejection fraction. Contours were traced to exclude papillary muscles and trabeculations.

7.3.2. Image analysis

7.3.2.1. Qualitative LGE assessment

Maximum scar transmuralty was visually assessed using a 5 point scale (0=no LGE, 1=1-25%, 2=26-50%, 3=51-75%, 4=76-100%). Confidence in scar detection and degree of transmuralty was assessed using a 4 point scale (1=non-diagnostic, 2=low, 3=moderate, 4=high confidence).

7.3.2.2. Quantitative LGE assessment

Quantitative assessment of the myocardial scar burden was performed using the semi-automated full-width half-maximum method (threshold of 50% of the maximum intensity within the scar) which has been proposed as the most reproducible method (180, 343). On the 2D BN, MN and T1 ρ LGE short-axis images endocardial and epicardial contours were manually outlined (excluding trabeculations and papillary muscles); manual delineation of two separate user-defined ROIs were then made on the LGE short axis slice where infarcted myocardium was present. One ROI was drawn in remote myocardium (where no scar was present); a second ROI was drawn within hyperenhanced myocardium where infarcted myocardium was present. Scar tissue mass (grams) was then calculated on the BN, MN and T1 ρ LGE LV short axis slice based on these ROIs.

7.3.2.3. CNR measurement

ROIs were drawn on each single slice MN, BN, and T1 ρ LGE images in areas of hyper-enhancement, a remote area of normal myocardium, and in the blood pool. ROIs contained at least 30 pixels, aside from the areas of hyper-enhancement where size of the ROI was governed by the size of the scar. A further ROI covering the entire LV myocardium was drawn on the corresponding noise image, the standard deviation of this measurement was then used to calculate CNR measurements. CNR was calculated as the ratio of the difference in mean signal intensity between ROIs on the LGE images to the standard deviation of signal intensity in the whole LV ROI from the separate noise image. CNR was calculated for difference between scar and blood pool ($CNR_{\text{scar-blood}}$), scar and myocardium ($CNR_{\text{scar-myo}}$) and between blood and remote myocardium ($CNR_{\text{blood-myo}}$).

7.3.3. Statistical analysis

Continuous variables are expressed as means \pm SD. Categorical variables are expressed as N (%) or proportions. Normality of data was tested using a Shapiro-Wilk test. Repeated measures ANOVA with post hoc Bonferroni correction was used to compare means of the three groups. $P < 0.05$ was considered statistically significant. Coefficient of variation was used to assess interobserver and intraobserver variability for scar size. Cohen κ statistic was used for interobserver and intraobserver agreement for transmural assessment and the image confidence score. Statistical analysis was performed using IBM SPSS® Statistics 22.0 (IBM Corp., Armonk, NY).

7.4. Results

7.4.1. Study population

A total of 30 patients (26/30 male, mean age 63.8 ± 10.7 years; mean BMI $26.3 \pm 3.6 \text{ kg/m}^2$; mean LV ejection fraction $47 \pm 11\%$; LVEDV $167 \pm 53 \text{ ml}$; LVEDVi $87 \pm 25 \text{ ml/m}^2$; LVSV $75 \pm 17 \text{ ml/m}^2$; LVESV $92 \pm 48 \text{ ml}$) were prospectively examined.

7.4.2. MR imaging

Imaging using routine PSIR, blood nulled PSIR and T1 ρ were successfully completed in all patients with no imaging failures. There was no significant difference in time of image acquisition between the three pulse sequences MN 17.58 ± 0.53 minutes BN 18.07 ± 0.47 minutes T1 ρ 18.11 ± 0.46 minutes $P = 1$ between timing of all sequences.

7.4.3. Qualitative image analysis

7.4.3.1. Transmurality assessment

The transmural extent was deemed significantly larger in the BN ($66 \pm 34\%$) and T1 ρ ($66 \pm 36\%$) compared to MN $48 \pm 37\%$, ($P < 0.001$ compared to both

BN and T1 ρ). Interobserver agreement for transmural assessment was excellent for all methods ($\kappa = 0.81$ (MN), 0.95 (BN), 0.85 (T1 ρ)). Intraobserver agreement for transmural assessment was also good or excellent for all methods ($\kappa = 0.70$ (MN), 0.85 (BN), T1 ρ 0.85 (T1 ρ)).

7.4.3.2. Confidence scores for assessment of transmural

No images were deemed non-diagnostic. Confidence scores were significantly higher for BN (3.87 ± 0.346) compared to MN (3.10 ± 0.76 $P < 0.001$) and T1 ρ (3.20 ± 0.71 $P < 0.001$), there was no difference in confidence scores for T1 ρ compared to MN ($P = 0.977$). Interobserver agreement was excellent for the three methods ($\kappa = 0.843$ (MN), 0.865 (BN), 0.870 (T1 ρ)). Intraobserver agreement was also excellent for all three methods ($\kappa = 0.948$ (MN), 0.839 (BN), 0.865 (T1 ρ)). In one patient both BN and T1 ρ identified sub-endocardial scar that was mistaken for outflow tract by both readers on the MN LGE image (figure 7-2; further representative images are seen in figures 7-3 and 7-4).

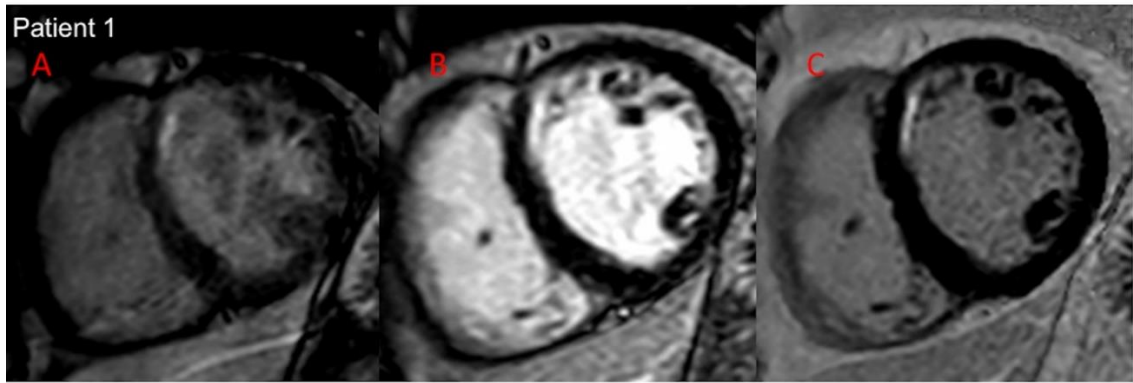


Figure 7-2 A, B, C (Patient 1) shows a small sub-endocardial anterior infarct imaged with each of the pulse sequences.

A is T1p, B is MN and C is BN. B shows limited contrast between the blood pool and scar and it could be mistaken for outflow tract, whereas in C the scar is clearly apparent. A demonstrates increased contrast between scar and blood pool but limited contrast between myocardium and blood pool.

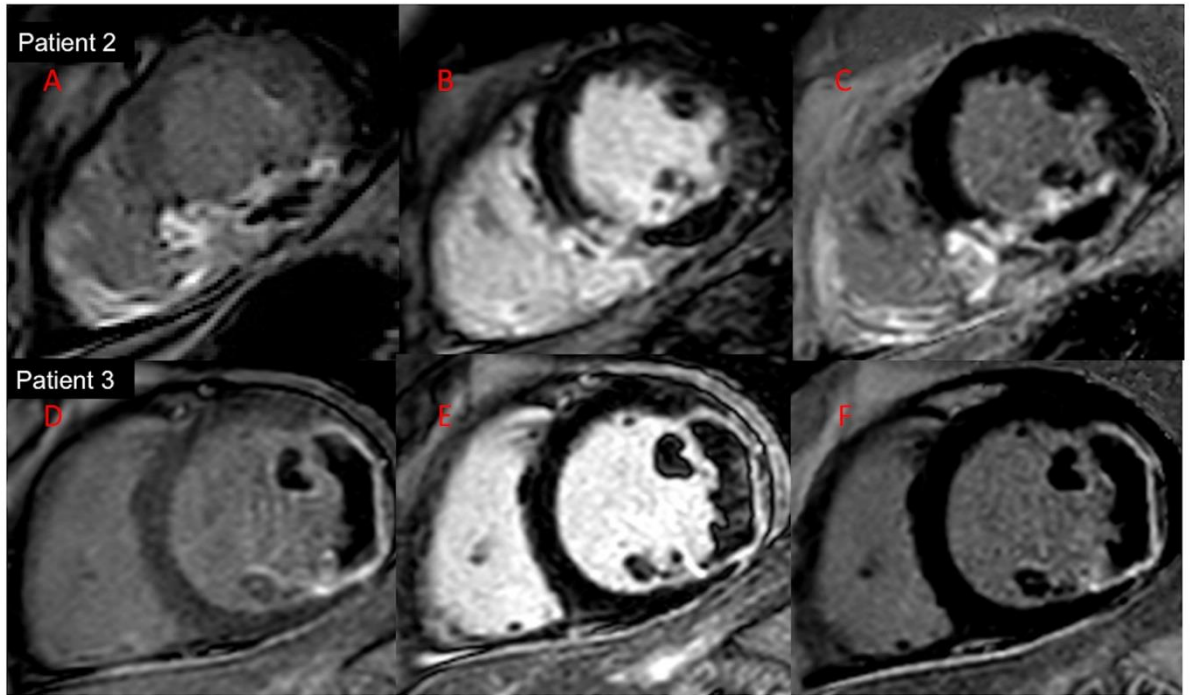


Figure 7-3 shows 2 patients with acute infarctions with each of the pulse sequences.

A, B, C (Patient 2) shows an acute inferior infarction with RV involvement and microvascular obstruction (MVO). B is MN compared to A, and C (T1 ρ and BN respectively) it is difficult to discern the extent of the RV infarction. **D, E and F (Patient 3)** show an acute lateral infarction with extensive MVO imaged with T1 ρ , MN and BN respectively. It is difficult to discern the papillary muscle MVO except in the T1 ρ (D).

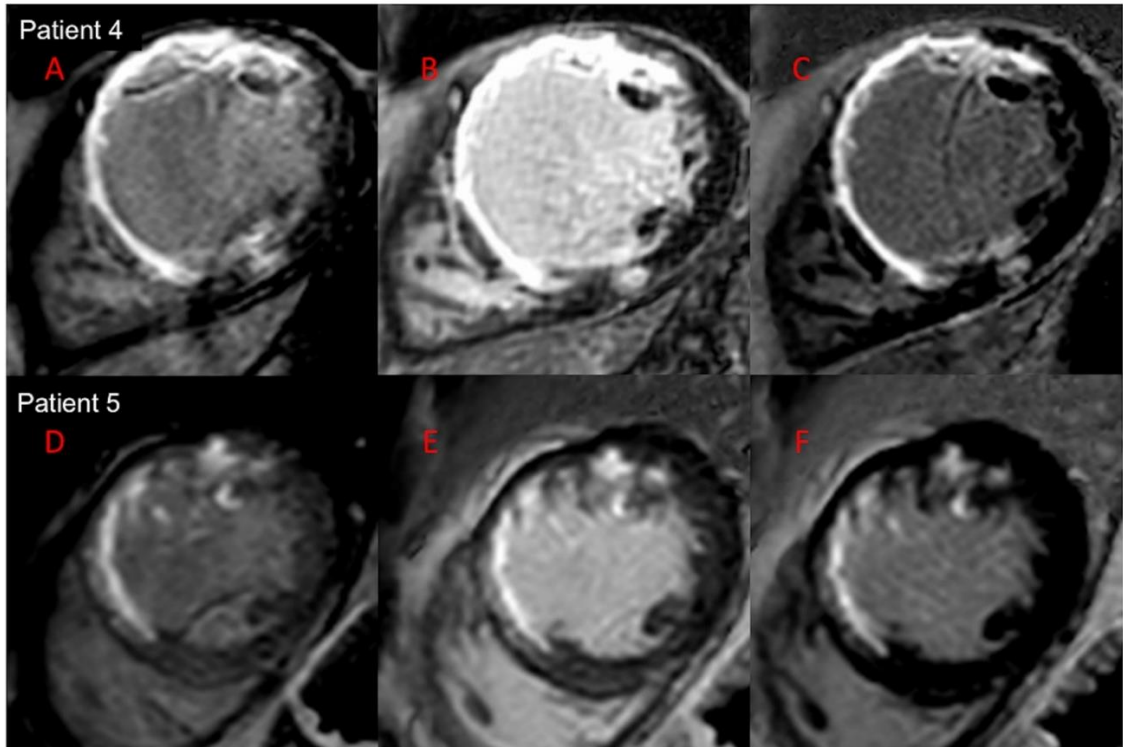


Figure 7-4 shows 2 patients with chronic infarction imaged with each of the pulse sequences:

A and D are T1 ρ , B, E is MN and C, F BN.

7.4.4. Quantitative image analysis

7.4.4.1. Scar size

There was no significant difference in scar size between the three LGE methods: MN ($2.28 \pm 1.58\text{g}$) BN ($2.16 \pm 1.57\text{g}$) and T1 ρ ($2.29 \pm 2.5\text{g}$) (MN:BN $P=0.066$, BN:T1 ρ $P=0.385$, MN: T1 ρ $P=1$). Interobserver coefficient of variation was good for all three methods (MN 9.32%, BN 7.63%, T1 ρ 9.40%.) Intraobserver coefficient of variation for scar size was also good for all three methods (MN 7.36%, BN 7.39%, T1 ρ 9.18%).

7.4.4.2. CNR analysis

The $\text{CNR}_{\text{scar-blood}}$ was significantly increased for both the BN (27.1 ± 10.4) and the T1 ρ (30.2 ± 15.1) compared to the MN (15.3 ± 8.4 $P<0.001$ for both sequences) (Figure 7-5). There was no significant difference in $\text{CNR}_{\text{scar-myocardium}}$

between BN (55.9 ± 17.3) and MN (51.1 ± 17.8 $P=0.512$); these both had significantly higher $CNR_{scar-myocardium}$ compared to the T1p (42.6 ± 16.9 $P=0.007$ and $P=0.014$ respectively). The $CNR_{blood-myocardium}$ was significantly higher for MN compared to BN (28.0 ± 12 $P<0.001$); $CNR_{blood-myocardium}$ was also significantly higher for both MN and BN compared to T1p (13.6 ± 7.2 $P<0.001$ for both sequences).

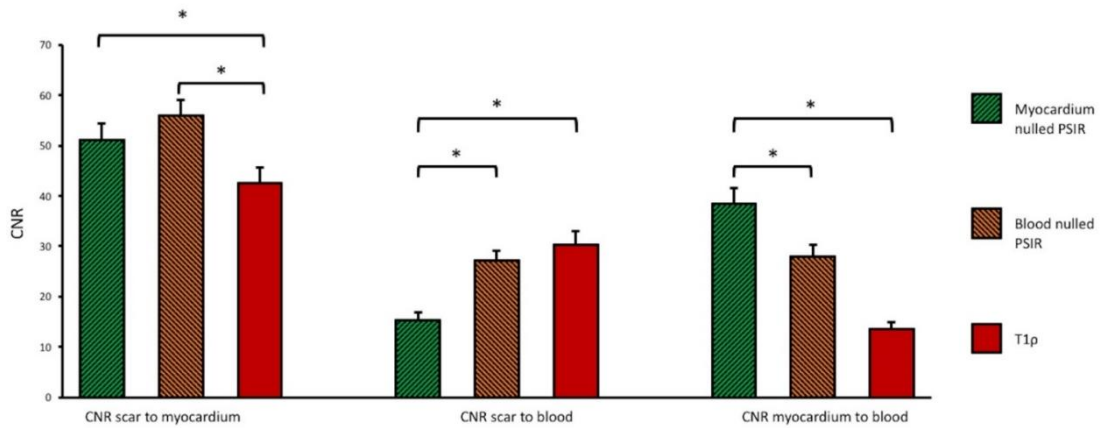


Figure 7-5 shows CNR for the respective sequences. Downward lines of the asterisked (*) bars demarcate significant difference between the CNRs of the respective pulse sequences.

7.5. Discussion

The main findings of this study are: i) both PSIR with TI set for blood nulling and the T1p LGE sequence demonstrated significantly higher scar to blood CNR compared to routine MN; ii) PSIR with TI set for blood nulling demonstrated significantly higher reader confidence scores compared to both routine MN and the novel T1p LGE sequence iii.) quantitative LGE scar size measurement showed no statistical difference between the three LGE methods.

Current conventional LGE imaging using IR and PSIR spoiled gradient echo sequences give high resolution images that are firmly established as the

reference standard for viability imaging by CMR. Accurate determination of transmural extent is vital to guide revascularisation; currently however a significant limitation is that of the limited contrast between hyperenhanced scar and residual contrast in the LV blood pool. Several previous studies have used a variety of different preparation pulses, including T2 preparation, double and triple inversion recovery, or T1p with spin locking to produce dark or black blood LGE images (172–178). Most recently focus has been concentrated on using a T2 preparation pulse to null the blood pool; Basha et al noted a significantly increased signal ratio between scar to blood using a T2 preparation pulse sequence versus a standard inversion recovery LGE sequence (361). Furthermore, recently a non-breath held motion corrected method using an inversion recovery T2 preparation combined with SSFP imaging demonstrated an increase in CNR of 13% for scar to blood compared to standard IR LGE sequence (177). This sequence has subsequently been assessed in 172 patients and identified significantly more LGE compared to standard LGE imaging (362). Most of these sequences currently remain research investigations and are vendor/platform specific and are yet to see mainstream clinical adoption. The recent study by Holtackers et al demonstrated an increased scar to blood contrast when nulling blood in a standard PSIR pulse sequence, without the need for additional preparation pulses (179).

Both the T1p and blood nulling PSIR LGE images in our study significantly increased the CNR between scar and blood pool compared to routine myocardium nulling PSIR images. Notably this only led to an increased reader confidence in the BN, but not however for the T1p sequence despite this increased CNR. The lower confidence scores for the T1p compared to the BN are likely representative of the lower $CNR_{\text{blood-myocardium}}$ for the T1p compared to the BN leading to difficulty in ascertaining the true anatomy of the left ventricle (distinction between remote myocardium and blood pool); this finding suggests that high $CNR_{\text{scar-blood}}$ is not the only facet necessary for high reader confidence. The anatomy of the ventricle can potentially be derived from the previously acquired SSFP images and transposed onto the T1p images in

order to clarify scar location; this however would add time to reader interpretation. The BN images retain the excellent image quality that characterise routine 2D MN PSIR images, whilst increasing the confidence of the reader for the identification of scar border. Quantitatively derived scar size was not significantly different between the three LGE methods despite the two dark blood methods objectively identifying greater transmural extent of scar to the two readers. Other LGE studies have demonstrated an increase in scar size using dark blood sequences, however these have been by visual assessment only or using less conventional methods of LGE quantitation (179, 362). There is no histological correlation for these findings, this corroborates those seen previously where histological correlation was performed (358).

This is the first study to compare PSIR with blood nulling and myocardium nulling to a dark blood sequence using additional preparation pulses. A primary benefit of the BN method is that the acquisition used in pulse sequence is already established in routine clinical use and requires no additional magnetisation pulses to perform. Importantly, this makes it simple for standard clinical adoption as it requires very little radiographer/clinician training to employ. This is in contrast to the recently described T2 sequence that led to a comparative doubling of acquisition time for a stack of 9 short axis slices (typically 12 short axis slices are acquired suggesting this length of time would increase further) (177). As CMR becomes ever more established in clinical guidelines efficient workflow in CMR departments is vital especially given that viability assessment is currently the third highest indication for CMR assessment in Europe (171).

7.5.1. Limitations

In this study, we only used single slices and did not cover the entire ventricle with the three different acquisitions. This approach however minimised the time elapsed between acquisition of the different sequences and consequent reduced the observed change in CNR to be due to the washout kinetics of the

gadolinium contrast agent. There was no histological reference standard to compare the actual presence or size of scar detected by the three sequences.

7.5.2. Conclusion

Both BN images and T1 ρ increase CNR for scar to blood compared to MN images with the TI set to null the myocardium. Routine adoption of the blood nulled PSIR would seem appropriate as reader confidence is heightened compared to MN images and T1 ρ sequences; as this LGE sequence is already in clinical use it requires little training to enable widespread clinical implementation.

8. Discussion

The mortality from cardiovascular disease remains the number one cause of death worldwide and continues to form a significant burden on modern healthcare systems.

Multi-parametric CMR is well-established to diagnose and guide the management of patients presenting with IHD. Progressively CMR methods are developed that allow insights to be gained into the pathophysiology of cardiovascular disease and diagnostic accuracy to be improved.

CMR imaging is ideally suited to investigative cardiovascular research due to the lack of ionising radiation for the acquisition of images and the high quality of image generation enables highly reproducible quantitative comparison of studies across patient groups. The central aim of this thesis was to study and refine the utility of both existing and emerging CMR imaging techniques in the context of IHD, with a particular emphasis on prior myocardial infarction and LGE techniques, risk prediction and diagnostic accuracy of ischaemia testing in severe CAD.

Chapter 3 compares the accuracy of non-invasive imaging methods of CMR with MPS-SPECT to identify significant left main coronary artery disease.

Chapter 4 uses quantitative analysis of myocardial function to give insights into myocardial mechanics and differentiate ischaemic and non-ischaemic cardiomyopathy that can appear phenotypically very similar.

Chapter 5 aimed to refine and update the Diamond and Forrester risk stratification score, commonly advocated in clinical practice guidelines, in order to risk stratify and identify those patients presenting with chest pain who should be sent for further investigation.

Chapters 7 and 8 are CMR method development chapters aiming to refine and advance upon existing LGE imaging techniques that are the cornerstone of viability and scar assessment in CMR.

8.1. Discussion, study limitations and future direction relating to Chapter 3

Chapter 3 “A Comparison of Cardiovascular Magnetic Resonance and Single Photon Emission Computed Tomography (SPECT) Perfusion Imaging in Left Main Stem or Equivalent Coronary Artery Disease” aimed to compare the diagnostic accuracy of the non-invasive imaging modalities of CMR and MPS-SPECT to identify significant left main coronary artery disease as measured by quantitative coronary angiography. Additionally, quantitative CMR perfusion analysis was compared to routine visual CMR analysis in the investigation of left main coronary artery disease. Significant left main stem coronary disease is associated with high mortality rates and is a relatively common finding in patients presenting with symptoms of stable coronary disease. Modern methods of coronary revascularisation have demonstrated significant survival benefits for patients with left main stem coronary disease. Data on the diagnostic accuracy of non-invasive imaging modalities for the assessment of coronary disease are often limited to observational retrospective studies in respect to MPS-SPECT, or not at all in respect to the utility of CMR. Both these imaging modalities are well established in the investigation of stable CAD and the findings seen on both CMR and SPECT have been related to prognosis and long term outcomes.

In this study, we demonstrated that in patients with stable suspected CAD, CMR first-pass perfusion imaging as part of a multi-parametric protocol more accurately detected evidence of CAD in LMS patients (AUC: 0.95; 0.85-0.99) than MPS-SPECT (AUC: 0.63; 0.49-0.76) ($p=0.0001$). Furthermore, although quantitative CMR perfusion showed high diagnostic accuracy for the detection of LMS disease with a global MBF $<2.08\text{ml/g/min}$ had sensitivity of 78% and

specificity of 85% for diagnosis of LMS disease, as the most diagnostic quantitative marker (AUC: 0.87; 0.75-0.94); quantitative perfusion however did not outperform visual CMR perfusion analysis ($p=0.18$) however was significantly more accurate than investigation with MPS-SPECT ($p=0.003$).

There were some limitations to this study, the numbers of patients with LMS disease in this prospective study are limited. In this study MPS-SPECT analysis did not use attenuation correction; this was however not routine practice when the CE-MARC study was undertaken (264). In this study, anatomical assessment with QCA was used as the endpoint for coronary angiography rather than FFR which has been used as a more contemporary method of physiological assessment. The CMR perfusion imaging pulse sequence used in CE-MARC was not fully optimised for quantitative analysis. The pulse sequence used a single preparation pulse for all three slices and a relatively high contrast agent dose that potentially may have led to a lower performance of quantitative analysis in this study compared to more recently developed methods. Studies comparing dual-bolus and uncorrected single bolus myocardial blood flow estimates however have not shown significant differences in diagnostic accuracy (266), and our diagnostic accuracy values corroborate other comparable studies in the literature, suggesting these limitations have not significantly affected our results.

Future directions in this area of research should build upon this exploratory analysis of the CE-MARC dataset. Further studies in this area should include a larger sized patient population. Furthermore, using a more contemporary pulse sequence that have been optimised for quantitative perfusion analysis would also add merit to further studies. Additionally, using a physiological reference standard such as FFR or alternatively IVUS that are often used in contemporary invasive assessment of left main coronary disease would add merit to further studies of non-invasive imaging in LMS disease.

8.2. Discussion, study limitations and future direction relating to Chapter 4

Chapter 4 “Quantitative deformation analysis differentiates ischaemic and non-ischaemic cardiomyopathy” aimed to investigate the relationship between strain-derived parameters of myocardium and the aetiology of patients with heart failure with reduced ejection fractions and hypothesised that in a prospectively recruited random sample of HFrEF patients with ICM and NICM would have distinctive myocardial torsion patterns. LV torsion results as a consequence of the fibrous architecture of the heart and is altered by different loading conditions such as hypertension, athletic training and alters with increasing age. Thus far there have been no comparisons of LV mechanics performed between different aetiologies of HFrEF.

This study demonstrated that all quantitatively derived CMR myocardial mechanical parameters including strain, twist and torsion were reduced in HF patients compared to healthy age-matched controls. Furthermore, despite patients being phenotypically comparable with analogous left ventricular dimensions, EF and strain parameters, patients with NICM generate significantly less LV twist and torsion than patients with ICM. Twist, torsion and strain are reduced in patients with cardiomyopathy compared to controls. Torsion and twist are significantly lower in patients with NICM compared to ICM, despite similar volumetric dimensions, circumferential and longitudinal strain parameters and LVEF.

Our observational study has a number of limitations. Overall this is a relatively small sample size with some differences in baseline demographics, comorbidities and treatment that may potential have led to a degree of bias. However this study was prospectively enrolled and age matched in both cardiomyopathy groups and controls particularly as age has been shown to affect the myocardial mechanics (strain, torsion and twist) measured here

(303). A recognised limitation of 2D tagging methods is through plane motion, the 2D method used in our paper has consistently been demonstrated to be reliable and reproducible in a variety of patient groups (233, 286, 304, 305) , and 2D and 3D tagging methods for LV torsion have been shown to strongly related (306). Current 3D methods of CMR tagging are time consuming requiring multiple breath holds of long duration (307, 308, 363), thus from a pragmatic point of view we used a reproducible 2D method that required a single breath hold per slice that HF patients would be able to tolerate. This 2D tagging method may potentially have had an effect on our results due to the global deformation changes seen in NICM versus local changes in contractile properties in ICM.

Future directions in this area of research should endeavour to build upon the findings of this study. Potential areas of work would be to reproduce these findings in a larger cohort of patients. Furthermore, different groups of heart failure subtypes and varying severity of disease phenotype could be investigated to further increase understanding of different pathophysiology. Additionally, the myocardial mechanical indices measured here by CMR could potentially be used to investigate patient response to medications or clinical interventions and be related to patient prognosis.

8.3. Discussion, study limitations and future direction relating to Chapter 5

Chapter 5 “Development and validation of a contemporary pre-test likelihood model of coronary artery disease referenced to invasive angiography, with comparison to pre-existing risk models” sought to both develop and validate a contemporary multivariable risk model based entirely on invasive coronary angiographic data (using data from two recently published contemporary UK studies of stable coronary artery disease (CE-MARC and CE-MARC 2: Clinical evaluation of magnetic resonance imaging in coronary heart disease study)), and to compare this to pre-existing risk models that are currently used

in clinical practice guidelines (35, 63, 96, 203). Non-invasive imaging is increasingly used as a first line investigation in stable CAD and advocated by societal practice guidelines prior to invasive assessment by X-ray coronary angiography; the use of PTL scores help to quantify risk of CAD and to guide choice of investigation. Historical risk scores based on X-ray angiography have been shown to overestimate the risk of coronary artery disease most likely as a consequence of being derived from highly selective higher risk populations that do not represent the lower risk populations undergoing assessment seen in current practice; whilst more modern risk scores are typically derived from heterogeneous populations derived from non-invasive imaging studies often using CTCA as the marker of presence of CAD with no invasive reference standard.

In this study, we corroborated the findings of previous studies that have indicated that the pre-existing Diamond and Forrester and Duke scores overestimate the risk of CAD in a contemporary population. Additionally, the more recent models by the CAD Consortium (recommended in the ESC guidelines) slightly under-estimated risk of CAD, but performed well once this was accounted for. The CE-MARC risk model that we developed in this study, that was derived from a large contemporary UK population undergoing invasive angiography, performed very well for estimation of PTL in the independent validation sample that again used invasive x-ray coronary angiography as the reference standard for the diagnosis of stenotic coronary artery disease, without needing any adjustment for different risk prevalence or for miscalibration.

There are a few limitations to this study. The total sample size of 1044 patients of the prospective development and validation datasets are comparatively small to the standard set by the CAD Consortium study. In this study some established clinical predictors were not found to be statistically significant (smoking, hypertension, type II diabetes) which may well be due to the sample size. Furthermore, while our development dataset was sufficiently-sized (in

terms of events per variable), and was derived from a study with low risk of work-up bias, this was however a single-centre study. Similarly, although the validation set was developed from a 6-centre randomised controlled trial, adding the enrichment population led to almost two thirds of the data being derived from the same hospital as the development set. A significant miscalibration effect was observed (-0.305; 95%CI -0.611, 0.000; P=0.050) if the enrichment set was removed from the validation of the CE-MARC model; this was due to the study population of CE-MARC 2 having a Duke PTL between 10-90%, (removing the enrichment set would mean the validation population would not have the same distribution of PTL as the development population). Excluding the enrichment set from the validation of the CE-MARC model did not however change the overall calibration in the large.

Future directions in this area would be to increase the overall sample size with a more even spread across the different risk groups derived from multiple centres and additionally with a larger representation of those in the older age groups and in the lower risk groups that are progressively more prevalent in rapid access chest pain clinics in contemporary practice.

8.4. Discussion, study limitations and future direction relating to Chapter 6

Chapter 6 “Feasibility Study of a Single Breath-hold, 3D mDIXON Pulse Sequence for Late Gadolinium Enhancement Imaging of Ischaemic Scar” utilised a novel mDIXON 3D-LGE imaging sequence in the setting of both acute and chronic MI. Multiple 3D LGE sequences have been proposed as an alternative to the standard 2D sequences that are used in clinical practice that cover the entire left ventricle in a single breath hold (156, 326–329) or via navigator based free breathing sequences (330–334); clinical adoption however has not occurred as these often compromise image quality and require long breath hold durations. The primary objectives of this study were

to prospectively evaluate the mDIXON 3D-LGE sequence for the detection and quantification of myocardial scarring and compare it to a standard 2D PSIR acquisition sequence used in routine practice.

In this study 3D mDIXON LGE was shown to offer a comparable level of image quality for the evaluation of ischaemic scar in the setting of both acute and chronic MI compared to standard 2D PSIR LGE imaging. Additionally using quantitative LGE assessment, 3D mDIXON LGE has high agreement with 2D LGE imaging for both scar mass and transmural. Furthermore, the 3D mDIXON LGE sequence evaluated in this study had a significantly shorter overall scan duration with an acceptable single breath-hold time compared to 2D LGE for coverage of the entire LV.

Limitations of our study include the difference in slice thickness between the 2D and 3D acquisitions. Additionally, the 3D mDIXON LGE scan that we used in this study does not employ a PSIR reconstruction, and consequently the image contrast is more sensitive to correct inversion time selection. A further limitation is that there is no pathology based reference standard to compare the true size and presence of myocardial infarction from the quantitative analysis of either 2D or 3D LGE approaches.

Studies of LGE imaging techniques are often limited by the lack of a histological reference standard. Further studies based on this work could utilise pathology as the reference standard for quantification of myocardial scarring. This study was performed in the setting of IHD and this method could be evaluated in patients presenting with alternative forms of cardiomyopathy with scarring from patchy fibrosis to mid wall fibrosis. Additionally, the utility of 3D mDIXON LGE imaging should be clinically evaluated to assess if its adoption improves clinical workflow.

8.5. Discussion, study limitations and future direction relating to Chapter 7

Chapter 7 “Clinical Evaluation of two dark blood methods of late gadolinium quantification of ischaemic scar” aimed to prospectively evaluate a novel T1 ρ dark blood sequence and compare this to blood nulled PSIR and standard myocardium nulled PSIR for the detection and quantification of myocardial scarring in the setting of IHD.

The principle findings of this chapter were that both PSIR with the TI set for blood nulling and the T1 ρ LGE sequence demonstrated significantly higher scar to blood CNR compared to routine MN PSIR. The study also showed that PSIR with TI set for blood nulling demonstrated significantly higher reader confidence scores compared to both routine MN and the novel T1 ρ LGE sequence. For quantitative LGE scar size measurement there was no statistical difference demonstrated between the three LGE methods.

Limitations In this study, are the use of only single slices rather than covering the entire ventricle with the three different acquisitions. This was a pragmatic approach that minimised the time elapsed between acquisition of the different pulse sequences and consequently reduced the observed change in CNR to be due to the washout kinetics of the gadolinium contrast agent. There was no histological reference standard to compare the actual presence or size of scar detected by the three sequences.

As with the previous chapter, future studies evaluating dark blood LGE imaging could utilise histology as the reference standard for quantification of myocardial scarring. A larger patient group could be used in order to identify if scarring was missed on the bright blood sequences that were identified on the dark blood sequences. This study was performed in the setting of IHD and this method could be evaluated in patients presenting with alternative forms of cardiomyopathy with scarring from patchy fibrosis to mid wall fibrosis.

Additionally, comparison of the blood nulled PSIR could be made to other dark blood sequences that are being adopted on differing platforms.

8.6. Overall future directions

CMR is now recognised as the reference standard for cardiac volumetric analysis and function (88, 89) and highly diagnostic for myocardial ischaemia and scarring; consequently CMR is firmly established in clinical practice guidelines for the investigation and management of IHD. Progress and future directions for CMR will come from progression of technological advances and their application to improve diagnostic accuracy as well as speed up clinical workflow; perhaps more importantly will be the application of CMR to demonstrate altered clinical outcomes.

Despite rapid progress in CMR technology, clinical CMR scanning due to its multi-parametric nature remains relatively time consuming compared to other non-invasive imaging modalities used in the investigation of IHD (47). Technological advances in accelerated CMR methods aim to improve temporal and spatial resolution as well as reduce overall scan durations. Accelerated methods utilising parallel imaging and kt undersampling are well established in clinical MR imaging (364). Recently interest has turned to compressed sensing (365); like k-t methods compressed sensing also exploits sparsity in a transform domain but instead of reducing the overlap in the transform domain, compressed sensing uses incoherent sampling and non-linear reconstruction. Compressed sensing techniques have been demonstrated to acquire a full cardiac cycle LV cine stack in a single breath hold with high reproducibility (352, 366).

In addition to the improvement in scanner hardware and pulse sequences, improvements to analysis software should enable improved clinical workflow and speed of reporting. Machine learning and the use of artificial intelligence

are both being adopted to accelerate software analysis (367, 368). The most recent update of Circle CVI uses machine learning in order to provide automatic contouring for left ventricular volumetric analysis and ejection fraction. Despite the progress in technological advances in CMR that continue apace, this is not however the only area of research that requires focus for progress in the field of CMR. Technological advances remain a technical endeavour without clinical application.

8.6.1. Studies showing outcomes in ischaemic heart disease

Progressively studies involving non-invasive imaging are using hard endpoints of mortality (322, 369). Thus far despite basic science studies showing improvement of function following viability assessment and suggestion from meta-analyses showing improved outcomes for patients using viability testing to improved patient outcomes, this has yet to be borne out in clinical studies (152, 370). The STICH viability substudy investigated this subject and showed no benefit to patient outcomes using viability assessment; however this was a sub-study of a negative trial and was fraught with confounders (12). Despite this viability assessment remains the 3rd highest indication for CMR in Europe (171); a randomised controlled trial of revascularisation versus optimal medical therapy in patients with viability as measured by LGE is surely clinically warranted.

Progressively non-invasive imaging studies are used as a gatekeeper to invasive coronary angiography. Despite the publication of the PROMISE trial as yet it is not clear whether functional imaging or anatomical imaging should be the imaging method of choice prior to angiography (322). A multi-centre study comparing functional imaging (CMR or DSE) compared to anatomical imaging (CTCA) to guide the management of patients with suspected CAD using a physiological reference standard such as FFR is another avenue that should be explored.

Newer methods of quantitative perfusion have been developed that are readily accessible to the clinician and that have been shown to have good correlation with PET (129, 130). This modality is beginning to be placed beyond a research tool and into clinical practice. Clinical trials using quantitative perfusion should be performed to assess whether it has any benefit compared to qualitative assessment for management of patients with suspected CAD and has utility other than as a research tool. Additionally quantitative perfusion is ideally placed to assess the concept of prognostic benefit being derived from revascularisation in patients with >10% ischaemia burden; a figure derived from historical observational studies (371).

8.7. Conclusions

CMR with its multiparametric nature and high reproducibility is ideally suited to the diagnosis of ischaemic heart disease and its sequelae, as well as providing insights into disease mechanisms.

In this thesis CMR has been demonstrated to have higher diagnostic accuracy over MPS-SPECT for the investigation of significant left main coronary artery disease. Using MR derived strain indices, it has been demonstrated that patients with non-ischaemic cardiomyopathy generate significantly less LV twist and torsion than patients with ischaemic cardiomyopathy. A contemporary risk score to assess the pre-test likelihood of coronary artery disease has been developed and validated in patients presenting with chest pain. A novel 3D mDIXON LGE method has been shown to generate comparable image quality for the evaluation of ischaemic scar compared to routine 2D LGE imaging in an overall greatly shorter scan time. Additionally this thesis has validated a novel method for dark blood late gadolinium imaging that does not utilise extra preparation pulses.

9. References

1. WHO | The top 10 causes of death. Available at: <http://www.who.int/mediacentre/factsheets/fs310/en/>. Accessed November 3, 2015.
2. Townsend N, Nichols M, Scarborough P, Rayner M. Cardiovascular disease in Europe - Epidemiological update 2015. *Eur. Heart J.* 2015;36:2696–2705.
3. Mozaffarian D, Benjamin EJ, Go AS, et al. Heart Disease and Stroke Statistics—2016 Update. *Circulation* 2016;133:e38–e360.
4. Bhatnagar P, Wickramasinghe K, Williams J, Rayner M, Townsend N. The epidemiology of cardiovascular disease in the UK 2014. *Heart* 2015;101:1182–1189.
5. Moschetti K, Petersen SE, Pilz G, et al. Cost-minimization analysis of three decision strategies for cardiac revascularization: results of the “suspected CAD” cohort of the european cardiovascular magnetic resonance registry. *J. Cardiovasc. Magn. Reson.* 2016;18:3.
6. Heal. Soc. Care Inf. Centre. Hosp. Epis. Stat. Admit. Patient Care—England, 2014–15 Prim. diagnosis, 3 characters table. Available at: <http://www.hesonline.nhs.uk/>. Accessed October 16, 2016.
7. Goodacre S, Cross E, Arnold J, Angelini K, Capewell S, Nicholl J. The health care burden of acute chest pain. *Heart* 2005;91:229–30.
8. Montalescot G, Sechtem U, Achenbach S, et al. 2013 ESC guidelines on the management of stable coronary artery disease: the Task Force on the management of stable coronary artery disease of the European Society of Cardiology. *Eur. Heart J.* 2013;34:2949–3003.

9. Thygesen K, Alpert JS, Jaffe AS, et al. Third universal definition of myocardial infarction. *Eur. Heart J.* 2012;33:2551–2567.
10. Sutton MG, Sharpe N. Left ventricular remodeling after myocardial infarction: pathophysiology and therapy. *Circulation* 2000;101:2981–8.
11. Camici PG, Prasad SK, Rimoldi OE. Stunning, hibernation, and assessment of myocardial viability. *Circulation* 2008;117:103–14.
12. Bonow RO, Maurer G, Lee KL, et al. Myocardial viability and survival in ischemic left ventricular dysfunction. *N. Engl. J. Med.* 2011;364:1617–25.
13. Allman KC, Shaw LJ, Hachamovitch R, Udelson JE. Myocardial viability testing and impact of revascularization on prognosis in patients with coronary artery disease and left ventricular dysfunction: a meta-analysis. *J. Am. Coll. Cardiol.* 2002;39:1151–8.
14. Sheifer SE, Manolio TA, Gersh BJ. Unrecognized myocardial infarction. *Ann. Intern. Med.* 2001;135:801–11.
15. Ross R. Inflammation or Atherogenesis. *N. Engl. J. Med.* 1999;340:115–126.
16. Yahagi K, Kolodgie FD, Otsuka F, et al. Pathophysiology of native coronary, vein graft, and in-stent atherosclerosis. *Nat. Rev. Cardiol.* 2016;13:79–98.
17. Libby P. Mechanisms of Acute Coronary Syndromes and Their Implications for Therapy. *N. Engl. J. Med.* 2013;368:2004–2013.
18. Virmani R, Burke AP, Farb A, Kolodgie FD. Pathology of the Vulnerable Plaque. *J. Am. Coll. Cardiol.* 2006;47:C13–C18.
19. Farb A, Burke AP, Tang AL, et al. Coronary plaque erosion without rupture into a lipid core. A frequent cause of coronary thrombosis in sudden coronary death. *Circulation* 1996;93:1354–63.
20. Reimer KA, Jennings RB. The “wavefront phenomenon” of myocardial

ischemic cell death. II. Transmural progression of necrosis within the framework of ischemic bed size (myocardium at risk) and collateral flow. *Lab. Invest.* 1979;40:633–44.

21. Thygesen K, Alpert JS, Jaffe AS, et al. Fourth universal definition of myocardial infarction (2018). *Eur. Heart J.* 2018;33:2551–2567.

22. Masci PG, Bogaert J. Post myocardial infarction of the left ventricle: the course ahead seen by cardiac MRI. *Cardiovasc. Diagn. Ther.* 2012;2:113–127.

23. Fishbein MC, Maclean D, Maroko PR. The histopathologic evolution of myocardial infarction. *Chest* 1978;73:843–849.

24. Ganame J, Messalli G, Masci PG, et al. Time course of infarct healing and left ventricular remodelling in patients with reperfused ST segment elevation myocardial infarction using comprehensive magnetic resonance imaging. *Eur. Radiol.* 2011;21:693–701.

25. Masci PG, Ganame J, Francone M, et al. Relationship between location and size of myocardial infarction and their reciprocal influences on post-infarction left ventricular remodelling. *Eur. Heart J.* 2011;32:1640–1648.

26. Springeling T, Uitterdijk A, Rossi A, et al. Evolution of reperfusion post-infarction ventricular remodeling: New MRI insights. *Int. J. Cardiol.* 2013;169:354–358.

27. Fihn SD, Gardin JM, Abrams J, et al. 2012 ACCF/AHA/ACP/AATS/PCNA/SCAI/STS Guideline for the diagnosis and management of patients with stable ischemic heart disease: a report of the American College of Cardiology Foundation/American Heart Association Task Force on Practice Guidelines, and the J. Am. Coll. Cardiol. 2012;60:e44–e164.

28. Tonino PAL, De Bruyne B, Pijls NHJ, et al. Fractional flow reserve

versus angiography for guiding percutaneous coronary intervention. *N. Engl. J. Med.* 2009;360:213–24.

29. Patel MR, Peterson ED, Dai D, et al. Low diagnostic yield of elective coronary angiography. *N. Engl. J. Med.* 2010;362:886–95.

30. Skinner JS, Smeeth L, Kendall JM, Adams PC, Timmis A, Chest Pain Guideline Development Group. NICE guidance. Chest pain of recent onset: assessment and diagnosis of recent onset chest pain or discomfort of suspected cardiac origin. *Heart* 2010;96:974–8.

31. Morise AP, Diamond GA. Comparison of the sensitivity and specificity of exercise electrocardiography in biased and unbiased populations of men and women. *Am. Heart J.* 1995;130:741–7.

32. Gianrossi R, Detrano R, Mulvihill D, et al. Exercise-induced ST depression in the diagnosis of coronary artery disease. A meta-analysis. *Circulation* 1989;80:87–98.

33. Diamond GA, Forrester JS. Analysis of probability as an aid in the clinical diagnosis of coronary-artery disease. *N. Engl. J. Med.* 1979;300:1350–8.

34. Nagel E, Shaw LJ. The assessment of ischaemic burden: Thoughts on definition and quantification. *Eur. Heart J. Cardiovasc. Imaging* 2014;15:610–611.

35. Greenwood JP, Ripley DP, Berry C, et al. Effect of Care Guided by Cardiovascular Magnetic Resonance, Myocardial Perfusion Scintigraphy, or NICE Guidelines on Subsequent Unnecessary Angiography Rates: The CE-MARC 2 Randomized Clinical Trial. *JAMA* 2016;316:1051–60.

36. NICE CG95 Chest pain Recent onset Assess. diagnosis Updat. Novemb. 2016. Available at:
<https://www.nice.org.uk/guidance/CG95/chapter/Recommendations#people-presenting-with-stable-chest-pain>. Accessed December 1, 2016.

37. Rumberger JA, Simons DB, Fitzpatrick LA, Sheedy PF, Schwartz RS. Coronary artery calcium area by electron-beam computed tomography and coronary atherosclerotic plaque area. A histopathologic correlative study. *Circulation* 1995;92:2157–2162.

38. Hou Z, Lu B, Gao Y, et al. Prognostic Value of Coronary CT Angiography and Calcium Score for Major Adverse Cardiac Events in Outpatients. *JACC Cardiovasc. Imaging* 2012;5:990–999.

39. Polonsky TS, McClelland RL, Jorgensen NW, et al. Coronary artery calcium score and risk classification for coronary heart disease prediction. *JAMA* 2010;303:1610–1616.

40. Knez A, Becker A, Leber A, et al. Relation of coronary calcium scores by electron beam tomography to obstructive disease in 2,115 symptomatic patients. *Am. J. Cardiol.* 2004;93:1150–1152.

41. Villines TC, Hulten EA, Shaw LJ, et al. Prevalence and severity of coronary artery disease and adverse events among symptomatic patients with coronary artery calcification scores of zero undergoing coronary computed tomography angiography: results from the CONFIRM (Coronary CT Angiography Evalu. *J. Am. Coll. Cardiol.* 2011;58:2533–2540.

42. Maurovich-Horvat P, Ferencik M, Voros S, Merkely B, Hoffmann U. Comprehensive plaque assessment by coronary CT angiography. *Nat. Rev. Cardiol.* 2014;11:390–402.

43. Budoff MJ, Raggi P, Beller GA, et al. Noninvasive Cardiovascular Risk Assessment of the Asymptomatic Diabetic Patient. *JACC Cardiovasc. Imaging* 2016;9:176–192.

44. Heijnenbrok-Kal MH, Fleischmann KE, Hunink MGM. Stress echocardiography, stress single-photon-emission computed tomography and electron beam computed tomography for the assessment of coronary artery disease: a meta-analysis of diagnostic performance. *Am. Heart J.*

2007;154:415–23.

45. Paech DC, Weston AR. A systematic review of the clinical effectiveness of 64-slice or higher computed tomography angiography as an alternative to invasive coronary angiography in the investigation of suspected coronary artery disease. *BMC Cardiovasc. Disord.* 2011;11:32.

46. Mowatt G, Cook JA, Hillis GS, et al. 64-Slice computed tomography angiography in the diagnosis and assessment of coronary artery disease: systematic review and meta-analysis. *Heart* 2008;94:1386–93.

47. Yilmaz A, Sechtem U. Ischaemia testing in patients with stable angina: which test for whom? *Heart* 2014;100:1886–1896.

48. Zarins CK, Taylor CA, Min JK. Computed fractional flow reserve (FFR_{CT}) derived from coronary CT angiography. *J. Cardiovasc. Transl. Res.* 2013;6:708–714.

49. Min JK, Taylor CA, Achenbach S, et al. Noninvasive Fractional Flow Reserve Derived From Coronary CT Angiography: Clinical Data and Scientific Principles. *JACC. Cardiovasc. Imaging* 2015;8:1209–22.

50. Koo BK, Erglis A, Doh JH, et al. Diagnosis of ischemia-causing coronary stenoses by noninvasive fractional flow reserve computed from coronary computed tomographic angiograms: Results from the prospective multicenter DISCOVER-FLOW (Diagnosis of Ischemia-Causing Stenoses Obtained Via Noninvasive Fractional Flow Reserve) Study. *J. Am. Coll. Cardiol.* 2011;58:1989–1997.

51. Nørgaard BL, Leipsic J, Gaur S, et al. Diagnostic performance of noninvasive fractional flow reserve derived from coronary computed tomography angiography in suspected coronary artery disease: The NXT trial (Analysis of Coronary Blood Flow Using CT Angiography: Next Steps). *J. Am. Coll. Cardiol.* 2014;63:1145–1155.

52. Curzen NP, Nolan J, Zaman AG, Nørgaard BL, Rajani R. Does the

Routine Availability of CT-Derived FFR Influence Management of Patients With Stable Chest Pain Compared to CT Angiography Alone?: The FFRCT RIPCORDER Study. *JACC. Cardiovasc. Imaging* 2016;9:1188–1194.

53. Douglas PS, De Bruyne B, Pontone G, et al. 1-Year Outcomes of FFRCT-Guided Care in Patients With Suspected Coronary Disease: The PLATFORM Study. *J. Am. Coll. Cardiol.* 2016;68:435–45.

54. Cook CM, Petraco R, Shun-Shin MJ, et al. Diagnostic Accuracy of Computed Tomography-Derived Fractional Flow Reserve : A Systematic Review. *JAMA Cardiol.* 2017;2:803–810.

55. Menke J, Unterberg-Buchwald C, Staab W, Sohns JM, Seif Amir Hosseini A, Schwarz A. Head-to-head comparison of prospectively triggered vs retrospectively gated coronary computed tomography angiography: Meta-analysis of diagnostic accuracy, image quality, and radiation dose. *Am. Heart J.* 2013;165:154–63.e3.

56. Baron KB, Choi AD, Chen MY. Low Radiation Dose Calcium Scoring: Evidence and Techniques. *Curr. Cardiovasc. Imaging Rep.* 2016;9:12.

57. Layland J, Carrick D, Lee M, Oldroyd K, Berry C. Adenosine. *JACC Cardiovasc. Interv.* 2014;7:581–591.

58. Iskandrian AE, Bateman TM, Belardinelli L, et al. Adenosine versus regadenoson comparative evaluation in myocardial perfusion imaging: results of the ADVANCE phase 3 multicenter international trial. *J. Nucl. Cardiol.* 14:645–58.

59. Perrin M, Djaballah W, Moulin F, et al. Stress-first protocol for myocardial perfusion SPECT imaging with semiconductor cameras: high diagnostic performances with significant reduction in patient radiation doses. *Eur. J. Nucl. Med. Mol. Imaging* 2015;42:1004–11.

60. Rybicki FJ, Mather RT, Kumamaru KK, et al. Comprehensive

assessment of radiation dose estimates for the CORE320 study. *AJR. Am. J. Roentgenol.* 2015;204:W27-36.

61. Wolk MJ, Bailey SR, Doherty JU, et al. ACCF/AHA/ASE/ASNC/HFSA/HRS/SCAI/SCCT/SCMR/STS 2013 multimodality appropriate use criteria for the detection and risk assessment of stable ischemic heart disease: a report of the American College of Cardiology Foundation Appropriate Use Criteria Task Force. *J. Am. Coll. Cardiol.* 2014;63:380–406.

62. de Jong MC, Genders TSS, van Geuns R-J, Moelker A, Hunink MGM. Diagnostic performance of stress myocardial perfusion imaging for coronary artery disease: a systematic review and meta-analysis. *Eur. Radiol.* 2012;22:1881–1895.

63. Greenwood JP, Maredia N, Younger JF, et al. Cardiovascular magnetic resonance and single-photon emission computed tomography for diagnosis of coronary heart disease (CE-MARC): a prospective trial. *Lancet* 2012;379:453–460.

64. Greenwood JP, Motwani M, Maredia N, et al. Comparison of Cardiovascular Magnetic Resonance and Single-Photon Emission Computed Tomography in Women With Suspected Coronary Artery Disease From the Clinical Evaluation of Magnetic Resonance Imaging in Coronary Heart Disease (CE-MARC) Trial. *Circulation* 2014;129:1129–1138.

65. Klocke FJ, Baird MG, Lorell BH, et al. ACC/AHA/ASNC guidelines for the clinical use of cardiac radionuclide imaging--executive summary: a report of the American College of Cardiology/American Heart Association Task Force on Practice Guidelines (ACC/AHA/ASNC Committee to Revise the 1995 Guideli. *Circulation* 2003;108:1404–18.

66. Douglas PS, Khandheria B, Stainback RF, et al. ACCF/ASE/ACEP/AHA/ASNC/SCAI/SCCT/SCMR 2008 appropriateness

criteria for stress echocardiography: a report of the American College of Cardiology Foundation Appropriateness Criteria Task Force, American Society of Echocardiography, American College of Emerg. *Circulation* 2008;117:1478–1497.

67. Supariwala A, Makani H, Kahan J, et al. Feasibility and prognostic value of stress echocardiography in obese, morbidly obese, and super obese patients referred for bariatric surgery. *Echocardiography* 2014;31:879–885.

68. Varga A, Garcia MAR, Picano E. Safety of stress echocardiography (from the International Stress Echo Complication Registry). *Am. J. Cardiol.* 2006;98:541–543.

69. Geleijnse ML, Krenning BJ, van Dalen BM, et al. Factors affecting sensitivity and specificity of diagnostic testing: dobutamine stress echocardiography. *J. Am. Soc. Echocardiogr.* 2009;22:1199–1208.

70. Schinkel AFL, Bax JJ, Elhendy A, et al. Long-term prognostic value of dobutamine stress echocardiography compared with myocardial perfusion scanning in patients unable to perform exercise tests. *Am. J. Med.* 2004;117:1–9.

71. Tillisch J, Brunken R, Marshall R, et al. Reversibility of Cardiac Wall-Motion Abnormalities Predicted by Positron Tomography. *N. Engl. J. Med.* 1986;314:884–888.

72. Bergmann SR, Weinheimer CJ, Markham J, Herrero P. Quantitation of myocardial fatty acid metabolism using PET. *J. Nucl. Med.* 1996;37:1723–30.

73. Takx RAP, Blomberg B a., El Aidi H, et al. Diagnostic accuracy of stress myocardial perfusion imaging compared to invasive coronary angiography with fractional flow reserve meta-analysis. *Circ. Cardiovasc. Imaging* 2015;8:e002666–e002666.

74. Joshi N V, Vesey AT, Williams MC, et al. 18F-fluoride positron emission tomography for identification of ruptured and high-risk coronary atherosclerotic plaques: a prospective clinical trial. *Lancet (London, England)* 2014;383:705–13.
75. Dweck MR, Chow MWL, Joshi N V., et al. Coronary arterial 18F-sodium fluoride uptake: a novel marker of plaque biology. *J. Am. Coll. Cardiol.* 2012;59:1539–48.
76. Nallamothu BK, Spertus JA, Lansky AJ, et al. Comparison of clinical interpretation with visual assessment and quantitative coronary angiography in patients undergoing percutaneous coronary intervention in contemporary practice: the Assessing Angiography (A2) project. *Circulation* 2013;127:1793–800.
77. Isner JM, Kishel J, Kent KM, Ronan JA, Ross AM, Roberts WC. Accuracy of angiographic determination of left main coronary arterial narrowing. Angiographic--histologic correlative analysis in 28 patients. *Circulation* 1981;63:1056–64.
78. Cameron A, Kemp HG, Fisher LD, et al. Left main coronary artery stenosis: angiographic determination. *Circulation* 1983;68:484–9.
79. Davies JE, Sen S, Dehbi H-M, et al. Use of the Instantaneous Wave-free Ratio or Fractional Flow Reserve in PCI. *N. Engl. J. Med.* 2017;376:1824–1834.
80. Götberg M, Christiansen EH, Gudmundsdottir IJ, et al. Instantaneous Wave-free Ratio versus Fractional Flow Reserve to Guide PCI. *N. Engl. J. Med.* 2017;376:1813–1823.
81. Bech GJ, De Bruyne B, Pijls NH, et al. Fractional flow reserve to determine the appropriateness of angioplasty in moderate coronary stenosis: a randomized trial. *Circulation* 2001;103:2928–34.
82. De Bruyne B, Pijls NHJ, Kalesan B, et al. Fractional Flow Reserve–

Guided PCI versus Medical Therapy in Stable Coronary Disease. *N. Engl. J. Med.* 2012;367:991–1001.

83. Smits PC, Abdel-Wahab M, Neumann F-J, et al. Fractional Flow Reserve–Guided Multivessel Angioplasty in Myocardial Infarction. *N. Engl. J. Med.* 2017;376:1234–1244.

84. Engstrøm T, Kelbæk H, Helqvist S, et al. Complete revascularisation versus treatment of the culprit lesion only in patients with ST-segment elevation myocardial infarction and multivessel disease (DANAMI-3—PRIMULTI): an open-label, randomised controlled trial. *Lancet (London, England)* 2015;386:665–71.

85. McMurray JJ V., Adamopoulos S, Anker SD, et al. ESC Guidelines for the diagnosis and treatment of acute and chronic heart failure 2012: The Task Force for the Diagnosis and Treatment of Acute and Chronic Heart Failure 2012 of the European Society of Cardiology. Developed in collaboration with the Heart. *Eur. Heart J.* 2012;33:1787–1847.

86. Windecker S, Kolh P, Alfonso F, et al. 2014 ESC/EACTS Guidelines on myocardial revascularization: The Task Force on Myocardial Revascularization of the European Society of Cardiology (ESC) and the European Association for Cardio-Thoracic Surgery (EACTS) Developed with the special contribution o. *Eur. Heart J.* 2014;35:2541–619.

87. Foley JRJ, Plein S, Greenwood JP. Assessment of stable coronary artery disease by cardiovascular magnetic resonance imaging: Current and emerging techniques. *World J. Cardiol.* 2017;9:92–108.

88. Grothues F, Smith GC, Moon JCC, et al. Comparison of interstudy reproducibility of cardiovascular magnetic resonance with two-dimensional echocardiography in normal subjects and in patients with heart failure or left ventricular hypertrophy. *Am. J. Cardiol.* 2002;90:29–34.

89. Grothues F, Moon JC, Bellenger NG, Smith GS, Klein HU, Pennell

- DJ. Interstudy reproducibility of right ventricular volumes, function, and mass with cardiovascular magnetic resonance. *Am. Heart J.* 2004;147:218–23.
90. Ibrahim E-SH. Myocardial tagging by Cardiovascular Magnetic Resonance: evolution of techniques--pulse sequences, analysis algorithms, and applications. *J. Cardiovasc. Magn. Reson.* 2011;13:36.
91. Claus P, Omar AMS, Pedrizzetti G, Sengupta PP, Nagel E. Tissue Tracking Technology for Assessing Cardiac Mechanics Principles, Normal Values, and Clinical Applications. *JACC Cardiovasc. Imaging* 2015;8:1444–1460.
92. Steg PG, James SK, Atar D, et al. ESC Guidelines for the management of acute myocardial infarction in patients presenting with ST-segment elevation. *Eur. Heart J.* 2012;33:2569–619.
93. Al Jaroudi W, Iskandrian AE. Regadenoson: a new myocardial stress agent. *J. Am. Coll. Cardiol.* 2009;54:1123–30.
94. Nguyen K-L, Bandettini WP, Shanbhag S, Leung SW, Wilson JR, Arai AE. Safety and tolerability of regadenoson CMR. *Eur. Heart J. Cardiovasc. Imaging* 2014;15:753–60.
95. Jaarsma C, Leiner T, Bekkers SC, et al. Diagnostic performance of noninvasive myocardial perfusion imaging using single-photon emission computed tomography, cardiac magnetic resonance, and positron emission tomography imaging for the detection of obstructive coronary artery disease: a meta-anal. *J. Am. Coll. Cardiol.* 2012;59:1719–28.
96. Greenwood JP, Maredia N, Radjenovic A, et al. Clinical evaluation of magnetic resonance imaging in coronary heart disease: the CE-MARC study. *Trials* 2009;10:62.
97. Greenwood JP, Motwani M, Maredia N, et al. Comparison of cardiovascular magnetic resonance and single-photon emission

computed tomography in women with suspected coronary artery disease from the clinical evaluation of magnetic resonance imaging in coronary heart disease (CE-MARC) trial. *Circulation* 2014;129:1129–1138.

98. Schwitter J, Wacker CM, Wilke N, et al. MR-IMPACT II: Magnetic Resonance Imaging for Myocardial Perfusion Assessment in Coronary artery disease Trial: perfusion-cardiac magnetic resonance vs. single-photon emission computed tomography for the detection of coronary artery disease: a comparative . *Eur. Heart J.* 2013;34:775–81.

99. Ripley DP, Motwani M, Brown JM, et al. Individual component analysis of the multi-parametric cardiovascular magnetic resonance protocol in the CE-MARC trial. *J. Cardiovasc. Magn. Reson.* 2015;17:59.

100. Li M, Zhou T, Yang L, Peng Z, Ding J, Sun G. Diagnostic Accuracy of Myocardial Magnetic Resonance Perfusion to Diagnose Ischemic Stenosis With Fractional Flow Reserve as Reference. *JACC Cardiovasc. Imaging* 2014;7:1098–1105.

101. Greulich S, Steubing H, Birkmeier S, et al. Impact of arrhythmia on diagnostic performance of adenosine stress CMR in patients with suspected or known coronary artery disease. *J. Cardiovasc. Magn. Reson.* 2015;17:94.

102. Plein S, Schwitter J, Suerder D, Greenwood JP, Boesiger P, Kozerke S. k-Space and time sensitivity encoding-accelerated myocardial perfusion MR imaging at 3.0 T: comparison with 1.5 T. *Radiology* 2008;249:493–500.

103. Cheng ASH, Pegg TJ, Karamitsos TD, et al. Cardiovascular magnetic resonance perfusion imaging at 3-tesla for the detection of coronary artery disease: a comparison with 1.5-tesla. *J. Am. Coll. Cardiol.* 2007;49:2440–9.

104. Bernhardt P, Walcher T, Rottbauer W, Wöhrle J. Quantification of myocardial perfusion reserve at 1.5 and 3.0 Tesla: a comparison to

fractional flow reserve. *Int. J. Cardiovasc. Imaging* 2012.

105. Ebersberger U, Makowski MR, Schoepf UJ, et al. Magnetic resonance myocardial perfusion imaging at 3.0 Tesla for the identification of myocardial ischaemia: comparison with coronary catheter angiography and fractional flow reserve measurements. *Eur. Hear. J. – Cardiovasc. Imaging* 2013;14:1174–1180.

106. Bernstein MA, Huston J, Ward HA. Imaging artifacts at 3.0T. *J. Magn. Reson. Imaging* 2006;24:735–46.

107. Rajiah P, Bolen MA. Cardiovascular MR imaging at 3 T: opportunities, challenges, and solutions. *Radiographics* 2014;34:1612–35.

108. Motwani M, Jogiya R, Kozerke S, Greenwood JP, Plein S. Advanced cardiovascular magnetic resonance myocardial perfusion imaging: high-spatial resolution versus 3-dimensional whole-heart coverage. *Circ. Cardiovasc. Imaging* 2013;6:339–48.

109. Maredia N, Radjenovic A, Kozerke S, Larghat A, Greenwood JP, Plein S. Effect of improving spatial or temporal resolution on image quality and quantitative perfusion assessment with k-t SENSE acceleration in first-pass CMR myocardial perfusion imaging. *Magn. Reson. Med.* 2010;64:1616–24.

110. Motwani M, Maredia N, Fairbairn TA, Kozerke S, Greenwood JP, Plein S. Assessment of ischaemic burden in angiographic three-vessel coronary artery disease with high-resolution myocardial perfusion cardiovascular magnetic resonance imaging. *Eur. Heart J. Cardiovasc. Imaging* 2014;15:701–8.

111. Plein S, Kozerke S, Suerder D, et al. High spatial resolution myocardial perfusion cardiac magnetic resonance for the detection of coronary artery disease. *Eur. Heart J.* 2008;29:2148–55.

112. Motwani M, Maredia N, Fairbairn TA, et al. High-resolution versus standard-resolution cardiovascular MR myocardial perfusion imaging for the detection of coronary artery disease. *Circ. Cardiovasc. Imaging* 2012;5:306–13.

113. Lockie T, Ishida M, Perera D, et al. High-resolution magnetic resonance myocardial perfusion imaging at 3.0-tesla to detect hemodynamically significant coronary stenoses as determined by fractional flow reserve. *J. Am. Coll. Cardiol.* 2011;57:70–75.

114. Jogiya R, Kozerke S, Morton G, et al. Validation of dynamic 3-dimensional whole heart magnetic resonance myocardial perfusion imaging against fractional flow reserve for the detection of significant coronary artery disease. *J. Am. Coll. Cardiol.* 2012;60:756–65.

115. Manka R, Paetsch I, Kozerke S, et al. Whole-heart dynamic three-dimensional magnetic resonance perfusion imaging for the detection of coronary artery disease defined by fractional flow reserve: determination of volumetric myocardial ischaemic burden and coronary lesion location. *Eur. Heart J.* 2012;33:2016–24.

116. Manka R, Wissmann L, Gebker R, et al. Multicenter evaluation of dynamic three-dimensional magnetic resonance myocardial perfusion imaging for the detection of coronary artery disease defined by fractional flow reserve. *Circ. Cardiovasc. Imaging* 2015;8.

117. Shaw LJ, Berman DS, Picard MH, et al. Comparative Definitions for Moderate-Severe Ischemia in Stress Nuclear, Echocardiography, and Magnetic Resonance Imaging. *JACC Cardiovasc. Imaging* 2014;7:593–604.

118. Hachamovitch R, Hayes SW, Friedman JD, Cohen I, Berman DS. Comparison of the short-term survival benefit associated with revascularization compared with medical therapy in patients with no prior coronary artery disease undergoing stress myocardial perfusion single

photon emission computed tomography. *Circulation* 2003;107:2900–7.

119. Jogiya R, Morton G, De Silva K, et al. Ischemic burden by 3-dimensional myocardial perfusion cardiovascular magnetic resonance: comparison with myocardial perfusion scintigraphy. *Circ. Cardiovasc. Imaging* 2014;7:647–54.

120. McDiarmid AK, Ripley DP, Mohee K, et al. Three-dimensional whole-heart vs. two-dimensional high-resolution perfusion-CMR: a pilot study comparing myocardial ischaemic burden. *Eur. Heart J. Cardiovasc. Imaging* 2015;jev231.

121. Schuster A, Zarinabad N, Ishida M, et al. Quantitative assessment of magnetic resonance derived myocardial perfusion measurements using advanced techniques: microsphere validation in an explanted pig heart system. *J. Cardiovasc. Magn. Reson.* 2014;16:82.

122. Jogiya R, Makowski M, Phinikaridou A, et al. Hyperemic stress myocardial perfusion cardiovascular magnetic resonance in mice at 3 Tesla: initial experience and validation against microspheres. *J. Cardiovasc. Magn. Reson.* 2013;15:62.

123. Biglands JD, Magee DR, Sourbron SP, Plein S, Greenwood JP, Radjenovic A. Comparison of the Diagnostic Performance of Four Quantitative Myocardial Perfusion Estimation Methods Used in Cardiac MR Imaging: CE-MARC Substudy. *Radiology* 2015;275:393–402.

124. Morton G, Chiribiri A, Ishida M, et al. Quantification of absolute myocardial perfusion in patients with coronary artery disease: comparison between cardiovascular magnetic resonance and positron emission tomography. *J. Am. Coll. Cardiol.* 2012;60:1546–55.

125. Miller CA, Naish JH, Ainslie MP, et al. Voxel-wise quantification of myocardial blood flow with cardiovascular magnetic resonance: effect of variations in methodology and validation with positron emission tomography. *J. Cardiovasc. Magn. Reson.* 2014;16:11.

126. Weng AM, Ritter CO, Lotz J, Beer MJ, Hahn D, Köstler H. Automatic postprocessing for the assessment of quantitative human myocardial perfusion using MRI. *Eur. Radiol.* 2010;20:1356–65.
127. Biglands JD, Ibraheem M, Magee DR, Radjenovic A, Plein S, Greenwood JP. Quantitative Myocardial Perfusion Imaging Versus Visual Analysis in Diagnosing Myocardial Ischemia: A CE-MARC Substudy. *JACC. Cardiovasc. Imaging* 2018;11:711–718.
128. Foley JRJ, Kidambi A, Biglands JD, et al. A comparison of cardiovascular magnetic resonance and single photon emission computed tomography (SPECT) perfusion imaging in left main stem or equivalent coronary artery disease: a CE-MARC substudy. *J. Cardiovasc. Magn. Reson.* 2017;19:84.
129. Kellman P, Hansen MS, Nielles-Vallespin S, et al. Myocardial perfusion cardiovascular magnetic resonance: optimized dual sequence and reconstruction for quantification. *J. Cardiovasc. Magn. Reson.* 2017;19:1–14.
130. Engblom H, Xue H, Akil S, et al. Fully quantitative cardiovascular magnetic resonance myocardial perfusion ready for clinical use: A comparison between cardiovascular magnetic resonance imaging and positron emission tomography. *J. Cardiovasc. Magn. Reson.* 2017;19:1–9.
131. Bruder O, Schneider S, Pilz G, et al. 2015 Update on Acute Adverse Reactions to Gadolinium based Contrast Agents in Cardiovascular MR. Large Multi-National and Multi-Ethnic Population Experience With 37788 Patients From the EuroCMR Registry. *J. Cardiovasc. Magn. Reson.* 2015;17:58.
132. Kribben A, Witzke O, Hillen U, Barkhausen J, Daul AE, Erbel R. Nephrogenic Systemic Fibrosis. *J. Am. Coll. Cardiol.* 2009;53:1621–1628.
133. Nagel E, Lehmkuhl HB, Bocksch W, et al. Noninvasive diagnosis of

ischemia-induced wall motion abnormalities with the use of high-dose dobutamine stress MRI: comparison with dobutamine stress echocardiography. *Circulation* 1999;99:763–70.

134. Wahl A, Paetsch I, Gollesch A, et al. Safety and feasibility of high-dose dobutamine-atropine stress cardiovascular magnetic resonance for diagnosis of myocardial ischaemia: experience in 1000 consecutive cases. *Eur. Heart J.* 2004;25:1230–6.

135. Nandalur KR, Dwamena BA, Choudhri AF, Nandalur MR, Carlos RC. Diagnostic performance of stress cardiac magnetic resonance imaging in the detection of coronary artery disease: a meta-analysis. *J. Am. Coll. Cardiol.* 2007;50:1343–53.

136. Manka R, Jahnke C, Gebker R, Schnackenburg B, Paetsch I. Head-to-head comparison of first-pass MR perfusion imaging during adenosine and high-dose dobutamine/atropine stress. *Int. J. Cardiovasc. Imaging* 2011;27:995–1002.

137. Gebker R, Frick M, Jahnke C, et al. Value of additional myocardial perfusion imaging during dobutamine stress magnetic resonance for the assessment of intermediate coronary artery disease. *Int. J. Cardiovasc. Imaging* 2012;28:89–97.

138. Mordi I, Stanton T, Carrick D, et al. Comprehensive dobutamine stress CMR versus echocardiography in LBBB and suspected coronary artery disease. *JACC. Cardiovasc. Imaging* 2014;7:490–8.

139. Roger VL, Jacobsen SJ, Pellikka PA, Miller TD, Bailey KR, Gersh BJ. Prognostic value of treadmill exercise testing: a population-based study in Olmsted County, Minnesota. *Circulation* 98:2836–41.

140. Fleischmann KE, Hunink MG, Kuntz KM, Douglas PS. Exercise echocardiography or exercise SPECT imaging? A meta-analysis of diagnostic test performance. *JAMA* 1998;280:913–20.

141. Thavendiranathan P, Dickerson JA, Scandling D, et al. Comparison of treadmill exercise stress cardiac MRI to stress echocardiography in healthy volunteers for adequacy of left ventricular endocardial wall visualization: A pilot study. *J. Magn. Reson. Imaging* 2014;39:1146–52.
142. Sukpraphrute B, Drafts BC, Rerkpattanapipat P, et al. Prognostic utility of cardiovascular magnetic resonance upright maximal treadmill exercise testing. *J. Cardiovasc. Magn. Reson.* 2015;17:103.
143. Gusso S, Salvador C, Hofman P, et al. Design and testing of an MRI-compatible cycle ergometer for non-invasive cardiac assessments during exercise. *Biomed. Eng. Online* 2012;11:13.
144. Forouzan O, Flink E, Warczytowa J, et al. Low Cost Magnetic Resonance Imaging-Compatible Stepper Exercise Device for Use in Cardiac Stress Tests. *J. Med. Device.* 2014;8:0450021-450028.
145. Gargiulo P, Dellegrottaglie S, Bruzzese D, et al. The Prognostic Value of Normal Stress Cardiac Magnetic Resonance in Patients With Known or Suspected Coronary Artery Disease: A Meta-analysis. *Circ. Cardiovasc. Imaging* 2013;6:574–582.
146. Lipinski MJ, McVey CM, Berger JS, Kramer CM, Salerno M. Prognostic value of stress cardiac magnetic resonance imaging in patients with known or suspected coronary artery disease: a systematic review and meta-analysis. *J. Am. Coll. Cardiol.* 2013;62:826–38.
147. Buckert D, Dewes P, Walcher T, Rottbauer W, Bernhardt P. Intermediate-Term Prognostic Value of Reversible Perfusion Deficit Diagnosed by Adenosine CMR. *JACC Cardiovasc. Imaging* 2013;6:56–63.
148. Korosoglou G, Elhmidi Y, Steen H, et al. Prognostic value of high-dose dobutamine stress magnetic resonance imaging in 1,493 consecutive patients: assessment of myocardial wall motion and perfusion. *J. Am. Coll. Cardiol.* 2010;56:1225–34.

149. Greenwood JP, Herzog BA, Brown JM, et al. Prognostic Value of Cardiovascular Magnetic Resonance and Single-Photon Emission Computed Tomography in Suspected Coronary Heart Disease: Long-Term Follow-up of a Prospective, Diagnostic Accuracy Cohort Study. *Ann. Intern. Med.* 2016;1–10.
150. Wagner A, Mahrholdt H, Holly TA, et al. Contrast-enhanced MRI and routine single photon emission computed tomography (SPECT) perfusion imaging for detection of subendocardial myocardial infarcts: an imaging study. *Lancet (London, England)* 2003;361:374–9.
151. Kwong RY, Chan AK, Brown KA, et al. Impact of unrecognized myocardial scar detected by cardiac magnetic resonance imaging on event-free survival in patients presenting with signs or symptoms of coronary artery disease. *Circulation* 2006;113:2733–43.
152. Kim RJ, Fieno DS, Parrish TB, et al. Relationship of MRI delayed contrast enhancement to irreversible injury, infarct age, and contractile function. *Circulation* 1999;100:1992–2002.
153. Mollet NR, Dymarkowski S, Volders W, et al. Visualization of ventricular thrombi with contrast-enhanced magnetic resonance imaging in patients with ischemic heart disease. *Circulation* 2002;106:2873–6.
154. Srichai MB, Junor C, Rodriguez LL, et al. Clinical, imaging, and pathological characteristics of left ventricular thrombus: a comparison of contrast-enhanced magnetic resonance imaging, transthoracic echocardiography, and transesophageal echocardiography with surgical or pathological validation. *Am. Heart J.* 2006;152:75–84.
155. Bulluck H, Chan MHH, Paradies V, et al. Incidence and predictors of left ventricular thrombus by cardiovascular magnetic resonance in acute ST-segment elevation myocardial infarction treated by primary percutaneous coronary intervention: a meta-analysis. *J. Cardiovasc. Magn. Reson.* 2018;20:72.

156. Goetti R, Kozerke S, Donati OF, et al. Acute, subacute, and chronic myocardial infarction: quantitative comparison of 2D and 3D late gadolinium enhancement MR imaging. *Radiology* 2011;259:704–11.
157. Pierce IT, Keegan J, Drivas P, Gatehouse PD, Firmin DN. Free-breathing 3D late gadolinium enhancement imaging of the left ventricle using a stack of spirals at 3T. *J. Magn. Reson. Imaging* 2015;41:1030–7.
158. Kim RJ, Wu E, Rafael A, et al. The use of contrast-enhanced magnetic resonance imaging to identify reversible myocardial dysfunction. *N. Engl. J. Med.* 2000;343:1445–53.
159. Romero J, Xue X, Gonzalez W, Garcia MJ. CMR imaging assessing viability in patients with chronic ventricular dysfunction due to coronary artery disease: a meta-analysis of prospective trials. *JACC. Cardiovasc. Imaging* 2012;5:494–508.
160. Baer FM, Theissen P, Schneider CA, et al. Dobutamine magnetic resonance imaging predicts contractile recovery of chronically dysfunctional myocardium after successful revascularization. *J. Am. Coll. Cardiol.* 1998;31:1040–8.
161. Shah DJ, Kim HW, James O, et al. Prevalence of regional myocardial thinning and relationship with myocardial scarring in patients with coronary artery disease. *JAMA* 2013;309:909–18.
162. Nagel E, Schuster A. Myocardial viability: dead or alive is not the question! *JACC. Cardiovasc. Imaging* 2012;5:509–12.
163. Bree D, Wollmuth JR, Cupps BP, et al. Low-dose dobutamine tissue-tagged magnetic resonance imaging with 3-dimensional strain analysis allows assessment of myocardial viability in patients with ischemic cardiomyopathy. *Circulation* 2006;114:133-6.
164. Schuster A, Paul M, Bettencourt N, et al. Cardiovascular magnetic resonance myocardial feature tracking for quantitative viability

assessment in ischemic cardiomyopathy. *Int. J. Cardiol.* 2013;166:413–20.

165. Schuster A, Paul M, Bettencourt N, et al. Myocardial feature tracking reduces observer-dependence in low-dose dobutamine stress cardiovascular magnetic resonance. *PLoS One* 2015;10:e0122858.

166. Hendel RC, Patel MR, Kramer CM, et al. ACCF/ACR/SCCT/SCMR/ASNC/NASCI/SCAI/SIR 2006 appropriateness criteria for cardiac computed tomography and cardiac magnetic resonance imaging: a report of the American College of Cardiology Foundation Quality Strategic Directions Committee Appropriateness C. *J. Am. Coll. Cardiol.* 2006;48:1475–97.

167. Patel MR, Dehmer GJ, Hirshfeld JW, Smith PK, Spertus JA. ACCF/SCAI/STS/AATS/AHA/ASNC/HFSA/SCCT 2012 Appropriate Use Criteria for Coronary Revascularization Focused Update. *J. Am. Coll. Cardiol.* 2012;59:857–881.

168. Velazquez EJ, Lee KL, Deja MA, et al. Coronary-artery bypass surgery in patients with left ventricular dysfunction. *N. Engl. J. Med.* 2011;364:1607–16.

169. Schinkel AFL, Bax JJ, Poldermans D, Elhendy A, Ferrari R, Rahimtoola SH. Hibernating myocardium: diagnosis and patient outcomes. *Curr. Probl. Cardiol.* 2007;32:375–410.

170. Gerber BL, Rousseau MF, Ahn S a., et al. Prognostic Value of Myocardial Viability by Delayed-Enhanced Magnetic Resonance in Patients With Coronary Artery Disease and Low Ejection Fraction. *J. Am. Coll. Cardiol.* 2012;59:825–835.

171. Bruder O, Wagner A, Lombardi M, et al. European Cardiovascular Magnetic Resonance (EuroCMR) registry--multi national results from 57 centers in 15 countries. *J. Cardiovasc. Magn. Reson.* 2013;15:9.

172. Basha T, Roujol S, Kissinger K V, Goddu B, Manning WJ, Nezafat R. Black blood late gadolinium enhancement using combined T2 magnetization preparation and inversion recovery. *J. Cardiovasc. Magn. Reson.* 2015;17:O14.
173. Farrelly C, Rehwald W, Salerno M, et al. Improved detection of subendocardial hyperenhancement in myocardial infarction using dark blood-pool delayed enhancement MRI. *Am. J. Roentgenol.* 2011;196:339–348.
174. Peel SA, Morton G, Chiribiri A, Schuster A, Nagel E, Botnar RM. Dual Inversion-Recovery MR Imaging Sequence for Reduced Blood Signal on Late Gadolinium-enhanced Images of Myocardial Scar. *Radiology* 2012;264:242–249.
175. Liu CY, Wieben O, Brittain JH, Reeder SB. Improved delayed enhanced myocardial imaging with T2-Prep inversion recovery magnetization preparation. *J. Magn. Reson. Imaging* 2008;28:1280–1286.
176. Muscogiuri G, Rehwald WG, Schoepf UJ, et al. T(Rho) and magnetization transfer and INvErsion recovery (TRAMINER)-prepared imaging: A novel contrast-enhanced flow-independent dark-blood technique for the evaluation of myocardial late gadolinium enhancement in patients with myocardial infarction. *J. Magn. Reson. Imaging* 2016:1–9.
177. Kellman P, Xue H, Olivieri LJ, et al. Dark blood late enhancement imaging. *J. Cardiovasc. Magn. Reson.* 2016;18:77.
178. Kim HW, Rehwald WG, Wendell DC, et al. Flow-Independent Dark-blood DeLayed Enhancement (FIDDLE): validation of a novel black blood technique for the diagnosis of myocardial infarction. *J. Cardiovasc. Magn. Reson.* 2016;18:1–3.
179. Holtackers RJ, Chiribiri A, Schneider T, Higgins DM, Botnar RM. Dark-blood late gadolinium enhancement without additional

- magnetization preparation. *J. Cardiovasc. Magn. Reson.* 2017;19:64.
180. Flett AS, Hasleton J, Cook C, et al. Evaluation of techniques for the quantification of myocardial scar of differing etiology using cardiac magnetic resonance. *JACC Cardiovasc. Imaging* 2011;4:150–156.
181. Nicolosi GL, Latini R, Marino P, et al. The prognostic value of pre-discharge quantitative two-dimensional echocardiographic measurements and the effects of early lisinopril treatment on left ventricular structure and function after acute myocardial infarction in the GISSI-3 Trial. Gruppo Italia. *Eur. Heart J.* 1996;17:1646–56.
182. Klem I, Shah DJ, White RD, et al. Prognostic value of routine cardiac magnetic resonance assessment of left ventricular ejection fraction and myocardial damage: an international, multicenter study. *Circ. Cardiovasc. Imaging* 2011;4:610–9.
183. Zemrak F, Petersen SE. Late gadolinium enhancement CMR predicts adverse cardiovascular outcomes and mortality in patients with coronary artery disease: systematic review and meta-analysis. *Prog. Cardiovasc. Dis.* 2011;54:215–29.
184. Schelbert EB, Cao JJ, Sigurdsson S, et al. Prevalence and prognosis of unrecognized myocardial infarction determined by cardiac magnetic resonance in older adults. *JAMA* 2012;308:890–6.
185. Scott PA, Morgan JMJ, Carroll N, et al. The extent of left ventricular scar quantified by late gadolinium enhancement MRI is associated with spontaneous ventricular arrhythmias in patients with coronary. *Circ. Arrhythmia Electrophysiol.* 2011;4:324–330.
186. Gao P, Yee R, Gula L, et al. Prediction of arrhythmic events in ischemic and dilated cardiomyopathy patients referred for implantable cardiac defibrillator evaluation of multiple scar quantification measures for late gadolinium enhancement magnetic resonance imaging. *Circ. Cardiovasc. Imaging* 2012;5:448–456.

187. Demirel F, Adiyaman A, Timmer JR, et al. Myocardial scar characteristics based on cardiac magnetic resonance imaging is associated with ventricular tachyarrhythmia in patients with ischemic cardiomyopathy. *Int. J. Cardiol.* 2014;177:392–9.
188. Scott PA, Rosengarten JA, Curzen NP, Morgan JM. Late gadolinium enhancement cardiac magnetic resonance imaging for the prediction of ventricular tachyarrhythmic events: a meta-analysis. *Eur. J. Heart Fail.* 2013;15:1019–27.
189. Klem I, Weinsaft JW, Bahnson TD, et al. Assessment of myocardial scarring improves risk stratification in patients evaluated for cardiac defibrillator implantation. *J. Am. Coll. Cardiol.* 2012;60:408–20.
190. Roes SD, Borleffs CJW, van der Geest RJ, et al. Infarct tissue heterogeneity assessed with contrast-enhanced MRI predicts spontaneous ventricular arrhythmia in patients with ischemic cardiomyopathy and implantable cardioverter-defibrillator. *Circ. Cardiovasc. Imaging* 2009;2:183–90.
191. Zeidan-Shwiri T, Yang Y, Lashevsky I, et al. Magnetic resonance estimates of the extent and heterogeneity of scar tissue in ICD patients with ischemic cardiomyopathy predict ventricular arrhythmia. *Heart Rhythm* 2015;12:802–8.
192. White J a., Yee R, Yuan X, et al. Delayed enhancement magnetic resonance imaging predicts response to cardiac resynchronization therapy in patients with intraventricular dyssynchrony. *J. Am. Coll. Cardiol.* 2006;48:1953–60.
193. Wong JA, Yee R, Stirrat J, et al. Influence of pacing site characteristics on response to cardiac resynchronization therapy. *Circ. Cardiovasc. Imaging* 2013;6:542–50.
194. Taylor RJ, Umar F, Panting JR, Stegemann B, Leyva F. Left ventricular lead position, mechanical activation, and myocardial scar in

relation to left ventricular reverse remodeling and clinical outcomes after cardiac resynchronization therapy: A feature-tracking and contrast-enhanced cardiovascular magnetic r. *Heart Rhythm* 2016;13:481–9.

195. Younger JF, Plein S, Crean A, Ball SG, Greenwood JP. Visualization of coronary venous anatomy by cardiovascular magnetic resonance. *J. Cardiovasc. Magn. Reson.* 2009;11:26.

196. Heidenreich PA, Trogdon JG, Khavjou OA, et al. Forecasting the future of cardiovascular disease in the United States: a policy statement from the American Heart Association. *Circulation* 2011;123:933–44.

197. Walker S, Girardin F, McKenna C, et al. Cost-effectiveness of cardiovascular magnetic resonance in the diagnosis of coronary heart disease: an economic evaluation using data from the CE-MARC study. *Heart* 2013;99:873–81.

198. Boldt J, Leber AW, Bonaventura K, et al. Cost-effectiveness of cardiovascular magnetic resonance and single-photon emission computed tomography for diagnosis of coronary artery disease in Germany. *J. Cardiovasc. Magn. Reson.* 2013;15:30.

199. Pletscher M, Walker S, Moschetti K, et al. Cost-effectiveness of functional cardiac imaging in the diagnostic work-up of coronary heart disease. *Eur. Hear. J. - Qual. Care Clin. Outcomes.* 2016;in press.

200. Petrov G, Kelle S, Fleck E, Wellnhofer E. Incremental cost-effectiveness of dobutamine stress cardiac magnetic resonance imaging in patients at intermediate risk for coronary artery disease. *Clin. Res. Cardiol.* 2015;104:401–9.

201. Moschetti K, Favre D, Pinget C, et al. Comparative cost-effectiveness analyses of cardiovascular magnetic resonance and coronary angiography combined with fractional flow reserve for the diagnosis of coronary artery disease. *J. Cardiovasc. Magn. Reson.* 2014;16:13.

202. Hendel RC, Berman DS, Di Carli MF, et al. ACCF/ASNC/ACR/AHA/ASE/SCCT/SCMR/SNM 2009 Appropriate Use Criteria for Cardiac Radionuclide Imaging: A Report of the American College of Cardiology Foundation Appropriate Use Criteria Task Force, the American Society of Nuclear Cardiology, the American Col. J. Am. Coll. Cardiol. 2009;53:2201–29.
203. Ripley DP, Brown JM, Everett CC, et al. Rationale and design of the Clinical Evaluation of Magnetic Resonance Imaging in Coronary heart disease 2 trial (CE-MARC 2): a prospective, multicenter, randomized trial of diagnostic strategies in suspected coronary heart disease. Am. Heart J. 2015;169:17–24.e1.
204. Desai NR, Bradley SM, Parzynski CS, et al. Appropriate Use Criteria for Coronary Revascularization and Trends in Utilization, Patient Selection, and Appropriateness of Percutaneous Coronary Intervention. JAMA 2015;314:2045–53.
205. Chan PS, Patel MR, Klein LW, et al. Appropriateness of Percutaneous Coronary Intervention. JAMA 2011;306:53–61.
206. Hussain ST, Paul M, Plein S, et al. Design and rationale of the MR-INFORM study: stress perfusion cardiovascular magnetic resonance imaging to guide the management of patients with stable coronary artery disease. J. Cardiovasc. Magn. Reson. 2012;14:65.
207. Boden WE, O'Rourke RA, Teo KK, et al. Optimal medical therapy with or without PCI for stable coronary disease. N. Engl. J. Med. 2007;356:1503–16.
208. Frye RL, August P, Brooks MM, et al. A randomized trial of therapies for type 2 diabetes and coronary artery disease. N. Engl. J. Med. 2009;360:2503–15.
209. Shaw LJ, Berman DS, Maron DJ, et al. Optimal medical therapy with or without percutaneous coronary intervention to reduce ischemic burden:

results from the Clinical Outcomes Utilizing Revascularization and Aggressive Drug Evaluation (COURAGE) trial nuclear substudy. *Circulation* 2008;117:1283–1291.

210. Shaw LJ, Weintraub WS, Maron DJ, et al. Baseline stress myocardial perfusion imaging results and outcomes in patients with stable ischemic heart disease randomized to optimal medical therapy with or without percutaneous coronary intervention. *Am. Heart J.* 2012;164:243–50.

211. Shaw LJ, Cerqueira MD, Brooks MM, et al. Impact of left ventricular function and the extent of ischemia and scar by stress myocardial perfusion imaging on prognosis and therapeutic risk reduction in diabetic patients with coronary artery disease: results from the Bypass Angioplasty Revasculariza. *J. Nucl. Cardiol.* 2012;19:658–69.

212. Hundley WG, Bluemke DA, Finn JP, et al. ACCF/ACR/AHA/NASCI/SCMR 2010 expert consensus document on cardiovascular magnetic resonance: a report of the American College of Cardiology Foundation Task Force on Expert Consensus Documents. *J. Am. Coll. Cardiol.* 2010;55:2614–62.

213. Ripley DP, Saha A, Teis A, et al. The distribution and prognosis of anomalous coronary arteries identified by cardiovascular magnetic resonance: 15 year experience from two tertiary centres. *J. Cardiovasc. Magn. Reson.* 2014;16:34.

214. Kim WY, Danias PG, Stuber M, et al. Coronary magnetic resonance angiography for the detection of coronary stenoses. *N. Engl. J. Med.* 2001;345:1863–9.

215. Kato S, Kitagawa K, Ishida N, et al. Assessment of coronary artery disease using magnetic resonance coronary angiography: a national multicenter trial. *J. Am. Coll. Cardiol.* 2010;56:983–91.

216. Hamdan A, Asbach P, Wellnhofer E, et al. A prospective study for

- comparison of MR and CT imaging for detection of coronary artery stenosis. *JACC. Cardiovasc. Imaging* 2011;4:50–61.
217. Bettencourt N, Ferreira N, Chiribiri A, et al. Additive value of magnetic resonance coronary angiography in a comprehensive cardiac magnetic resonance stress-rest protocol for detection of functionally significant coronary artery disease: a pilot study. *Circ. Cardiovasc. Imaging* 2013;6:730–8.
218. Ripley DP, Motwani M, Plein S, Greenwood JP. Established and emerging cardiovascular magnetic resonance techniques for the assessment of stable coronary heart disease and acute coronary syndromes. *Quant. Imaging Med. Surg.* 2014;4:330–44.
219. Garg P, Underwood SR, Senior R, Greenwood JP, Plein S. Noninvasive cardiac imaging in suspected acute coronary syndrome. *Nat. Rev. Cardiol.* 2016:1–10.
220. Carrick D, Haig C, Rauhalampi S, et al. Prognostic significance of infarct core pathology revealed by quantitative non-contrast in comparison with contrast cardiac magnetic resonance imaging in reperfused ST-elevation myocardial infarction survivors. *Eur. Heart J.* 2016;37:1044–59.
221. Carberry J, Carrick D, Haig C, et al. Remote Zone Extracellular Volume and Left Ventricular Remodeling in Survivors of ST-Elevation Myocardial Infarction. *Hypertension* 2016:HYPERTENSIONAHA.116.07222.
222. Friedrich MG, Karamitsos TD. Oxygenation-sensitive cardiovascular magnetic resonance. *J. Cardiovasc. Magn. Reson.* 2013;15:43.
223. Jahnke C, Gebker R, Manka R, Schnackenburg B, Fleck E, Paetsch I. Navigator-gated 3D blood oxygen level-dependent CMR at 3.0-T for detection of stress-induced myocardial ischemic reactions. *JACC Cardiovasc. Imaging* 2010;3:375–384.

224. Arnold JR, Karamitsos TD, Bhamra-Ariza P, et al. Myocardial oxygenation in coronary artery disease: Insights from blood oxygen level-dependent magnetic resonance imaging at 3 Tesla. *J. Am. Coll. Cardiol.* 2012;59:1954–1964.
225. Mekkaoui C, Reese TG, Jackowski MP, Bhat H, Sosnovik DE. Diffusion MRI in the heart. *NMR Biomed.* 2017;30:e3426.
226. Ferreira PF, Nielles-Vallespin S, Scott AD, et al. Evaluation of the impact of strain correction on the orientation of cardiac diffusion tensors with in vivo and ex vivo porcine hearts. *Magn. Reson. Med.* 2018;79:2205–2215.
227. Khalique Z, Ferreira PF, Scott AD, et al. Diffusion Tensor Cardiovascular Magnetic Resonance of Microstructural Recovery in Dilated Cardiomyopathy. *JACC Cardiovasc. Imaging* 2018.
228. Garg P, Westenberg JJM, van den Boogaard PJ, et al. Comparison of fast acquisition strategies in whole-heart four-dimensional flow cardiac MR: Two-center, 1.5 Tesla, phantom and in vivo validation study. *J. Magn. Reson. Imaging* 2018;47:272–281.
229. Olsson LE, Chai C-M, Axelsson O, Karlsson M, Golman K, Petersson JS. MR coronary angiography in pigs with intraarterial injections of a hyperpolarized ¹³C substance. *Magn. Reson. Med.* 2006;55:731–7.
230. Witte KK, Byrom R, Gierula J, et al. Effects of Vitamin D on Cardiac Function in Patients With Chronic HF. *J. Am. Coll. Cardiol.* 2016;67:2593–2603.
231. Vogel-Claussen J, Finn JP, Gomes AS, et al. Left ventricular papillary muscle mass: relationship to left ventricular mass and volumes by magnetic resonance imaging. *J. Comput. Assist. Tomogr.* 2006;30:426–432.

232. Myerson SG, Bellenger NG, Pennell DJ. Assessment of left ventricular mass by cardiovascular magnetic resonance. *Hypertension* 2002;39:750–755.
233. Swoboda PP, Larghat A, Zaman A, et al. Reproducibility of myocardial strain and left ventricular twist measured using complementary spatial modulation of magnetization. *J. Magn. Reson. Imaging* 2014;39:887–894.
234. Young AA, Cowan BR. Evaluation of left ventricular torsion by cardiovascular magnetic resonance. *J. Cardiovasc. Magn. Reson.* 2012;14:49.
235. El-Menyar AA, Al Suwaidi J, Holmes DR. Left main coronary artery stenosis: state-of-the-art. *Curr. Probl. Cardiol.* 2007;32:103–93.
236. Conley MJ, Ely RL, Kisslo J, Lee KL, McNeer JF, Rosati RA. The prognostic spectrum of left main stenosis. *Circulation* 1978;57:947–52.
237. Taylor H a, Deumite NJ, Chaitman BR, Davis KB, Killip T, Rogers WJ. Asymptomatic left main coronary artery disease in the Coronary Artery Surgery Study (CASS) registry. *Circulation* 1989;79:1171–9.
238. Serruys PW, Morice M-C, Kappetein AP, et al. Percutaneous coronary intervention versus coronary-artery bypass grafting for severe coronary artery disease. *N. Engl. J. Med.* 2009;360:961–72.
239. Naik H, White AJ, Chakravarty T, et al. A meta-analysis of 3,773 patients treated with percutaneous coronary intervention or surgery for unprotected left main coronary artery stenosis. *JACC. Cardiovasc. Interv.* 2009;2:739–47.
240. Beller GA, Zaret BL. Contributions of nuclear cardiology to diagnosis and prognosis of patients with coronary artery disease. *Circulation* 2000;101:1465–78.
241. Berman DS, Kang X, Slomka PJ, et al. Underestimation of extent of

ischemia by gated SPECT myocardial perfusion imaging in patients with left main coronary artery disease. *J. Nucl. Cardiol.* 2007;14:521–8.

242. Afonso L, Mahajan N. Single-photon emission computed tomography myocardial perfusion imaging in the diagnosis of left main disease. *Clin. Cardiol.* 2009;32:E11-5.

243. Shiba C, Chikamori T, Hida S, et al. Important parameters in the detection of left main trunk disease using stress myocardial perfusion imaging. *J. Cardiol.* 2009;53:43–52.

244. Rehn T, Griffith LS, Achuff SC, et al. Exercise thallium-201 myocardial imaging in left main coronary artery disease: sensitive but not specific. *Am. J. Cardiol.* 1981;48:217–23.

245. Cerqueira MD, Weissman NJ, Dilsizian V, et al. Standardized myocardial segmentation and nomenclature for tomographic imaging of the heart. A statement for healthcare professionals from the Cardiac Imaging Committee of the Council on Clinical Cardiology of the American Heart Association. *Circulation* 2002;105:539–42.

246. Jerosch-Herold M, Wilke N, Stillman AE. Magnetic resonance quantification of the myocardial perfusion reserve with a Fermi function model for constrained deconvolution. *Am. Assoc. Phys. Med.* 1998;25:73–84.

247. Biglands J, Magee D, Boyle R, Larghat A, Plein S, Radjenović A. Evaluation of the effect of myocardial segmentation errors on myocardial blood flow estimates from DCE-MRI. *Phys. Med. Biol.* 2011;56:2423–43.

248. DeLong ER, DeLong DM, Clarke-Pearson DL. Comparing the areas under two or more correlated receiver operating characteristic curves: a nonparametric approach. *Biometrics* 1988;44:837–45.

249. Youden WJ. Index for rating diagnostic tests. *Cancer* 1950;3:32–5.

250. Schwitter J, Wacker CM, Wilke N, et al. MR-IMPACT II: Magnetic

Resonance Imaging for Myocardial Perfusion Assessment in Coronary artery disease Trial: perfusion-cardiac magnetic resonance vs. single-photon emission computed tomography for the detection of coronary artery disease: a comparative . *Eur. Heart J.* 2013;34:775–781.

251. Schwitter J, Wacker CM, Van Rossum AC, et al. MR-IMPACT: comparison of perfusion-cardiac magnetic resonance with single-photon emission computed tomography for the detection of coronary artery disease in a multicentre, multivendor, randomized trial. *Eur. Heart J.* 2008;29:480–489.

252. Pijls NHJ, De Bruyne B, Peels K, et al. Measurement of fractional flow reserve to assess the functional severity of coronary-artery stenoses. *N. Engl. J. Med.* 1996;334:1703–8.

253. Reyes E. Detection of left main stem and three-vessel coronary artery disease by myocardial perfusion SPECT imaging. *EuroIntervention* 2010;6:G72–G78.

254. Ragosta M, Bishop AH, Lipson LC, et al. Comparison Between Angiography and Fractional Flow Reserve Versus Single-Photon Emission Computed Tomographic Myocardial Perfusion Imaging for Determining Lesion Significance in Patients With Multivessel Coronary Disease. *Am. J. Cardiol.* 2007;99:896–902.

255. Chung S-Y, Lee K-Y, Chun EJ, et al. Comparison of stress perfusion MRI and SPECT for detection of myocardial ischemia in patients with angiographically proven three-vessel coronary artery disease. *AJR. Am. J. Roentgenol.* 2010;195:356–62.

256. Schwitter J, Wacker CM, Wilke N, et al. Superior diagnostic performance of perfusion-cardiovascular magnetic resonance versus SPECT to detect coronary artery disease: The secondary endpoints of the multicenter multivendor MR-IMPACT II (Magnetic Resonance Imaging for Myocardial Perfusion Assessm. *J. Cardiovasc. Magn. Reson.*

2012;14:61.

257. Kidambi A, Sourbron S, Maredia N, et al. Factors associated with false-negative cardiovascular magnetic resonance perfusion studies: A Clinical evaluation of magnetic resonance imaging in coronary artery disease (CE-MARC) substudy. *J. Magn. Reson. Imaging* 2016;43:566–73.

258. Abidov A, Bax JJ, Hayes SW, et al. Transient ischemic dilation ratio of the left ventricle is a significant predictor of future cardiac events in patients with otherwise normal myocardial perfusion SPECT. *J. Am. Coll. Cardiol.* 2003;42:1818–25.

259. McLaughlin MG, Danias PG. Transient ischemic dilation: a powerful diagnostic and prognostic finding of stress myocardial perfusion imaging. *J. Nucl. Cardiol.* 2002;9:663–7.

260. Williams KA, Schneider CM. Increased stress right ventricular activity on dual isotope perfusion SPECT: a sign of multivessel and/or left main coronary artery disease. *J. Am. Coll. Cardiol.* 1999;34:420–7.

261. Mannting F, Zabrodina Y V, Dass C. Significance of increased right ventricular uptake on 99mTc-sestamibi SPECT in patients with coronary artery disease. *J. Nucl. Med.* 1999;40:889–94.

262. Nagel E, Klein C, Paetsch I, et al. Magnetic resonance perfusion measurements for the noninvasive detection of coronary artery disease. *Circulation* 2003;108:432–7.

263. Patel AR, Antkowiak PF, Nandalur KR, et al. Assessment of advanced coronary artery disease: advantages of quantitative cardiac magnetic resonance perfusion analysis. *J. Am. Coll. Cardiol.* 2010;56:561–9.

264. Greenwood JP, Brown JM, Dickinson CJ, Ball SG, Plein S. CMR versus SPECT for diagnosis of coronary heart disease – Authors' reply.

Lancet 2012;379:2147–2148.

265. Broadbent DA, Biglands JD, Ripley DP, et al. Sensitivity of quantitative myocardial dynamic contrast-enhanced MRI to saturation pulse efficiency, noise and t1 measurement error: Comparison of nonlinearity correction methods. *Magn. Reson. Med.* 2016;75:1290–300.

266. Groothuis JGJ, Kremers FPPJ, Beek AM, et al. Comparison of dual to single contrast bolus magnetic resonance myocardial perfusion imaging for detection of significant coronary artery disease. *J. Magn. Reson. imaging* 2010;32:88–93.

267. Braunwald E. Heart failure. *JACC. Heart Fail.* 2013;1:1–20.

268. Yancy CW, Jessup M, Bozkurt B, et al. 2013 ACCF/AHA guideline for the management of heart failure: a report of the American College of Cardiology Foundation/American Heart Association Task Force on Practice Guidelines. *J. Am. Coll. Cardiol.* 2013;62:e147-239.

269. Ponikowski P, Voors AA, Anker SD, et al. 2016 ESC Guidelines for the diagnosis and treatment of acute and chronic heart failure: The Task Force for the diagnosis and treatment of acute and chronic heart failure of the European Society of Cardiology (ESC). Developed with the special contribution . *Eur. J. Heart Fail.* 2016;18:891–975.

270. D'Elia N, D'hooge J, Marwick TH. Association Between Myocardial Mechanics and Ischemic LV Remodeling. *JACC Cardiovasc. Imaging* 2015;8:1430–1443.

271. Streeter DD, Spotnitz HM, Patel DP, Ross J, Sonnenblick EH. Fiber orientation in the canine left ventricle during diastole and systole. *Circ. Res.* 1969;24:339–347.

272. Hansen DE, Daughters GT, Alderman EL, Stinson EB, Baldwin JC, Miller DC. Effect of acute human cardiac allograft rejection on left ventricular systolic torsion and diastolic recoil measured by

intramyocardial markers. *Circulation* 1987;76:998–1008.

273. Buchalter MB, Rademakers FE, Weiss JL, Rogers WJ, Weisfeldt ML, Shapiro EP. Rotational deformation of the canine left ventricle measured by magnetic resonance tagging: effects of catecholamines, ischaemia, and pacing. *Cardiovasc. Res.* 1994;28:629–35.

274. Bertini M, Delgado V, Nucifora G, et al. Left ventricular rotational mechanics in patients with coronary artery disease: differences in subendocardial and subepicardial layers. *Heart* 2010;96:1737–43.

275. Paetsch I, Föll D, Kaluza A, et al. Magnetic resonance stress tagging in ischemic heart disease. *Am. J. Physiol. Heart Circ. Physiol.* 2005;288:H2708-14.

276. Setser RM, Smedira NG, Lieber ML, Sabo ED, White RD. Left ventricular torsional mechanics after left ventricular reconstruction surgery for ischemic cardiomyopathy. *J. Thorac. Cardiovasc. Surg.* 2007;134:888–896.

277. Sade LE, Demir Ö, Atar I, Müderrisoglu H, Özin B. Effect of Mechanical Dyssynchrony and Cardiac Resynchronization Therapy on Left Ventricular Rotational Mechanics. *Am. J. Cardiol.* 2008;101:1163–1169.

278. Young AA, Axel L, Dougherty L, Bogen DK, Parenteau CS. Validation of tagging with MR imaging to estimate material deformation. *Radiology* 1993;188:101–8.

279. Rüssel IK, Götte MJW, Bronzwaer JG, Knaapen P, Paulus WJ, van Rossum AC. Left Ventricular Torsion. An Expanding Role in the Analysis of Myocardial Dysfunction. *JACC Cardiovasc. Imaging* 2009;2:648–655.

280. Yeon SB, Reichek N, Tallant BA, et al. Validation of in vivo myocardial strain measurement by magnetic resonance tagging with sonomicrometry. *J. Am. Coll. Cardiol.* 2001;38:555–561.

281. Messroghli DR, Bainbridge GJ, Alfakih K, et al. Assessment of regional left ventricular function: Accuracy and reproducibility of positioning standard short-axis sections in cardiac MR imaging. *Radiology* 2005;235:229–236.
282. Foley JRJ, Swoboda PP, Fent GJ, et al. Quantitative deformation analysis differentiates ischaemic and non-ischaemic cardiomyopathy: sub-group analysis of the VINDICATE trial. *Eur. Heart J. Cardiovasc. Imaging* 2017:1–8.
283. Velazquez EJ, Lee KL, Jones RH, et al. Coronary-Artery Bypass Surgery in Patients with Ischemic Cardiomyopathy. *N. Engl. J. Med.* 2016;374:1511–20.
284. Arts T, Reneman RS, Veenstra PC. A model of the mechanics of the left ventricle. *Ann. Biomed. Eng.* 1979;7:299–318.
285. Beyar R, Sideman S. Left ventricular mechanics related to the local distribution of oxygen demand throughout the wall. *Circ. Res.* 1986;58:664–77.
286. Swoboda PP, Erhayiem B, McDiarmid AK, et al. Relationship between cardiac deformation parameters measured by cardiovascular magnetic resonance and aerobic fitness in endurance athletes. *J. Cardiovasc. Magn. Reson.* 2016;18:48.
287. Greenbaum RA, Ho SY, Gibson DG, Becker AE, Anderson RH. Left ventricular fibre architecture in man. *Heart* 1981;45:248–263.
288. Lorenz CH, Pastorek JS, Bundy JM. Delineation of normal human left ventricular twist throughout systole by tagged cine magnetic resonance imaging. *J. Cardiovasc. Magn. Reson.* 2000;2:97–108.
289. Ono S, Waldman LK, Yamashita H, Covell JW, Ross J. Effect of coronary artery reperfusion on transmural myocardial remodeling in dogs. *Circulation* 1995;91:1143–53.

290. Homans DC, Pavek T, Laxson DD, Bache RJ. Recovery of transmural and subepicardial wall thickening after subendocardial infarction. *J. Am. Coll. Cardiol.* 1994;24:1109–1116.
291. Wu MT, Tseng WYI, Su MYM, et al. Diffusion tensor magnetic resonance imaging mapping the fiber architecture remodeling in human myocardium after infarction: Correlation with viability and wall motion. *Circulation* 2006;114:1036–1045.
292. Abate E, Hoogslag GE, Leong DP, et al. Association between multilayer left ventricular rotational mechanics and the development of left ventricular remodeling after acute myocardial infarction. *J. Am. Soc. Echocardiogr.* 2014;27:239–48.
293. Becker M, Ocklenburg C, Altiok E, et al. Impact of infarct transmurality on layer-specific impairment of myocardial function: a myocardial deformation imaging study. *Eur. Heart J.* 2009;30:1467–76.
294. Karaahmet T, Gürel E, Tigen K, et al. The effect of myocardial fibrosis on left ventricular torsion and twist in patients with non-ischemic dilated cardiomyopathy. *Cardiol. J.* 2013;20:276–286.
295. Sengupta PP, Krishnamoorthy VK, Abhayaratna WP, et al. Disparate Patterns of Left Ventricular Mechanics Differentiate Constrictive Pericarditis From Restrictive Cardiomyopathy. *JACC Cardiovasc. Imaging* 2008;1:29–38.
296. van Dalen BM, Caliskan K, Soliman OII, et al. Left ventricular solid body rotation in non-compaction cardiomyopathy: a potential new objective and quantitative functional diagnostic criterion? *Eur. J. Heart Fail.* 2008;10:1088–93.
297. Kanzaki H, Nakatani S, Yamada N, Urayama SI, Miyatake K, Kitakaze M. Impaired Systolic torsion in dilated cardiomyopathy: Reversal of apical rotation at mid-systole characterized with magnetic resonance tagging method. *Basic Res. Cardiol.* 2006;101:465–470.

298. Meluzin J, Spinarova L, Hude P, et al. Left ventricular mechanics in idiopathic dilated cardiomyopathy: systolic-diastolic coupling and torsion. *J. Am. Soc. Echocardiogr.* 2009;22:486–93.
299. Antoni ML, Mollema SA, Delgado V, et al. Prognostic importance of strain and strain rate after acute myocardial infarction. *Eur. Heart J.* 2010;31:1640–7.
300. Mignot A, Donal E, Zaroui A, et al. Global longitudinal strain as a major predictor of cardiac events in patients with depressed left ventricular function: A multicenter study. *J. Am. Soc. Echocardiogr.* 2010;23:1019–1024.
301. Garg P, Kidambi A, Foley JRJ, et al. Ventricular longitudinal function is associated with microvascular obstruction and intramyocardial haemorrhage. *Open Hear.* 2016;3:e000337.
302. Rademakers FE, Rogers WJ, Guier WH, et al. Relation of regional cross-fiber shortening to wall thickening in the intact heart. Three-dimensional strain analysis by NMR tagging. *Circulation* 1994;89:1174–82.
303. Lumens J. Impaired subendocardial contractile myofiber function in asymptomatic aged humans, as detected using MRI. *AJP Hear. Circ. Physiol.* 2006;291:H1573–H1579.
304. Larghat AM, Swoboda PP, Biglands JD, Kearney MT, Greenwood JP, Plein S. The microvascular effects of insulin resistance and diabetes on cardiac structure, function, and perfusion: a cardiovascular magnetic resonance study. *Eur. Heart J. Cardiovasc. Imaging* 2014;15:1368–76.
305. Musa T Al, Uddin A, Swoboda PP, et al. Cardiovascular magnetic resonance evaluation of symptomatic severe aortic stenosis: association of circumferential myocardial strain and mortality. *J. Cardiovasc. Magn. Reson.* 2017;19:1–10.

306. Rüssel IK, Tecelão SR, Kuijer JPA, Heethaar RM, Marcus JT. Comparison of 2D and 3D calculation of left ventricular torsion as circumferential-longitudinal shear angle using cardiovascular magnetic resonance tagging. *J. Cardiovasc. Magn. Reson.* 2009;11:8.
307. Rutz AK, Ryf S, Plein S, Boesiger P, Kozerke S. Accelerated whole-heart 3D CSPAMM for myocardial motion quantification. *Magn. Reson. Med.* 2008;59:755–63.
308. Stoeck CT, Manka R, Boesiger P, Kozerke S. Undersampled Cine 3D tagging for rapid assessment of cardiac motion. *J. Cardiovasc. Magn. Reson.* 2012;14:60.
309. Pryor DB, Shaw L, McCants CB, et al. Value of the history and physical in identifying patients at increased risk for coronary artery disease. *Ann. Intern. Med.* 1993;118:81–90.
310. Cheng VY, Berman DS, Rozanski A, et al. Performance of the Traditional Age, Sex, and Angina Typicality-Based Approach for Estimating Pretest Probability of Angiographically Significant Coronary Artery Disease in Patients Undergoing Coronary Computed Tomographic Angiography: Results From the Mul. *Circulation* 2011;124:2423–2432.
311. Genders TSS, Steyerberg EW, Alkadhi H, et al. A clinical prediction rule for the diagnosis of coronary artery disease: Validation, updating, and extension. *Eur. Heart J.* 2011;32:1316–1330.
312. Genders TSS, Steyerberg EW, Hunink MGM, et al. Prediction model to estimate presence of coronary artery disease: retrospective pooled analysis of existing cohorts. *BMJ* 2012;344:e3485.
313. Bittencourt MS, Hulten E, Polonsky TS, et al. European Society of Cardiology-Recommended Coronary Artery Disease Consortium Pretest Probability Scores More Accurately Predict Obstructive Coronary Disease and Cardiovascular Events Than the Diamond and Forrester Score: The Partners Registry. *Circulation* 2016;134:201–11.

314. Genders TSS, Coles A, Hoffmann U, et al. The External Validity of Prediction Models for the Diagnosis of Obstructive Coronary Artery Disease in Patients With Stable Chest Pain: Insights From the PROMISE Trial. *JACC. Cardiovasc. Imaging* 2017;1–10.
315. Timmis A, Roobottom CA. National Institute for Health and Care Excellence updates the stable chest pain guideline with radical changes to the diagnostic paradigm. *Heart* 2017;heartjnl-2015-308341.
316. Diamond GA. A clinically relevant classification of chest discomfort. *J. Am. Coll. Cardiol.* 1983;1:574–5.
317. White IR, Royston P, Wood AM. Multiple imputation using chained equations: Issues and guidance for practice. *Stat. Med.* 2011;30:377–99.
318. Li P, Stuart EA, Allison DB. Multiple Imputation: A Flexible Tool for Handling Missing Data. *JAMA* 2015;314:1966–7.
319. Rubin Donald B. Multiple Imputation for Nonresponse in Surveys. 2004th ed. Wiley-Interscience; 2004.
320. Harrell FE, Lee KL, Mark DB. Multivariable prognostic models: issues in developing models, evaluating assumptions and adequacy, and measuring and reducing errors. *Stat. Med.* 1996;15:361–87.
321. Bhatnagar P, Wickramasinghe K, Wilkins E, Townsend N. Trends in the epidemiology of cardiovascular disease in the UK. *Heart* 2016;102:1945–1952.
322. Douglas PS, Hoffmann U, Patel MR, et al. Outcomes of anatomical versus functional testing for coronary artery disease. *N. Engl. J. Med.* 2015;372:1291–300.
323. Wasfy MM, Brady TJ, Abbara S, et al. Comparison of the diamond-forrester method and duke clinical score to predict obstructive coronary artery disease by computed tomographic angiography. *Am. J. Cardiol.* 2012;109:998–1004.

324. Cremer PC, Nissen SE. The National Institute for Health and Care Excellence update for stable chest pain: poorly reasoned and risky for patients. *Heart* 2017:heartjnl-2017-311410.
325. Kellman P, Arai AE. Cardiac imaging techniques for physicians: late enhancement. *J. Magn. Reson. Imaging* 2012;36:529–42.
326. Foo TKF, Stanley DW, Castillo E, et al. Myocardial viability: breath-hold 3D MR imaging of delayed hyperenhancement with variable sampling in time. *Radiology* 2004;230:845–51.
327. Dewey M, Laule M, Taupitz M, Kaufels N, Hamm B, Kivelitz D. Myocardial viability: assessment with three-dimensional MR imaging in pigs and patients. *Radiology* 2006;239:703–9.
328. Jablonowski R, Nordlund D, Kanski M, et al. Infarct quantification using 3D inversion recovery and 2D phase sensitive inversion recovery; validation in patients and ex vivo. *BMC Cardiovasc. Disord.* 2013;13:110.
329. Peukert D, Laule M, Taupitz M, Kaufels N, Hamm B, Dewey M. 3D and 2D Delayed-Enhancement Magnetic Resonance Imaging for Detection of Myocardial Infarction: Preclinical and Clinical Results. *Acad. Radiol.* 2007;14:788–794.
330. Nguyen TD, Spincemaille P, Weinsaft JW, et al. A fast navigator-gated 3D sequence for delayed enhancement MRI of the myocardium: comparison with breathhold 2D imaging. *J. Magn. Reson. Imaging* 2008;27:802–8.
331. van den Bosch HCM, Westenberg JJM, Post JC, et al. Free-breathing MRI for the assessment of myocardial infarction: clinical validation. *AJR. Am. J. Roentgenol.* 2009;192:W277-81.
332. Kino A, Zuehlsdorff S, Sheehan JJ, et al. Three-dimensional phase-sensitive inversion-recovery turbo FLASH sequence for the evaluation of left ventricular myocardial scar. *AJR. Am. J. Roentgenol.*

2009;193:W381-8.

333. Peters DC, Appelbaum EA, Nezafat R, et al. Left ventricular infarct size, peri-infarct zone, and papillary scar measurements: A comparison of high-resolution 3D and conventional 2D late gadolinium enhancement cardiac MR. *J. Magn. Reson. Imaging* 2009;30:794–800.

334. Yin G, Zhao S, Lu M, et al. Assessment of left ventricular myocardial scar in coronary artery disease by a three-dimensional MR imaging technique. *J. Magn. Reson. Imaging* 2013;38:72–79.

335. Morsbach F, Gordic S, Gruner C, et al. Quantitative comparison of 2D and 3D late gadolinium enhancement MR imaging in patients with Fabry disease and hypertrophic cardiomyopathy. *Int. J. Cardiol.* 2016;217:167–73.

336. Bratis K, Henningson M, Grigoratos C, et al. Clinical evaluation of three-dimensional late enhancement MRI. *J. Magn. Reson. Imaging* 2016:1–9.

337. Shaw JL, Knowles BR, Goldfarb JW, Manning WJ, Peters DC. Left atrial late gadolinium enhancement with water-fat separation: The importance of phase-encoding order. *J. Magn. Reson. Imaging* 2014;40:119–125.

338. Eggers H, Brendel B, Duijndam A, Herigault G. Dual-echo Dixon imaging with flexible choice of echo times. *Magn. Reson. Med.* 2011;65:96–107.

339. Dixon WT. Simple proton spectroscopic imaging. *Radiology* 1984;153:189–94.

340. Guerini H, Omoumi P, Guichoux F, et al. Fat Suppression with Dixon Techniques in Musculoskeletal Magnetic Resonance Imaging: A Pictorial Review. *Semin. Musculoskelet. Radiol.* 2015;19:335–347.

341. Ma J. Dixon techniques for water and fat imaging. *J. Magn. Reson.*

Imaging 2008;28:543–558.

342. Reeder SB, Wen Z, Yu H, et al. Multicoil Dixon chemical species separation with an iterative least-squares estimation method. *Magn. Reson. Med.* 2004;51:35–45.

343. Amado LC, Gerber BL, Gupta SN, et al. Accurate and objective infarct sizing by contrast-enhanced magnetic resonance imaging in a canine myocardial infarction model. *J. Am. Coll. Cardiol.* 2004;44:2383–2389.

344. Lapinskas T, Schnackenburg B, Kouwenhoven M, et al. Fatty metaplasia quantification and impact on regional myocardial function as assessed by advanced cardiac MR imaging. *MAGMA* 2017.

345. Goldfarb JW, Roth M, Han J. Myocardial fat deposition after left ventricular myocardial infarction: assessment by using MR water-fat separation imaging. *Radiology* 2009;253:65–73.

346. Hernando D, Kellman P, Haldar JP, Liang ZP. A network flow method for improved MR field map estimation in the presence of water and fat. *Conf. Proc. ... Annu. Int. Conf. IEEE Eng. Med. Biol. Soc.* 2008;2008:82–5.

347. Shin T, Lustig M, Nishimura DG, Hu BS. Rapid single-breath-hold 3D late gadolinium enhancement cardiac MRI using a stack-of-spirals acquisition. *J. Magn. Reson. Imaging* 2014;40:1496–1502.

348. Morita K, Utsunomiya D, Oda S, et al. Comparison of 3D Phase-Sensitive Inversion-Recovery and 2D Inversion-Recovery MRI at 3.0 T for the Assessment of Late Gadolinium Enhancement in Patients with Hypertrophic Cardiomyopathy. *Acad. Radiol.* 2013;20:752–757.

349. Kühn HP, Papavasiliu TS, Beek AM, Hofman MBM, Heusen NS, van Rossum AC. Myocardial viability: rapid assessment with delayed contrast-enhanced MR imaging with three-dimensional inversion-recovery

prepared pulse sequence. *Radiology* 2004;230:576–82.

350. Bauner KU, Muehling O, Theisen D, et al. Assessment of Myocardial Viability with 3D MRI at 3 T. *AJR. Am. J. Roentgenol.* 2009;192:1645–50.

351. Bizino MB, Tao Q, Amersfoort J, et al. High spatial resolution free-breathing 3D late gadolinium enhancement cardiac magnetic resonance imaging in ischaemic and non-ischaemic cardiomyopathy: quantitative assessment of scar mass and image quality. *Eur. Radiol.* 2018:1–9.

352. Vincenti G, Monney P, Chaptinel J, et al. Compressed sensing single-breath-hold CMR for fast quantification of LV function, volumes, and mass. *JACC Cardiovasc. Imaging* 2014;7:882–892.

353. Akçakaya M, Rayatzadeh H, Basha TA, et al. Accelerated late gadolinium enhancement cardiac MR imaging with isotropic spatial resolution using compressed sensing: initial experience. *Radiology* 2012;264:691–9.

354. Basha TA, Akçakaya M, Liew C, et al. Clinical performance of high-resolution late gadolinium enhancement imaging with compressed sensing. *J. Magn. Reson. Imaging* 2017;46:1829–1838.

355. Roujol S, Basha TA, Akçakaya M, et al. 3D late gadolinium enhancement in a single prolonged breath-hold using supplemental oxygenation and hyperventilation. *Magn. Reson. Med.* 2014;72:850–7.

356. Kelle S, Roes SD, Klein C, et al. Prognostic value of myocardial infarct size and contractile reserve using magnetic resonance imaging. *J. Am. Coll. Cardiol.* 2009;54:1770–7.

357. Kellman P, Arai AE, McVeigh ER, Aletras AH. Phase-sensitive inversion recovery for detecting myocardial infarction using gadolinium-delayed hyperenhancement. *Magn. Reson. Med.* 2002;47:372–83.

358. Kim HW, Rehwald WG, Jenista ER, et al. Dark-Blood Delayed Enhancement Cardiac Magnetic Resonance of Myocardial Infarction.

JACC Cardiovasc. Imaging 2017;1–12.

359. Witschey WRT, Pilla JJ, Ferrari G, et al. Rotating frame spin lattice relaxation in a swine model of chronic, left ventricular myocardial infarction. *Magn. Reson. Med.* 2010;64:1453–60.

360. Witschey WRT, Borthakur A, Elliott MA, et al. Artifacts in T1 rho-weighted imaging: compensation for B(1) and B(0) field imperfections. *J. Magn. Reson.* 2007;186:75–85.

361. Basha TA, Tang MC, Tsao C, et al. Improved dark blood late gadolinium enhancement (DB-LGE) imaging using an optimized joint inversion preparation and T2 magnetization preparation. *Magn. Reson. Med.* 2017;00.

362. Francis R, Kellman P, Kotecha T, et al. Prospective comparison of novel dark blood late gadolinium enhancement with conventional bright blood imaging for the detection of scar. *J. Cardiovasc. Magn. Reson.* 2017;19:1–12.

363. Ryf S, Spiegel MA, Gerber M, Boesiger P. Myocardial tagging with 3D-CSPAMM. *J. Magn. Reson. Imaging* 2002;16:320–325.

364. Axel L, Otazo R. Accelerated MRI for the assessment of cardiac function. *Br. J. Radiol.* 2016;89:20150655.

365. Axel L, Sodickson DK. The need for speed: Accelerating CMR imaging assessment of cardiac function. *JACC Cardiovasc. Imaging* 2014;7:893–895.

366. Kido T, Kido T, Nakamura M, et al. Compressed sensing real-time cine cardiovascular magnetic resonance: Accurate assessment of left ventricular function in a single-breath-hold. *J. Cardiovasc. Magn. Reson.* 2016;18:1–11.

367. Deo RC. Machine Learning in Medicine. *Circulation* 2015;132:1920–1930.

368. Lecun Y, Bengio Y, Hinton G. Deep learning. *Nature* 2015;521:436–444.

369. SCOT-HEART investigators. CT coronary angiography in patients with suspected angina due to coronary heart disease (SCOT-HEART): an open-label, parallel-group, multicentre trial. *Lancet (London, England)* 2015;385:2383–91.

370. Inaba Y, Chen JA, Bergmann SR. Quantity of viable myocardium required to improve survival with revascularization in patients with ischemic cardiomyopathy: A meta-analysis. *J. Nucl. Cardiol.* 2010;17:646–54.

371. Hachamovitch R, Hayes S, Friedman JD, et al. Determinants of risk and its temporal variation in patients with normal stress myocardial perfusion scans: what is the warranty period of a normal scan? *J. Am. Coll. Cardiol.* 2003;41:1329–40.

10. Appendix

10.1. Ethical approval, Patient information sheets and consent form for Chapters 3 and 5

NHS
National Research Ethics Service

Leeds (West) Research Ethics Committee
A/B Floor, Old Site
Leeds General Infirmary
Great George Street
Leeds
LS1 3EX

Telephone: 0113 392 6788
Facsimile: 0113 392 2663

25 September 2007

Professor Stephen Ball
Professor of Cardiology
Leeds Teaching Hospitals NHS Trust
Institute of Cardiovascular Research
G Floor, Jubilee Building
Leeds General Infirmary
Leeds
LS1 3EX

Dear Professor Ball

Full title of study: Cardiac Magnetic Resonance Imaging in Coronary Heart
Disease: From Research to Clinical Practice
REC reference number: 051012051128

The REC gave a favourable ethical opinion to this study on 23 August 2005.

Further notification(s) have been received from local site assessor(s) following site-specific assessment. On behalf of the Committee, I am pleased to confirm the extension of the favourable opinion to the new site(s). I attach an updated version of the site approval form, listing all sites with a favourable ethical opinion to conduct the research.

R&D approval

The Chief Investigator or sponsor should inform the local Principal Investigator at each site of the favourable opinion by sending a copy of this letter and the attached form. The research should not commence at any NHS site until approval from the R&D office for the relevant NHS care organisation has been confirmed.

Statement of compliance

The Committee is constituted in accordance with the Governance Arrangements for Research Ethics Committees (July 2001) and complies fully with the Standard Operating Procedures for Research Ethics Committees in the UK.

051012051128

Please quote this number on all correspondence.



CE-MARC STUDY

Clinical Evaluation of Magnetic Resonance imaging in Coronary heart disease

Patient information Leaflet

Version 2.1 December 2005

Dear patient,

You are being invited to take part in a research study. Before you decide it is important for you to understand why the research is being done and what it will involve. Please take time to read the following information carefully and discuss it with friends, relatives and your GP if you wish. Ask us if there is anything that is not clear or if you would like more information. Take time to decide whether or not you wish to take part.

WHY HAVE I BEEN CHOSEN?

This study is looking at people like you, who have been referred to a cardiology clinic with chest pain. We will be asking 750 people to take part in this study.

WHAT IS THE PURPOSE OF THE STUDY?

We currently have several tests available to help us find out if chest pain is caused by heart disease. These include treadmill exercise testing, coronary angiography and SPECT perfusion imaging. More recently we have begun to use another test, Magnetic Resonance Imaging (MRI) to obtain pictures of the heart. MRI produces pictures with much greater detail than with other types of heart scans. Importantly, MRI is also a safer test than most other heart scans, because it does not expose patients to any harmful radiation and pictures of the heart can be taken "from the outside". Because

of all of these qualities, MRI might become one of the most important tests in patients who suffer with chest pain and coronary heart disease. As for any new test, before being able to use MRI on a daily basis, we need to find out how accurate it really is compared with the currently available tests. This is why we are carrying out this research study.

DO I HAVE TO TAKE PART?

It is up to you to decide whether or not to take part. If you do decide to take part you will be given this information sheet to keep and be asked to sign a consent form. If you decide to take part you are still free to withdraw at any time and without giving a reason. This will not affect the standard of care you receive.

WHAT WILL HAPPEN TO ME IF I TAKE PART?

All patients in this study will have three or four heart tests. One of the tests is the MRI scan, which is done solely for research purposes. The other three tests are those that are currently used to detect coronary heart disease, namely an exercise treadmill test, a SPECT myocardial perfusion study (to obtain information on the blood flow to the heart muscle) and an x-ray angiogram (to detect any blockages in the heart arteries). Of these other three tests, your hospital consultant may want you to have some or even all anyway. However, because for this study all patients must have all four tests (to allow us to compare them with each other), if any of the other three tests are not requested by your hospital consultant, we will carry them out for this research study.

All tests will be performed at the Leeds General Infirmary and we will try to carry out as many as possible on the same day to minimise the time you have to spend travelling to the hospital. Information leaflets that give you more details about all of the tests will be provided.

1. The MRI scan will take approximately 60 minutes to complete. You lie in a short 'tunnel', which holds a large magnet. Short bursts of magnetic fields and radio waves from the MRI scanner allow images to be created. You will hear periodical loud "banging" noises while we are acquiring the images of your heart. We will remain in communication with you throughout the scan. Twice during the scan, we will inject an MRI contrast medication into a vein in your arm. The needle used for this will feel like a sharp scratch. Usually people are not aware of the contrast dye injection. At one point we will also inject a medication (Adenosine) into a vein in your arm, which is a drug to increase the blood flow to your heart. This can cause a brief feeling of warmth, breathlessness or chest discomfort. However all of these feelings, if they occur, usually settle within one or two minutes.

2. The exercise treadmill test requires you to walk on a treadmill while your heart trace (ECG) and blood pressure are measured. This test will of course only be carried out if you are physically able to walk on the treadmill. Almost all patients referred to hospital with chest pain have a treadmill test anyway.

3. The SPECT perfusion study is carried out on two separate days and takes approximately 2 hours on each day. On one day pictures of the heart will be taken at rest and on the second day after injection of the same medication (Adenosine) that we use for the MRI scan to increase the blood flow to your heart. On both days you will also have an injection of a radioactive dye into the blood, which is taken up by the heart muscle. Usually people are not aware of the contrast dye injection. One hour after the injection, pictures of the heart are taken with a special camera that slowly moves around you while you lie on a bed with one arm raised above your head. Taking these pictures takes approximately 20 minutes.

4. With the x-ray angiogram, we take x-ray pictures of the heart arteries. This test requires you to come into hospital for one day. You will be taken to an x-ray room and lie down on your back. After cleaning the groin area, local anaesthetic is given into the groin or the forearm and a needle put into the artery in the groin or arm. Because of the local anaesthetic putting the needle in should not be painful. A fine, hollow tube called a 'catheter' is then introduced into the artery and is gently advanced through the blood vessels to the heart. The catheter is roughly the diameter of the lead in a lead pencil. You will not feel the catheter being moved around inside your chest. A dye is then injected into the heart blood vessels and X-rays taken from several angles. Some injections cause a hot, flushing sensation which lasts a few seconds. When the test is over, the catheter is removed and simple pressure is applied to the leg or arm for about 10 minutes. Most patients referred to hospital with chest pain will have an x-ray angiogram at some point.

In addition to the heart scans you will have one blood sample taken and stored to measure a number of biochemical markers of cardiovascular risk. The sample would be taken by a qualified nurse or doctor and if at all possible will be taken at a time when you are having blood taken for another reason.

After you have had the heart tests, we will monitor your progress for three years. This will involve a short telephone call once a year to find out how your health has been.

Sometimes we collaborate with commercial companies to pursue our research. This may be necessary for example if we find a new blood marker and need to develop a kit to measure it. Although this may involve the use of samples or research results from patients, these would be anonymised and there would be no direct financial gain to patients taking part in the study.

WHAT ARE THE RISKS AND DISCOMFORTS?

Magnetic Resonance Imaging (MRI) is safe and no x-rays or radiation are used for this scan. There are no known risks from this technique. Some patients may experience claustrophobia. The staff will provide every possible means to reduce this sensation. The contrast medication which we use is very safe but, as with any injection, reactions may occur. These include a warm sensation at the injection site, nausea or vomiting and transient skin rash. These effects usually only last for a few minutes. People with a history of allergy are more likely to suffer a more severe reaction, but this is rare (less than 1 in 3000). The department is equipped to cope with allergic reactions if they happen.

Adenosine, the medication we use to increase the blood flow to the heart, can cause flushing, breathlessness and chest discomfort. However, all of these feelings usually subside within one or two minutes or even more quickly if the medication is stopped.

The Exercise treadmill test can cause angina or heart rhythm changes in some people. Should you develop such side effects, the test would be stopped immediately.

SPECT imaging is very safe but exposes patients to a small amount of radiation. As for MRI, Adenosine, the medication we use to increase the blood flow to the heart, can cause flushing, breathlessness and chest discomfort. However, all of these feelings usually subside within one or two minutes or even more quickly if the medication is stopped.

The most common complication of the X-ray angiogram is for a bruise to form in the groin. This is not serious, but may be inconvenient for a few days. Serious complications are very rare, but there is a small risk of the test causing a heart attack, stroke or kidney damage (about 1 in 1000). The test also exposes patients to a small amount of radiation.

All radiation doses carry a small risk. The radiation dose that you would receive from all the tests in this study together would be equivalent to between two and ten years of exposure to natural background radiation.

BENEFITS TO YOU

If you take part in this study, your chest pain will be studied very thoroughly and a lot of information about the health of your heart will be obtained. Most, but not all of this information would be gathered if you did not take part in the study and some of the information could help to plan what is the best treatment for you.

EXPENSES

We will provide reasonable travel expenses should this be necessary for you to attend the follow-up scan. We are also happy to arrange transport to the hospital and return you home if needs be.

WILL MY TAKING PART BE KEPT CONFIDENTIAL?

All information, which is collected about you during the course of the research will be kept strictly confidential. This information will be securely stored at the Clinical Trials Research Unit (CTRU) at the University of Leeds and at the Cardiac MRI Unit at Leeds General Infirmary on paper and electronically, under the provisions of the 1998 Data Protection Act. You will not be identified in any publication that may result from this research.

We will inform your General Practitioner (GP) of your participation in this study as well as in the event of an unexpected abnormality on the scan. We will also contact the Office of National Statistics at a later stage for information that they already hold on patients treated in the UK.

With your permission, your data may also provide a resource for future studies. If any information from this study is used to develop new research, data protection regulations will be observed and strict confidentiality maintained. Ethical approval will be obtained for any future studies involving your data. You will not be identified in the results of any future studies.

If you withdraw consent from further study follow-up, your data will remain on file and will be included in the final study analysis.

WHAT WILL HAPPEN TO THE RESULTS OF THE RESEARCH STUDY?

When the study is complete the results will be published in a medical journal, but no individual patients will be identified. If you would like a copy of the published results, please ask your doctor.

INDEMNITY/COMPENSATION

If you are harmed as a direct result of taking part in this study, there are no special compensation arrangements. If you are harmed due to someone's negligence, then you may have grounds to a legal action. Regardless of this, if you have any cause to complain about any aspect of the way you have been approached or treated during the course of this study, the normal National Health Service complaints mechanisms are available to you.

If you have a private medical insurance please ensure that participation in the study does not affect your cover.

WHO IS ORGANISING AND FUNDING THE STUDY?

This is a research project of the Cardiac MRI department at Leeds General Infirmary, which is funded by the British Heart Foundation.

WHO HAS REVIEWED THE STUDY?

The study has been reviewed and approved by an independent local NHS Research Ethics Committee

For further information please contact:

Dr. Neil Maredia, Research Fellow, or
Petra Bijsterveld, Research Nurse
British Heart Foundation Cardiac MRI Department,
B Floor, Clarendon Wing,
Leeds General Infirmary.
Tel: 0113 39 2 5481 Mobile: 07922 512 887.
<http://www.cmr.leeds.ac.uk/>



When you attend for your Cardiology out-patient appointment, a Doctor or Nurse connected with the research programme will talk to you about the study and give you further information.

If, after reading this information leaflet you definitely do not want to consider this study, please tear off this slip and give it to the receptionist with your name written below.

Name:

.....
.....

Thank you for your time.

CE-MARC Study
Clinical Evaluation of Magnetic Resonance imaging in
Coronary heart disease

Patient Study Number:

Date of Birth:

Hospital Number:

Initials:

Please initial

boxes

1. I have read the Patient Information Sheet dated December 2005 (Version 2.1) for the above study and I have had the opportunity to ask questions and discuss the research study and I am satisfied with the answers to my questions.
2. I have received enough information about this study.
3. I understand that my participation is voluntary and that I am free to withdraw from the study at any time without giving a reason and without affecting my future care.
4. I understand that my medical records may be looked at by authorised individuals from the Clinical Trials Research Unit in order to check that the study is being carried out correctly.
5. I understand that information held by the NHS and records maintained by the Office of National Statistics (ONS) may be used to follow up my health status, should I lose contact with my hospital doctor. I give permission for this information to be obtained from the ONS and/or NHS if necessary.
6. I agree that my medical data may be used to help develop future research studies and I understand that my identity will remain anonymous.
7. I understand that my samples may be used in future research projects which may involve collaborations with commercial companies and I understand that I will not benefit financially if the research leads to the development of a new test or treatment.
8. I agree to take part in this research study.

Signature.....

Name (block capitals)..... Date.....

Signature of witness.....

Name (block capitals).....Date.....



Health Research Authority

NRES Committee Yorkshire & The Humber - South Yorkshire
Millside
Mill Pond Lane
Meanwood
Leeds
LS6 4RA

Telephone: 01133050108

18 September 2012

Petra Bijsterveld
Research Nurse
CMR Clinical Research Group
Cardiovascular Research
G Floor Jubilee Wing
Leeds General Infirmary
LS1 3EX

Dear Petra

Full title of study: Clinical Evaluation of Magnetic Resonance imaging in
Coronary heart disease 2
REC reference number: 12/YH/0404

Thank you for your email of 17/09/2012 I can confirm the REC has received the documents listed below as evidence of compliance with the approval conditions detailed in our letter dated 30 August 2012. Please note these documents are for information only and have not been reviewed by the committee.

Documents received

The documents received were as follows:

Document	Version	Date
Covering Letter	Ms Bijsterveld Email	17 September 2012
Participant Consent Form: CE-Marc 2	1.1	17 September 2012
Participant Information Sheet: CE-Marc 2	1.1	17 September 2012

You should ensure that the sponsor has a copy of the final documentation for the study. It is the sponsor's responsibility to ensure that the documentation is made available to R&D offices at all participating sites.

12/YH/0404 Please quote this number on all correspondence

Yours sincerely

Hazel Robinson
Assistant Co-ordinator

E-mail: hazel.robinson9@nhs.net

Copy to: Dr John P Greenwood
Mrs Rachel de Souza, University of Leeds
Ms Anne Gowing, R&D Department, Leeds Teaching Hospitals NHS Trust



Health Research Authority

NRES Committee Yorkshire & The Humber - South Yorkshire

Millside
Mill Pond Lane
Meanwood
Leeds
LS6 4RA

Telephone: 0113 3050116
Facsimile: 0113 8556191

12 September 2012

Dr John P Greenwood
Consultant Cardiologist, Senior Lecturer
University of Leeds
Academic Unit of Cardiovascular Medicine
G floor, Jubilee Wing
Leeds General Infirmary
LS1 3EX

Dear Dr Greenwood

Study title: Clinical Evaluation of Magnetic Resonance imaging in
Coronary heart disease 2
REC reference: 12/YH/0404
IRAS Project reference: 109822

The Research Ethics Committee reviewed the above application at the meeting held on 30 August 2012. Thank you for sending Ms Petra Bijsterveld to discuss the study.

Ethical opinion

Discussion with Ms Bijsterveld

- The Committee asked the Researcher whilst determining CMR guided care and CV events (MACE) in the study, if a large number of false negatives are identified going through CMR, will it be stopped? The Researcher confirmed that a Safety Monitoring Committee will be established on the study. She stated that the previous C-MARC study has already monitored this, so it is highly unlikely that these patients will be missed.
- The Committee informed the Researcher that they had agreed that the Participant Information Sheet was rather lengthy, but informative. However, they asked that some wording be changed i.e. under the section 'Purpose of the study' the wording in the 8th line down states 'Importantly, MRI is also a safer test than most other heart scans, because it does not use radiation'. The Committee stated that it should only state 'MRI does not use radiation', as at this point they have not been allocated into one of the three groups. They also stated that the word 'No' should be inserted at the beginning of the paragraph under the heading 'Do I have to take part?'

The members of the Committee present gave a favourable ethical opinion of the above

research on the basis described in the application form, protocol and supporting documentation, subject to the conditions specified below.

Ethical review of research sites

NHS Sites

The favourable opinion applies to all NHS sites taking part in the study, subject to management permission being obtained from the NHS/HSC R&D office prior to the start of the study (see "Conditions of the favourable opinion" below).

Non NHS sites

The Committee has not yet been notified of the outcome of any site-specific assessment (SSA) for the non-NHS research site(s) taking part in this study. The favourable opinion does not therefore apply to any non-NHS site at present. I will write to you again as soon as one Research Ethics Committee has notified the outcome of a SSA. In the meantime no study procedures should be initiated at non-NHS sites.

Conditions of the favourable opinion

The favourable opinion is subject to the following conditions being met prior to the start of the study.

Management permission or approval must be obtained from each host organisation prior to the start of the study at the site concerned.

Management permission ("R&D approval") should be sought from all NHS organisations involved in the study in accordance with NHS research governance arrangements.

Guidance on applying for NHS permission for research is available in the Integrated Research Application System or at <http://www.rdforum.nhs.uk>.

Where a NHS organisation's role in the study is limited to identifying and referring potential participants to research sites ("participant identification centre"), guidance should be sought from the R&D office on the information it requires to give permission for this activity.

For non-NHS sites, site management permission should be obtained in accordance with the procedures of the relevant host organisation.

Sponsors are not required to notify the Committee of approvals from host organisations

It is responsibility of the sponsor to ensure that all the conditions are complied with before the start of the study or its initiation at a particular site (as applicable).

You must notify the REC in writing once all conditions have been met (except for site approvals from host organisations) and provide copies of any revised documentation with updated version numbers. The REC will acknowledge receipt and provide a final list of the approved documentation for the study, which can be made available to host organisations to facilitate their permission for the study. Failure to provide the final versions to the REC may cause delay in obtaining permissions.

Approved documents

The documents reviewed and approved at the meeting were:

<i>Document</i>	<i>Version</i>	<i>Date</i>
Covering Letter		10 August 2012
Evidence of insurance or indemnity		28 September 2011
Investigator CV		10 August 2012
Letter of invitation to participant	1.0	10 August 2012
Other: Study Flow Diagram/ Study Summary		
Other: General Practitioner Information Sheet	1.0	10 August 2012
Participant Information Sheet	1.0	10 August 2012
Protocol	1.0	10 August 2012
Questionnaire: Seattle Angina Questionnaire		
Questionnaire: Your Health & Wellbeing		
Questionnaire: Health Questionnaire		
REC application		23 July 2012

Membership of the Committee

The members of the Ethics Committee who were present at the meeting are listed on the attached sheet.

Dr Rhona Bratt (co-opted member) expressed that the Research Nurse attending on behalf of the Chief Investigator, Petra Bijsterveld, was once a Committee Member on the REC that she chairs. The Committee agreed that Rhona Bratt remain in the room and take part in all deliberations and decision making for this study, as they did not deem this to be a conflict of interest.

Statement of compliance

The Committee is constituted in accordance with the Governance Arrangements for Research Ethics Committees and complies fully with the Standard Operating Procedures for Research Ethics Committees in the UK.

After ethical review

Reporting requirements

The attached document "After ethical review – guidance for researchers" gives detailed guidance on reporting requirements for studies with a favourable opinion, including:

- Notifying substantial amendments
- Adding new sites and investigators
- Notification of serious breaches of the protocol
- Progress and safety reports
- Notifying the end of the study

The NRES website also provides guidance on these topics, which is updated in the light of changes in reporting requirements or procedures.

Feedback

You are invited to give your view of the service that you have received from the National Research Ethics Service and the application procedure. If you wish to make your views known please use the feedback form available on the website.

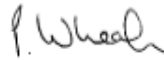
Further information is available at National Research Ethics Service website > After Review

12/YH/0404	Please quote this number on all correspondence
------------	--

With the Committee's best wishes for the success of this project

Yours sincerely

pp



Mr Neil Marsden
Vice-Chair

Email: trish.wheat@nhs.net

*Enclosures: List of names and professions of members who were present at the meeting and those who submitted written comments
"After ethical review – guidance for researchers"*

Copy to: Rachel de Souza, University of Leeds

Ms Anne Gowing, R&D Department, Leeds Teaching Hospitals NHS Trust

CE-MARC 2

Clinical Evaluation of Magnetic Resonance imaging in Coronary heart disease.

QUICK GUIDE

(v 4.0 June 12 2013)

- You are invited to take part in a research study, comparing different ways of investigating patients who have chest pain.
- The study is funded by the British Heart Foundation.
- If you consent to take part in the study you will be randomly assigned to be in one of three groups:

Group 1	This group will be investigated with an MRI scan of the heart
Group 2	This group will be investigated with a SPECT scan of the heart
Group 3	This group will be investigated following national (NICE) guidelines and you will either have a CT scan, a SPECT scan or an X-Ray angiogram (depending on the likelihood of you having narrowings in your heart arteries).

- The test you have will be reported and if it is abnormal you will have an X-Ray coronary angiogram (unless that was your 1st test anyway) with measurement of the blood flow in the heart arteries.
- All patients will be followed up and therefore members of the research team will have access to your records during and after study participation
- You will not benefit directly from taking part in the study
- You do not have to take part if you do not want to, in which case you would receive standard care instead.

If you would like to read more the study is explained in detail in the information sheet which follows. The research team will also be happy to explain the study to you in person.

CE-MARC 2
Clinical Evaluation of Magnetic Resonance imaging in Coronary heart disease.

PATIENT INFORMATION SHEET
Version 4.0 June 12 2013

Chief Investigator: Prof J Greenwood

Dear Patient,

You are being invited to take part in a research study. Before you decide it is important for you to understand why the research is being done and what it will involve. Please take time to read the following information carefully and discuss it with friends, relatives and your GP if you wish. Ask us if there is anything that is not clear or if you would like more information. Take time to decide whether or not you wish to take part.

Purpose of the study

We have several tests available to help us find out if chest pain is caused by narrowings of the heart arteries (coronary heart disease). Currently many patients in whom coronary artery disease is suspected, have an angiogram (=X-ray test taking pictures of the heart arteries). We know from other studies that some of these angiograms will show normal heart arteries. Before having an angiogram many patients have had another heart test, for instance a CT scan or a SPECT scan. Doctors are always looking to develop and improve tests that can reliably tell us if a patient needs an angiogram as their next test or not. Nowadays we can use Magnetic Resonance Imaging (MRI) to obtain pictures of the heart and see how well the heart is supplied with blood and oxygen. MRI is becoming an important test in patients who suffer with chest pain and coronary heart disease, and may eventually reduce the need for invasive tests such as coronary angiograms. Doctors have been doing research for many years to see how accurate MRI is compared to other heart tests. This study is part of that on-going research. In this study we will be using a magnet with a stronger magnetic field (called 3Tesla) than used in our previous CEMARC I study. This gives sharper pictures with even more detail.

Why have I been chosen?

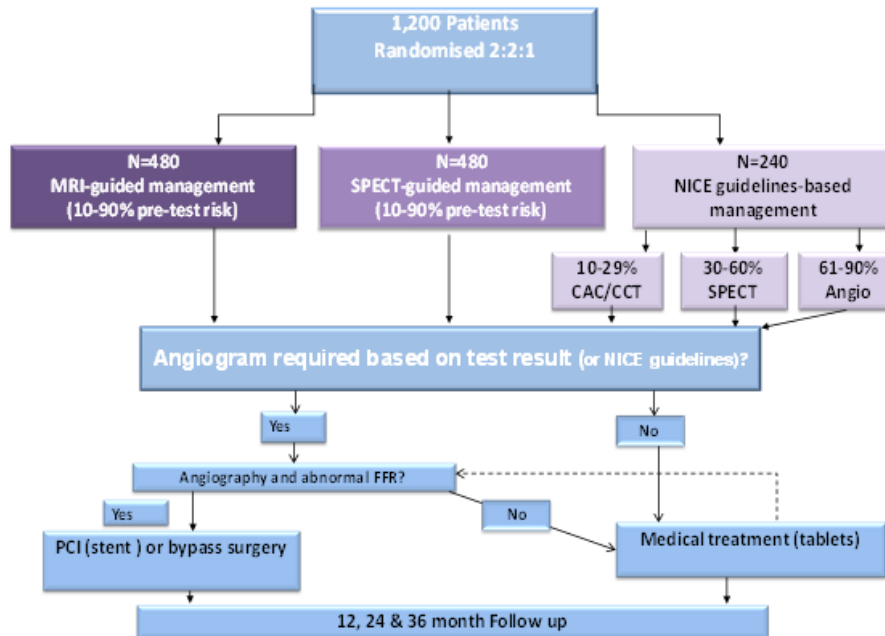
This study is looking at people like you, who have been referred to a cardiology clinic with chest pain. We will be asking 1200 people, in several UK hospitals, to take part in this study.

Do I have to take part?

No. It is up to you to decide whether or not to take part. If you do decide to take part you will be given this information sheet to keep and be asked to sign a consent form. If you decide to take part you are still free to withdraw at any time and without giving a reason. This will not affect the standard of care that you receive from the NHS. If there is a possibility that you might be pregnant, you should not take part in the study. Our research team will be happy to discuss any other questions that you may have concerning your suitability for the study, before you decide whether to take part.

What will happen to me if I take part?

If you take part in this study you will be assigned to one of three groups. We call one group 'MRI guided' , the second group SPECT-guided, and the third group 'NICE guidelines based'. The choice will be made randomly, like tossing a coin. Neither you nor your doctor can influence what group you will be in. The groups will not be the same size: you have more chance of being in either the MRI or the SPECT group than of being in the NICE guidelines group. As the names suggest, your treatment in this study will be guided by the results of either the MRI scan, the SPECT scan, or one of the tests recommended by NICE (which also includes SPECT).



1. MRI guided group: (480 out of the 1200 patients will be in this group). If you are allocated to the MRI group you will have an **MRI scan** next. The scan will take approximately 60 minutes to complete. You lie in a short 'tunnel', which holds a large magnet. Short bursts of magnetic fields and radio waves from the MRI scanner allow images to be created. You will hear periodical loud "banging" noises while we are acquiring the images of your heart, though we do protect your ears with headphones. You can listen to the radio, or to one of your own CDs. We will remain in communication with you throughout the scan. During the scan, we will inject an MRI contrast medication into a vein in your arm. At one point we will also inject a medication (Adenosine) into a vein in your other arm, which is a drug to increase the blood flow to your heart. This medication is used routinely in many heart tests. **What happens next:** The MRI scan will be reported by a consultant who is an expert in this area. If the test is normal your further treatment will be decided by your own cardiologist. If the test shows that there may be one or more narrowings in your heart arteries you will be offered a further test called an X-Ray coronary angiogram (see page 4).

2. SPECT guided group: (480 out of the 1200 patients will be in this group). If you are allocated to the SPECT group you will have a **SPECT scan** next. The SPECT perfusion study is carried out on two separate days and each visit takes approximately 2 hours. On one day pictures of the heart will be taken at rest, and on a second day after injection of a medication (Adenosine) to increase the blood flow to your heart. On both days you will also have an injection of a radioactive dye into the blood, which is taken up by the heart muscle. One hour after the injection, pictures of the heart are taken with a special camera that slowly moves around you while you lie on a bed with one arm raised above your head. Taking these pictures takes approximately 20 minutes. **What happens next:** The SPECT scan will be reported by a consultant who is an expert in this area. If the test is normal your further treatment will be decided by

your own cardiologist. If the test shows that there may be one or more narrowings in your heart arteries you will be offered a further test called an X-Ray coronary angiogram (see page 4).

3. NICE guidelines group: (240 out of the 1200 patients will be in this group). If you are allocated to the NICE guidelines group you will have the heart test recommended by these guidelines, published by NICE, the National Institute for Health and Clinical Excellence, in 2010. This will be one of the following: a CT calcium score (followed by a CT coronary angiogram if required), a SPECT scan, or an X-Ray coronary angiogram. Which test you are offered depends on how likely it is that you have narrowings of the heart arteries. We can calculate this from your medical history and you will fall into either a low, intermediate, or high likelihood group.

a. For patients with a low likelihood:

CT calcium score: CT stands for 'computerised tomography' and is a sophisticated type of X-ray. You will lie on a bed under a scanner and will be asked to hold your breath briefly for the scan to be performed. This scan will let us see how much calcium there is in your heart arteries. If there is very little then the scan will be stopped at that point and you will have no further tests. If there is a lot of calcium the scan will also be stopped and you will be offered an X-Ray coronary angiogram (see below). If there is a moderate amount of calcium we will continue to see whether there are any narrowings, this is called a **CT coronary angiogram**. For this you will receive an injection of a contrast dye into a vein in your arm. You may also receive an injection of a medicine (a beta-blocker) to slow your heart rate down a little bit. This can help reduce the time you will need to hold your breath for.

b. For patients with an intermediate likelihood:

SPECT scan: this is the same scan as the patients in the SPECT guided group have, and is described on page 3. If the test shows that there may be one or more narrowings in your heart arteries you will be offered a further test called an X-Ray coronary angiogram (see below).

c. For patients with a high likelihood:

X-Ray Coronary angiography: This test requires you to come into hospital for one day. With a coronary angiogram we take X-ray pictures of the heart arteries. You will be taken to an X-ray room and asked to lie down on a bed. After cleaning the skin, local anaesthetic is given and a needle put into the artery in the wrist or occasionally the groin. A fine, hollow tube called a "catheter" is then introduced into the artery and is gently advanced through the blood vessels to the heart. You will not feel the catheter being moved around inside your chest. A dye is then injected into the heart blood vessels and X-rays taken from several angles. A narrowing or a blockage may be seen which would confirm the diagnosis of coronary artery disease. To assess the importance of a narrowing in a heart artery a **pressure wire** will be used. This technique is increasingly used during a coronary angiogram to guide further treatment. This is a very small wire inserted through the catheter into the vessel of the heart to measure the blood flow. It also involves the injection of Adenosine to improve blood flow to the heart. When the test is over, the catheter is removed and simple pressure is applied to the wrist (or groin).

After the angiogram the doctor carrying out the test will discuss the findings with you, and the options for treatment if any narrowings were found. Any treatment you receive is not part of the study and will be carried out following current best practice. If you do need an angiogram for any reason within a year of joining the study we will do the pressure wire test on narrowings seen in your heart arteries.

Health Questionnaires

If you agree to participate in this study, you will be asked to complete three simple health questionnaires when you join the study, after six months, and then once a year for three years.

Follow-up: As part of the study we would like to see how you are getting on once a year for three years. We may telephone you to ask you some simple questions about your health. With your permission we may also look at your hospital records, request access to your GP records, central NHS records and/or use information from The Health and Social Care Information Centre.

It is very helpful if we can continue to track your health condition over a long term period. The Health and Social Care Information Centre (HSCIC) allows us to access health information about you with your permission. In order to this we are seeking your permission to provide HSCIC with some of your personal details (including your name, date of birth, address and NHS number) and with this information HSCIC will be able to provide us with simple health information about you beyond the 3 year follow up period of this study, for a period of up to 20 years. It is very important to understand the long term health condition of patients to find out if the treatments we are giving are effective. Information will be provided to HSCIC in strict confidence and will be kept securely by them and will not be released to a third party.

What are the possible disadvantages and risks of taking part? It is important to remember that if you were not in the study you would be having one of these tests anyway.

MRI scan: Magnetic Resonance Imaging (MRI) at 3Tesla is safe and no radiation is used for this scan. There are no known risks from the technique. Some people may experience claustrophobia. Our MRI staff will do all that they can to make you feel comfortable during the scan, and will be monitoring you via a video camera and an audio link. If we are unable to make you feel comfortable in the scanner, we will not go ahead with scanning. We will need to insert two small tubes (cannulae) into your arms for the contrast dye and the adenosine medication. The contrast medication we use during the scan is very safe but, as with any injection, reactions may occur. These include a warm sensation at the injection site, nausea or vomiting and transient skin rash. These effects usually only last for a few minutes. People with a history of allergy are more likely to suffer a more severe reaction, but this is rare (less than 1 in 3000). The department is equipped to cope with allergic reactions if they happen. Adenosine, the medication we use to increase the blood flow to the heart, can cause flushing, breathlessness and chest discomfort. However, all of these feelings usually subside within one or two minutes or even more quickly when the medication is stopped.

SPECT scan: SPECT imaging is very safe but exposes patients to a small amount of radiation. The dose is equivalent to receiving approximately 3 years of natural background radiation in the UK. We will need to insert one small tube (cannula) into your arm for the contrast dye and the adenosine medication. Adenosine, the medication we use to increase the blood flow to the heart, can cause flushing, breathlessness and chest discomfort. However, all of these feelings usually subside within one or two minutes after the medication is stopped.

CT coronary angiogram: CT imaging is very safe but exposes patients to a small amount of radiation. The dose of a CT calcium score only scan is equivalent to receiving approximately 6 months to 1 year of natural background radiation in the UK. The dose of a CT angiogram is equivalent to receiving approximately 3 years of natural background radiation in the UK. We will need to insert one small tube (cannula) into your arm for the contrast dye. The contrast medication we use during the scan is very safe but, as with any injection, reactions may occur. The department is equipped to cope with allergic reactions if they happen. You may also be given a medication (by mouth or into a vein) to slow your heart rate down a little, this is called a beta-blocker. If this is the case you will usually be kept under observation until the after effects of any possible light headedness have worn off, which is usually for about half an hour.

X-Ray Coronary angiography and pressure wire:

At present most patients with chest pain or other symptoms consistent with coronary artery disease will have an angiogram at some point. The advantage of an angiogram is that it can look inside the arteries. However this also means that it is invasive and bears some risks. The most common complication of the X-ray angiogram is for a bruise to form on the wrist or in the groin. This is not serious, but may be inconvenient for a few days. Allergic reactions to the iodine based dye are rare and the department is equipped to cope with reactions. Other serious complications are very rare, but the test can cause a heart attack, stroke or kidney damage. This is estimated at about 1 or 2 in every 1000 people. However the level of risk depends on your overall health and your individual heart condition. A

pressure wire test is safe, but as a wire is passed down the coronary artery a small risk of damage to the blood vessel wall or heart muscle is added.

The amount of radiation you are exposed to during a coronary angiogram is approximately equivalent to the radiation you are exposed over the course of 3 years from the natural environment.

What are the alternatives?

If you do not wish to take part in the study you will have the heart test your cardiologist chooses for you.

Benefits to you

We cannot promise the study will directly benefit you, but the information we get from this study might help the treatment of future patients. If you take part in a study you will have more contact with us, and have more opportunities to ask questions and be informed about your health, which some patients find helpful.

Expenses

You will not be asked to undergo any extra tests as a result of taking part in this study, so you will incur no extra expenses.

Will my taking part be kept confidential?

All information collected about you during the course of the study will be kept strictly confidential. This information will be securely stored, electronically on Leeds Teaching Hospitals NHS Trust and University of Leeds secure servers, and on paper, under the provisions of the 1998 Data Protection Act. Images (scans) and data, after your personal details have been removed, may be sent to participating study centres, or to an independent laboratory, for analysis. Your data, including personal data such as your name, address and NHS number will be sent to the Clinical Trials Research Unit at the University of Leeds. The data collected will be coded and your personal details will be kept entirely separately from details about your health and treatment. You will not be identified in any publication that may result from this research.

We may contact the Health and Social Care Information Centre or other central NHS UK bodies at a later stage for information which they hold on your health status. This means some of your personal data will be shared with the Health and Social Care Information Centre. Any information exchanged between us Health and Social Care Information Centre will be subject to strict data protection regulations.

With your permission, your data may also provide a resource for future studies. If any information from this study is used to develop new research, data protection regulations will be observed and strict confidentiality maintained. Any information about you which leaves the hospital will have your name and address removed so that you cannot be identified. Your data and or images may be sent to institutions in the UK, the European Economic Area or outside the EEA. Ethical approval will be obtained for any future studies involving your data. With your consent we may also wish to contact you in future about new studies you may wish to participate in. We will never give your personal details to any researchers outside of our department.

If you withdraw consent from further study follow-up, or if you were to become incapacitated, any data collected about you up to that point will remain on file and will be included in the final study analysis.

What will happen to the results of the research study?

When the study is complete the results will be published in a medical journal, but no individual patients will be identified. If you would like a copy of the published results, please ask your doctor.

Indemnity/Compensation

If you are harmed as a direct result of taking part in this study, there are no special compensation arrangements. If you are harmed due to someone's negligence, then you may have grounds to a legal action. Regardless of this, if you have

any cause to complain about any aspect of the way you have been approached or treated during the course of this study, the normal National Health Service complaints mechanisms are available to you.

The research organisation

This is a research project of the Cardiac MRI department at the University of Leeds and the Leeds Teaching Hospitals NHS Trust, in collaboration with the Clinical Trials Research Unit at the University of Leeds. It is being funded by the British Heart Foundation.

Who has reviewed the study?

The study has been reviewed and approved both by the South Yorkshire Research Ethics Committee and by your hospital trust's Research and Development Office. More details can be provided, on request, by your study doctor.

For further information please contact:

CONSENT FORM v 4.0 June 12th 2013
CE-MARC 2
Clinical Evaluation of Magnetic Resonance imaging in Coronary heart disease.
CI: Prof John Greenwood

Patient Study Number: Patient Initials.....

NHS number: Date of Birth:

Please initial boxes

1. I have read the Patient Information Sheet dated June 12th 2013 (version 4.0) for the above study and I have had the opportunity to ask questions and discuss the research study and I am satisfied with the answers to my questions.
2. I understand that my participation is voluntary and that I am free to withdraw from the study at any time without giving a reason.
3. I give my consent for my General Practitioner to be informed, and I understand that my cardiologist will be informed only if we find any abnormality over and above what is already known.
4. I understand that data and images collected will be stored on a computer system, and, after my personal details have been removed, may be sent to participating study centres or to an independent laboratory, and may be available to researchers at other institutions in the UK, the EEA, and countries outside the EEA.
5. I understand that relevant sections of my medical notes and data collected during the study (including personal data) may be looked at by individuals from the University of Leeds, the Clinical Trials Research Unit, from regulatory authorities, or from the Leeds Teaching Hospitals NHS Trust, where it is relevant to my taking part in this research. I give permission for these individuals to have access to my records.

6. I understand that information held by the NHS, by my General Practitioner, and information held and managed by the Health and Social Care Information Centre and other central UK NHS bodies, may be used to contact me and provide information about my health status. I give permission for this information to be obtained from The Health and Social Care Information Centre, the NHS Central Register and/or my GP if necessary. To do this, I understand that my details (including my name, address, NHS number and date of birth) will be shared with The Health and Social Care Information Centre.
7. If I were to lose capacity or withdraw consent for further follow-up I understand that data already collected will be kept and used for the purposes of the study.
8. I agree to take part in this research study and that the general results of the study will be made available to the medical community most likely through publication in a reputable medical journal.
9. I am willing to be contacted again in the future with regard to potentially taking part (without any obligation) in further related research studies.
10. I agree to a copy of this consent form being sent to the Clinical Trials Research Unit.

Signature.....

Name (block capitals)..... Date.....

Signature of researcher.....

Name (block capitals).....Date.....

1 copy for patient, 1 copy for the CTRU, 1 copy for medical records and 1 copy for Investigator Site File

10.2. Ethical approval, Patient information and consent forms for Chapter 4

NRES Committee Yorkshire & The Humber - Leeds Central

Yorkshire and Humber REC Office
First Floor, Millside
Mill Pond Lane
Meanwood
Leeds
LS6 4RA

Telephone: 0113 3050127
Facsimile: 0113 8556191

03 May 2012

Dr Klaus Witte
Senior Lecturer and Consultant Cardiologist
Leeds Teaching Hospitals NHS Trust
Great George Street
Leeds
LS1 3EX

Dear Dr Witte

Study title: VINDICATE: Vitamin D treating patients with Chronic
heArT failurE
REC reference: 12/YH/0206

The Research Ethics Committee reviewed the above application at the meeting held on 20 April 2012. Thank you for attending to discuss the study.

Ethical opinion

Members commended you on the involvement of patients in the development of this study.

The Committee asked you to explain the recruitment process. You stated that potential participants will be identified as a result of their low levels of vitamin D. You explained that the Vitamin D test was now part of standard in the department due to the link between vitamin D and chronic heart failure. The test forms part of the unit's audit procedure and allows clinicians to stratify risk e.g. low risk patients can return to GP managed care.

The members of the Committee present gave a favourable ethical opinion of the above research on the basis described in the application form, protocol and supporting documentation, subject to the conditions specified below.

Ethical review of research sites

NHS Sites

The favourable opinion applies to all NHS sites taking part in the study, subject to management permission being obtained from the NHS/HSC R&D office prior to the start of the study (see "Conditions of the favourable opinion" below).

Non NHS sites

The Committee has not yet been notified of the outcome of any site-specific assessment (SSA) for the non-NHS research site(s) taking part in this study. The favourable opinion does not therefore apply to any non-NHS site at present. I will write to you again as soon as

one Research Ethics Committee has notified the outcome of a SSA. In the meantime no study procedures should be initiated at non-NHS sites.

Conditions of the favourable opinion

The favourable opinion is subject to the following conditions being met prior to the start of the study.

Management permission or approval must be obtained from each host organisation prior to the start of the study at the site concerned.

Management permission ("R&D approval") should be sought from all NHS organisations involved in the study in accordance with NHS research governance arrangements.

Guidance on applying for NHS permission for research is available in the Integrated Research Application System or at <http://www.rdforum.nhs.uk>.

Where a NHS organisation's role in the study is limited to identifying and referring potential participants to research sites ("participant identification centre"), guidance should be sought from the R&D office on the information it requires to give permission for this activity.

For non-NHS sites, site management permission should be obtained in accordance with the procedures of the relevant host organisation.

Sponsors are not required to notify the Committee of approvals from host organisations

- 1. The GP letter should include the correct REC name.**

It is responsibility of the sponsor to ensure that all the conditions are complied with before the start of the study or its initiation at a particular site (as applicable).

You should notify the REC in writing once all conditions have been met (except for site approvals from host organisations) and provide copies of any revised documentation with updated version numbers. Confirmation should also be provided to host organisations together with relevant documentation

Approved documents

The documents reviewed and approved at the meeting were:

Document	Version	Date
Covering Letter		12 March 2012
Evidence of insurance or indemnity		28 September 2011
GP/Consultant Information Sheets	1	12 March 2012
Investigator CV		12 January 2012
Letter of invitation to participant	1	12 March 2012
Other: Data from proof of concept & observational study		
Other: CV - J Gierula		02 April 2012
Other: CV - R Byrom		21 March 2012
Other: CV - M Kearney		08 November 2011
Participant Consent Form	1	12 March 2012
Participant Information Sheet	1	12 March 2012
Protocol	1	12 March 2012

REC application		12 March 2012
Summary/Synopsis		

Membership of the Committee

The members of the Ethics Committee who were present at the meeting are listed on the attached sheet.

Statement of compliance

The Committee is constituted in accordance with the Governance Arrangements for Research Ethics Committees and complies fully with the Standard Operating Procedures for Research Ethics Committees in the UK.

After ethical review

Reporting requirements

The attached document "After ethical review – guidance for researchers" gives detailed guidance on reporting requirements for studies with a favourable opinion, including:

- Notifying substantial amendments
- Adding new sites and investigators
- Notification of serious breaches of the protocol
- Progress and safety reports
- Notifying the end of the study

The NRES website also provides guidance on these topics, which is updated in the light of changes in reporting requirements or procedures.

Feedback

You are invited to give your view of the service that you have received from the National Research Ethics Service and the application procedure. If you wish to make your views known please use the feedback form available on the website.

Further information is available at National Research Ethics Service website > After Review

12/YH/0206	Please quote this number on all correspondence
-------------------	---

With the Committee's best wishes for the success of this project

Yours sincerely

Dr Margaret L. Faulk
Chair

Email: nicola.mallender-ward@nhs.net

Enclosures: List of names and professions of members who were present at the meeting and those who submitted written comments

"After ethical review – guidance for researchers"

Copy to:

Mrs Clare Skinner, University of Leeds

Mrs Amanda Burd, Research & Development LTHT



UNIVERSITY OF LEEDS

The Leeds Teaching Hospitals 
NHS Trust

Dr Klaus Witte
Division of Cardiovascular and Diabetes Research
Leeds Institute for Genetics, Health and Therapeutics
The LIGHT Laboratories
University of Leeds
Leeds LS2 9JT



Developmental Clinical Studies:

VINDICATE: VitamIN D treating patIents with Chronic heArT failurE

Patient Information Sheet

Chief Investigator: Dr. Klaus K Witte (Tel: 0113 3926642)

Title: VINDICATE: VitamIN D treating patients with Chronic heArT failurE

You are being asked to take part in a research study. Before agreeing to participate in this study, it is important that you read and understand the following explanation of the proposed study procedures. The following information describes the purpose, procedures, benefits, discomforts, risks and precautions associated with this study. It also describes your right to refuse to participate or withdraw from the study at any time.

In order to decide whether you wish to participate in this research study, you should understand enough about its risks and benefits to be able to make an informed decision. This is known as the informed consent process. Please ask the study doctor or study staff to explain any words you don't understand. Make sure all your questions have been answered to your satisfaction before signing the consent form.

Part 1

Purpose of the study

We want to find out whether supplementing vitamin D in patients with chronic heart failure helps improve their symptoms, the function of their heart, their exercise capacity and some of the other features seen in chronic heart failure.

Vitamin D is a substance that can be made in the skin in response to sunlight. As a result of low levels of sunlight, many adults in the UK have low levels. This is particularly common in patients with heart failure. It is well known that vitamin D improves bone strength by causing calcium deposition in the bone matrix. Patients with osteoporosis ('thinning of the bones') often receive low doses of vitamin D and calcium to help reduce their chances of fractures.

In addition to its effects on bone strength, recent information has suggested that vitamin D might have widespread additional effects on the heart's pumping function, muscle, kidney and immune system function, insulin production and release, and artery relaxation. Many of these are abnormal in heart failure and we want to find out if by giving vitamin D for a year will improve these abnormalities. In order to do this we are performing a study in 100 patients with heart failure. The study will involve patients taking either vitamin D or a placebo (dummy tablet) daily for twelve months (one year). Neither you nor your doctor will know whether you are taking the vitamin D or the placebo. This is called 'blinding' and is common in studies of this type to reduce 'bias'.

Why have I been invited to take part?

We have invited you to take part in this study because you have heart failure and have been attending our Heart Failure Clinic. During one of your routine blood tests we have found that you have a low vitamin D level. Normally vitamin D is not supplemented to patients unless they have suffered broken bones. However, it is possible that vitamin D has other effects as described above.

Do I have to take part?

It is up to you to decide. We will describe the study and go through this information sheet, which we will then give to you. If you agree to take part we will then ask you to sign a consent form to show that you understand what is involved in the study. You will remain free to withdraw at any time, without giving a reason. This would not affect the standard of care you receive.

What will happen if I take part?

If you agree to participate in this study, we will ask you to come to our research clinic for the 'baseline' visit.

First 'baseline' visit

During this visit we will ask you to sign a consent form to say that you are happy to take part. This first visit will involve several tests in order to try to keep the number of extra trips to a minimum.

We will ask you to fill in a questionnaire about your symptoms and one about your recent visits to hospital. A nurse will help you with this if you wish. A doctor will examine you and we will take some further blood tests. We will take about a table spoonful of blood at this visit. We will then perform an echocardiogram (ultrasound scan of the heart). You will have had one of these before.

The final test during this visit will be a walk test lasting 6 minutes. You will be asked to walk up and down a corridor at your own pace for 6 minutes. You can stop and rest at any point, although we would like you to do as much as you can. A nurse will be present throughout the test and there are chairs at both ends for you to rest.

The project involves two further tests but these are not mandatory. We would like as many people to do these two tests as possible, but if you are not keen on them please discuss this with the nurse or the doctor.

At the end of this visit you will be given the tablets which are pleasant tasting (of

blackcurrant) and chewable. *If you have agreed to participate in the two optional tests listed below, please do not start taking the tablets until the research nurse telephones you after the tests have been done.*

Two optional tests

The first is an exercise test on a treadmill to measure your exercise capacity. This will be done on E-floor in the cardiology department and usually takes about 30 minutes. During this test we will ask you to walk until you are exhausted. Throughout the test we will collect the air you breathe in and out to measure your oxygen consumption. If you have never performed an exercise test on the treadmill before we will ask you to come back a week later to repeat this as described below.

The second optional test is a cardiac magnetic resonance scan (CMR). You will only be invited to participate in this part of the study if you are being included at the Leeds centre. This is a detailed scan of the heart which will require another visit. You might have had one of these before. It involves you lying on a bed which then moves into a tunnel to image the heart. Some people find this enclosing. If you get claustrophobic you might not be able to tolerate this scan. In this case we would still like you to take part in the study but we will omit the CMR scan.

Once you have had these baseline tests, one of the nurses will telephone you to start taking the tablets. Whether you take the vitamin D or the placebo tablets is decided randomly (like the toss of a coin). Neither you nor the doctors will know whether you are taking the vitamin or the placebo.

Follow-up visits

After three months, six months and nine months, we will invite you back to the clinic to check how you are getting on with the treatment and to review your symptoms. We will also perform a blood test (one teaspoonful of blood) to monitor your vitamin D levels at each visit, ask you to fill in the questionnaires again and repeat the 6 minute walk test.

End of the study visits

After one year of treatment, we will organise another set of tests similar to those you had at baseline. This will include assessments of your symptoms, the questionnaires, the blood tests (one tablespoonful). If you had them at baseline, we will also repeat the exercise test, and the cardiac magnetic resonance scan of your heart. During these tests you should continue to take the tablets. Once the final scan has been performed, we will tell you that you can stop taking them.

Risks

The risk of any adverse event as a result of taking vitamin D is very low. There have been no incidences of adverse events with the dose we will be using in this study. We have recently completed a 60 patient study with no adverse events attributable to the vitamin D. The risks associated with any of the scans is very low, and the blood testing might leave a little bruise. The risk from exercise testing is likewise very small (less than 1 percent). Adverse effects could include the development of chest pain, hypotension (low blood pressure) or arrhythmias (irregular or abnormal heart beats). A physician will be present to supervise all testing.

Benefits

The study aims to see if there are benefits of vitamin D in patients with heart failure who are otherwise taking optimal therapy. In order to demonstrate this, all patients will initially be managed with all therapy so far proven to be of benefit. All participants will be investigated thoroughly and followed-up carefully. In addition to optimal therapy half of the patients will be taking dummy pills (placebo). If during the study it becomes apparent that there are clear benefits of vitamin D we will stop the study early and all subjects will be transferred to the vitamin D tablets.

Participation

Your participation in this study is voluntary. You can choose not to participate or you may withdraw at any time without affecting your medical care. Since you are being asked to come to the hospital more frequently, we can compensate you for reasonable for travel expenses. We will inform your GP that you are participating in this study.

Compensation

If you become ill or are physically injured as a result of participation in this study, medical treatment will be provided. In no way does signing this consent form waive your legal rights nor does it relieve the investigators, sponsors or involved institutions from their legal and professional responsibilities.

Part 2

What if relevant new information becomes available?

Sometimes we get new information about your condition, based upon the results of the tests. If this happens, your research doctor will tell you and discuss whether you should continue in the study. If you decide not to carry on, your research doctor will make arrangements for your care to continue. If the study is stopped for any other reason, we will tell you and arrange your continuing care. Similarly if it becomes apparent that vitamin D is proving to be of benefit before the end of the study, we will stop the study early and convert all participants to vitamin D.

What if I don't want to carry on with the study?

You can withdraw from the study at any time. We might use information collected while you were taking part.

Complaints

If you have a concern about any aspect of this study, you should ask to speak to a member of the study team who will do his best to answer your questions (0113 3926642). If you remain unhappy and wish to complain formally, you can do this through the NHS Complaints Procedure. Details can be obtained from the hospital.

In the event that something does go wrong and you are harmed during the research and this is due to someone's negligence then you may have grounds for a legal action for compensation against Leeds University or Leeds Teaching Hospitals NHS Trust but you may have to pay your legal costs. The normal National Health Service complaints mechanisms will still be available to you.

Confidentiality

All information obtained during the study will be held in strict confidence. You will be

identified with a study number only. No names or identifying information will be used in any publication or presentations. No information identifying you will be transferred outside the investigators in this study. During the regular monitoring of your study or in the event of an audit, your medical record may be reviewed by the Hospital Research Ethics Board. We will however make your General Practitioner aware that you are participating in this study.

What will happen to the results of the study?

We will inform all participants of the results of the study and the results will be published in international peer-reviewed journals.

Who has reviewed the study?

All research in the NHS is investigated by independent group of people, called a Research Ethics Committee to protect your safety, rights, wellbeing and dignity. This study has been reviewed and given favourable opinion by Leeds West Research Ethics Committee.

Questions

If you have any further questions about the study, please call Dr Klaus Witte at 0113 3926642.



UNIVERSITY OF LEEDS

The Leeds Teaching Hospitals 
NHS Trust

Dr Klaus Witte
Division of Cardiovascular and Diabetes Research,
Leeds Institute for Genetics, Health and Therapeutics
University of Leeds
Leeds LS2 9JT

Centre Number: 1

Study Number: 1

Patient Identification Number for this trial:

CONSENT FORM

Title of Project: VINDICATE: Vitamin D treating patients with Chronic heart failure

Name of Investigators: Dr Klaus Witte

Please initial box

1. I confirm that I have read and understand the information sheet dated 12th March 2012 (version 1.0) for the above study. I have had the opportunity to consider the information, ask questions and have had these answered satisfactorily.

2. I understand that my participation is voluntary and that I am free to withdraw at any time without giving any reason, without my medical care or legal rights being affected.

3. I understand that relevant sections of my medical notes and data collected during the study may be looked at by regulatory authorities or from the NHS Trust, where it is relevant to my taking part in this research. I give permission for these individuals to have access to my records.

4. I agree to my GP being informed of my participation in the study

5. I agree to take part in the above study.

Name of Subject

Date

Signature

Name of Person
taking consent

Date

Signature

When completed, 1 for patient; 1 for researcher site file; 1 (original) to be kept in medical notes

10.3. Ethical approval, Patient information and consent forms for Chapters 6 and 7

18 APR 2012



NRES Committee Yorkshire & The Humber - Leeds West
First Floor
Milleide
Mill Pond Lane
Leeds
LS6 4RA

Telephone: 0113 3050122
Facsimile: 0113 8556191

18 April 2012

Dr Sven Plein
Consultant Cardiologist, British Heart Foundation Senior Clinical Research Fellow
University of Leeds
Academic Unit of Cardiovascular Medicine
G floor, Jubilee Wing
Leeds General Infirmary
LS1 3EX

Dear Dr Plein

Study title: QUANTITATIVE EVALUATION OF MYOCARDIAL CHARACTERISTICS IN REPERFUSED ST-ELEVATION MYOCARDIAL INFARCTION – A 3 TESLA CARDIOVASCULAR MAGNETIC RESONANCE STUDY
REC reference: 12/YH/0169

The Research Ethics Committee reviewed the above application at the meeting held on 13 April 2012. The Committee would like to thank Dr Kidambi for attending the meeting.

Ethical opinion

The procedure for dealing with identification of an unexpected condition was queried; Dr Kidambi explained that if the participant is still an inpatient their cardiologist would be informed; if they have been discharged their GP and cardiologist would be notified. Members asked that this is included in the participant information sheet and GP letter.

The members of the Committee present gave a favourable ethical opinion of the above research on the basis described in the application form, protocol and supporting documentation, subject to the conditions specified below.

Ethical review of research sites

NHS Sites

The favourable opinion applies to all NHS sites taking part in the study, subject to management permission being obtained from the NHS/HSC R&D office prior to the start of the study (see "Conditions of the favourable opinion" below).

Conditions of the favourable opinion

The favourable opinion is subject to the following conditions being met prior to the start of the study.

Management permission or approval must be obtained from each host organisation prior to

After ethical review

Reporting requirements

The attached document "After ethical review – guidance for researchers" gives detailed guidance on reporting requirements for studies with a favourable opinion, including:

- Notifying substantial amendments
- Adding new sites and investigators
- Notification of serious breaches of the protocol
- Progress and safety reports
- Notifying the end of the study

The NRES website also provides guidance on these topics, which is updated in the light of changes in reporting requirements or procedures.

Feedback

You are invited to give your view of the service that you have received from the National Research Ethics Service and the application procedure. If you wish to make your views known please use the feedback form available on the website.

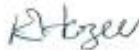
Further information is available at National Research Ethics Service website > After Review

12/YH/0169

Please quote this number on all correspondence

With the Committee's best wishes for the success of this project

Yours sincerely



pp
Dr Rhona Bratt
Chair

Email: Elaine.hazell@nhs.net

Enclosures: List of names and professions of members who were present at the meeting and those who submitted written comments "After ethical review – guidance for researchers"

Copy to: Mrs Rachel E De Souza

Mrs Anne Gowing, Leeds Teaching Hospitals NHS Trust

the start of the study at the site concerned.

Management permission ("R&D approval") should be sought from all NHS organisations involved in the study in accordance with NHS research governance arrangements.

Guidance on applying for NHS permission for research is available in the Integrated Research Application System or at <http://www.rdforum.nhs.uk>.

Where a NHS organisation's role in the study is limited to identifying and referring potential participants to research sites ("participant identification centre"), guidance should be sought from the R&D office on the information it requires to give permission for this activity.

For non-NHS sites, site management permission should be obtained in accordance with the procedures of the relevant host organisation.

Sponsors are not required to notify the Committee of approvals from host organisations

1 The GP letter should make it clear that if an unexpected condition is identified they will be informed.

2 The participant information sheet should make it clear that the GP and cardiologist will be informed if any unexpected condition is identified.

It is responsibility of the sponsor to ensure that all the conditions are complied with before the start of the study or its initiation at a particular site (as applicable).

You should notify the REC in writing once all conditions have been met (except for site approvals from host organisations) and provide copies of any revised documentation with updated version numbers. Confirmation should also be provided to host organisations together with relevant documentation

Approved documents

The documents reviewed and approved at the meeting were:

<i>Document</i>	<i>Version</i>	<i>Date</i>
✓ Evidence of insurance or indemnity		28 September 2011
✓ GP/Consultant Information Sheets	1	01 March 2012
Investigator CV		
✓ Participant Consent Form	1	01 March 2012
✓ Participant Information Sheet	1	01 March 2012
✓ Protocol	1	04 March 2012
REC application		12 March 2012

Membership of the Committee

The members of the Ethics Committee who were present at the meeting are listed on the attached sheet.

Statement of compliance

The Committee is constituted in accordance with the Governance Arrangements for Research Ethics Committees and complies fully with the Standard Operating Procedures for Research Ethics Committees in the UK.

NRES Committee Yorkshire & The Humber - Leeds West

Attendance at Committee meeting on 13 April 2012

Committee Members:

<i>Name</i>	<i>Profession</i>	<i>Present</i>	<i>Notes</i>
Miss Brygitta Atraszkiewicz	Information Analyst	Yes	
Professor Howard Bird	Consultant Rheumatologist	Yes	
Dr Rhona Bratt	Retired Multimedia Project Manager	Yes	
Mr David Bryant	Pharmacist	No	
Dr Martin Elliott	Consultant Paediatric Oncologist	No	
Dr Sheila E. Fisher	NCRI Associate Director for PPI	Yes	
Mr Peter Margerison	Retired Solicitor	Yes	
Mr Jerry Masterson	Practice Learning Facilitator	Yes	
Dr Wendy Neil	Consultant Psychiatrist	No	
Dr Vera Neumann	Consultant in Rehabilitation Medicine	No	
Dr Jane Orton	Consultant Oncologist	Yes	
Dr Reema Sirriyeh	Research Fellow	No	
Professor Anne Topping	Director, Centre for Health and Social Care Research	Yes	

Also in attendance:

<i>Name</i>	<i>Position (or reason for attending)</i>
Mrs Elaine Hazell	REC Co-ordinator
Ms Ariana Mihoc	Observer
Mrs Shobhana Ningoo	Assistant Co-ordinator

Study code 3T-STEMI

**Quantitative evaluation of myocardial characteristics in reperfused
ST- elevation myocardial infarction – a 3 Tesla cardiovascular
magnetic resonance study**

PATIENT INFORMATION SHEET
Version 1.2; February 13 2015

Chief Investigator: Dr S Plein

Dear Patient,

You are being invited to take part in a research study. Before you decide it is important for you to understand why the research is being done and what it will involve. Please take time to read the following information carefully and discuss it with friends, relatives and your GP if you wish. Ask us if there is anything that is not clear or if you would like more information. Take time to decide whether or not you wish to take part.

Purpose of the study

Magnetic Resonance Imaging (MRI) is a test, which produces detailed pictures of your internal organs by putting you within a strong magnetic field. With Cardiac MRI we are able to detect several important abnormalities that are caused by heart disease, for example the scarring of the heart from heart attacks and the restrictions of blood flow to the heart muscle that lead to angina. Also, MRI produces pictures of the heart with much greater detail than with other types of heart scans. Importantly, MRI is also a safer test than most other heart scans, because it does not expose patients to any harmful radiation and pictures of the heart can be taken "from the outside". Because of all of these qualities, MRI may become one of the most important tests in patients who suffer with different types of heart disease.

We have been doing MRI scans of the heart in Leeds since 1995. We are continuously carrying out research into improving the images and thereby improving patient care.

During a heart attack the heart muscle cells are damaged. Some heart muscle will not return to normal and will be replaced by a scar. Other parts of the heart muscle are less severely affected by the heart attack and can recover to normal over time.

With MRI the consequences of a heart attack can be shown in much greater detail than with other tests.

In this research we aim to find out how heart attacks affect the heart early on and in the recovery phase that follows. We would therefore like to scan patients like you twice or three times over a 3 month period.

Why have I been chosen?

This study is looking at people like you, who have recently had a heart attack and had the blocked blood vessel reopened. We are hoping to recruit 150 patients like you into this study.

Do I have to take part?

It is up to you to decide whether or not to take part. If you do decide to take part you will be given this information sheet to keep and be asked to sign a consent form. If you decide to take part you are still free to withdraw at any time and without giving a reason. This will not affect the standard of care that you receive from the NHS. If there is a possibility that you might be pregnant, you should not take part in the study. Our research team will be happy to discuss any other questions that you may have concerning your suitability for the study, before you decide whether to take part.

What will happen to me if I take part?

All patients in this study will have two or three MRI scans. We would aim to scan you twice within the first ten days after your heart attack, which is important to find out how changes in the heart evolve, though circumstances (including how you are feeling) may limit us to just one scan during this period. The final scan will take place 3 months later.

The MRI scans will be performed at the Leeds General Infirmary and will each take approximately 60 minutes to complete. You lie in a short 'tunnel', which holds a large magnet. Short bursts of magnetic fields and radio waves from the MRI scanner allow images to be created. You will hear periodical loud "banging" noises while we are acquiring the images of your heart, though we do protect your ears with headphones. You can listen to the radio, or to one of your own CDs. We will remain in communication with you throughout the scan. During the scan, we will inject an MRI contrast medication into a vein in your arm. For this we will insert a small tube (cannula) in a vein in your arm. If you come down from the ward with a cannula (whilst you are staying in hospital) we would use the one that is already there. Usually people are not aware of the actual contrast dye injection.

Whilst you are an in-patient on the ward you will have a blood sample taken every day. This would happen regardless of whether you are in the study or not. We will use some of the results for the research study. We will also take a blood sample (at most 15 mls = 3 teaspoons) from you at every scan visit. We will take this from the cannula we have to insert to inject the contrast dye so there are no extra needles involved. With your permission we will store these samples and analyze them at the end of the study for markers of heart function. Any use of your samples after this study could only happen if an ethics committee approved it.

As part of the study we would like to make a follow-up telephone call to you after one year and at 3 years to ask you some simple questions about your health. With your permission we may also look at your hospital records, request access to your GP records, central NHS records and/or use information from the NHS Information Centre.

After you leave hospital it is very helpful if we can continue to track your health condition over a long term period. The Medical Research Information Service (MRIS) allows us to access health information about you with your permission. In order to this we are seeking your permission to provide MRIS with some of your personal details (including your name, date of birth, address and NHS number) and with this information MRIS will be able to provide us with simple health information about you beyond the 3 year follow up period of this study. It is very important to understand the long term health condition of patients after a heart attack to find out if the treatments we are giving are effective. Information will be provided to MRIS in strict confidence and will be kept securely by them and will not be released to a third party.

Risks and discomforts

Magnetic Resonance Imaging (MRI) at 3 Tesla is safe and no x-rays or radiation are used for this scan. There are no known risks from this technique. Some people may experience claustrophobia. Our MRI staff will do all that they can to make you feel comfortable during the scan, and will be monitoring you via a video camera and an audio link. If we are unable to make you feel comfortable in the scanner, we will not go ahead with scanning. The contrast medication we use during the scan is very safe but, as with any injection, reactions may occur. These include a warm sensation at the injection site, nausea or vomiting and transient skin rash. These effects usually only last for a few minutes. People with a history of allergy are more likely to suffer a more severe reaction, but this is rare (less than 1 in 3000). The department is equipped to cope with allergic reactions if they happen.

Benefits to you

This study does not form part of your normal clinical care and is done solely for research purposes.

Expenses

We will provide reasonable travel expenses should this be necessary for you to attend the MRI scan. We are also happy to arrange transport to the hospital and return you home if needs be.

Will my taking part be kept confidential?

All information collected about you during the course of the study will be kept strictly confidential. This information will be securely stored, electronically on the Leeds General Infirmary secure server, and on paper, under the provisions of the 1998 Data Protection Act. The data collected will be coded and your personal details will be kept separately. You will not be identified in any publication that may result from this research.

With your permission we will inform your GP of your participation in the study. If any unexpected abnormality or condition were found we would inform your GP and your cardiologist.

We may contact the NHS Information Service at a later stage for information, which they hold on your health status. This means some of your personal data will be shared with the NHS Information Service. Any information exchanged between us and the NHS Information Service will be subject to strict data protection regulations.

With your permission, your data may also provide a resource for future studies. If any information from this study is used to develop new research, data protection regulations will be observed and strict confidentiality maintained. Any information about you which leaves the hospital will have your name and address removed so that you cannot be identified. Your data and or images may be sent to institutions in the UK, the European Economic Area or outside the EEA. Ethical approval will be obtained for any future studies involving your data.

If you withdraw consent from further study follow-up, or if you were to become incapacitated, any data collected about you up to that point will remain on file and will be included in the final study analysis.

What will happen to the results of the research study?

When the study is complete the results will be published in a medical journal, but no individual patients will be identified. If you would like a copy of the published results, please ask your doctor.

Indemnity/Compensation

If you are harmed as a direct result of taking part in this study, there are no special compensation arrangements. If you are harmed due to someone's negligence, then you may

have grounds to a legal action. Regardless of this, if you have any cause to complain about any aspect of the way you have been approached or treated during the course of this study, the normal National Health Service complaints mechanisms are available to you.

The research organisation

This is a research project of the Cardiac MRI department of the Leeds General Infirmary and the University of Leeds.

Who has reviewed the study?

The study has been reviewed and approved both by a nationally approved Research Ethics Committee and your hospital Research and Development Office. More details can be provided, on request, by your study doctor.

For further information please contact:

Dr Pankaj Garg
Research Fellow in Cardiac MRI
British Heart Foundation Cardiac MRI Department
B Floor, Clarendon Wing
Leeds General Infirmary
Leeds
LS1 3EX
T 0113 392 5909

Or

Lisa Clark, Fiona Richards, Annabel Nixon
Research Nurses
Cardiology Research
X47 Sunshine Corridor
Leeds General Infirmary
Leeds
LS1 3EX
T 0113 392 5224
M 07922 512 887

Thank you.

CONSENT FORM v 1.2; February 13 2015

**Quantitative evaluation of myocardial characteristics in reperfused ST- elevation myocardial infarction – a 3 Tesla cardiovascular magnetic resonance study.
CI: Dr S Plein**

Patient Study Number:

Date of Birth:

Please initial boxes

1. I have read the Patient Information Sheet dated February 13 2015 (Version 1.2) for the above study and I have had the opportunity to ask questions and discuss the research study and I am satisfied with the answers to my questions.
2. I understand that my participation is voluntary and that I am free to withdraw from the study at any time without giving a reason.
3. I give my consent for my General Practitioner to be informed, and I understand that my cardiologist will be informed only if we find any abnormality over and above which is already known.
4. I understand that data and images collected will be stored on a computer system, and, after my personal details have been removed, may be available to researchers at other institutions in the UK, the EEA, and countries outside the EEA.
5. I understand that some of the blood samples taken from me will be stored and may be analyzed in the future for markers of a heart attack.
6. I understand that relevant sections of my medical notes and data collected during the study may be looked at by individuals from the University of Leeds, from regulatory authorities, or from the Leeds Teaching Hospitals NHS Trust, where it is relevant to my taking part in this research. I give permission for these individuals to have access to my records.
7. I understand that information held by the NHS and records maintained by the NHS Information Centre, the NHS Central Register and by my General Practitioner may be used to contact me and provide information about my health status. I give permission for this information to be obtained from the NHS Information Centre, the NHS Central Register and/or my GP if necessary.
8. If I were to lose capacity or withdraw consent for further follow-up I understand that data already collected will be kept and used for the purposes of the study.
9. I agree to take part in this research study and that the general results of the study will be made available to the medical community most likely through publication in a reputable medical journal.

Signature.....

Name (block capitals)..... Date.....

Signature of witness.....

Name (block capitals)..... Date.....